Univerzita Karlova v Praze

Přírodovědecká fakulta

Studijní program: aplikovaná geologie

RNDr. Lenka Thinová

Radioaktivita hornin a ovzduší ve vybraných podzemních prostorách a jejich zdravotní dopady

Disertační práce

Školitel: Prof. RNDr. Milan Matolín, DrSc.

Praha, 2013

Charles University in Prague

Faculty of Science

Study program: applied geology

RNDr. Lenka Thinová

Radioactivity of the rock and the environment in selected underground areas, and its impact on human health

Dissertation

Supervisor: Prof. RNDr. Milan Matolín, DrSc.

Prague, 2013

Prohlášení:

Prohlašuji, že jsem závěrečnou práci zpracovala samostatně a že jsem uvedla všechny použité informační zdroje a literaturu. Tato práce ani její podstatná část nebyla předložena k získání jiného nebo stejného akademického titulu.

V Praze, 07.04.2013

Podpis

Abstrakt

Disertační práce je tematicky zaměřena na posouzení radioaktivity a absorbovaných dávek záření v jeskyních ČR, z nichž některé vykazují vysoké koncentrace radonu. Předkládaná práce je souhrnem analýz a doporučení, vyplývajících z výsledků měření uskutečněných v podzemních prostorách v ČR za předchozích 10 let. Je zaměřena na posouzení zdrojů ozáření v prostředí jeskyní (a v prostředí využívaných pro speleoterapii), zvážení zdravotních dopadů jejich radiace, včetně zhodnocení vlivu jejich variability na externí a interní ozáření osob. Všechna měření byla provedena s cílem ověřit, případně zlepšit, existující metodický postup pro výpočet absorbované dávky od radonu v podzemních prostorách. Hlavním řešeným problémem bylo posouzení, zda jednotný „jeskynní faktor“ odpovídá skutečným vlastnostem tohoto prostředí. Měření byla prováděna ve všech veřejnosti přístupných jeskyních v ČR a v některých dalších podzemních prostorách. Dvě z jeskyní (Bozkovské dolomitové jeskyně a Zbrašovské aragonitové jeskyně) byly vybrány pro dlouhodobé experimenty. Nejdůležitějšími získanými výsledky jsou tyto: koncentrace radonu v podzemních prostorách není možné předpovídat na základě žádného geologického a geometrického modelu; efektivní dávka externího záření geologických zdrojů radiace dosahovala jednotek μSv a ve srovnání s efektivní dávkou způsobenou inhalací radonu a jeho přeměnových produktů byla zanedbatelná; vysoké koncentrace radonu v ovzduší nemohou být způsobeny koncentrací radonu v přítomné vodě, jejich zdrojem jsou koncentrace ^{226}Ra převážně v klastických sedimentech a zejména nízký koeficient výměny vzduchu; poměry ^{228}Th/^{226}Ra v klastických sedimentech byly vyšší než 1 (v průměru 1,5); typické hodnoty poměrů ^{228}Th/^{226}Ra v karbonátových horninách (včetně amfibolitu a erlánu) se pohybovaly mezi 0, 2 až 0,5; integrální detektory radonu RAMARN byly otestovány pro použití k získání vstupních dat k výpočtu dávky od radonu; perioda integrálního měření byla stanovena na období 1.10. až 31.3. (zimní sezóna) a 1.4. až 30.9. (letní sezóna); nebyly zjištěny rozdíly mezi koncentracemi radonu v pracovní a mimo pracovní dobu; měřené hodnoty volné frakce radioaktivních částic v ovzduší se pohybovaly mezi 0,03 až 0,6 (průměrná hodnota pro jeskyně v ČR byla f_p = 0,13); přítomnost aerosolových částic s průměrem 1-10 μm v jeskyni byla způsobena přítomností lidí (po uzavření jeskyně počet těchto částic rychle klesl); koncentrace částic s průměrem okolo 200 nm se ukázala být relativně stabilní (~10#/cm^3); částice s průměry ~10 nm byly tvořeny v průběhu intensivní práce v jeskyni či pohybu osob v jeskyni (100-1000#/cm^3); pro profil „Prohlídka jeskyně“ byly AMADy 144, 715 a 1900 nm; pro profil „Noc“ byly AMADy 140 a 710nm; závislost faktoru nerovnováhy F na volné frakci f_p byla popsána logaritmickým vztahem $\ln(1/f_p) = a*\ln(1/F)^b$, koeficienty *a* a *b* byly vypočteny ze všech měření volné frakce v podzemních prostorách přístrojem FRITRA4 (měření na mřížce) jako a = 1,85 a b = -1,096. Na základě výsledků aerosolové kampaně (uskutečněné v Bozkovské dolomitové jeskyni) a výsledků výpočtů konversních koeficientů pro převod koncentrace radonu v ovzduší na absorbovanou dávku záření programem LUDEP byly vypočteny pro všechny proměřené podzemní prostory individuální jeskynní faktory. Hodnoty jeskynních faktorů se pohybovaly od 1 do 2,4. Celková relativní chyba výpočtu dávky od radonu byla stanovena na 46%. Metodika pro stanovení dávky v podzemních prostorách byla na základě presentovaných výsledků novelizována ve spolupráci se SÚJB (RNDr. Ivana Ženatá) a aplikována v praxi. V závěru práce byl vytvořen jednoduchý MCNPX model pro výpočet vlivu gama záření vzdušného ^{214}Bi (energetické okno 1,66-1,86 MeV) v prostředí s vysokými koncentracemi radonu a složité geometrie měření na výsledky gama spektrometrie in situ, prováděné v jeskyních.

Abstract

The thesis is focused on measurement and assessment of absorbed doses of radiation in caves of the Czech Republic, out of which some exhibit high activity concentration of radon in air. This thesis presents an analysis and recommendations based on measurement results obtained in the underground caves over the past 10 years. The focus is on defining the sources of irradiation within the cave environment (and in areas used for speleotherapy), considering their potential health effect, including the variable dependence of external and internal irradiation influences. All of the measurements had as an objective to verify, and where possible improve, the existing methodology for assessing and calculating the dose from radon in underground spaces. The main issue that had to be resolved was whether a numerically specified *cave factor* value is applicable to all underground areas. The research measurements were carried out in all available show caves and in several underground areas, and were based on the initial results from an aerosol measurement campaign. Two caves (the *Bozkov Dolomite* Caves and the *Zbrašov Aragonite* Caves) were selected for advanced long-term measurements. A large number of long-term and short-term studies were carried out. The most important results for cave environments were: the values for the effective dose due to external radiation were not higher than units of μSv, and were considered negligible in comparison with the internal dose due to radon; radon in water cannot be the source of a high concentration of radon in the Czech caves; the ^{228}Th/^{226}Ra ratios in clastic sediments are generally higher than 1 (on an average, they are 1.5); typical values for the ^{228}Th/^{226}Ra ratio for carbonate rocks (including amphibolite and erlan) varied between 0.2 - 0.5; integral radon monitoring using RAMARN detectors can provide more consistent results for calculating the effective dose; no major differences were shown in the average radon activity concentration during working time as opposed to non-working time; the best period for "winter season" measurements was from October 1st to March 31st, while the remaining months are referred to as the "summer season"; the free fraction of radioactive particles in air ranged from 0.03 to 0.6, with arithmetical average $f_p = 0.13$; the presence of aerosol particles 1-10 μm in diameter is definitely caused by the presence of visitors or personnel; when the cave was closed, these particles rapidly dissipated; by contrast, the concentration of air particles about 200 nm in diameter is relatively stable (~10 #/cm^3); for the ~10 nm particle size group it seems that the aerosols are produced by intensive work or movement (the concentration is about 100-1000 #/cm^3); for the "Night" profile, the AMADs were 140 and 710nm; for the "Guided Tour" profile, the AMADs were 144, 715 and 1900 nm; using the LUDEP program, dose conversion factors were obtained for single radon decay products; the direct dependence between equilibrium factor F and the size of the free fraction f_p was described using the Log-Power expression $\ln(1/f_p) = a*\ln(1/F)^b$; the calculated values for coefficients *a* and *b* for measured free fraction values by FRITRA4 device from all measurements made in caves and in underground areas were $a = 1.85$ and $b = -1.096$. The *individual cave factor* for each investigated underground area was calculated on the basis of the aerosol measurement campaign in *Bozkov Dolomite* Caves, and the LUDEP program and results obtained through this research; the cave factor values varied between 1 and 2.4. The 46% relative error of the dose from radon was estimated and discussed. A new radon measurement methodology was prepared in collaboration with the State Office for Nuclear Safety (SONS), and it was put into operational use. A simple model using the MCNPX method was developed which describes the gamma-ray contribution of the high concentration of radon daughter ^{214}Bi in the air of underground environment and the contribution of gamma rays of rocks in the complex measurement geometry of the in situ gamma spectrometry in underground caves.

Acknowledgement

The measurements and the research presented here were financially supported by:

2002 – 2005: the Department of Dosimetry FNSPE CTU in Prague

2006 – 2007: the State Office for Nuclear Safety, the project № VaV 12/2006

2008 – 2012: the Czech Ministry of Education, Youth and Physical Culture (research plan № MSM6840770040)

2002 – 2012: the Cave Administration of the Czech Republic

Personal acknowledgement

I would like to thank my supervisor, Milan Matolín, for his patience and for his professional advice.

This thesis would not have been completed without support and help from a large group of people.

Firstly, I would like to thank the Cave Administration of the Czech Republic for its cooperation and for allowing me to look into the radon concentration measurement data registers (especially Jaroslav Hromas and Petr Zajíček). Many thanks for showing tremendous confidence in my work and for offering selfless help in all underground areas where measurements were made, especially in the Bozkov Dolomite Caves (Dušan Milka, Hanka Dlabalová), the Zbrašov Aragonite Caves (Bára Šimečková, Milan Geršl), and the Mladeč Caves (Drahomíra Coufalová).

The Faculty of Nuclear Sciences and Physical Engineering has always stood by me. I would like to thank Tomáš Čechák (Head of the Department of Dosimetry and Application of Ionizing Radiation) and Ladislav Musílek for long-time personal support and for financial support that enabled advanced measurements to be made using the most appropriate equipment. Among the group of students without whom such a large number and range of field measurements and calculations could not have been implemented, I give countless thanks to Kateřina Navrátilová Rovenská (Eva Brandejsová, Lenka Dragounová, Matěj Navrátil, and others).

Many thanks for collaboration with the NRPI Radon Expert Group (Ladisla Moučka, Aleš Froňka, Karel Jílek, Jan Hradecký), NRBCPI experts (Petr Otáhal) and ICPF (Vladimír Ždímal), without whose support for the aerosol measurements in the Bozkov Dolomite Caves the subsequent research could not have been carried out.

At last but not least, many thanks for revising my English and for personal support to Robin Healey, and to Petr Liška and others, who helped me along in a multitude of small tasks, too numerous to mention.

And, of course, my great appreciation to my daughters, Mirka and Zdeňka, for their unrelenting support and their faith in my ability to bring this work to a successful conclusion.

Contents

1. Introduction

The sources of irradiation in the underground are natural radionuclides, which are contained in the rock, clastic sediments and in the local air. However it must be kept in mind that the variability of radionuclides concentration in limestone (or other sedimentary rock) and in clastic sediments fulfilling the underground areas, and the variability of the characteristics of the underground environment is such, that it is not possible to predict any potential irradiation problem in the given underground area from general geological information. The health impact of the irradiation which is caused by radionuclides in general can be defined using annual effective dose, which consists of external and internal dose. Both of those values comprise the behavior of the people in the area under investigation and the time spent in this environment performing given activity (Figure 1).

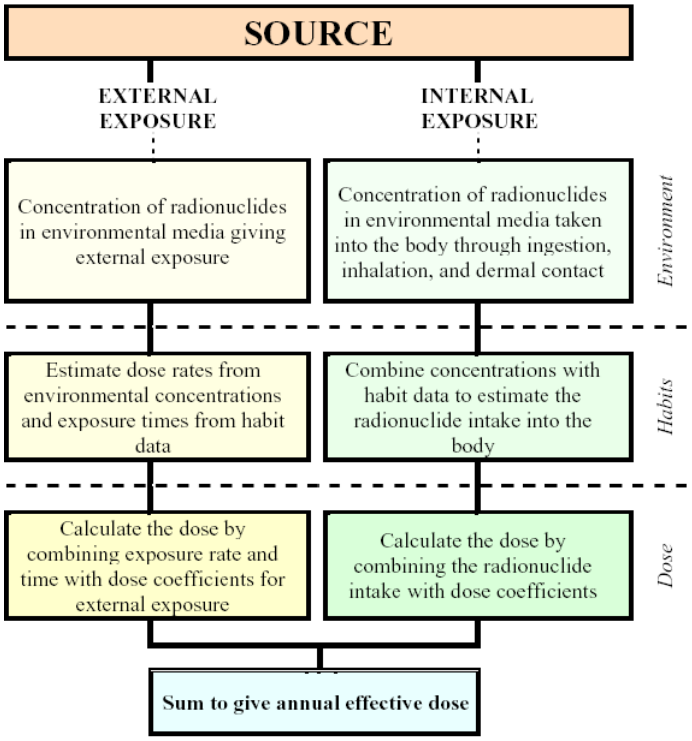

Figure 1 Assessing dose of the representative individual for the purpose of radiation protection for the public (ICRP, 2005).

Radon (^{222}Rn and ^{220}Rn) is major contributor to dose from natural sources and from all radiation sources as well (excluding medical applications) in most of countries around the world. Being a gas, radon can seep from a rock formation into the air, or water and can travel along lengthy paths. The Czech Republic is a country with relatively high natural radioactivity values (the average terrestrial gamma dose rate is 66 nGy/h (Manová, 1995), while the global world average is 55nGy/h (UNSCEAR, 2000)). As a result, there is a

comparatively high probability of a high radon concentration in dwellings and in workplaces. The radon concentration may vary abruptly from building to building, because the underlying geological and tectonic situation is often complex.

Historically, the existence of a high mortality among miners in central Europe was first recognized in the early 16th century. It was not until the 19th century that the cause was identified as a lung cancer and in 1924 it was attributed to radon gas exposure. Radon's role significance was not identified until the 1950's. Since 1970's it was evident that radon represents a health hazard not only for miners, but also for people living in dwellings and working in other underground places as well. From that period the radon problematic became component of human health impact studies. Efforts to lower the radon concentration in dwellings and workplaces have been aimed at decreasing the risk of initiating lung cancer.

Mainly on the basic of the miner studies, the International Agency for Research on Cancer classified radon as a Group 1 human carcinogen in 1988 and is considered by the World Health Organization to be a second cause of lung cancer after smoking (Mc Laughlin, 2012). In 1994, the International Commission on Radiological Protection recommended the adoption of a risk factor equivalent to a lifetime risk of death of 0.0001 for chronic exposure to a radon gas concentration of 1 Bq m^{-3}. On this basis, the estimated risk of contracting fatal lung cancer as a consequence of exposure to 200 Bq m^{-3} is about 2 in 100 (Solomon, 1996).

Despite radon being responsible for about of half of population irradiation, and it may seem that the human being are used to live with radon through the ages, except that in numerous workplaces, including below ground areas, the concentration of radon may reach levels of thousands Bq/m^3 . These concentrations exceed levels that have been established as safe by a range of radiation protection scientists (epidemiologists, radiobiologists and mathematical modelers) on the basis of long-term research, and it is clear that radon poses a wide-reaching potential threat to human health. When taking into account the number of hours spent in the underground, the risk for visitors or recreation cavers is much lower (one order or more) than for workers, who spent in these areas more than 100 hours annually. For this reason, the research was focused on workers with possible application to any member of the population.

It has been proven that natural radionuclides are present in certain types of workplaces, and that they can irradiate the people working in them. Radiation protection for these workers therefore became an important part of the legal framework for radiation protection. The workplace areas most usually affected by radon are underground workshops – non-uranium mines, caves accessible to the public, underground storage areas, underground water

processing facilities, pump stations, spas, and also areas used for speleotherapy. In these locations, workers (including medical personnel in the case of areas used for speleotherapy) can be subjected to a high level of irradiation by radon and its daughter products.

Earlier and current Czech legislation has established a detailed, well-prepared system of rules for protecting workers against irradiation from various sources. The reference levels and the limits for internal and external irradiation are subject to law number 18/1997 Sb., which addresses peaceful uses of nuclear energy and ionizing radiation (the Atomic Law), according to regulation № 307 regarding Radiation protection in accordance with the current regulations of the State Office for Nuclear Safety (SONS) № 499/2005 Sb., superseding regulation № 307/2002 Sb. (see Regulation № 499/2005 Sb. for a comprehensive list of workplaces).

Measurements of the radon activity concentration and the way of determining the effective dose at workplaces affected by radon are specified by the *Methodological procedures for measurements at workplaces where a significant increase in irradiation from natural sources can occur, and for determining the effective dose*, issued by SONS in January 2006 as *SONS Recommendations* (www.sujb.cz).

An action level for Rn of 1000 Bq m^{-3} was proposed. For workplaces with radon levels in excess of this *action level*, the preferred option is to modify the workplace conditions in order to reduce the radon levels to below 1000 Bq m^{-3}. If this reduction is not possible, then it may be necessary to implement radiation monitoring programs to ensure compliance with regulatory radiation limits.

The effective dose from radon and its short-lived daughters for workers was calculated on the basis of the ICRP65 Recommendations (ICRP, 1993) and could be expressed by equation 1

$$E = h_p . c_{V,Rn} . T \qquad \textbf{Equation 1}$$

where E is annual effective dose (usually in mSv)

h_p is dose conversion factor based on results from the epidemiological studies and is equal 3.1 nSv/(Bq.h.m^{-3}) for workers and 2.4 nSv/(Bq.h.m^{-3}) for members from public

T time spent in the area with activity radon concentration $c_{V,Rn}$ (h)

$c_{V,Rn}$ radon activity concentration (Bq.m^{-3}), which is recalculate from equivalent radon concentration using equilibrium factor F, which is for dwellings equal 0.4, based on AMAD = 1 and 250 nm, free fraction 6,5% and medium humidity

When the radon concentration decreases about 100 Bq.m^{-3}, the annual effective dose at work or at home decrease about 0,6 or 1.7 mSv.

A conservative methodology for estimation of a potential dose in caves employs solid state alpha track detectors. The integral radon concentration measurement data is converted into annual effective doses, using the equation № 1, and using an additional "cave factor j" for underground workplaces. This factor which was based on calculation with AMAD 1 a 250nm, 13.6% of unattached fraction obtained as average estimation from 3 grab sampling measurements in caves, 6.5 % of unattached fraction for dwellings, expresses the differences between dwellings and for caves environment and was equal 1.5 (Thomas, 1999), (Thomas, 1999a).

Out of the thirteen caves in the Czech Republic that were open to the public in 2006 (some of these caves were also used for speleotherapy), about one half of them (e.g. the Bozkov Dolomite Caves) had action level effective doses that might exceed 6mSv.

This thesis presents measurement results gathered over the past 10 years, and the core of the research is defined by the VaV SUJB 2006 project "Enhancement of personal dosimetry for workers in publicly accessible caves and in caves used for speleotherapy, with a view to including other underground workplaces". Some measurement results presented here are not required for the dose calculation; however they provide interesting information about the cave environment, which could influence variability of the measured values and have to be considered within errors estimation process.

Individual parts of the equation №1 are verified by following the gradual process which leads to assessment of health impact of the underground environment. The research concept description for this multidisciplinary topic starts in chapter 3, where the methodology is discussed. In this chapter are outlined all the steps necessary to describe the investigated environment through various measurements aimed to obtain the necessary data pertinent to the objective of the research. This is followed in chapter 4 by presenting a summary of the present state of research in the area of sources of irradiation and their evaluation in the process of effective dose calculation. The chapter 4 also contains the description of the investigated environment supported by examples of dependencies which were noted in the process of the underground areas measurement. A dedicated part of this chapter focuses on aerosol in the environment characterization, because dose conversion factor is based on a proportion of free and attached fractions of radon daughters.

Chapter 5 is an important section of the thesis, covering all the measurements performed. Firstly there is listing of all the measuring equipment and software used, including its specifications and characteristic. Some parameters investigated in the underground were analyzed more thoroughly such as integral and continual radon concentration, or laboratory measurement of radionuclides present in the rock samples, due to the greater importance of these parameters to health impact. Other parameters with lesser importance were not evaluated in a great detail, partly due to the lack of specialized equipment (long term unattached fraction of radon daughters measurement, thoron measurement etc.) or due to shorter time allotment (long term continual air flow measurement etc.). One parameter concerning proportion of the free fraction from aerosol measurement had to be estimated (using a standard published value) due to large inherent equipment error in the area of the smallest aerosol particles. Individual measurements are described sequentially, while the results are summarized and commented in detail within the chapter 6. The above results were used for actualization of the methodology for radon measurement in the underground. In conclusion of the chapter 6, there is described the detailed calculation process for determination of the individual cave factor for the *Bozkov Dolomite* Cave. That refined calculation process was also used for determining the cave factors for all other caves and some underground areas as detailed in the chapter 7. Conclusions in chapter 8 summarize and discus all results of the above described research processes. Using these results the assessment of the health impact of the irradiation sources in the underground was made more precise. The more precisely determined value of cave factor would have significant impact on the time the guides or cavers may spend in the underground.

Very important component in the establishment of a radiation dose concerns the errors in the entire process. These errors are elaborated and discussed in the Appendix 1. The established relative errors are integrated in the practical outcome of the thesis, which is the new version of the methodology for the dose calculation in the underground areas (Appendix 2).

Some differences in results have occurred between the data from laboratory gamma spectrometry measurement of rock samples in comparison with the in situ gamma spectrometry measurement (Zimák, 2004b). A simple model using MCNPX method was developed with focus to explain these differences, which may be caused by high concentration of radon daughter ^{214}Bi in the underground atmosphere. The results are attached in Appendix 3 and they could form very useful base for the follow on research.

All measurements were conducted within the available time frame, with the level of complexity required for solving the main task – to evaluate the impact on human health of exposure to irradiation in specific underground environments. Presented results were selected to point out some of the possible circumstances and to prove that, in order to uncover the applicable dependences, it is necessary to monitor the selected parameters consistently and continuously over a period of several years.
By 2010, the focus had turned to aerosol measurements, and to determining the unattached and attached fraction (ICRP, 2010). This is a major shift, and the new focus now requires high-quality the measuring equipment.

The volume of the intended research was such that it required support from several organizations listed below, according to the year of their involvement. The results obtained by specific organization are referenced throughout the thesis:

CA CR	2002-2012
NRPI	2002, 2006-2007
NRCBPI	2006-2007
ICPF	2002

In the course of the research of radioactivity health impact in caves, the following students´ theses were prepared under the supervision of this thesis author: (Brandejsová, 2004), (Rovenská, 2007). Some results from the above theses were listed in text with appropriate references.

Please note:

- When no other definition is listed, the isotope is ^{222}Rn throughout the text.
- Radon activity concentration is expressed using $c_{V,Rn}$ (Bq/m^3) which means that the contribution of thoron is not considered.

The chapters in this paper are based on results that we have obtained, some of which have already been published. References are quoted in text. The following papers have been published and presented as an outcome of research and studies carried out in connection with the aims of this thesis:

Published papers, with impact factor:

Thinova L., Burian I. (2008): Effective Dose Assessment for Workers in Caves in the Czech Republic: Experiments with Passive Radon Detectors. Radiation Protection Dosimetry. vol. 130, no. 1, p. 48-51. (ISSN 0144-8420) (IF = 0,528)

Rovenska K., Thinova L., Zdimal V. (2008): Assessment of the Dose from Radon and its Decay Products in the Bozkov Dolomite Cave. Radiation Protection Dosimetry. vol. 130, no. 1, p. 34-37. (ISSN 0144-8420) (IF = 0,528)

Thinova L., Rovenska K., Otahal P. (2010): Environmental and radon measurements in the underground workplaces in Czech Republic. Nucleonika Journal. Vol 55, no.4, p. 491-494. ISSN 0029-5922 (IF=0,321)

Rovenska K., Thinova L. (2010): Seasonal variation of radon in the Bozkov cave. Nucleonika Journal. Vol 55, no.4, p. 483-490. ISSN 0029-5922 (IF=0,321)

Thinova L., Rovenska K. (2011): Radon dose calculation methodology for underground workers in the Czech Republic. Radiation Protection Dosimetry. vol. 145, no. 2-3, p. 1233-237. (ISSN 0144-8420) (IF = 0,966).

Briestensky M., Thinova L., Stemberk J., Rowberry M. D. (2011): The use of caves as observatories for recent geodynamic activity and radon gas concentrations in the Western Carpathians and the Bohemian Massif. Radiation Protection Dosimetry. vol. 145, no. 2-3, p. 166-172. (ISSN 0144-8420) (IF = 0,966).

Reviewed papers:

Thinova L., Rovenska K. (2008): Radon Dose Determination for Cave Guides in the Czech Republic. In The Natural Radiation Environment. Melville, New York: American Institute of Physics, vol. 1, p. 141-144. (ISBN 978-0-7354-0559-2)

Methodology:

Ženatá I., Thinová L., Rovenská K.(2009): Novelizace-Metodický návod pro měření na pracovištích, kde může dojít k významnému zvýšení ozáření z přírodních zdrojů, a určení efektivní dávky. SÚJB 2009. (metodika)

Invited lecture:

7th HLNRRA 24-26 November 2010, Mumbai, India.

Thinova L., Rovenska K. (2010): Radioactivity of underground workplaces and a discussion about the accuracy of dose estimates (oral presentation)

International conferences (2006 – 2010):

Radon Investigation in the Czech Republic XI and the 8th International Workshop on the Geological Aspects of Radon Risk Mapping, 10-15 September, Prague, Czech Republic

Thinova L., Cechak T., Moucka L., Fronka A. (2006) The Determination of an Effective Dose for Workers in Caves (oral presentation)

5th International Conference on Protection against Radon at Home and at Work, 9-15 September 2007, Prague, Czech Republic

Thinova L., Burian I. (2007) Effective Dose Assessment for Workers in Caves in the CR: Experiments with Passive Radon Detectors (oral presentation)

Rovenska K., Thinova L., Zdimal V. (2007) Assessment of the Dose from Radon and its Decay Products in the Bozkov Dolomite Cave (oral presentation)

Peano R.G., Peano G., Villavecchia E., Thinova, L., Fronka, A. (2007) Atmospheric Radon in Bossea Cave: Results of Collaborative Measurements in Bossea Cave (CTU Prague - Stazione Scientifica di Bossea) (poster presentation)

Thinova L., Bula V. (2007) Microdosimetric Approach to Dose Calculation from Radon Progeny (poster presentation)

8th NRE Symposium, 10-15 October 2007, Rio de Janeiro, Brasil

Thinova L., Jilek K., Rovenska, K. (2007) Radon Dose Determination for Cave Guides in the Czech Republic (oral presentation)

RADON in ENVIRONMENT 2009, 10-14 May 2009, Zakopane, Poland

Thinova L., Rovenska K., Otahal P. (2009) Environmental and radon measurements in the underground workplaces in the Czech Republic (oral presentation)

6th International Conference on Protection against Radon at Home and at Work, 13-17 September 2010, Prague, Czech Republic

Thinova L., Fronka A., Rovenska K. (2010): A pilot study of the dependence of radon concentration on tectonic structures, using simple geophysical methods (oral)

Thinova L., Rovenska K. (2010): Radon dose calculation methodology for underground workers in the Czech Republic (poster presentation)

Briestensky M., Thinova L., Stemberk J., Rowberry M.D. (2010): The use of caves as observatories for recent geodynamic activity and radon gas concentrations in the Western Carpathians and the Bohemian Massif (poster presentation)

2. Thesis objectives

This thesis attempts to classify the exposure, to irradiation from natural ionizing radiation sources, of workers in Czech show caves and in caves used for speleotherapy, with further applicability to other underground workplaces. The title of thesis "Radioactivity of the rock and the environment in selected underground areas, and its impact on human health" indicates an interdisciplinary study aimed at comprehensively resolving this complex issue.

The caves and other underground spaces are characterized in contrast to dwellings by the following characteristic: the absence of aerosol sources (the aerosol concentration in caves is approx. 100 times lower than in the outdoor atmosphere); high humidity; a low ventilation rate and the uneven surfaces. A health impact assessment has to be based on good knowledge about sources of irradiation in the investigated underground areas. It is not possible to predict any potential irradiation problem in the given underground area from general geological information. The sources of radioactivity (terrestrial radionuclides) must be inspected with regard to their origin, behaviour, propagation and variability. All newly obtained results were used for meeting the specific research aims in the area of health impact. The goal was to verify present approaches to dose calculation based on the recommendations of international organizations (IRCP, UNSCEAR, WHO). A comparison was also made with the procedures used in other countries, together with a critical evaluation of the methodology used in the Czech Republic (SÚJB, 2006). Presently available equipment and theoretical knowledge about the impact of radon on human health were utilized in order to meet the objectives stated here.

After all available underground areas had been examined (Bílková, et al., 2002), show caves were selected as representative research sites, because they offered the most suitable combination of relevant factors (a complex geological environment, presence of workers, ability to monitor the time spent underground by employees, availability of historical monitoring data, etc.). The results of presented research were subsequently applied to other underground workplaces.

The success of the research was aided by the support provided by the Czech Cave Administration, and by the openness of the Administration's staff.

3. Thesis methodology

The working arrangements enabled continuous monitoring and long-term observation of selected cave and underground area parameters. To meet the research objective, it was necessary to divide the research into several phases that overlapped in time, because obtaining certain working conclusions influenced the research steps within the other phases of the research. The research strategy focused on obtaining as many data sets as possible in 2006 – 2007, when the research was receiving financial support under project VaV 12/2006.

The starting point was based on previous experience of comparable measurements, which were carried out in the *Koněprusy* Caves (from 2001 to 2003) and in the *Bozkov Dolomite* Caves, after 2002. The Head of the *Bozkov Dolomite* Caves expressed the opinion that our mutual collaboration was very positive, and this turned out to be a crucial factor for the follow up measurements.

Many underground areas (where workers and guides spent more than 100 hours per year) were made available for monitoring. Because the optimum period of time for monitoring cave parameters that have an impact on human health is a year or longer, two caves of different origin (the *Bozkov Dolomite* Caves and the *Zbrašov Aragonite* Caves) were chosen for complex long-term experiments. In other areas, including the remaining show caves, speleotherapy facilities, wine cellars, underground mine museums, underground fortresses, etc., only measurements of short-term radioactivity and environmental conditions were carried out (usually around three days in duration).

The methodology was based on parallel related research tasks, which required good cooperation and coordination among the ongoing investigations. Two main methodology components had to be realized – acquisition of new theoretical knowledge, followed by carrying out measurements and processing the results from the measurements. The measurements were limited by the quality and the number of available devices (chapter 5.1). An extensive study of this kind would have been impossible to carry out without the given by the Radon expert group from the National Radiation Protection Institute (NRPI) in Prague. The collaboration with the National Radiation, Chemical and Biological Protection Institute (NRCBPI) in Kamenná-Milín in the field of radon exhalation rate and thoron concentration measurements was crucial. The help provided by students of the Faculty of Nuclear Sciences and Physical Engineering (FNSPE) of the Czech Technical University in Prague was also very much appreciated. The time necessary for verifying the calibration of the devices and for

checking the results, based on repeated measurements, also had to be incorporated into the research time schedule.

The methodology for the project gained further support through the author's work in organizing an international radon conference and workshop, which was arranged as a component of the *5th International Conference on Protection against Radon at Home and at Work,* held in Prague in September 2007. The main theme of the conference was "Radon dose calculation", and the aim of the workshop was to discuss the variability of the environmental conditions in caves, including the pros and cons of various approaches to radon dose calculation. The workshop took place in the *Bozkov Dolomite* Caves, and was supported by the Czech Caves Administration.

The selected research approach

After a thorough evaluation (see chapter 4) the following research approach was selected: the methodology for determining the impact on human health of radioactivity in underground spaces was based on the source of irradiation analysis, and on verifying the dose calculation. This meant that each dose calculation component had to be verified. An important component of the calculation must be a more precise determination of the *cave factor* "j" (see chapter 1). For a more accurate calculation of the radon dose, it was necessary to carry out long-term and short-term measurements, and to verify the cave factor for the dose calculations, including an estimation of the errors involved. An available set of previous measurements of aerosol spectra in the *Bozkov Dolomite* Cave was used.

The first phase of the research was an evaluation process, which utilized the results of previous research efforts. This included the results of the author's own previous measurements in caves (a 5-day aerosol particle-size spectrum campaign to determine the free fraction and to compare the aerosol spectra in an apartment and in a cave, and also long-term continuous radon monitoring - both campaigns in cooperation with the *Bozkov Dolomite* Caves). In addition, a literature search was carried out in Czech and international publications. In the early stages of the project, it was beneficial to obtain more information about the current status of calculations of the dose from radon in underground areas used in other European countries (see chapter 4).

The focus of this phase was on defining the sources of irradiation within the cave environment (and in the areas used for speleotherapy), considering their potential health effect, including

the variable dependence of external and internal influences. The caves are very special workplaces from the radiation protection point of view, due to the stability of their protected environment, which is maintained in order to enable the geological processes to continue. The summation and a critical evaluation of approaches to the evaluation of lung irradiation were important considerations in this phase of our study.

The second phase of the research lasted more than two years. The results from this phase built on the theoretical foundations established within the first phase. All of the measurements had as an objective to verify, and where possible improve, the existing methodology for measuring radon in underground spaces (SÚJB, 2006). The research measurements were carried out in all available caves, and were based on the initial results. Two caves (the *Bozkov Dolomite* Caves and the *Zbrašov Aragonite* Caves) were selected for advanced long-term measurements. Each of these caves offered a very interesting environment, and in addition their managements were very willing to provide the necessary support for all required activities. The second phase focused on the following field activities:

- Evaluate the natural radioactive element content present in the sedimentary rocks and in the cave subsoil, using a laboratory gamma spectrometry method on the collected samples.
- Make in situ measurements of the radon concentration in water samples collected inside and outside the caves.
- Make continuous radon concentration measurements using RADIM3 devices in a special box with a desiccant.
- Make regular measurements of radon and radon daughters, using a grab sampling procedure to specify the proportion of radon daughters and the equilibrium factor.
- Make regular indoor air flow measurements to study the locations of the radon supply and the transfer of the air pockets among the areas within the cave.
- Make comparative measurements, monitoring radon and various radon daughters to study the measurement capability in areas with relative humidity near 100% (including FRITRA4, a device for simultaneous detection of radon concentration and the concentration of unattached and attached fractions of radon daughters).
- Monitor the behaviour of guides and visitors (or speleotherapy nurses) by recording the time spent by them in the cave, in relation to the continuously monitored levels of

radon concentration, in order to determine differences in radon concentration between working hours and rest of the 24-hour period.

- Test the ability of certain types of dosimeters to detect radon and its daughters, for purposes of personal dosimetry.
- Make comparisons between the RAMARN detectors and the SSNTDs that were used for integral radon measurements, in a high humidity environment, focusing on the optimum location for integral radon measurements in the areas of interest, including international comparisons.
- Verify a random set of data (repeated measurements under different conditions, or a comparison of different monitoring devices).
- Extend the measurement locations to other underground areas, e.g. tunnels, old mines, wine cellars, and underground fortresses.
- Utilize previously obtained measurements and results of surveys carried out in unusual spaces.

The third phase was characterized by an analysis of approaches toward the establishment of a more precise definition, and by defining correct procedures for determining the effective dose for workers in caves. This was based on the results of integral measurements of radon concentration activity, and on the time spent by workers in the caves, using a study of various approaches to the evaluation of lung irradiation. Each approach was critically appraised. In the Czech Republic, the calculations for the radon dose were based on the equation № 1 (according to ICRP 65 Recommendation) using an additional "cave factor j" for underground workplaces:

$$\mathbf{E\ (mSv) = j.h_{p}.T.c_{V,Rn}} \qquad \textbf{Equation 2}$$

where **j** was the "cave factor" and the value was calculated to be 1.5, according to research carried out by Dr. J. Thomas (Thomas, 1999) for all underground areas (more information about cave factor in (Thinová, 2007)). The main issue that had to be resolved was whether the general cave factor value is indeed applicable to all underground areas. Part of the analysis included seminars and discussions with radon experts interested in increasing the precision of cave monitoring.

The fourth phase was implemented by concentrating all data obtained and entered into the calculation process, using the LUDEP dose-in-lungs model. The effective dose was recalculated fairly precisely using the method described in chapter 6.5 and chapter 7. Our results indicated that the caves show great environmental differences that need to be addressed by an *individual cave factor*. An essential component of the methodology was the integration of the relative errors, which have a major impact on the calculated output values.

The **final phase** was important for the practical application of our conclusions. A new measurement methodology was prepared in collaboration with the State Organization for Nuclear Safety (SONS), and it was put into operational use (Ženatá, et al., 2009). The new methodology has had a significant impact on obligatory cave monitoring.

As was mentioned above, the research activities were divided into three groups: long-term and short-term activities, and calculation processes.

Long-term research activities (lasting more than one year) were carried out in the *Bozkov Dolomite* caves and in the *Zbrašov Aragonite* Caves, as follows:

1. Study sources of irradiation, their behavior and variability.
2. Observe the behavior of guides and other workers in the underground spaces, in connection with the local, daily and seasonal variations in radon concentration.
3. Verify the integral radon measurements, based on the RAMARN detection system by continuous monitoring. Note the differences between the level of radon concentration assessed during working hours and in non-working hours.
4. Verify the RAMARN detection measurement system in spaces with almost 100% humidity.
5. Compare the old SSNTD measurement system with the RAMARN system.
6. Make continuous radon concentration measurements.
7. Study the seasonal radon variation to determine the best time interval for integral radon measurements, taking into account the opening hours for visitors to the cave.
8. Make air flow measurements. Perform regular indoor air flow measurements to study the radon supply and to understand the transfer of air pockets between individual areas in the cave, in order to determine the best location for integral measurements using RAMARN detectors.

Repeated **short-term research activities** were carried out in all the studied underground spaces, as follows:

1. Make regular measurements of radon and its daughters to estimate the equilibrium factor F and its variability.
2. Measure the thoron concentration.
3. Measure the radon concentration in samples of cave waters.
4. Measure the exhalation rate (clastic sediments and karst rock).
5. Make continuous measurements of unattached and attached fractions.
6. Carry out laboratory gamma spectrometry measurements of cave rock and clastic sediments samples, including subsoil material.
7. Measure the dose rate and the radon concentration profile along the route followed by visitors to the cave.
8. Make an assessment to compare the usability of personal dosimeters with the use of integral measurements.

The process of **verifying the cave factor** and **calculating the dose from radon** was carried out as follows:

1. Determine the ratio of the unattached fraction in each cave.
2. Determine the relationship between the equilibrium factor F and the unattached fraction f_p.
3. Calculate the individual cave factor “j”.
4. Work out the total error in the dose estimate from a radon calculation based on an assessment of the partial errors.
5. Test the proposals in practical applications, and finalize the recommendations.

4. Present state of the research

4.1 Determining the underground dose

Overview of approaches to estimating the radon dose to the lungs

The health impact of irradiation in underground spaces is mainly due to inhalation of radon and its progeny. The impact of cosmic radiation is negligible, as it is eliminated by the shielding effect of the rock massif. The external irradiation (caused by gamma radiation, which is released during radionuclide decay in rocks) should be on an average the same as on the Earth's surface. The typical mass concentration of radionuclides present in the rock (most of the Czech show caves were formed in limestone, with only a minority formed in dolomite or in some other type of rock) is usually lower than the average rock values, while the contribution of airborne ^{214}Bi depends on the radon activity concentration (see chapter 6.10 and Appendix 3). For these reasons, the research reviewed here deals mainly with the dose from radon.

The typical range of the effective individual dose varies from 0.2 to 10 mSv (UNSCEAR, 2000), but there are locations where the doses reach tens of mSv and more. The effective dose from radon and its progeny to the lung epithelium cannot be measured in vitro. Several approaches to evaluating the irradiation of human lungs have been investigated. Research efforts have systematically improved the dose conversion factor value, which represents the effect of unit exposure of lung epithelium to radon.

The approach to an effective dose calculation from the radon evolution history is described for example in Böhm (2003); ICRP, (2010); Vaillant (2012); McLaughlin (2012); Harley (2012), etc. The European pooling study re-analyzed data from 13 European case-control studies (Mc Laughlin, 2012). Smoking histories and 15-year or higher occupation, in an average concentration of radon, or in an actual concentration, were considered. The inter-year variability was also taken into account. This approach yielded an excess relative risk of 16% (95% CI: 5-31%) per 100Bq/m^3 increase in the long term average radon concentration. To put the excess relative risk of 16% per 100Bq/m^3 in context: the estimated risks at 0.00, 100 and 400 Bq/m^3 relative to lifelong non-smokers with no radon exposure are 1; 1.2; 1.6. For those continuing to smoke 15-25 cigarettes per day the estimated risks are 25.8, 29.9 and 42.3. In a joint analysis of 11 cohort studies of a total of 60,000 miners all over the world, the average excess relative risk (ERR) per WLM was estimated to be 0.44% (95 CI: 0.20-1.00%). Miners exposed to low radon progeny concentrations were found to have a higher ERR/WLM than

those exposed to higher concentrations. Residential studies in the period up to 2008 reported a positive association between childhood leukemia and radon.

A brief overview of the basic approaches (empiric, dosimetric and biological) is listed below.

All approaches deal with the following group data:

a. Epidemiological data on cohorts of miners (average and large exposures) and studies on animals (with studies of the different structure and radio-sensitivity of the respiratory tract).

b. Data from residential epidemiological studies.

c. Data analysis based on the effects of irradiation on survivors of the A-Bomb explosion in Hiroshima over a period of 45 years provided an opportunity to observe several groups of people according to gender and age categories, but only in the area of radiation with low LET.

1. Empirical approach (used in Czech legislation)

- Derives the dose conversion factor from epidemiological studies using the ratio of the risk of lung cancer in miners to the overall risk of cancer in the atomic bomb survivors (Vaillant, et al., 2012).

- Assesses the radon risk from the health effects directly observed in group a) and, more recently, in group b), in comparison with the effects observed in a non-exposed population.

2. Dosimetric approach (modeling the behaviour of aerosol particles in the lung; deals with group data source c))

- Uses the quality factor and calculates doses for individual tissues on the basis of mathematical models. The compartmental HRTModel is used for the bronchial dose (ICRP66) (Böhm, 2003), (Rovenská, 2007), (Harley, et al., 2012).

- Uses dosimetric models of the human respiratory tract to estimate the equivalent dose to the lung and the effective dose per unit radon exposure*.

**Note*: The main sources of variability and uncertainty in calculating the equivalent dose to lungs per unit exposure to radon progeny include: the activity size distribution of the radon progeny aerosol; the breathing rate; the model used to predict aerosol deposition in the respiratory tract; the absorption of the radon progeny from lungs to blood; the identification of target cells and their location within the bronchial and bronchiolar epithelium; the relative sensitivity of the different cell types to radiation; regional differences in the radiation sensitivity of the lung (ICRP115, 2010). An example of differences between the calculation results using several dosimetric models is expressed in table B.1 in Recommendation ICRP115. Published values of the effective dose

(mSv/WLM) to an adult male from the inhalation of radon and its progeny vary between 5.7 (indoors and outdoors, UNSCEAR 2000) and 21 (HRTM, (James, et al., 2004).

- Uses a tissue weighting factor for lung equal to 0.12 (the same in all ICRP Recommendations) and a radiation weighting factor for the alpha particle equal to 20. The ratio between the dose coefficients, based on the dosimetric model, which are based on the survivors' data, in comparison with the epidemiological approach dose coefficients, is equal 2-3.[1]

3. **Biological and micro-dosimetric approach (focusing more on tissue details)** (Böhm, 2003)

- Tries to define the relationship between energy deposition and subsequent processes (transformation, aberration, mutation).

- Creates biological models based on group data a). The last BEIRVI model analyses epidemiological cohort studies from eleven mines in different parts of the world. The BEIRVI model confirms linear dependence between exposure and the relative risk up to cumulative exposure values of 200 WLM. For higher exposures, the dependence is concave.
- Calculates the relative risk for different age groups, where the risk decreases with age (0.5-3% for each 100 WLM).
- Considers that non-irradiated cells exhibit irradiated effects as a result of signals received from nearby irradiated cells (bystander effect).
- Estimates that the total risk for the public is 10 times lower than for miners. Homogeneous distribution of the target nuclei depth dose underestimates the real radiation risk, particularly in deeper locations (Böhm, et al., 2002).

[1] A major change occurred recently with ICRP Publication 103 (2007), in which it is now recommended that any radon exposure should be reduced according to the ALARA principle below the reference level. Previous recommendations only focused on exposures above the action level. ICRP classified indoor radon in dwellings and workplaces as existing exposure radiation. ICRP103 retains the upper value of 10 mSv for the individual dose reference level. Reference levels in terms of activity concentrations of radon derived from this effective dose are 600 Bqm^{-3} for dwellings and 1500 Bqm^{-3} for workplaces. A lifetime lung cancer risk is recommended to be 5.10^{-4}/WLM. ICRP has moved to a dosimetric approach, and proposes that the same approach be applied to the intake of radon and progeny as for other radionuclides, using a reference biokinetics and dosimetric model (Vaillant, et al., 2012).

4.1.1 Dose from radon calculation in the Czech Republic

Recommendation ICRP65 adopted the epidemiological approach and used miners data (from seven cohorts), because it involved less uncertainty than indirect use of the epidemiology of low linear energy transfer radiation from the data for the survivors of the A-Bomb. The lifetime lung cancer risk was estimated at 2.8.10-4/WLM for workers and at DCF 5 (4) mSv/WML for the public. Action level was defined as "the concentration of radon at which intervention is recommended to reduce the exposure in dwellings and workplaces". The action level was derived as not exceeding the annual effective dose of 3-10 mSv. The corresponding radon concentration value in workplaces is about 500-1500 Bq/m^3 (assuming annual occupancy of 2000h and F = 0.4).

The Czech legislation adopted a general limit on the effective dose of 20 mSv per year, averaged over 5 years (100mSv in 5 years) for workers, and a limit of 1 mSv per year for members of the public. The effective dose from radon calculation is based on Recommendation ICRP65 (1993) (although new Recommendations ICRP103 and ICRP115 have been published).

In the Czech Republic, the reference level for the effective dose caused by inhalation of radon and its radon daughter products of 6mSv must not be exceeded. Based on the estimate of an annual 2000-hour exposure (i.e. typical annual working hours) in an area with the average $c_{V,Rn}$ value of 1000 Bq/m^3 (time integral = 2 MBq•h/m^3), the effective dose is determined, based on time of stay T, using the equation:

$$\boldsymbol{E = \frac{c_{V,Rn}.T}{2MBq.h/m^3}.6mSv} \qquad \textbf{Equation 3}$$

where:

E annual effective dose in mSv,

$c_{V,Rn}$ measured average radon activity concentration (Bq/m^3),

T duration of worker's presence in hours

Note: This is applicable given that F~0,4.

The measurement duration of $c_{V,Rn}$ should typically be half a year or one year. In the case of dwellings during the winter season, the measurement time may be shorter (two months).

Because caves and dwellings differ in types of aerosol spectra (AMAD), particle concentration (the particle concentration in caves is 100 times lower than in dwellings – see chapter 4.1.5; 6.5) (Thinova, 2005), the amount of unattached fraction, humidity, temperature and ventilation coefficient, the "cave factor" j = 1.5 was established for calculating the dose

from radon in caves in the Czech Republic (Thomas, 1999), (Thomas, 1999a). Equation № 1 $E = h_p . c_{V,Rn} T$ for effective dose calculation was modified to equation № 2: $E = h_p . \mathbf{j} . c_{V,Rn} T$. This calculation was based on AMAD 1 and 250nm, 13.6% of the unattached fraction obtained as an average estimation from three grab sampling measurements in caves, and took into account 6.5% of unattached fraction for dwellings (Marsh, et al., 1998), (Nazaroff, et al., 1988). The high radon concentration in some Czech caves (reaching 30 kBq/m^3) can lead to the reference limit of 6 mSv per year being exceeded. The question was whether the same cave factor is applicable to all underground spaces.

The measured radon concentration value that is used in the calculation depends on equilibrium factor F, which is one of most important components of dose calculation. Factor F describes the equilibrium between the radon concentration and the concentration of associated radon daughters in the air. Factor F is expressed using the ratio between the total alpha particle energy that the particular mixture of radon and its progeny will emit and the total energy emitted by the same concentration of radon gas, in perfect equilibrium with its radon daughters. For most environments, this ratio is considered to be constant, and usually F = 0.4 - 0.5 is used for the indoor radon activity concentration from radon daughter measurements and calculations. However, in some underground environments the value of F varies between 0.1 – 0.9, depending on the ventilation rate, sources of aerosol nuclei and the aerosol particle size spectrum (Cigna, 2005) etc.

SSNT detectors were used in former Czechoslovakia and then in the Czech Republic (after 1992) for almost two decades between 1985 and 2003 for integral radon concentration measurements, which were (and still are) used in the Czech Republic for calculations of the dose from radon in dwellings and under the ground. The exposure period was one year. This system never in fact received a type approval, because the response was dependent on the equilibrium factor (F) and on the occurrence of thoron. However, this approach was certainly adequate to provide a rough identification of locations with concentrations exceeding the investigation level. Since 2003, the new RAMARN system has been certified.

One part of research (chapter 6.1) has focused on a comparison between the old and new systems of measurement and on methods used in research laboratories elsewhere (Thinová, et al., 2006), (Thinova, et al., 2008), (Thinova, et al., 2008a).

The approach to calculating the dose from radon for underground workers is practically the same throughout Europe. These calculations are fully the responsibility of each country; however it is useful be aware of different approaches to dose calculation. It emerged from correspondence with responsible experts in various countries in 2006, that Recommendation

ICRP65 (expressed by the equation № 1: $E = 3.1*c_{V,Rn}*T$) is the approach mostly widely used around the world. Track-etch-detectors (based on the CR 39 detector) and different lengths of measuring time intervals were also used, but in practice nobody took into account the difference between the ratios of the unattached and attached fractions in dwellings, or of the very special conditions in caves. The calculation is often based on the short-term interval of integral $c_{V,Rn}$ measurements (with various types of corrections) or grab sampling. The following examples of particularly interesting information were selected (Thinová, et al., 2006):

In *Germany*, the dose conversion factor 3.1 mSv/MBq.h.m^{-3} (1.4 mSv/mJ.h.m^{-3}) was used, and F should fit the interval 0.2 - 0.7. When F was lower or higher, a PAEC (Potential Alpha Energy Concentration) measurement was required. Track-etch-detectors are mostly used.

In *Sweden*, the SSNTD was used (Solid State Nuclear Track Detector, based on CR39 detecting material), and the researchers usually took into account radon concentration rather than doses. They tried to explain to members of the public that smokers are more exposed to radon hazards than non-smokers (based on results in (Darby, et al., 2005)).

In *Estonia*, no measurements of radon in caves were conducted. The dose from radon was calculated on the basis of ICRP 65.

In *Norway*, the concentration of thoron, due to the high concentration of thorium, was taken into account. The measurement time interval implemented there was usually two periods of two months in the winter season. The values are corrected to an annual average concentration. SSNTDs were used for the measurements.

The most elaborate approach was used in *Slovenia*. PAEC was measured, rather than $c_{V,Rn}$, and an appropriate conversion factor was used (1.4 mSv/mJ.h.m^{-3}). For breathing rate 1.2 m^3/h and 2000 working hours, the calculation was equivalent to the Czech calculation. Sometimes, under special conditions, a different conversion factor was used. A factor of 2 was used (according to ICRP 32 Recommendation) for underground workplaces, which was similar to the Czech approach.

In *Italy*, a nomogram is used to assess the time that it is permissible to spend under the ground. The nomogram is a graphic expression of the equation $T=106* D/(7.784*F*C)$, where D is the dose constraint and C is the average concentration of radon (Cigna, 2005).

Studies of caves cover a long-term complex of activities and measurements. A large number of measurements have been made in cave environments. Scientists have studied the level and the variability of radon concentrations, the equivalent equilibrium radon concentration and the equilibrium factor. Interesting studies have correlated various parameters that influence the

radon concentration. Recent studies have yielded noteworthy results on the unattached and attached fraction ratio and on the aerosol particle size distribution for the purposes of dose (dose conversion factors) calculation. In a recent past, starting from the seventies, there were many excellent measurements conducted, and most of those results are forming reliable base for the continuation of the research today. The following conclusions were drawn on the basis of a simple indoor model (Porstendörfer, et al., 1978). The ratio of the concentration of radon and the free and attached decay products is greatly influenced by ventilation, exhalation and wall deposition of the free radioactive atoms. The radioactive aerosol itself deposits by sedimentation and diffusion, so there is no radioactive equilibrium between the emanations and their decay products. The attachment rate of the particles depends on the attachment coefficient and on the aerosol concentration. The recoil factor for the β-decays is negligible. The difference between the ^{214}Pb and ^{214}Bi (^{214}Po) concentrations is very small, and can be set as equal. The calculated deposition velocity for the attached and unattached fractions was compared with earlier studies, and the differences among the results for the models was very high (20-30x or more), (Knutson, et al., 1983), 1983), (Scott, 1983), (Toohey, et al., 1984).

Measurements of radon and its short-lived daughters in the air in tunnels were carried out by Shimo (Shimo, et al., 1984). The equilibrium equivalent unattached fraction (EEUF) was measured in air for various outdoor and indoor circumstances. The EEUF values varied according to the amount of pollutant in the air. An inverse correlation between EEUF and #/cm^3 was demonstrated. In a tunnel, the mean value of the unattached fraction of the potential alpha energy f_p was 0.12 (0.9-0.14). It was found that the total ^{218}Po concentration correlated well with the equilibrium equivalent ^{218}Po concentration obtained assuming radioactive equilibrium between daughters. The equilibrium equivalent unattached fraction can therefore be used instead of the unattached fraction.

In 1985, Raes (Raes, 1985) described two distinct physical forms of the radon progeny: the attached fraction and the unattached fraction, which is still in a form of ions, molecules or perhaps small clusters. Several experimental investigations on the properties of the unattached fraction studied the size resolution, the creation and growth of aerosols, and their diffusion coefficient. No consistent results were reported for the effect of relative humidity on the diffusion coefficient, although the theory predicts a decrease in the diffusion coefficient for higher relative humidity. Raes found that this mode that was very mobile, in contrast to the accumulation mode, and that its median value could be found between 1-10 nm.

The unattached fraction in the indoor environment was found to have a value between 5-15% without aerosol sources in the room. As a result of smoking, cooking, etc. the unattached

fraction can decrease below 5% (Vanmarcke, et al., 1989). Vanmarcke's analysis shows that the dose in the indoor environment is relatively independent of the equilibrium factor, meaning that it is better to use a conversion factor based on ^{222}Rn concentration rather than a conversion factor based on the EER. An average concentration of 20Bq/m^3 corresponds to an effective dose equivalent to 1mSv/y.

(Quinn, 1990) studied variations in temperatures and air flow. The factors that influence the release and concentration of radon in caves are many and complex: the orientation of the cave opening toward prevailing winds; the configuration of the cave (altitude difference between entrance and passageways), a more or less complicated system of corridors; surface shape etc.) These factors influence the sensitivity of changes in radon concentration to external effects (temperature, barometric pressure, precipitation), which is reflected by daily or seasonal variations. Radon daughters were measured in different locations in two "right-side-up" caves (grab sampling using filters). Although the caves were very similar, the radon concentration was different, mainly due to changes in air flow. A hypothesis that the concentration of radon daughters could be predicted on the basis of a set of various parameters was not confirmed.

In measurements in limestone caves (Solomon, et al., 1992), radium in water was found to have values between 2.0 and 3.2 Bq/l. The equilibrium factor F varied between 0.19 and 0.50, and the unattached fraction varied between 0.11 and 0.18 (which is in good agreement with the average f_p value measured in the Czech show caves). The unattached fraction was relatively constant. The activity size distributions of the ultrafine and accumulation modes for PAEC were bimodal, with an ultrafine mode at an activity median diameter (AMD) of 1.1 nm and an upper mode at an AMD of 170 nm (attached). The radon concentration varied between 18 and 1370 Bq/m^3, and the annual effective dose calculated for 45 min tours through the cave was 1.7 mSv (0.08-2.8mSv) for full-time guides.

(Cohen, 1993) studied the correlation between average indoor radon levels in 1600 U.S. counties (89% U.S. population) and the mortality rates in those counties from various types of cancer. This "ecological" study described the average effect on a large group of people (separately for males and females).The strongest correlation was for lung cancer in a group of males and also females. When the smoking parameter was added, the correlation between the radon level and the occurrence of lung cancer was stronger. For smoking, the strongest correlation was found for the thymus and the oral cavity.

(Porstendörfer, et al., 1994) studied the daily variation of the radon concentration indoors and outdoors and the influence of meteorological parameters. No correlation between atmospheric pressure and radon activity concentration was confirmed.

To estimate the radiation dose, one must know the amount and the place of deposition in the lung of the inhaled radon and thoron daughters. Three air activity parameters are important for these dose calculations: the concentration of the decay products; the concentration of the unattached fraction of the decay products; and the activity size distributions of the radioactive aerosols (Porstendörfer, et al., 1994). Outdoor radon concentration measurements show a mean F-factor of about 0.6 with a variation of between 0.4 and 0.8 at a height of 1.5 m above ground, and the mean value of the unattached fraction f_p-value is about 2%. Rising aerosol particle concentrations yield increasing equilibrium factors, because the attachment process is faster than the loss of the decay product clusters by plate out process. However, the unattached fraction decreases with increasing particle concentrations. The radon concentration indoors is mainly influenced by the strength of the sources and by the air exchange with the outdoor air. Both parameters can be affected by meteorological parameters, with human activities, mechanical ventilation and heating systems.

The dose to tissue from the inhalation of radon, thoron and their daughters cannot be measured. It has to be calculated by modeling the sequence of events involved: inhalation, deposition, clearance, retention and decay of the radionuclides (Porstendörfer, 1994). In general, all dosimetric models agree with the conclusion that the alpha dose to the bronchial target tissue from inhaled ^{222}Rn daughters is higher than the pulmonary alpha dose by a factor of about 2-80. This dosimetric result agrees with historical findings for Rn-exposed miners. Retention studies indicate a biological half-life of a few hours for inhaled radon and thoron daughters in the human lung. This means that the main fraction of the potential alpha energy of short-lived radon daughters deposited in the lung is absorbed in this organ; the dose to other tissues delivers a negligible contribution to the effective dose. The dose equivalent of radon daughters in the trachea-bronchial region is about 5 times higher than the dose equivalent in the pulmonary region.

Various measurements were carried out in 13 Italian caves (Cappa, et al., 1996). The radon concentration reached tens up to tens of thousands (Grotta Petruso) Bq/m^3. A limit of 20mSv/year (averaged over 5 years) was applied for workers, with an upper limit of 50 mSv/year. The effective dose was calculated according to Recommendation ICRP65. The researchers considered 1000 working hours/year and then the concentrations could reach 1000 Bq/m^3 in the case of the lower limit of 3mSv, and 3300 Bq/m^3 for the upper limit of 10mSv,

without exceeding the limits chosen for reference. When the concentration was higher, the researchers recommended reducing the time spent under the ground. An easy nomogram was presented for estimating the length of stay under the ground without exceeding the limits.

The HRTModel was used by Porstendörfer for dose calculations. The original deposition destination and the amount of inhaled activity deposited in the lung depend on the particle size (Porstendörfer, 2001). The effective dose from a radioactive mixture can be deduced by adding the effective doses of each decay product. The depth-dose distribution was weighted with the relative number distribution of basal and secretory cells in the epithelium. Because of the greater number of basal cells in the deeper epithelium tissue, the dose values to the secretory + basal cells of the bronchial lung region are significantly lower than the dose values to the secretory cells alone. The bronchial region makes the predominant contribution to the total lung dose in the size range of the cluster mode (<5nm), while the bronchiolar dose is highest in the size range of the aerosol attached activity (>10nm). Even in the size range from 10-100 nm with higher deposition particle efficiency in the alveolar region, the effective dose contribution of this region is more than five times lower than the effective dose of the bronchial and bronchiolar region.

Research on the cave environment and on basic radon daughter physics is presented in a paper by (Cigna, 2005). This coherent publication presents rather interesting information about radon concentration and equilibrium factors from caves around the world. The data from the Czech caves is represented through measurements made by Ivo Burian (Burian, et al., 1990). The average F from all of published measurements not only in Europe was 0.69, and the data from 220 different caves had a log normal distribution. Because it is neither possible nor advisable to change the cave atmosphere, Cigna recommended limiting the exposure time spent under the ground and offered a simple calculation using equation № 3.

(Wysocka, 2011) carried out measurements of the radon concentration in Jurassic caves. The equilibrium factor in these caves was equal to 0.5 on an average. The Denman and Parkinson assumption was adopted for calculating the dose (Denman, et al., 1996): Dose [mSv] = (radon concentration [Bq/m^3] x caving time [h])/126,000. The annual dose equivalents ranged from 0.002mSv to 15.3 mSv. The same approach to dose calculation was used in (Gillmore, et al., 2000).

Numerous research measurements have been carried out in *Postojna* Cave (Slovenia). (Vaupotič, 2008) presented nano-size radon short-lived decay product measurements. The dose conversion factors were calculated on the basis of the unattached fraction of radon decay

product values (f_{un} values) obtained during short-term monitoring in summer and in winter at two points in the *Postojna* Cave. The calculations were based on the concentrations of radon and radon decay products, the equilibrium factor, the unattached fraction of radon decay products (f_{un}), barometric pressure, relative air humidity in the cave and air temperature in the cave and outdoors. The outside temperature was described as the driving force for cave air exchange. Dependence of radon concentration on atmospheric pressure was observed only occasionally over a short period in the winter season. The working averages and the total averages for radon concentration did not differ much, not more than 4% for c_{Rn}, 6% for C_{RnDP}, 8% for F and 13% for f_p. The everyday minima for c_{Rn} were at about 20 h, for F and C_{RnDP} at about 14 h, and for f_p at 17-20 h.

The unattached fraction f_{un} was calculated using the equation $f_{un} = PAEC_{un}/(PAEC_{un} + PAEC_{at})$. c_{Rn} and f_{un} were significantly higher in the summer season than in winter, because the cave air is much more disturbed in summer, when there are visitors, than in winter, resulting in enhanced f_{un} values in summer. The f_{un} value obtained from systematic monitoring in this study (from 0.09 to 0.65) was much higher than the values measured in the *Postojna* Cave by Porstendörfer in the year 1992, which ranged from 0.056 to 0.16, and by (Solomon, et al., 1992) in a limestone cave, which ranged from 0.13 to 0.18.

Using f_{un} values, DCF_m and DCF_n were calculated (for mouth and nasal breathing). According to (Porstendörfer, 1996) $f_{un} = f_p$.

$DCF_{Dm} = 101 \times f_p + 6.7 \times (1-f_p)$

$DCF_{Dn} = 23 \times f_p + 6.2 \times (1-f_p)$

Combined nasal (X fraction) and mouth (1-X fraction) breathing

$DCF_{Dc} = X \times DCF_{Dm} + (1 - X) \times DCF_{Dn}$

Vaupotič calculated DCFc considering nasal and mouth breathing in combination, and the results were always higher than 5 mSv/WLM, by a factor of 11.5-14 in the summer season and 3.0-4.0 in the winter season at the lowest point in the cave (3.1-3.5 in summer and 1.5 – 1.7 in winter at the *Railway Station* cave location. (It is recommended to use these DCF for research purposes only.)

On the basis of these calculations and the results from integral track detectors, the effective doses were 5mSv for guides (429 hours) 2.8 for a locomotive driver (319 hours), 7.5 mSv for an electrician (230 hours, and more time spent in the lowest part), etc. If the effective dose of a worker for the first half of the year exceeds 2.0 mSv, that worker should spend a reduced time in the cave in the second half of the year. The highest uncertainty of the data used was 21% and 15% for $C_{Rn,Dp}$ and 20%- 30% for f_{un} at the lowest point and at the railway station.

Recent measurements in *Postojna* Cave are described in (Bezek, et al., 2012). The radon activity concentration and the short–lived radon daughters and size distribution of the background aerosol particles in the size range of 10-1100 nm were measured. On the basis of the measurement results, where f_p was 0.62 in the summer season and 0.13 in the winter season, Bezek concluded that an inverse relationship between total particle number concentration and the unattached fraction can be observed only if two distinct seasons are compared. However, this conclusion was made for particles larger than 10nm, while the unattached fraction ranges from 0.1 nm to 10nm.

4.2 Measurements of underground radioactivity

The radioactivity of underground spaces is influenced mainly by the presence of primary and secondary primordial radionuclides in the rock and air environment. The concentration of natural radionuclides in karst rock (mostly limestone and dolomite) in the rock composition of the Bohemian Massif and the Western Carpathians is lower (Mareš, 1979). The secular equilibrium in uranium and thorium decay chains can be disrupted due to the chemical properties of the rock, and is caused mainly by dissolution and recrystallization. Artificial radionuclides are present only in exceptional cases (^{137}Cs and ^{90}Sr isotopes may occur in allochthonous clastic sediments transported into a cave after the Chernobyl accident).

A classification of the natural and artificial underground in the territory of the Czech Republic was presented in (Bílková, et al., 2002). The best source of information about the origin, geology, environmental properties and radioactivity of all Czech caves is the book *The Caves* (Hromas, 2009). The information presented above indicates that natural underground areas are impossible to categorize, because each of them is individual in origin and in environment. In terms of health impact, only the number of hours spent under the ground can be used as a criterion for classification. The hypothesis that the concentration of radon daughters in underground environments could be predicted on the basis of a set of measurement parameters and on the basis of a theoretical model, was deliberated but has not been confirmed (Gillmore, et al., 2000), (Quinn, 1990).

The gamma spectrometric characteristics of cave rock measurements are not widely covered in the literature. The equilibrium in uranium or thorium decay chains is often evaluated for the purposes of dating rocks, geological layers or sinters, but the ESR method or mass spectrometry is usually used for determining the concentration of radionuclides. The minimum detection activity of these methods is several orders lower than for “classic” in situ

or laboratory gamma spectrometry measurements, which use a semiconductor detector (HPGe) or a scintillation detector (NaI(Tl) or BGO).

Even when there is a low concentration of radionuclides in karst rock, their presence can help in studies of stratigraphy and dating. (Hladil, 2003) presents an example where, in sections in Quaternary platform limestones on San Salvador Island, a gamma spectrometry method and magneto-susceptibility (κ) data confirmed that the characteristic geophysical patterns are coupled with depositional cycle boundaries. The positive κ-anomaly was coincident with the Th-spike. In cases where a buried cycle boundary forms the truncated floor of a horizontal cave that is filled with carbonate sediment, both U and Th anomalies are broadened.

The four processes responsible for generating aerosols in caves by alpha particles (ionization of the cave air; dislodging of atoms and ions out of the bedrock by high energy alpha particles into the air near the surface, or onto a thin layer on the surface; alphas knocking mineral fragments out from the bedrock) were studied by (Pashenko, et al., 1997). The mentioned hypothetical processes, though physically plausible, cannot play any essential role in the generation of cave aerosols, and much less in the formation of the speleothems.

(Gillmore, et al., 2000) described the variations within and between caves as a result of subtleties of the bedrock geology, fault patterns, and weathering. Gillmore's paper sets out a theoretical model of radon concentration as a result of geological principles concerning source, transport, and subsequent release in caves, which seeks to predict the probable variability in both space and time. This model illustrates that there is much that is not known. The Denman (Denman, et al., 1996) formula was used to estimate the effective dose. The measured average uranium content in cave samples of sedimentary rocks was between 2.0 and 8.2 ppm. Although most carbonates are low in uranium, the soil and residuum derived from them may often be very high in uranium and radium. Where there are carbonate bedrocks, uranium and radium may be absorbed into iron oxidate coatings. Radium occurs with organic material in associated soils, and tyuyamunite, carnotite, and uranophane occur in karst environments. The level of radon concentration can also be affected by factors such as the porosity, permeability and mineralization of the rocks composing individual parts of a cave, by uranium content, the nature of the material filling bottom, tectonics, fault zone features, hydrological conditions, and so on. Most radon escapes from heavily fractured rocks with abnormally high contents of secondary uranium minerals. In the process of bedrock weathering, uranium and hence radon may be released, particularly from secondary deposits.

In measurements carried out in limestone caves (Solomon, et al., 1992), the mass activities of ^{226}Ra in sediments and in soil were in the range of 20-50 Bq/kg (comparable with surface soil

samples). These results fit very well the mass activities obtained by the author through laboratory gamma spectrometry of clastic sediment measurements in the Czech show caves (chapter 6.10).

Cave ventilation, carbon dioxide degassing and temperature fluctuations actively controlled speleothem growth dynamics and therefore dictated how and when speleothems incorporate chemical components from the hydro-geological system (Smith, et al., 2013), when the *Ingleborough* Cave was investigated. Human visitors are known to change the carbon dioxide composition and the temperature of cave air over short temporal scales. A fan was installed at the cave entrance to reduce the radon build up and to ensure a safe working environment for the cave guides, by pumping external air into the cave throughout the public visiting days. However, a fan alters the natural cave atmosphere. The cave monitoring team investigated the atmospheric properties before, during and after a tourist visit. The impact of the cave visitors on the cave atmospheric CO_2 concentration, aerosol concentration and temperature change was measured. While the visitors were present in the cave, the temperature changed in the order of tenths of one ºC, the CO_2 concentration doubled, and anthropogenic aerosols increased as a result of two mechanisms: tourists' bodies acting as a vector for aerosol transport and transporting the particles on their clothing, and, secondly, people returning aerosols into the cave atmosphere by kicking dust from the path and by touching cave walls. The concentration of allogenic aerosols (influence of the fan) falls rapidly within the first 75m of the cave system. Autogenic aerosols are created in the area surrounding an active stream.

Information about the radioactivity of the Czech underground spaces (mainly caves and speleo-therapy areas) is well known. The characteristics of the speleotherapy areas are described in (Jirka, 2001). The presence of natural radionuclides in the rock of the Czech show caves has been measured and results have been published mainly by J. Zimák and J. Štelcl, from Palacký University, Olomouc and by their students (Abt, 2010), (Otáhal, 2006), etc.). Their publications from (Zimák, et al. 2004a,b,c,d,e), (Štelcl, et al., 2006), (Štelcl, et al., 1998), (Štelcl, et al., 2011) etc. summarized results from gamma spectrometry measurements in all Czech show caves and in areas utilized for speleotherapy, and contained a large number of results from in-situ and laboratory measurements. The maxima of ^{226}Ra mass concentrations in clastic sediments were measured in the *Zbrašov Aragonite* Caves (in the area of the "gas lakes") (521 Bq/kg; 324 Bq/kg on an average) and in the *Sloup-Šosůvka* Caves (195 Bq/kg; 53 Bq/kg on an average). The maxima for ^{226}Ra mass concentrations in limestone (1287 Bq/kg; 275 Bq/kg on average) and in sinters (543 Bq/kg; 268 Bq/kg on an average) were measured in the *Zbrašov Aragonite* Caves. The concentration of ^{226}Ra was

higher than 100 Bq/kg in the *Mladeč* Caves, in the *Sloup-Šosůvka* Caves and in the *Javoříčko* Caves (sinters and limestone); in the *Balcarka* Cave (limestone) and in the *Koněprusy* and *Bozkov Dolomite* Caves (dolomite). A comparison between the rock radioactivity results measured by mentioned researchers and these authors is presented in chapter 6.10 of this thesis.

Otáhal (Otáhal, 2006) presented the results from laboratory and in situ gamma spectrometry of natural radionuclide measurements in the Moravian Karst. The designation *cave clastic sediments* was used for all the material that speleologists refer to as "cave clay". This material contains mostly grains less than 2mm in size. The coloring of these sediments is usually gray-brown, yellow-brown, ochre-brown or red-brown. The concentration of CaO in the studied material was very low, indicating that there was no secondary calcification. The cave clastic sediments contained mostly SiO_2, except the samples from the *Balcarka* Cave and the *Císařská* Cave. Potassium was contained only in the illite. Otáhal concluded that the highest mass activities of natural radionuclides are present in cave clastic sediments. In a comparison of the results from the laboratory and the results from in-situ gamma spectrometry measurements (^{226}Ra and ^{232}Th in Bq/kg), the main disproportion occurred in the *Býčí skála* Cave and in the *Balcarka* Cave. (The factors that influence in-situ gamma spectrometry measurement results are discussed in chapter 6.10 and in Appendix 3).

A comparison of the CO_2 and ^{222}Rn concentrations in the speleo-atmosphere confirmed that these gases have similar dynamics.

For the health impact due to irradiation, it is useful to recalculate the concentration of natural radionuclides into gamma dose rates from the rock environment according to the IAEA Guidelines (IAEA, 2003a) (Table 1). This recalculation process is used in chapter 6.10 of this dissertation.

Table 1 Theoretical gamma ray exposure rates and gamma dose rates 1m above a plane and infinite homogeneous soil medium per unit radioelement concentration, assuming radioactive equilibrium in the U and Th decay series (IAEA, 1989, IAEA, 1991, Lovborg, 1984).

Radioelement concentration	Exposure Dose rate	
	(μR/h)	(nGy/h)
1% K	1.505	13.078
1 ppm U	0.653	5.675
1 ppm Th	0.287	2.494

4.3 Description of the environment

4.3.1 Introduction to cave geology

A very important aspect of cave environment research is collecting geological information about the genesis of a cave. The determining factors that have a substantial effect on the characteristics of a cave include the structural and geological settings of the karstic massive and the hydrography of the close area. Syngenetic caves were formed simultaneously with the emergence of the rock in which they are located. Among these caves, we can include travertine caves (caused, due to the elimination of travertine), lava caves (arising from the solidification of lava), coral caves, and boulder and crevasse.

Syngenetic caves, formed at the same time with rock formation, are presented by travertine crater caves, caves of travertine constructive waterfalls, volcano-exhalation and volcano-explosive caves (www.ssj.sk).

Epigenetic cave formation is not linked to the formation of the rock, in which they were formed. Examples of epigenetic caves formed by corrosion and water erosion (karst) are interlayer, ice, wave and wind caves. Epigenetic caves, formed by geomorphic process after the formation of rock are represented by corrosive, corrosive-collapsed, fluviokarst (corrosive-erosive), fluviokarst-collapsed, crevasse, crevasse-collapsed, crevasse-corrosive, debris, weathered caves and others (www.ssj.sk).

It is important to keep these considerations in mind in order to understand the relationships among sediments occurring in rock cavities. In the development of the Moravian Karst, there was a younger tectonic process that resulted in re-flooding of spaces earlier formed, filling them (cavities) with new sediments.

According to the water activity, we can distinguish the following cave types: dry, flooded, river caves, lake caves, underwater caves, spring caves and immersion caves. Other characterizations can be based on structural geology (peers, fractures, breaks), on climate, or on the spatial position of the cave (vertical, oblique, combined). Spatial position is of interest for the spread of radon from the bottom layer (Přibyl, 1992).

We consider the stratification zones for the water surface in karst caves to be as follows: the stratified phreatic zone, which is always at the surface (parallel to the zone of saturation in the soil), followed by the vadose zone, which includes part of the underground karst water that circulates due to gravity, vertically or diagonally above the phreatic zone (similar to aeration zone soils). Some of the monitored structures in caves are fillings that were potential sources

of radon. The highest concentrations of uranium, or ^{226}Ra, are found in igneous rocks. There are lower concentrations in metamorphic rocks, and the lowest concentrations are found in sedimentary rocks, where the major types of caves are formed.

The development of caves in the Bohemian Karst and in other karst regions has often taken place several hundred meters below the erosion base. The presence of permeable zones reaching a significant depth allows for deep water circulation and the formation of karstic structures (Bruthans, et al., 2001).

Cave deposits provide evidence about the development of caves, and about the geomorphological, paleohydrogeographic and paleoclimatic conditions during the period when they were formed and sedimented. The sediments could be flushed out of the formation, or could remain as deposits.

There are two genetical types of cave sediments: autochthonous and allochthonous. Autochthonous panels are formed directly in the cave. They take the form of rubble, rocky debris, Sintra, stalactites, ice, and condensed water sediments. Through hardening, these take the form of breccias. In the case of deluvial sediments, we take into account the slope runoff and the sediment deposited by R_{on} (run-on water) on the sloping walls and their bases.

Allochthonous cave fillings were dragged into the cave through secondary activity. These fillings can be due to windblown dust, blown-in snow, organic remains or hot earth gases. Other sediments may have been brought in by flowing water, seeping-in water or the activity of a thermal spring. The most widely found fillings are allochthonous fluvial sediments or alluvial sediments (sediments arising through water bed erosion or deposited by flowing water) from regular or underground flooding. These sediments can be transported over large distances and can be many tens of meters in thickness (Bosák, 1988).

The origin of a cave is what makes it unique. The origin or source of the sediments in the cave is one of the parameters influencing the sources of radon in it. Because of the very low natural radioactivity of the surrounding rock and the very low coefficient of emanation, the main sources of radon in caves are cave clastic sediments and the high radon concentration resulting from a very low ventilation rate. The (during orogenesis) strongly faulted and folded karst bodies provide wide transportation system of paths for radon emanation to transport from deeper parts of caves.

4.3.2 Geological characterization of the Czech show caves

The area of the Czech Republic consists of two basic geological units, which are components of a larger geological structure that forms the geological basis of Europe. The Czech karst

areas represent carbonate karst belonging to the *Central European Type of polycyclic and polygenetic karst* (Panoš, 1964). *Hydrothermal karst* represents a special type of karst. The diverse geological substructure led to the formation of two large karstic units and a number of karstic "islands".

These karstic systems have developed in bodies of limestone, dolomitic limestones, mostly from the Devon period, less frequently from Silurian period, in the framework of the Bohemian Massif, and from the Jurassic period in the area belonging to the Outer Western Carpathians region.

There are 1771 karstic caves, 456 pseudo-karstic caves and abysses in the Czech Republic, while 14 of these have been opened to the public. The show caves in the Czech Republic can be classified according to their genesis as **corrosive**, (i.e. formed through dissolution along cracks and surfaces with lower resistivity) (*Chýnov* Caves), (i.e. where the major carving factor was an active water flow) (*Na Špičáku* Cave), areas with a **combination of these corrosive and abrasive** (*Balcarka* Cave), and even, in a special case, as **hydrothermal** (caves created through the flow of warm mineral waters through the massif) (*Zbrašov Aragonite* Caves). Some caves still encompass an active underground stream.

The Kateřina´s Cave

A brief geological characterization of the caves included in the Czech show caves investigation project (Thinová, 2007) is given below. Maps of each cave are available on www.caves.cz, and detailed information about Czech underground areas is provided in (Hromas, 2009).

Chýnov Caves:

These caves developed in crystalline limestone up to 12 meters in thickness in colorful series of Bohemian moldanubian, located across the westernmost tip of the Bohemian-Moravian Highlands. This cave is shaped inside a limestone lens deposited in a series of monotonous Moldanubian gneisses. A feature of the cave is the crystalline limestone alternating with layers of colored amphibolite.

Koněprusy Caves:

These caves were formed at the top of the *Golden Horse* hill in the southwestern part of the Bohemian Karst. Geologically, the Bohemian Karst belongs to the Devonian Silurian-Lower Paleozoic core of the *Prague* Basin, which is part of the *Barrandian* massif. Bohemian Karst limestone bodies are separated by shale, volcanic rock, and include formations of platform Cretaceous sediments and Quaternary gravels.

Bozkov Dolomite Caves:

These caves are situated in a Lugian region. They were formed in crystalline dolomitic limestone (marble) up to calcareous dolomites of Silurian age in the *Krkonoše* foothills. The original Silurian metamorphic limestone was dolomitized in the course of Hercynian orogeny. These caves were created as part of the *Ponikelské* group, as labeled by (Chaloupský, 1989). Crystalline calcite and dolomite, together with chlorite-muskovitic phyllites form the youngest part of this group (Hladil, et al., 2003). Carbonate rocks occur in discontinuous streaks and lenses in this area (Hromas, 1997). The lens in which the *Bozkov* caves were formed is 300 m in length and has a maximum width of about 150 m (Skřivánek, et al., 1997). The cave is permeated by calcareous and siliceous dolomite lenses from the Silurian age, surrounded by phyletic shales.

Na Pomezí Caves:

These caves are located 2 km north of *Lipová* Spa. This is the longest cave complex formed by dissolving crystalline limestone. It was formed in metamorphic carbonates in the Devon age, and belongs to the *Branná* group, which forms a part of the *Hrubý Jeseník* Mountains.

The cave permeates an island of pure, white crystalline limestone 220 m in thickness. A rock formed through the karstic process surrounds quartzite, schist and fillies. The whole *Branná* group is very difficult to characterize stratigraphically, as it is formed by a series of rock areas that are intensely tectonically affected. A stratigraphic classification was attempted by Květoň (Květoň, 1951) who distinguished within the *Branná* group a Silurian lower section and a Devonian upper section. In addition to areas with strongly graphitic schist, quartzite, graphitic biotitic gneiss and calcific metalydites in the lower Silurian section, there are also lenses of limestone 100-200 meters in width that can be traced for several hundred meters.

Na Špičáku Cave:

This cave originated in the *Supíkovické* marbles between *Jeseník* and *Supíkovice*, which are allocated to the *Žulovský* massif. The rock is Devonian, and accompanies the crystalline core of *Hrubý Jeseník*. This type of rock usually includes ancillary calcific marbles, graphite, phlogopite, diopside, tremolite, etc. The *Žulovský* massif itself is an extensive body that forms a part of the *Rychlebské* Mountains. It is separated from the main part of the *Rychlebské* Mountains by a bordering *Sudeten* fracture. The whole pluton is raised along this fracture and protrudes within an area of 125 km^2. The pluton penetrates into some folded and metamorphic rock, believed to be Devonian.

Javoříčko Caves:

These caves were formed in the northern part of the *Konice - Mladeč* belt, as a part of the *Javoříčský* Karst. The oldest members of the *Konice - Mladeč* belt are basal clastic, which lie directly on pre-Devonian *Mladeč* metamorphic phyllites. The clastic near *Ludmírov* and *Vojtěchov* is between 20-50 m in thickness. From the direction of the overlying rock, the clastic changes into grayish, after weathering brownish and greenish, fine, often calcific shale, mostly strongly pressure disturbed. The thickness of the shale can be estimated at 20-50 m (Svoboda, 1966). The *Javoříčko* Caves were formed in Devonian carbonates within *Lažánecko - Macošské* limestone formations, which pass into the overlying *Vilémovické* limestone. Near *Vojtěchov*, the *Vilémovické* limestone massif is estimated to be 300 to 400 meters in thickness (Fabík, 1975).

Mladeč Caves:

These caves developed on the southern edge of the significant *Hornomoravský* valley depression. The *Mladeč* Caves, as part of the *Mladeč* Karst, located near the *Litovelské Pomoraví* protected area, were formed in the solid *Třesín* massif, which forms the northernmost part of the *Mladeč* belt line. These caves are located in *Vilémovic*e limestone, which is several hundred meters in thickness near *Mladeč* (Dvořák, 1994). The *Třesín* massif was probably formed in the course of the variscan tectogenesis by dragging anticlinal Devonian parts to Culm sediments. It can therefore be considered as a part of the Moravian-Silesian *Bradlové* zone, defined by (Přichystal, 1996). The bedrock is composed from the same rocks as the adjoining *Javoříčko* Caves.

Zbrašov Aragonite Caves:

Aragonite caves have formed in the *Hranice* karst, which is the easternmost protrusion of Moravian-Silesian Devon within the development of the Moravian karst. The *Hranice* karst forms the northeastern edge of the *Malenik* plate. The paleozoic bedrock in northern Moravia has not yet been significantly explored. Deep drilled wells located in this area reached deepest in the Lower Carboniferous sediments, e.g. the *High* borehole in 1967 reached a depth of 1711.6 meters. The borehole is located 10 kilometers west of the city *Hranice* (Suk, et al., 1991).

The occurrence of several Brunovistulicum outcrops near *Olomouc* suggests the rock filling the Paleozoic basement rock layer. These Aragonite caves were created in a massive *Vilémovice* - *Macocha* limestone formation and in the overlying honeycomb limestone of uncertain age (Dvořák, 2004).

Vilémovické limestones are light gray, very finely grained. They were previously marked as "coral", because of the abundant fossilized remains of corals. (Svoboda, et al., 1956) concluded according to the coral and stromatoporic fauna that sedimentation took place in a shallow water environment. (Dvořák, et al., 1978) consider this limestone as chemically very pure, being a product of a unique sedimentary environment.

In addition to *Vilémovice* calcite we can locate honeycomb calcite in the *Zbrašov Aragonite* Caves. The petrography of the honeycomb limestone is considerably variable, depending on the clay content. Crinoids and foraminifers have been identified among the fossil remains in the honeycomb calcite. According to the conodont fauna found there the limestone belongs to a higher Frasne layer (Dvořák, et al., 1978).

The *Moravian karst* geological situation:

The *Moravian* Karst region lies on the eastern edge of the *Bohemian* Massif, in the *Moravian-Silesian* Palaeozoic area. The western boundary is formed by Proterozoic igneous rocks of the *Brno* Massif, and the eastern boundary is formed by *Drahanský* Culm deep sea sediments (Lower Carboniferous). The geological development of the Moravian Karst began during the Variscan orogeny early Middle Devonian (about 390 million years ago), when it gradually began to develop into a sea basin in which no Moravian Karst limestone sedimentation occurred. The Moravian Karst bedrock consists of Precambrian rocks of the *Brno* Massif age. On this bedrock, the Devonian weathered surface began to settle in the lower Devonian fragmentary violet-colored deposits. This was followed by sedimentation in a marine environment, which did not present a uniform trend throughout the Moravian Karst area, but

resulted in two rudimentary developments: the *Macocha* formation and the *Líšeň* formation (Musil, 1993). The whole *Macocha* formation, with its close overburden beneath the *Líšeň* formation, covers a time period of approx. 20 million years (Hladil, 1994). The lower limit of the carbonate sedimentation is erosion based, modeled under low water surface levels during a hiatus (absence of deposition, erosion), or with transformed siliclastic sediments. The upper limit in the greater part of the plateau is also erosion based, and it created the conditions for a low sea level up to the Devon/Carbon border. The front of the carbonate plateau in the Moravian Karst was "drowned" by the subsidence plates. The Givet-Frasne plateaus from tropical Devonian periods are mostly on an average 400 m in thickness, and the development consists of 4 cycles. These cycle-originated layers have an average thickness of 40, 180, 150 and 300 m, and each cycle lasted approximately 5-6 million years. These cycles in the Moravian Karst were first described by (Hladil, 1983) as *Čelechovický, Býčiskalský, Ochozská and Mokerský* (Hladil, 1997). A stratigraphic overview of the Moravian karst Devon period is summarized in (Hladil, 1994).

We will now provide a brief description of the Moravian karst show caves studied in this dissertation: the *Sloup-Šošůvka* Caves, the *Balcarka* Cave, the *Punkva* Caves, and the *Kateřina's* Cave are briefly described below.

Punkva Caves:

The *Punkva* Caves are located in the *Pustý žleb* karst canyon, 2.5 km NE from a secluded mountain mill, about 6 km NE from *Blansko* in the *Punkva river spring* National Nature Reserve (NNR). There is a dynamic system of caves carrying the flow of the river *Punkva*, which connects these caves with the *Amatér* cave area. The underground areas form the largest cave system in the Czech Republic, with a current length of about 3900 m (Bílková, et al., 2002). The caves were formed in *Vilémovické - Macošské* and *Lažánecké* limestone strata. The cave system includes the most famous Czech chasm, the *Macocha* abyss. These caves were not included in our study due to the complexity of the groundwater system.

Kateřina's Cave:

The *Kateřina's* cave is located in the *Pustý žleb* cliff, 0.5 km south of the secluded *Mountain Mill*, about 6 km south west from *Blansko* in the *Punkva river spring NNR*. The cave was formed in the *Lažánecké* limestone flux by an unknown underground water stream, flowing from the northeast toward *Pustý žleb* into the limestone *Lažánecký* massif. With a total length

of about 950 m and a height of 63 m, the cave nowadays passes through the *Chobot* rock ridge (Bílková, et al., 2002).

Sloup-Šošůvka Caves:

The *Sloup-Šošůvka* Caves are located on the southern edge of the village of *Sloup*, 9 km north east from *Blansko*, in the *Sloup-Šošůvka* Cave NNR, which constitutes one of the main branches of the largest underground cave system in the Czech Republic. Geologically, it is located on the edge of the karst area in the *Vilémovické* limestone formation. The karst submersion of the *Sloupský* creek, one of the underground tributaries of the river *Punkva*, was formed by a vast double-decker system of spacious tunnels and caves 4200 m in length and 94 m in depth. They are connected through several giant chasms to the deepest gorges in the Czech Republic (Bílková, et al., 2002).

Balcarka Cave:

The entrance to the *Balcarka* Cave is located in the *Balcar Rock*, situated at the beginning of *Suchý Žleb*, 0.5 km south of *Ostrov u Macochy*, about 8 km east northeast of *Blansko* in the *Balcar Rock NNR*. The *Balcarka* Cave is a large maze of caves and also a well-known archaeological site. The cave areas that have been uncovered have a total length of 930 m, and they reach combine height of 18.5 meters, on two levels connected by high domes and chimneys. Their emergence into strongly folded *Vilémovické* limestone was due to erosion by an unknown underground stream (Bílková, et al., 2002).

One of Czech show caves, the *Na Turoldu* Cave, originated in a Jurassic limestone fragment. This cave developed in lithological horizons of *Ernsburk* limestone. Geographically, the *Na Turoldu* cave falls within the *Pavlov Hills* area. The karst *Pavlov Hills area* consists of Jurassic limestone fragments beneath the *Ždánický* massif belonging to the outside group of the *Flyšov* belt in the southern zone of the Western Carpathians.

Speleo-therapeutic caves and tunnels:

Speleo-therapeutic areas, which are mostly located in show caves, and form a special part of the caves, are at the center of interest in our study, which focuses on the impact of cave environments on human health. Speleotherapy has a long and successful history in treating the respiratory system of children and adults.

In the Czech Republic, five underground areas are currently in use for speleo-therapeutic purposes. The radioactivity of the environment in the following caves was measured:

- *Sloup-Šošůvka* Caves
- *Císařská* Cave
- *Ve Štole* Cave, also known as *Třesínská* Cave
- *Javoříčko* Caves
- *Zlaté Hory* – an old underground mining area

Speleotherapeutic underground spaces, in detail:

Sloup-Šošůvka Caves:

This is a well-known cave complex in the Moravian Karst under ANCLP (CR) management. It serves as a speleotherapy center for the Children's Hospital in *Ostrov u Macochy*. The *Amatér Cave* complex was also used in the past.

Císařská Cave:

This cave, located between *Ostrov u Macochy* and *Holštejn*, is not open to the public.

It is the only cave in Moravian Karst with terraced, stagnating surface of groundwater. The cave fills with flood water from *Lopač* creek. The Císařská Cave has formed in close vicinity of *Vilémovické* limestone massif over *Rostáňské* shale layers. The cave is surrounded by very complex geological setting. Among rock types are present *Vilemovické and Křtinské* limestone, *Ostrovní* shale and *Rostáňské* shale layers (Hromas, 2009).

Ve Štole Cave, also known as *Třesínská* Cave:

This cave is a part of the Devonian (360 million years old) *Třesín* limestone cliffs that formed during the Variscan orogeny by forming an anticline in the Culm sedimentary shale about 260 million years ago. The *Ve Štole* Cave is a part of the *Mladečský* Karst. The name comes from a tunnel, approximately 345 m in length, dug into the karst massif. About 120 m of tunnels within the limestone cave system are used for speleotherapeutic purposes. At the back of the cave, there is limestone folded into Culm shales. The sediments in the (man-made) cave entrance and also the cave soil are worth mentioning. The grain size is variable, alternating with dust fractions (grain size <63 μm) and sand fractions (grain size between 63 μm and 2 mm). Gamma-spectroscopic clay measurements indicate mass activity of 300-800 Bq/kg, and rock 200-600 Bq/kg) (Jirka, 2001).

Javoříčko Caves:

The speleotherapy medical facility is predominantly composed of light-grey limestone. A dominant part of the rock is composed of sparitic limestone with aggregates crystalline sparitic calcite. Some limestone can be described as sparitic limestones with "clots" or band of micrite (Jirka, 2001).

Zlaté Hory underground tunnels:

The hospice inside the *Golden Hills* uses about 1 600 meters of underground passageways on the second level, formed by sulfide ore deposit mining in the Golden Hills – South mine. The geological structure of the massif is formed by the locally morphed volcanic-sedimentary rock complex of Paleozoic, Devonian age (about 390 million years). The largest proportion of the metamorphic rocks contain: quartzite (quartz sandstone), muscovite slate, marble, rocks resulting from the conversion of acidic volcanic rock, usually a part of hornblende quartzite, which is difficult to distinguish from ordinary quartzite. Sulfide mineralization is developed inside the hornblende quartzite and also on the contact surfaces of the hornblende quartzite with (muscovite-chlorite) shale. It should be noted that the massif does not contain limestone, which is essential for the release of calcium ions (Jirka, 2001).

4.3.3 Environmental characterization of the caves

For the purposes of our study of the concentration of radon within underground spaces, it is important to establish which basic parameters influence the radon concentration in various types of underground spaces. It is not so important to categorize the different types of underground spaces according to whether they are of artificial or natural origin, because the type of origin has little effect on irradiation monitoring.

The environment of caves is typically characterized by 100% humidity, and the number of aerosol particles is around 10^2 times lower than outside (but the number of free ions is higher). The seasonal variations of $c_{V,Rn}$ are very high (up to tens of thousands of $Bq.m^{-3}$) and the development of variations is the reverse of the development observed in dwellings.

The major sources of irradiation under the ground are natural radionuclides (from the uranium and thorium decay chain and potassium ^{40}K). These natural radionuclides are present in the rock (and in man-made areas in the building materials as well), in the bedrock, in sedimentary material of various origins, in atmosphere, and in underground lakes or dripping water. When discussing underground irradiation, we should consider on the one hand the sources, and on the other hand the environmental conditions, which may play an essential role in the

distribution of radiation sources, and their time variability, because irradiation is caused mainly by inhalation of radon.

4.3.3.1 The main characteristics of an underground environment that influence radon concentrations

In the course of many years of cave environment monitoring, the author has obtained interesting measurement results, which have indicated that major radon sources can be categorized under the following headings:

The bedrock below the underground areas is one of the major sources of radon. The variability of the radionuclide content in the rock types in the Czech Republic provides numerous sources of radon with different radon potential. In most areas, the fault system enables radon to be transported over tens or hundreds of meters (Nazaroff, et al., 1988) (Smetanová, 2009). The more complicated the tectonic system is, the more it enables the transport of radon from the bedrock. The low ventilation rate of underground spaces, and the stack effect, significantly increase the impact of radon coming from the bedrock.

The rock present in the underground may have a quite variable content of radionuclides. In the case of karst rock (dolomite, limestone and gypsum) and sinters, the content of natural radionuclides (^{238}U and ^{232}Th decay chains members, and ^{40}K) is usually very low (Zimák, 2004b) (see chapter 6.10). Although the rugged rock surface forms a large area for radon emanation, the emanation coefficient is very low (see chapter 6.8). The rock filling some tectonic fault (clastic sediment) or a metamorphic material may bring a local increase in irradiation, especially when it is weathered (for example porfyroids in the *Bossea* Cave 43 Bg/kg ^{226}Ra, 64 Bq/kg ^{228}Th and 1340 Bq/kg ^{40}K, erlan or the iron-manganese filling in the *Chýnov* Cave 20 Bq/kg ^{226}Ra, etc). During geological processes such as erosion, sedimentation, melting and recrystallization, radionuclides in decay series can become fractionated relative to each other, due to variations in their chemistry or the structural site that they occupy. This results in a state of secular disequilibrium (Dickin, 2005).

In caves, underground tunnels and mines, ***clastic sediments*** are major sources of radon, because of the large volume of this material present inside and below the caves, and its higher content of ^{226}Ra than for karst rock. These deposits were influenced by some type of current;

the particle size is therefore a reflection of the amount of energy that transported the sediments to the place of deposition. The particle size of clastic sediments is usually characterized by the presence of gravel (all particles larger than 2 mm in diameter), sand (particles smaller than 2 mm, but larger than 0.0625 mm), and mud (particles smaller than 0.0625 mm). The clastic sediment in the cave comprises all sediments filling the underground caverns and chambers with particle size smaller than 2 mm (Panoš, 2001). The clastic sediments in caves can be categorized as follows:

a) cave speleogene dirt – residual loose cave sediment containing insoluble residues of karst rock; the typical form of transport is a short transportation path from the area of origin
b) allogene cave dirt – consisting of silt or material flushed from the surrounding sedimentary karst surface
c) fluvial cave sediments – transported into the cave areas by the flow of cave water.

Spectrometric analysis of the sediments enabled us to monitor the disturbance in the secular radioactive equilibrium in the given geochemical systems, using a study of the $^{238}U/^{226}Ra$ or $^{228}Th/^{224}Ra$ proportion. Among the chemical processes that lead to an imbalance in the secular radioactive equilibrium, it is worthwhile to depict the geochemical dynamics of the geological rock group that is being studied (oxidation and reducing reactions, dissolution, crystallization, partial melting, absorption, phase changes (fluid – gas) for the studied carbonate rocks, indicative of mostly dissolution and re-crystallization. Knowledge of the mass activities for ^{226}Ra, ^{40}K and ^{232}Th in each of the collected samples could be an important indicator for categorizing these samples into appropriate rock groups, in terms of their genesis. The $^{208}Tl/^{226}Ra$ ratio enabled an evaluation of the origin of the clastogene sediments (Dickin, 2005).

The aerosols in caves are cave-specific**.** The caves are characterized in contrast to dwellings by the following characteristic: the absence of aerosol sources (the aerosol concentration in caves is approx. 100 times lower than in the outdoor atmosphere); high humidity; a low ventilation rate and the uneven surfaces. The *conversion factor (mSv/WLM),* which plays a significant role in the calculation of the dose, is dependent on the aerosol particle size spectrum resolution, and on the distribution of radon daughters among the attached and unattached fractions. Aerosols are discussed in detail in chapter 4.3.5.

Water springs. Some underground water sources can distribute dissolved radon into the environment. There was a very interesting situation in the *Haničk*a underground military fortress, where the main source of radon was a local underground water spring with a high concentration of radon ($c_{A,Rn}$ was 240 Bq/l). The radon emanation from this spring had a significant influence on the radon concentration in the air (Figure 2). Another example was found in water samples in the *Bossea* Cave (Italy). The water sample measurement results are summarized in Table 2. Although there are several water streams inside the *Bossea* Cave, just one stream from a small tributary fissure, situated above the main cave dome, was the source of radon.

Table 2 Concentration of radon in water samples in the *Bossea* Cave, Italy

Sampling location	**$c_{A,Rn}$ (Bq/l)**
Above the "Waterfall"	0.4
Inside the "Waterfall"	0.4
Under the "Waterfall"	0.2
Lago under the "Waterfall"	0.4
Groundwater emanating above the "Waterfall" - closed part	6.2
Lago Muratore - closed part of the cave	0.6
Lago di Emastina	0.4

The *Haničk*a underground military fortress

The building material is concrete. The distance between the measurement locations varies according to the length and the complexity of the underground corridors, usually around ten meters in length. Each measurement point expresses the average radon concentration from a five-minute measurement.

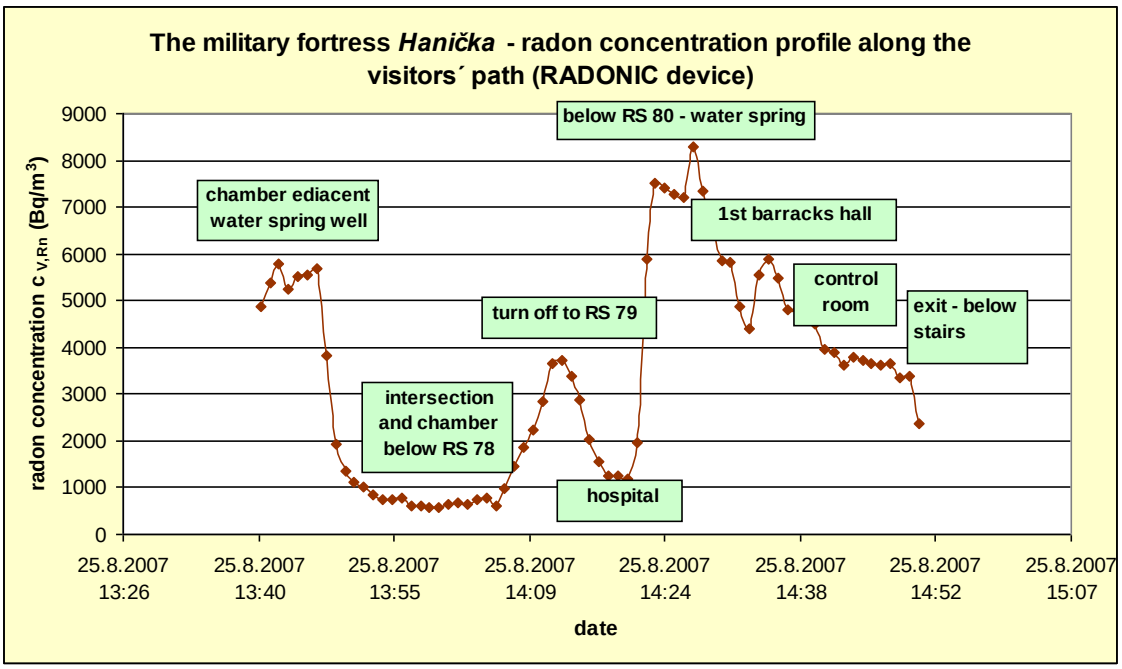

.

Figure 2 Radon concentration along the visitors' path (*Haničká* military fortress), which is influenced by radon released from a local water spring (240 Bq/l)

Climate dynamics - underground spaces have much smaller variations in daily and annual temperatures than are found in the outdoor atmosphere, but the variability among underground areas may be considerable. The underground climate is mainly influenced by the number and the location of the openings leading to the outdoor environment, and by the extensiveness and the jaggedness of the underground spaces, the presence of quarries (mining activities) in the vicinity of underground spaces, exhalation of gases, underground water, or the presence of surface water, etc.

The temperatures in the Czech show caves vary on an average between 14.3ºC, in the *Zbrašov Aragonite* Caves, and 6.2ºC in the *Sloup-Šosůvka* Caves (Sládek, 2009). The origin of the cave may also affect its temperature dynamics.

Underground areas with a single opening behave statically. There is almost no *airflow* within the enclosed spaces (when there is only one opening for exchange with the external environment).

Dynamic spaces have at least two openings, one of which may enable air inflow, while the other enables air outflow. The basic physical principle of the air exchange depends on different air temperatures at different vertical levels.

In a complicated underground situation, some area of the underground system may behave in isolation from the other chambers. Dynamic caves often contain some stato-dynamic areas.

The dynamics of the Czech caves has been studied in framework of master's projects by students from the Masaryk University (the *Chýnov* Caves - (Nováková, 2011), the *Císařská* Cave, the *Moravian* Karst Caves - (Lang, 2010), (Otáhal, 2006) etc., *Jesenický* Karst (Abt, 2010)).

Caves can be classified as dynamic or static, according to the air flow (Přibyl, 1992).

Dynamic caves have two or more entrances at different altitudes. In summer, the warm air entering the caves is cooled by the rocks, and it exits through the lower opening. The result is a continuous air flow. Thermal energy is passed into the rock, and the humidity increases due to the effort to establish thermodynamic equilibrium. Water vapor condenses on the walls after saturation, or it forms an aerosol on dust particles. In winter, the direction of flow reverses.

Static caves may also have several entrances that do not differ significantly in vertical position. In winter, warm air, heated by the rock, flows out of the cave and the cool air flows in. This exchange continues until thermal equilibrium is established. When there is an appropriate configuration of the cave spaces, the cold air in the cave can be preserved throughout the summer, and in special cases an ice cave can be created. In the opposite case, where the bulk of the space is located above the opening, the warm air inside the cave is preserved through the winter. The average temperature in the cave is then higher than the average temperature of the external environment.

There is also a type of cave designated as *stato-dynamic.* This type is a dynamic cave, where some entrances are closed in a certain period of the year, perhaps due to glaciation or flooding. The result is that the cave behaves statically for a certain period of the year, and dynamically at other times (Bosák, 1988).

Air flow, which is inseparably connected with climate dynamics, plays a crucial role for radon concentration levels (Figure 8, Figure 9). In the winter season, when the level of concentration is usually lower, the air flow may release "pockets" of radon. The radon concentration increases for a few hours, and this process is independent from the seismic activity (Thinová, 2007). The sources of high radon concentration are located in the deeper areas of caves. Closeness to the surface causes cave air and outside air to mix (Figure 6, Figure 7).

The following examples have been selected from the measurement results in various cave types:

The *Arnoldka* Cave

The dynamics of the radon concentration in different branches of the Arnoldka Cave was measured over a period of three weeks in 2008, as shown in the following figures (Figure 3, Figure 4, Figure 5). The entrance is located in the upper portion of the cave. Branch № 1 of this cave behaved dynamically during our measurements (it was located near a limestone quarry), while branch № 2 behaved statically. In the dynamic part of the cave, the radon concentration is influenced by the atmospheric pressure, and the concentration of radon is four times lower than in the static part. The correlation factor between radon concentration (after smoothing, using a moving average) and atmospheric pressure is R = -0.668. After shifting the time lag forward or back by a few hours the changes in the correlation factor are negligible (R = -0.669 when the pressure is shifted one hour ahead, etc.)

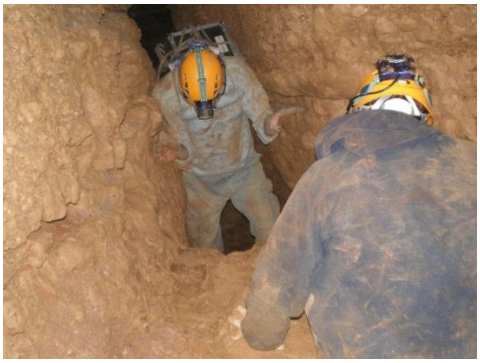

Photo: Radon measurement using RADONIC01 device in the Arnoldka Cave

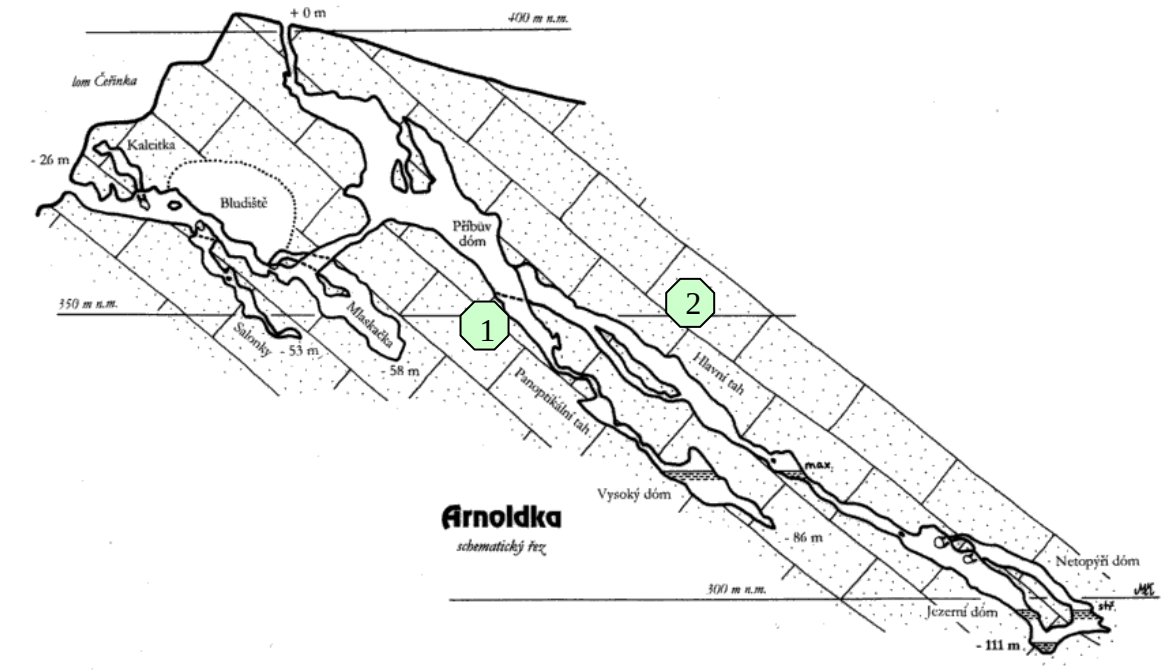

Figure 3 Layout of the *Arnoldka* Cave (author: Michal Kolčava)

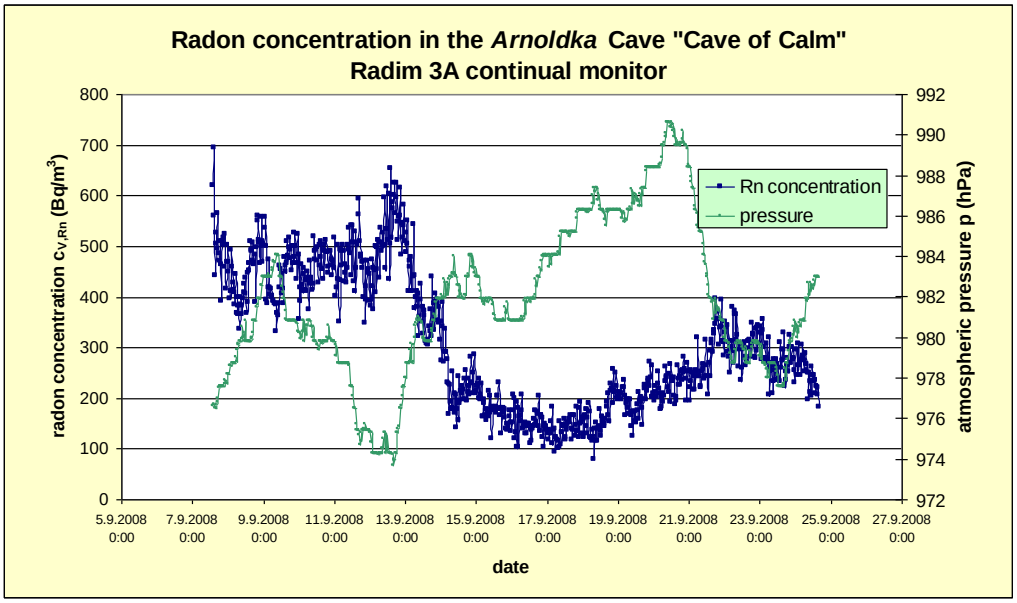

Figure 4 Radon concentration in the dynamic branch of the *Arnoldka* Cave

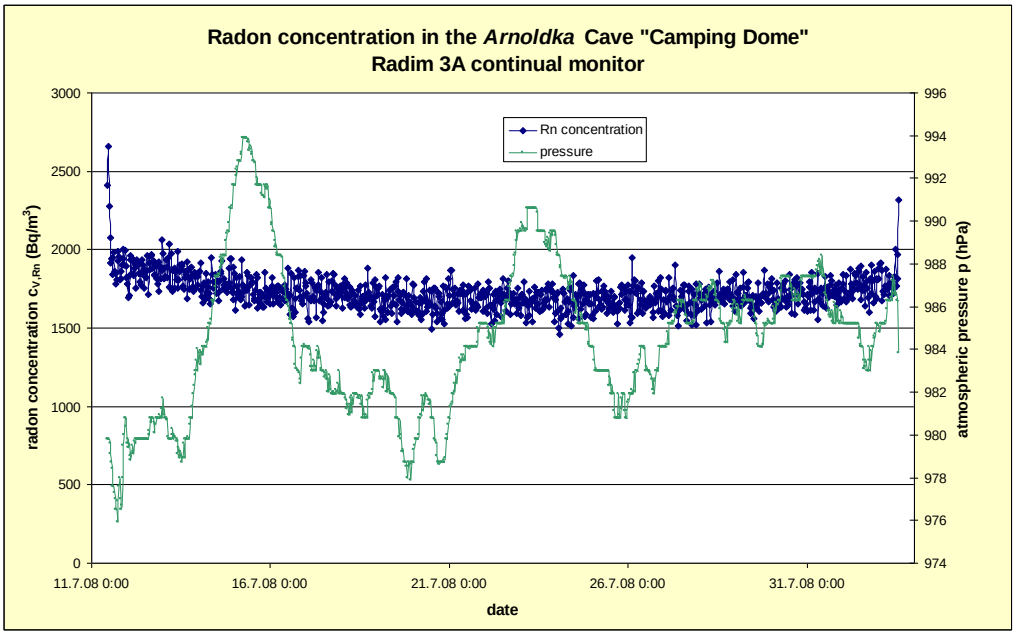

Figure 5 Example of a static cave – the radon concentration in branch № 2 of the *Arnoldka* Cave

The *Koněprusy* Caves

The exchange dynamics between the cave and the outside environment is shown in Figure 6. The measurement was carried out simultaneously in the *Koněprusy* Caves at different depths. The deepest part of the measured area was the *Old corridor*; the *Mint* area is located near the exit, near the surface. The radon concentration in the *Mint* is affected by intensive air

exchange. Figure 6 shows the influence of atmospheric pressure on the radon concentration at all depth levels.

The dependence between the radon concentration and the ratio of the temperatures outside/inside the cave (which is in practice equal to the outside temperature) and/or the atmospheric pressure is often studied based on measurement results. On the basis of 10 years of radon concentration measurements, it appears that the relationship is sometimes more closely related, and sometimes does not work. An example of daily variations that are independent from *atmospheric pressure* is shown in Figure 7.

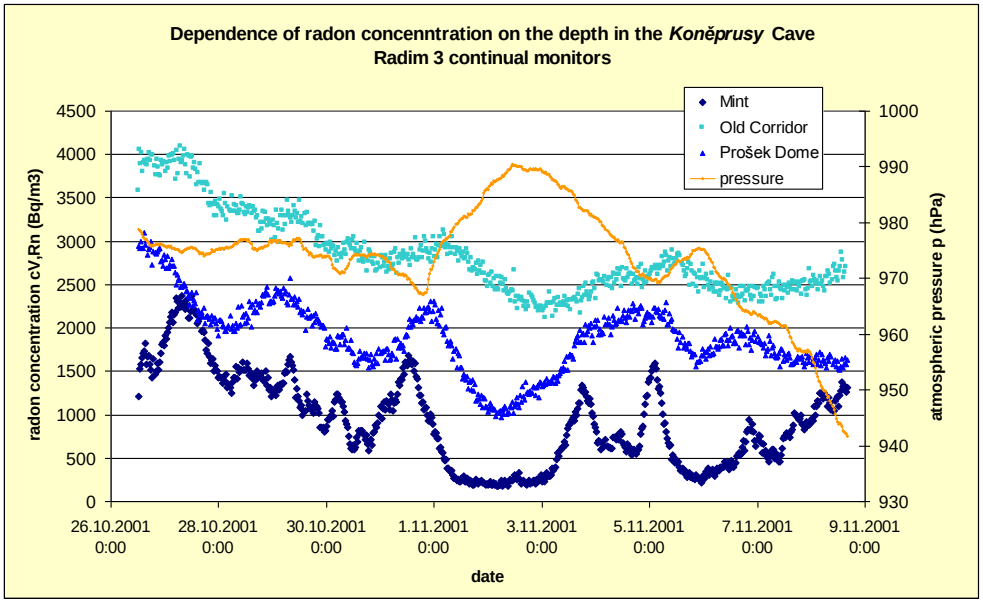

Figure 6 The influence of an increase in atmospheric pressure on a decrease in radon concentration at different depths in the *Koněprusy* Cave

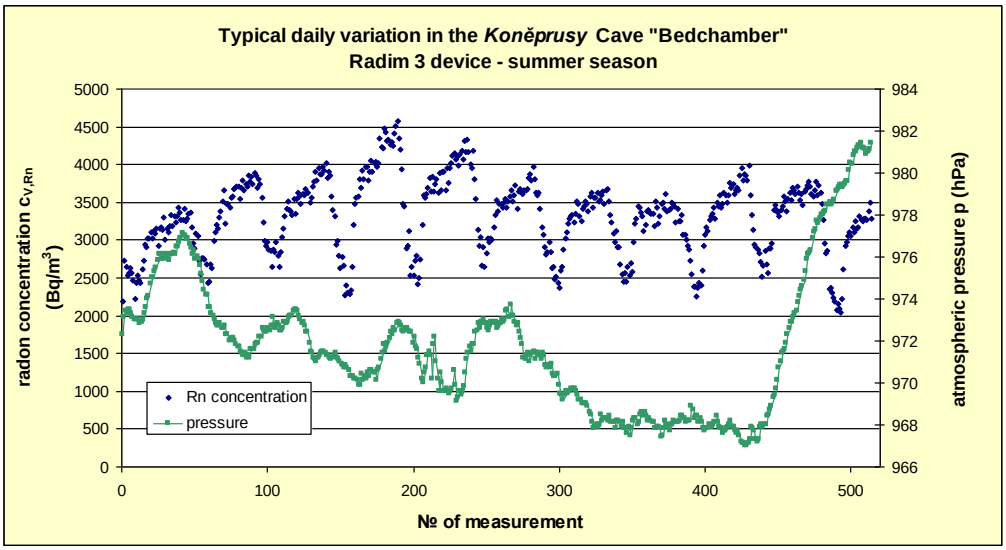

Figure 7 Typical daily variation during the summer season in the dynamic part of the *Koněprusy* Caves

The *Zbrašov Aragonite* Caves

The air flow has a significant effect on the level of radon concentration in the course of the year. Figure 7 shows a short part of the profile along the visitors' path - the junction of the air flow from three different directions.

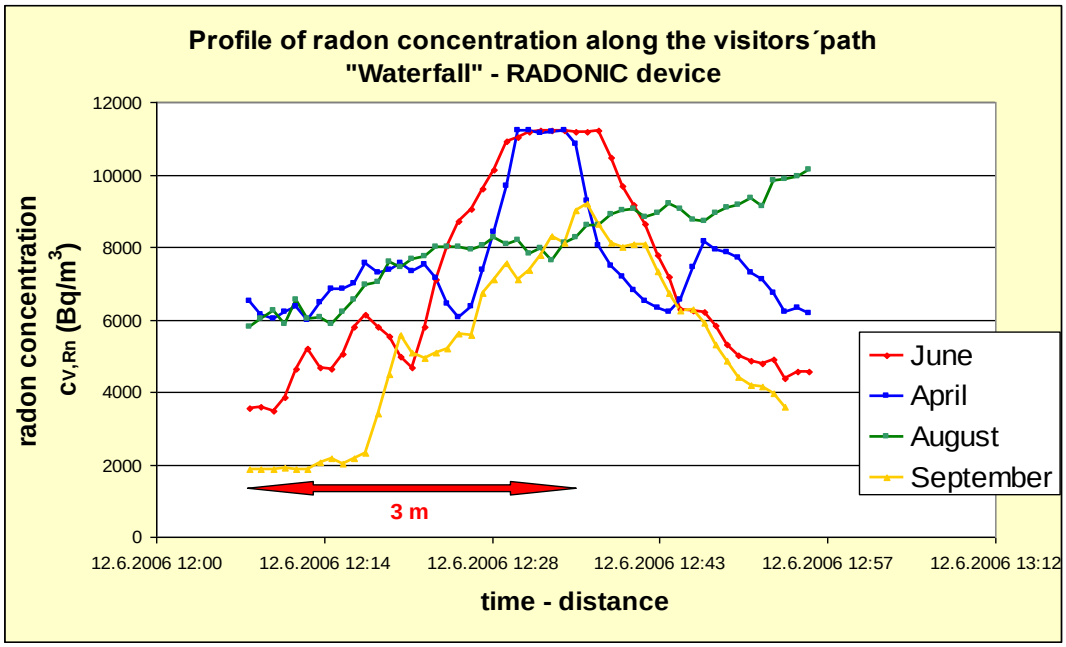

Figure 8 Decrease in radon concentration at the meeting point of three air flow directions (*Waterfall*, the *Zbrašov Aragonite* Caves) and its time variability

The air flow in the *Waterfall* area was measured using a Testo device, and was studied using an infrared camera. The detailed measurements of the radon concentration in this area are presented in chapter 6.2.4.

Figure 9 shows how the changes in air flow may affect the radon concentration in the *Zbrašov Aragonite* Caves. The ratio between daytime and night-time temperatures determines how much the cave environment "works". The maximum outside temperature during the measurements in June was 23ºC, and in September the maximum temperature was 22ºC, but the temperatures during the night in June were around 7ºC, while in September the night temperatures were around 17ºC! During the summer period, the air exchange is more intensive, so the levels of radon concentration are higher. (The outside temperature data was obtained from a meteorological station outside the *Zbrašov Aragonite* Caves).

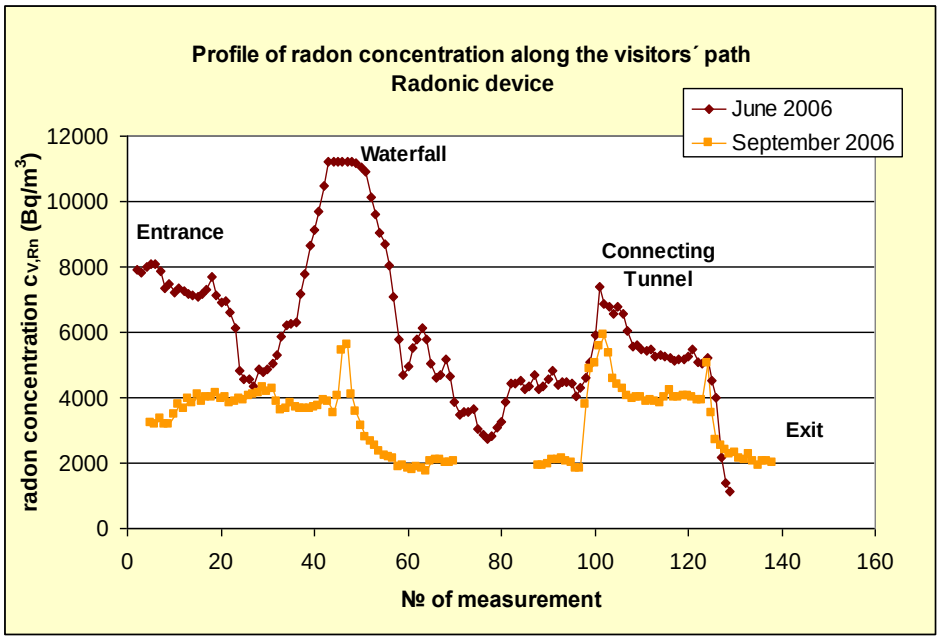

Figure 9 The profile along the visitors' path in different air flow conditions (the *Zbrašov Aragonite* Caves)

The correlation between the radon concentration in two different areas of the *Zbrašov Aragonite* Caves and the outside temperatures is presented in Figure 10. The shift between the temperature maxima and the radon concentrations in *Jurik's* Dome (further from the entrance, deeper part of the cave) is approx. 3.5 hours. The shift between temperature maxima and radon concentrations in *Gallaš's* Dome is 0.5 hour. The radon concentrations during the weekend time period (more visitors in the cave) are significantly lower. No impact of atmospheric pressure is evident (Figure 11).

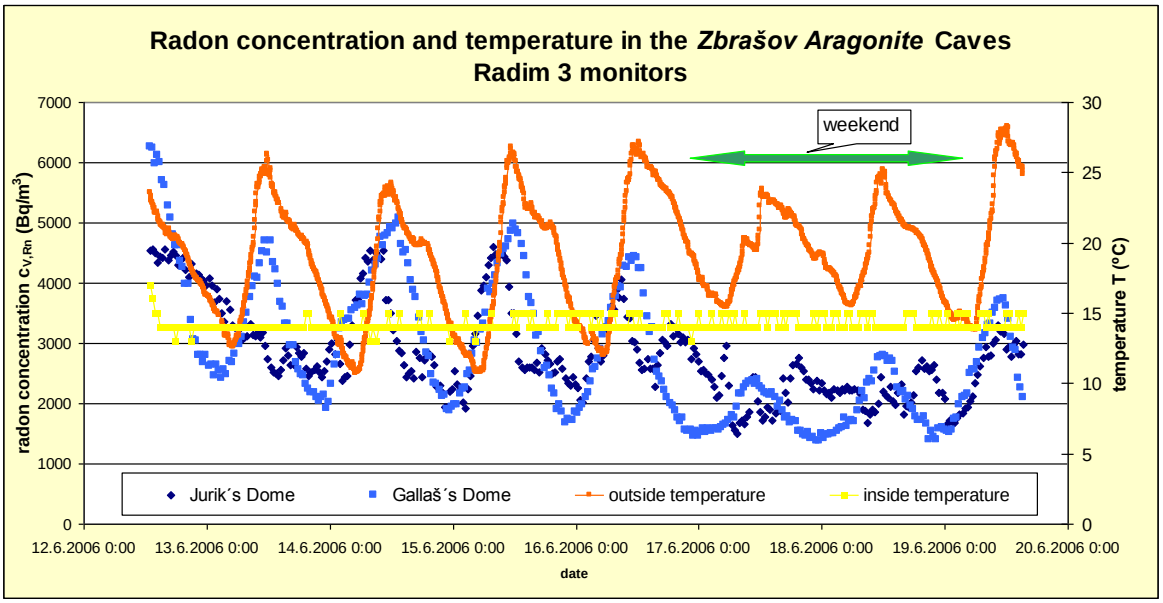

Figure 10 Correlation between outside temperatures and radon concentration inside the *Zbrašov Aragonite* Caves

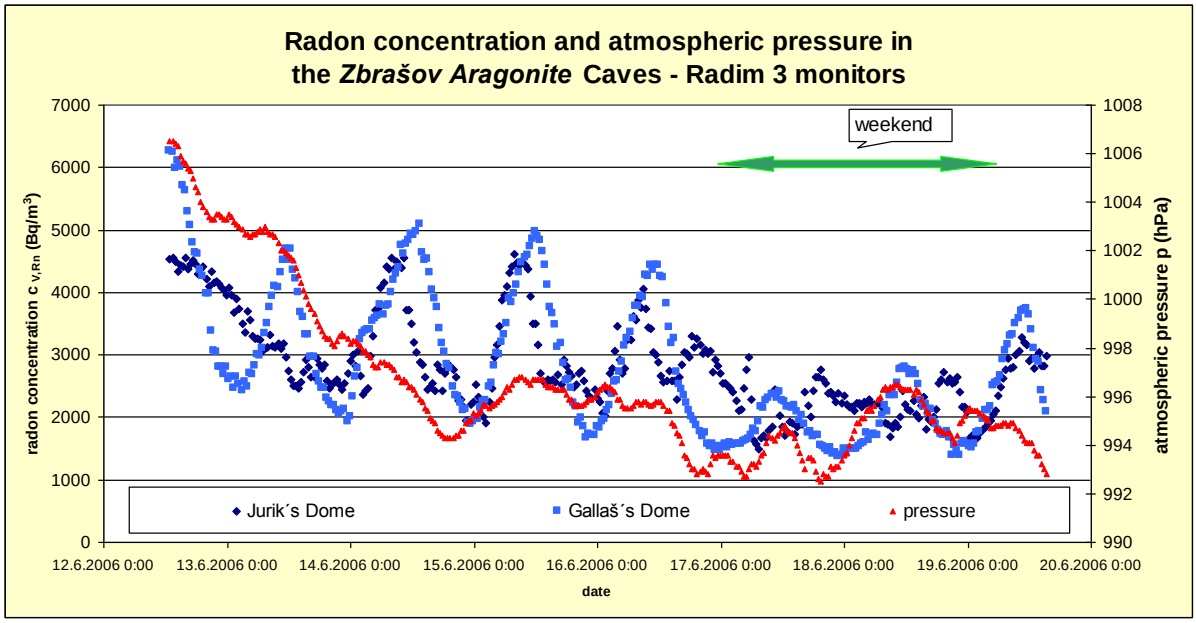

Figure 11 Correlation between atmospheric pressure and radon concentration inside the *Zbrašov Aragonite* Caves

An example of changes in radon concentration being influenced by atmospheric pressure and also by outside temperatures is shown in Figure 12, Figure 13, Figure 14 and Figure 15. The situation is most probably affected by the artificial ventilation system.

The shift between the radon concentration maxima in *Gallaš's* Dome and in *Jurik's* Dome is approx. 0.5 hour, which is the same as in June. As in June, the shift between the maxima in

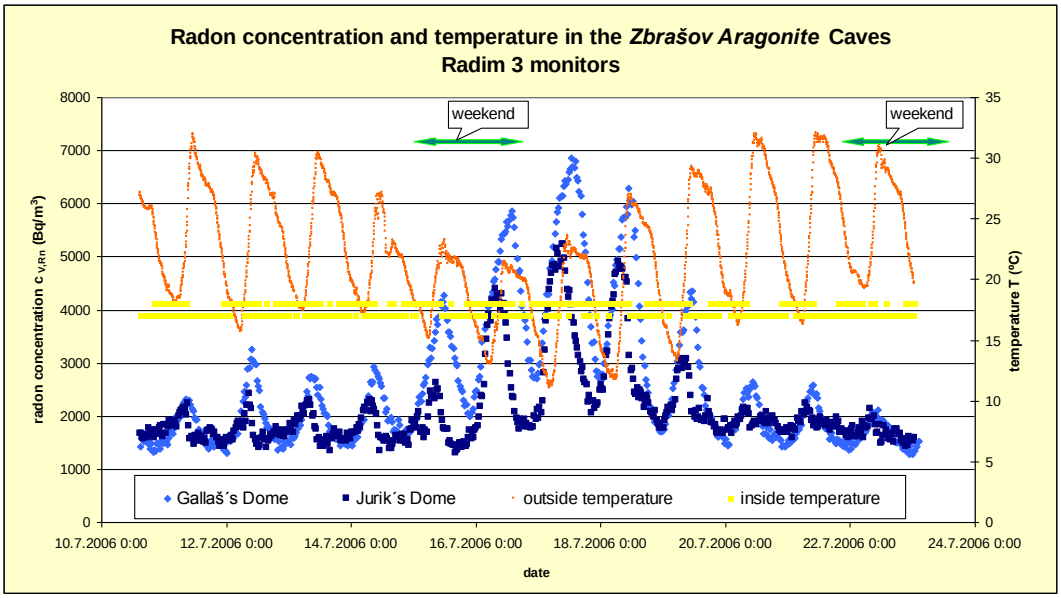

Figure 12 The continual simultaneous radon concentration, outside and inside temperature measurements in two different areas of the *Zbrašov Aragonite* Cave

temperatures and in radon concentrations in *Jurik's* Dome (further from the entrance, deeper part of cave) is approx. 3.5 hours. The shift between the temperature maxima and the radon concentrations in *Gallaš's* Dome is 0.5 hour. The shift between the radon concentration maxima in these two cave chambers is approx. 4 hours, whereas the maxima in *Jurik's* Dome come before the temperature maxima.

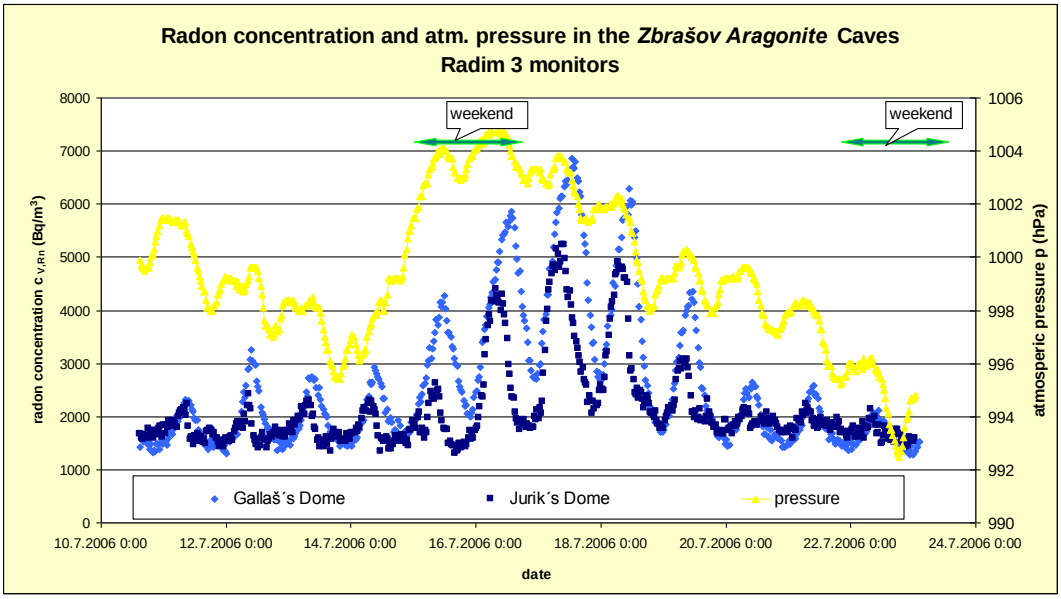

Figure 13 Course of the radon concentration and the atmospheric pressure in the *Zbrašov Aragonite* Caves, in July 2006

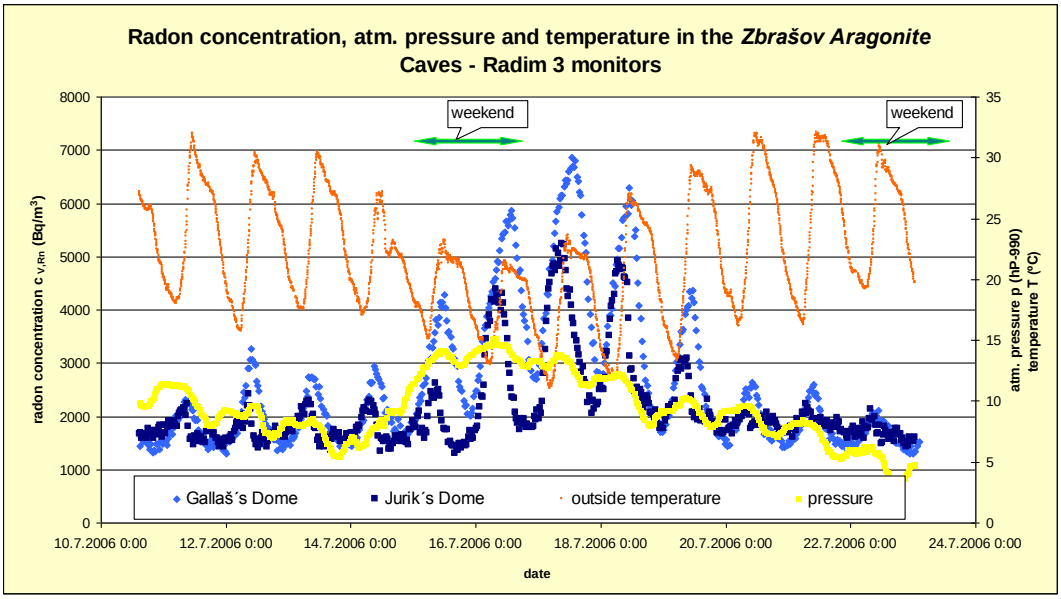

Figure 14 Environmental conditions in the *Zbrašov Aragonite* Caves

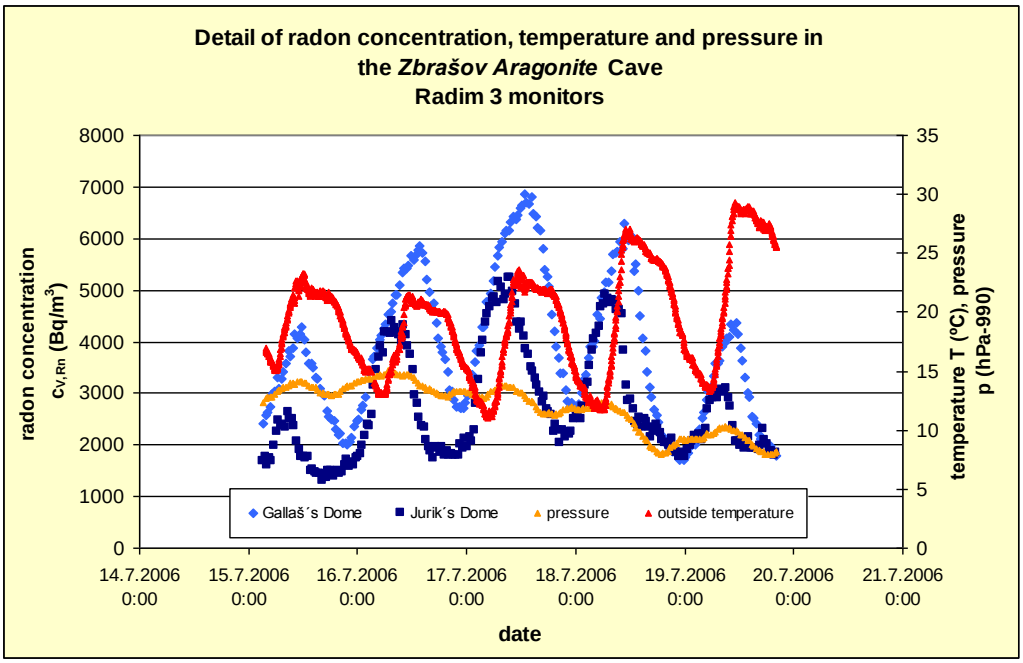

Figure 15 Environmental conditions in the *Zbrašov Aragonite* Caves, in detail

The *Bozkov Dolomite* Caves

The data time line for continual radon measurements, outside temperatures and atmospheric pressure obtained from long term monitoring in the *Bozkov Dolomite* Caves was processed, and the results were published in (Rovenska, et al., 2010). The main results were:

1) there is a strong correlation between both temperature and pressure difference, and radon concentration;

2) the time shift between changes in temperature and radon is in the range of 2 to 12 hours, depending on the season.

Simultaneous measurements in four areas in the cave are depicted in Figure 16. Despite the double door, which protects the cave environment, both curves – the *Chapel*, near the entrance, and the *Lake*, near the exit, – are affected by air exchange between the outdoor and indoor atmosphere. *Hell* is the deepest area of the cave, which communicates with inaccessible areas where radon is cumulated. Short-term increases of radon concentration in *Hell* occurred during the winter seasons, as a result of the release of air "pockets" from the inaccessible areas.

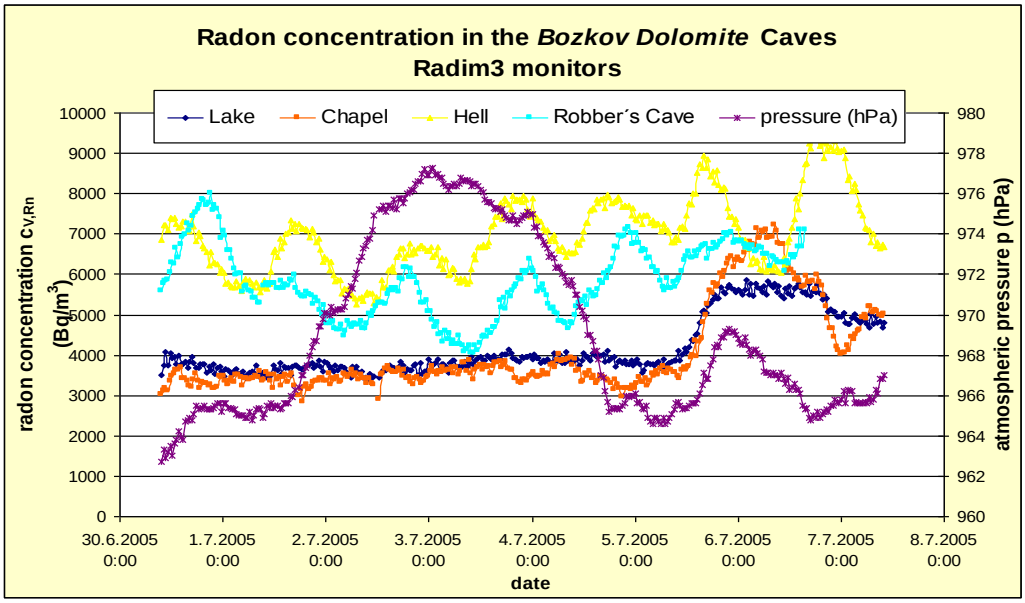

Figure 16 Simultaneous radon concentration measurements in the *Bozkov Dolomite* Caves

Seasonal variations

Seasonal variations may have a significant impact on integral radon concentration measurements. The radon concentration may change rapidly within a short time interval. In general, we distinguish two main seasons, summer and winter, when the air flow causes significantly different levels of radon concentration. Continuous monitored radon concentration data over a short period of time can be described successfully using statistical forecasting programs based on the process, including an evaluation of existing data (SPSS, StatGraphic etc. – see Figure 17, Figure 18).

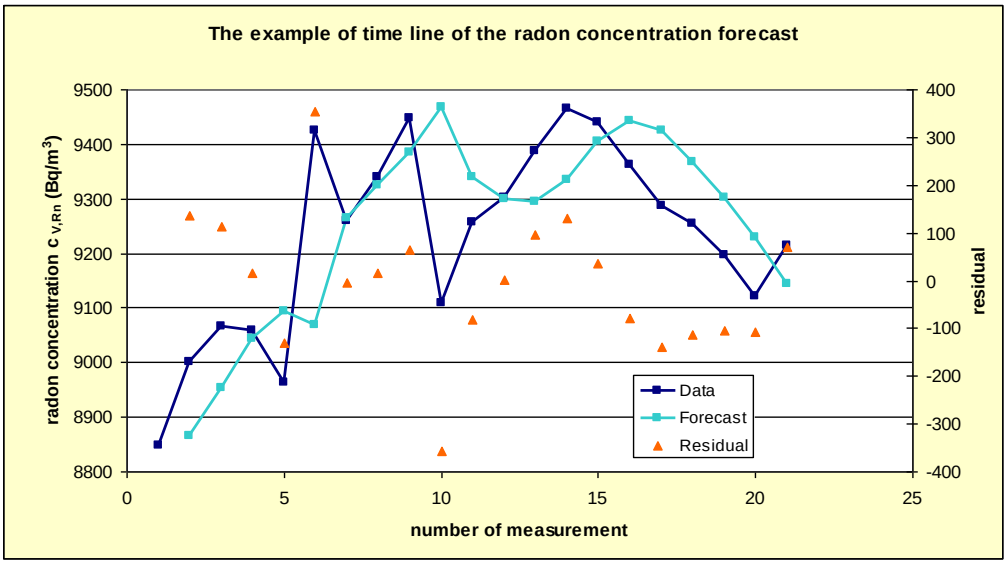

Figure 17 Example of a continuous radon monitoring forecast result (StatGraphic® statistical program)

However, the time line of radon concentrations is absolutely unpredictable toward the future (see Figure 18, last red part of the curve, which is a forecast). The seasons for integral measurements were determined on the basis of knowledge of continual radon monitoring over the previous few years. The selection of the season (see chapter 6.2.2) was statistically verified in 2012 (Štolba, 2012).

The *Bozkov Dolomite* Caves

The cave dynamics and the seasonal variations in radon concentration were studied on the basis of a long-term data set obtained in the *Bozkov Dolomite* Caves. Data of continual $c_{V,Rn}$ sequences measured using a Radim 3 continuous monitor in the *Bozkov Dolomite* Caves in 2008 - 2010 using 0.5 hour steps was processed statistically (Štolba, 2012). The Box-Jenkins methodology, based on examining the process interdependence, was used for the processing. This methodology creates a relationship where the monitored values show dependence on the monitoring results in the previous period and on the time dependence of a random component in the process. The initial tool in this methodology is correlation and regressive analysis. These modeling methods were presented under the designation ARIMA Models. These are auto-regressive models (processes) using sliding averages, which we use to analyze the time sequence values and form a prognosis for a future period. The result is a very interesting confirmation of the behavior of the cave environment, showing a significant parameter change in the ARIMA(1,1,2) model within the winter season for months January, February, March, April 2009 (see Table 3). For the winter period, the three-parameter ARIMA(1,1,2) model could be replaced by a single parameter model of a simple exponential smoothing that confirms the simpler curve shape for continuous radon measurements in caves in the winter period. Practically the same results were found as a result of radon concentration analyses in years 2008 through 2012.

Table 3 shows that the model parameters during the winter season are quite different - parameter *p* and parameter *q* even have the opposite sign. This situation can also be expressed by a 3D model (Figure 19). Points 1, 2 (January – April from Table 3) are outlying, and show different behavior of the measured radon concentration values during the winter season. In this time interval, the radon concentration could be described by a single parameter model of simple exponential smoothing, because the differences between the outside and inside temperatures are smaller than during the winter season, which results in minimum variability of the radon concentrations.

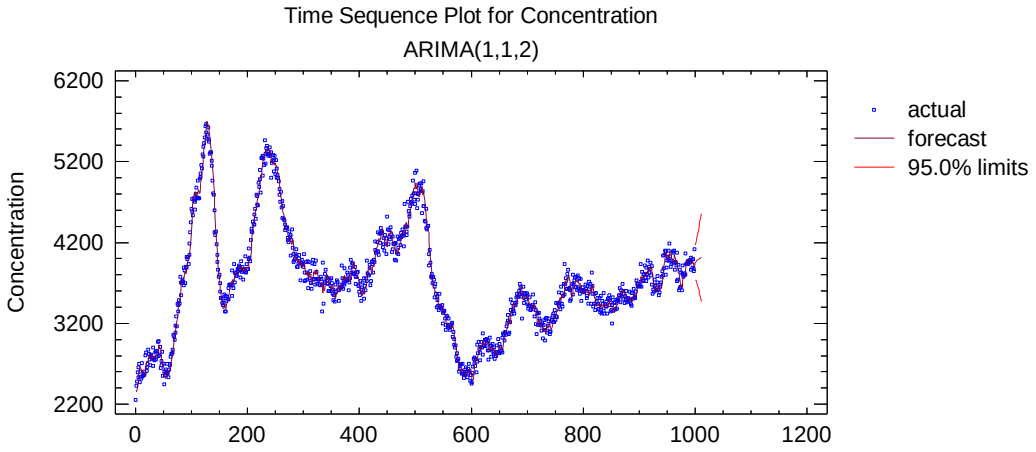

Figure 18 Example of applying the ARIMA(1,1,2) prediction model to radon concentration measurements in the *Bozkov Dolomite* Caves (Štolba, 2012). X axis – $c_{V,Rn}$ in Bq/m^3.

Table 3 ARIMA(1,1,2) model parameters *p, d, q* for 2009 (Štolba, 2012)

		AR(1)	MA(1)	MA(2)
1	Rn09JanFeb	-0.292284	0.532014	0.199994
2	Rn09MarApr	-0.199414	0.370018	0.094478
3	Rn09Apr	0.908544	1.51928	-0.63773
4	Rn09May	0.903666	1.5793	-0.692605
5	Rn09Jun	0.83528	1.48792	-0.634767
6	Rn09AugSep	0.846514	1.29217	-0.480196
7	Rn09Sep	0.795869	1.27614	-0.513944

Parameters AR(p), MA(d) and MA(q) express:

p - degree of the auto-regress part of the AR model

d - degree of difference

q - degree of smoothing of part of the MA model

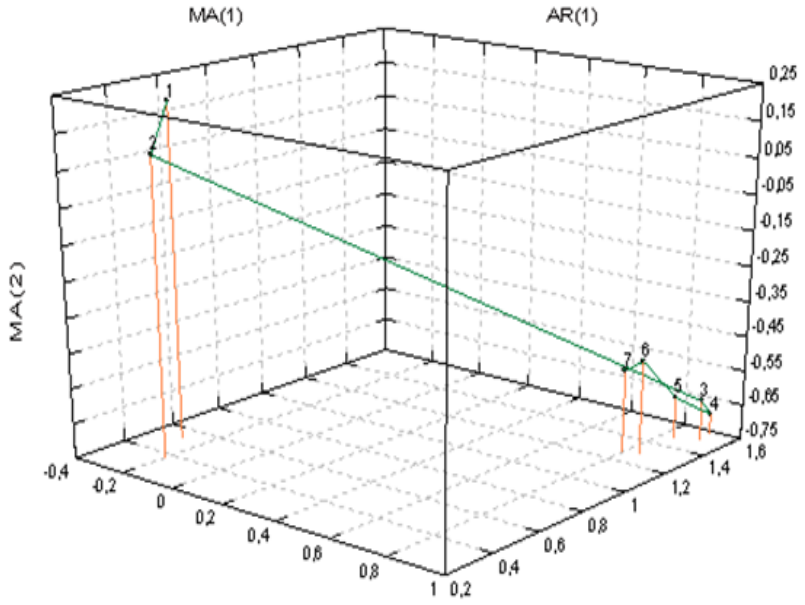

Figure 19 3D projection of the ARIMA model parameters for the time period January - September 2009 (Štolba, 2012)

4.3.4 Characteristics of the speleotherapeutic areas

The radioactivity in the Czech speleotherapy areas was measured by (Štelcl, et al., 2011). A laboratory method and an in-situ gamma spectrometry method were used in the speleotherapeutic centers in the *Císařská* Cave and in the *Sloup-Šosůvka* Caves (Moravian Karst). On the basis of the mean value of the equivalent mass activity of ^{226}Ra equal to 125 Bq kg^{-1} (approx. 10 ppm eU), clastic sediments (cave soils and fluvial sediments) were identified as the main source of natural radioactivity in both caves.

Climatic and environmental aspects of speleotherapy

Typical conditions in the underground spaces used for speleotherapy treatment are described in (Jirka, 2001):

- air velocity: < 0,15 m/s
- relative air humidity: 90-100%
- average temperature: 6-10°C
- pH: 4-4,5
- a slightly higher concentration of CO_2
- no harmful emissions (NH_3, NO_X, SO_X)
- the speleoaerosol is negatively ionized
- radioactivity

In terms of the cave climate (the endoclimate), speleotherapeutic spaces are subject to several requirements. The air velocity should not exceed 0.15 m/s, the relative humidity should be stable in the range of 90-100%, the average annual temperature of 6-10°C should have a

deviation of more than 1°C, pH around 4 - 4.5 prevents bacteria living and reproducing, slightly higher CO_2 (up to ten times the normal values in the outer atmosphere) stimulates calcium ionization, and also (with high humidity) deepens patients' breathing. An important finding is that the cave rooms are free of ozone, O_3 and NH_3 emissions, NO_X, and SO_X.

A substantial part of the cave air is humidity. Firstly, this ensures stability of the temperature conditions in the hall space, and consequently stimulates the development of the flora and fauna important for the self-cleaning capacity of the underground area, in the form of a vapor or an aerosol forming a matrix for ions affecting therapeutic effects. The cave aerosol known as the *speleoaerosol* is formed through the impact of water droplets forming a mist, and is naturally geo-electrically negatively ionized. Through contact with the rock, the aerosol obtains rocks ions. In lung tissue these ions reduce muscle spasms (especially through the activity of Ca ions) or otherwise support the positive effects on the condition of the patient's lungs and on the entire immune system.

The attached radioactive isotopes are bound to the speleoaerosol. This is now considered (together with the presence of aerosols and the ionization environment) to be one of the most important factors affecting treatment. Due to the complex dynamics of the underground spaces that are used for therapeutic purposes, it is necessary to know the value of the radiation when the human body is exposed to it. Speleotherapy counts with a positive effect of small amounts of radon (^{222}Rn and mostly ^{220}Rn isotope) and its daughter products in an ionization environment that also destroys bacteria. However, it is necessary to identify the sources of radon, to measure the presence of heavy metals in the environment, and to utilize gamma spectrometry to determine the natural radioactivity.

Table 4 Basic physical information about the speleotherapeutic environment (Jirka, 2001)

Sanatorium	temperature (°C)	rel. humidity (%)	ions concentration (cm^{-3})	$c_{V,Rn}$ ($Bq \cdot m^{-3}$)
Zlaté Hory -Edel	7.8-8.4	95	460-14000	35-580
Mladeč Caves	10	99		max 3800
Javoříčko Caves	7.4-7.7	100	2800-44000	112-7500
Sloup-Šosůvka Caves	7.3-8.3	99-100	14300-22000	148-2030
Císařská Cave	7.8-8.0	97-99	200-17350	350-2000

4.3.5 Brief characterization of aerosols in the environment

Aerosols are two-phase systems, consisting of particles and the gas in which they are suspended (Hinds, 1998). Atmospheric aerosols are a mixture of gases and particles (liquid or solid) that exhibits some stability in a gravitational field. Aerosol particles are formed by condensation of gases or vapours (fine particles) or by mechanical processes (coarse mode). They can change by growing (coagulation, condensation) or can even disappear on contact with a surface or be diluted by air movement. The concentration of aerosols can vary from some hundreds # per cm^3 (over the ocean) to millions # per cm^3 (Papastefanou, 2008).

Particle size is the most important parameter for characterizing the behavior of aerosols. All properties depend on particle size, some of them very strongly (Hinds, 1998). Depending on the source of the aerosols, one to three distinct maxima may form in the surface, volume or mass distributions (Table 5), (Figure 20). The mass of fine particles smaller than 2.0 μm in size is almost equal to the mass of coarse particles larger than 2.0 μm in size. Some particles serve as nuclei and cloud condensation nuclei, and carry electrical charges. Their stability depends on their having such a charge (Papastefanou, 2008).

Table 5 Atmospheric aerosol mode distributions consist basically of three separate modes (Papastefanou, 2008)

Mode	Diameter	i.e.	
Aitken nuclei	smaller than 0.1 μm	0.015 μm	
Accumulation	smaller than 2.0 μm	0.3 μm	larger than 0.1 μm
Coarse		10.0 μm	larger than 2.0 μm

Particles belonging to the *Aitken nuclei mode* originate primarily from the condensation and coagulation of highly supersaturated vapours. This mode rarely accounts for more than a few percent of the total aerosol mass.

Accumulation mode originates through mechanisms of coagulation and condensation of one material to another. Radioactive aerosols peak in accumulation mode, as this is the main mode in terms of surface area distribution. In accumulation mode, the geometric mean size is almost equal to the mass or volume geometric mean size.

In *coarse mode*, practically all particles at relative humidity up to 100% originate from mechanical processes. Coarse particles are produced by anthropogenic or natural mechanic processes, or originate from the condensation processes in the atmosphere.

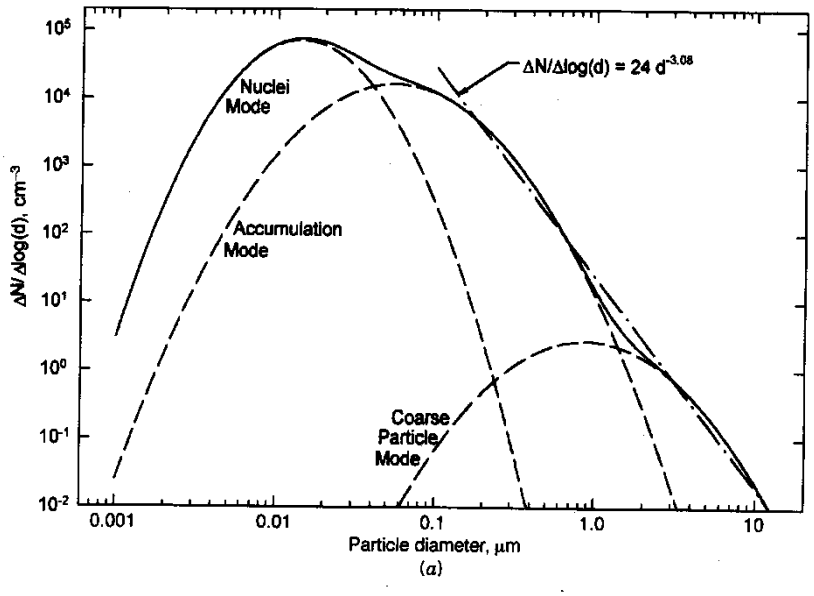

Figure 20 Average urban aerosol size distribution represented by three lognormal distributions (Hinds, 1998)

The activity size distribution of a radionuclide-associated aerosol particle is a surface distribution. Radioactive aerosols can be classified in the following categories (Papastefanou, 2008):

a) radioactive aerosols associated with radioactive nuclides of cosmogenic origin
b) radon and thoron decay product aerosols
c) fission product radionuclide aerosols

Category b) is the most important from the point of view of radon dose calculation.
The decay of ^{222}Rn and ^{220}Rn in the atmosphere produces low vapour pressure decay products (mostly positive charged), which coagulate or condense to create radioactive aerosols. These radionuclides include ^{218}Po ($T_{1/2}$=3.05 min), ^{214}Pb ($T_{1/2}$=26.8 min), and ^{212}Pb ($T_{1/2}$=10.64 h). The long-lived ^{210}Po isotope ($T_{1/2}$=22.3 y) is produced about one hour after attachment of ^{218}Po. The air is ionized by the radionuclides of different origin that are present, and the total energy dissipated per decay of ^{222}Rn depends on the equilibrium ratio of the radon decay products. The mobility of the decay product and the attachment to the aerosol particles is

mostly accomplished by diffusion, which is characterized by diffusion coefficient D (range from 0.03 to 0.085 cm^2s^{-1}) (Papastefanou, 2008).

The experimental measurement procedure provides no direct information about the structure or the concentration of the aerosol particles which carry the radioactive atoms. To obtain the activity-weighted size distribution, the information on how the activity is distributed according to the size of the aerosol particles, it is necessary to measure each stage of the impactor or wire screen of a diffusion battery. The acronym AMAD (activity median aerodynamic diameter) is used for reporting about the activity size distribution. AMAD marks the halfway diameter where aerosol particles with a greater aerodynamic diameter possess 50% of the total activity, and aerosol particles with a smaller aerodynamic diameter possess the remaining 50% of the total activity. AMAD is the same as the geometric mean of the diameter (Schery, 2001). Size distribution of the short-lived radon decay products under different conditions shows the Figure 21.

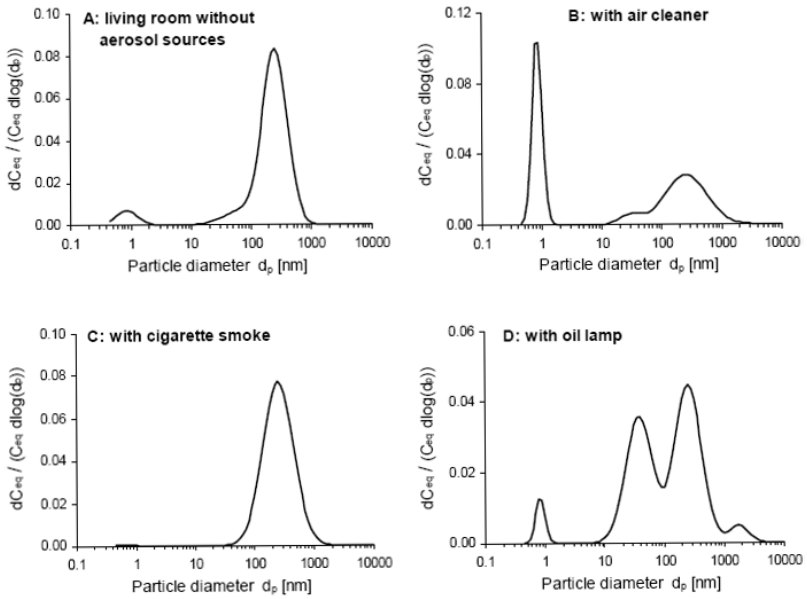

Figure 21 Size distribution of the short-lived radon decay products under different conditions. The size distributions were normalized to an area of beneath the curves (Haninger, 1997)

From the number of aerosol spectra measurements in different conditions, the following example of a result from outdoor air measurements was selected. (Grundel, et al., 2004) described the activity size distribution of short-lived radon decay products, consisting of about 12-19% in nucleation mode (0.05-60nm) and 81-88% in accumulation mode (60-1000 nm), and the coarse mode was missing. The activity median aerodynamic diameter (AMAD) of the

accumulation mode of short-lived decay products (337-343 nm) was significantly shifted to larger values for long-lived decay products and thoron (382-421 nm) (Papastefanou, 2008).

As a result of the measurements presented above, it is understandable that the activities of decay products in indoor or outdoor air are mostly absorbed on aerosol particles in the accumulation size range. From the measurement of NRBCPI and ICPF in 2012 (results as yet not published), it is apparent that there are no differences between "normal" and "activity" aerosol spectra.

The behavior of aerosol particles in air is described in Figure 22 and Figure 23.

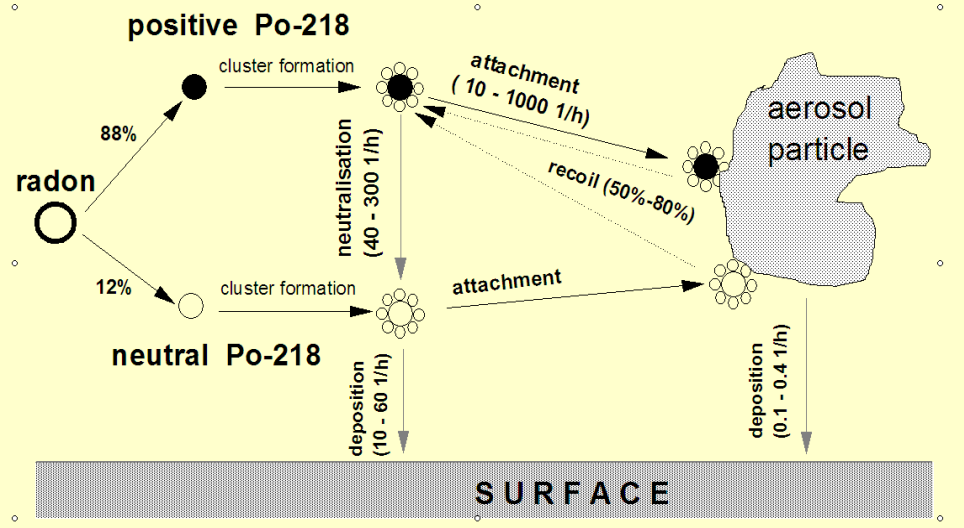

Figure 22 Behavior of radon daughters – cluster formation, absorption to an aerosol or deposition on the surface (Porstendörfer, 2007)

After their formation the unattached products are positively charged. They form charged and neutral clusters by reactions with water vapour and atmospheric gases in the air. The relative activity size distribution of the unattached radon progeny cluster as a function of the cluster diameter d depends on the concentration of water vapour, trace gases and the electrical charge distribution of the radionuclide in the atmosphere. The neutralization rate increases with higher humidity and radon concentration in air (Porstendörfer, 2001).

The positive fraction of the ^{218}Po clusters and the ^{214}Pb clusters in indoor air depends on the neutralization rate, which is a function of the ion production rate. The influence of humidity in the range RH = 30% - 95% (temperature: 20°C) is negligible (Porstendörfer, 2007).

The most commonly measured aerosol property, and the most important one for health and environmental effects, is mass concentration (g/cm^3). However, from the point of view of radiation protection (deposition in the lungs) the particle aerodynamic diameter is the most important value.

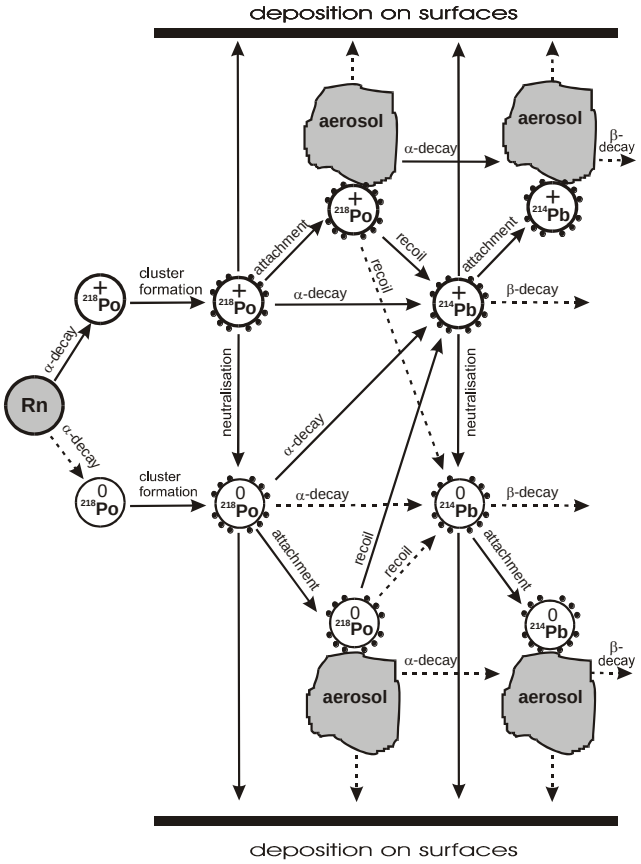

Figure 23 Processes of ^{218}Po and ^{214}Pb in air (Porstendörfer, 2007); (Papastefanou, 2008)

With reference to the diameter of an atom or the nucleus of an atom, the size of aerosol particles ranges from fractions of nm (the so-called unattached fraction – clusters of atoms or molecules), to several hundreds of μm (the so-called attached fraction – isotopes absorbed on the aerosol). The unattached fraction is usually up to 10 nm in aerodynamic diameter, but different researchers have reached different conclusions and the situation is influenced by the quality of the measurement methods. The measurement of the unattached clusters (d<10nm) under realistic environmental conditions is difficult (Porstendörfer, 2001).

For evaluations of the radiation health impact, the potential alpha energy concentration (PAEC) of the unattached fraction is defined as

$$f_p = PAEC_u / (PAEC_u + PAEC_a) \qquad \textbf{Equation 4}$$

where $PAEC_u$ is the potential alpha energy concentration of the unattached aerosol fraction, and $PAEC_a$ is the potential alpha energy concentration of the attached aerosol fraction (Böhm, 2003).

The unattached fraction is usually measured using an appropriate wire screen (grid) (usually 120 mesh/inch), a combination of filters, using electrostatic deposition, a diffusion tube, etc. The indoor unattached fraction varies on an average between 1% and 10% on the list of international measurement results (Papastefanou, 2008) Tab 2.5. The maximum is 33% in the open air and 49% in a tunnel. The recommended unattached fraction value for ambient air is 0.5 – 1%, for dwellings up to 5% (ICRP, 1981) or up to 3% (Reineking, et al., 1992).

The f_p values vary between 0% and 30%. Many working places have aerosol sources due to human activities and combustion and technical processes with a high particle concentration, Z > $4x10^4$ #/cm^3, and therefore f_p values below 1%. The f_p values are higher than 10% for workplaces with Z < $4x10^4$ #/cm^3. This is the case of poorly ventilated rooms, without aerosol sources or low ventilated underground caves (Porstendörfer, 2001).

Table 6 Best assessment of the indoor aerosol spectra characteristic (Marsh, et al., 1998)

	Unattached fraction	**Attached fraction**	**Attached fraction**	**Attached fraction**
		Nuclei mode	Accumulation mode	Coarse mode
Fraction of total PAEC	8%	25.8%	64.4%	1.8%
Fraction of attached PAEC		28%	70%	2%
Aerosol particle size	0.9nm AMTD	50nm AMAD	250nm AMAD	1500 AMAD
Dispersion σ_g	1.3	2.0	2.0	1.5
Particle density (g/cm^3)	1	1.4	1.4	1.4
Shape factor	1	1.1	1.1	1.1
Growth factor	1	1.5	1.5	1.5
F	0.4			

The unattached fraction is independent from the radon concentration in the air, but depends on the aerosol conditions in the studied environment, which influence the value of the equilibrium factor.

The main parameter that influences the unattached fraction value is the attachment rate, which depends on the number concentration of aerosol Z (cm^{-3}), and can be estimated by equation 4. This relationship was derived from aerosol particle concentration measurement results in various conditions – indoors, outdoors and in mines (Porstendörfer, 2001):

$f_{p,Rn} = (k_1\lambda_1 + k_2\lambda_2 * r)/ \beta * Z = 414/Z$ **Equation 5**

where $k_1 = 0.105$; $k_2 = 0.516$; $r = 0.8$ (recoil factor); $\beta = 1.4*10^{-6}$ $cm^3.s^{-1}$ (average attachment coefficient for an atmospheric aerosol).

For the unattached thoron fraction, we can use the equation

$f_{p,Tn} = 150/Z$ **Equation 6**

The activity size distribution of the radon products unattached fraction depends on humidity, trace gases and the electrical charge distribution of the radionuclides in the air.
The dose from radon caused by inhalation of radon is significantly influenced by the unattached fraction value (Figure 24, Figure 25). The dominant contribution to the effective dose is the contribution to the lung. The decay products are deposited in different regions of the lung, depending on their size and on the person's breathing rate.

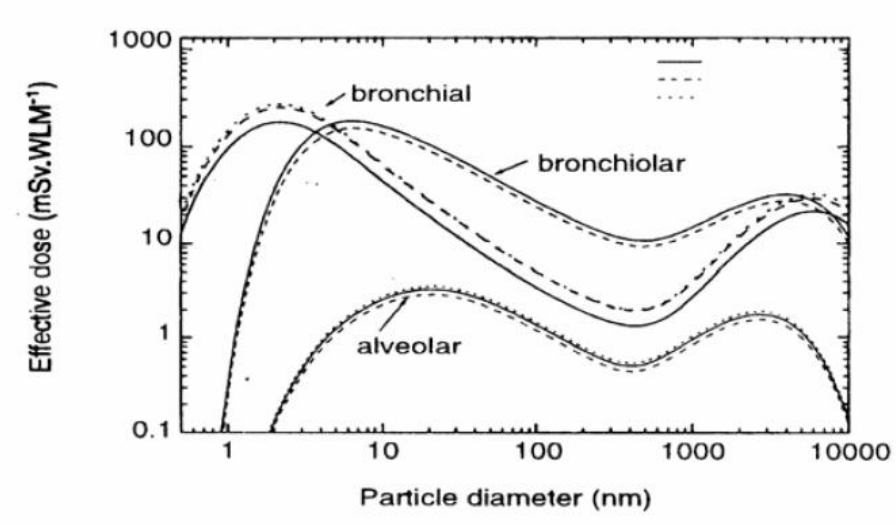

Figure 24 Effective dose per unit exposure of thoracic regions as a function of particle diameter ($w_t = 0.12$, $w_R = 20$, nasal breathing v = 0.75 $m^3.h^{-1}$ (Porstendörfer, 2001)

____ ^{218}Po; -----^{214}Pb; …… $^{214}Bi/^{214}Po$

The dosimetric approach to dose calculation is based on the Respiratory Human Respiratory Track Model (ICRP, 1994), which divides the lung into three main compartments (bronchial BB, bronchiolar bb, and alveolar-interstitial AI). The weighting factor ratio for the individual compartments are 0.333BB : 0.333bb : 0.333AI : 0.001 LN(TH) (LN(TH) is area of nodes) (ICRP, 1994). In (Porstendörfer, 2001) the relative cancer sensitivity between compartments is expressed in the ratio 0.8BB : 0.15bb : 0.05AI, which leads to higher effective dose caused by particles less than 5nm in diameter (Figure 24). The dose conversion factors are also dependent on breathing type – via nose or mouth. Figure 25 shows that the difference is mainly for small (nanometers) and large (tenths and hundreds of micrometers) particles.
The smallest particles (around 1nm) are well captured in the nose or mouth and their contribution to the dose is negligible. However, as a result of chemical or physical processes in the environment they can extend their size up to 3-5 nm and then contribute more to the dose in BB region. Particles larger than 10 nm are deposited deeper in the lung, in the AI region. However the surface activity in this region is low, because the activity is deposited on a large surface. The diffusion and the deposition ability of the aerosol particles into the lung decreases as the particles grow (Böhm, 2003).

The main parameters are the activity size distribution of the radon daughters and the original deposition destination, i.e. the particle size distribution. The calculation is based on the dose conversion factor, DCF, which expresses the relationship between the potential alpha energy concentration (PAEC) of the short-lived radon decay products exposure $C_p t$ and the dose

$$DCF = D / C_p t \qquad \textbf{Equation 7}$$

where D is dose, and t is time of inhalation (Porstendörfer, 2001).
For practical DCF calculations, three main factors must be considered (Papastefanou, 2008):

- the size distribution of the unattached fraction,
- the size distribution of the radioactive aerosol particles,
- unattached fractions in terms of PAEC.

Not only the unattached fraction but also a different aerosol size distribution has a great influence on the values of the dose conversion factors (Porstendörfer, 2001). The parameters that affected DCF_D most, are: unattached fraction of short-lived radon daughters (f_p), the

nucleation aerosol size, the nucleation fraction, the unattached aerosol size, and (March, et al., 2002). These factors depend on the interaction processes of radon daughters in air (attachment to aerosol particles, cluster formation, neutralization, plate-out on surfaces, etc.) and on the air conditions (humidity, aerosol distribution, presence of gases, etc.). The radiation weighting factor w_r=20 for alpha particles and the tissue weighting factor w_t=0.12 must be taken into account when the dose is calculated. The critical target cells for lung cancer induction processes are the nuclei of secretoric and basal cells.

A comparison between different environments (indoor, outdoor and workplace environment), obtained from continuous measurements over a period of three weeks, is shown in Table 7 (Papastefanou, 2008). $AMAD_a$ for indoor air (210 nm) without cigarette smoke or any other source of aerosols is shifted to a smaller size than for workplaces (300 nm). The results of the measurements carried out at 19 different workplaces show also activity size distributions with three modes (Porstendörfer, 2001).

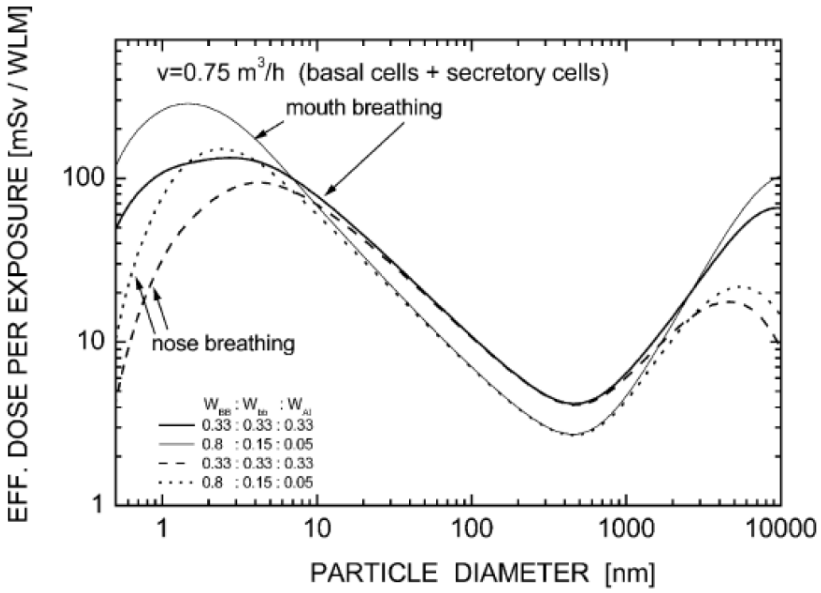

Figure 25 Effective dose per unit exposure as a function of particle diameter for different relative cancer sensitivity distributions between the bronchial (w_{BB}), bronchiolar (w_{bb}), and alveolar (w_{AI}) region of the thoracic lung (w_t = 0.12, w_R = 20) (Porstendörfer, 2001)

Table 7 Parameters of the activity size distribution of aerosol-attached short-lived radon decay products in air in different locations

n…nucleation mode; a…accumulation mode; c…coarse mode; Z…aerosol particle concentrations

Mode		outdoor air		indoor air		workplaces	
	Z (10^3.cm^{-3})	10-70		2-500		10-500	
nucleation	$AMAD_n$ (nm)	30-40		20-40		15-40	
	σ_{gn}	1.9-2.2		1.7-2.1		1.6-2.2	
	f_{pn}	0.3	0.2-0.4	0.3	0/0.4	0.3	0.2-0.5
accumulation	$AMAD_a$ (nm)	310	250-450	210	120-350	300	150-450
	σ_{ga}	2.1	1.8-3	2.2	1.6-3.0	2.5	1.8-4
	f_{pa}	0.67	0.4-0.8	0.7	0.6-1	0.6	0.3-0.8
coarse	$AMAD_c$ (nm)	3000	2000-6000			5000	3000-8000
	σ_{gc}	1.7	1.6-2.0			1.8	1.1-2.8
	f_{pc}	0.03	0-0.1			0.1	0-0.3

Examples of conversion factor values for a comparison between indoor, outdoor and workplace environments are summarized in

Table 8. Typical aerosol conditions, e.g. aerosol concentration and activity size distribution were assumed for the places that were presented. Nose breathing and the relative cancer sensitivity distribution (0.8:0.15:0.05) were taken into account (Papastefanou, 2008).

A comparison between DCF_u, DCF_{ae} and DCF_{total} (based on Table 8) is shown in Figure 26.

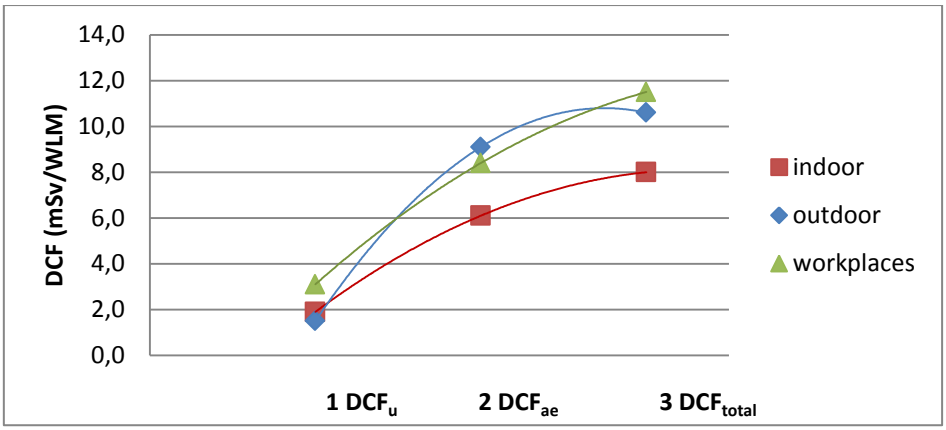

Figure 26 The difference between DCF_u, DCF_{ae} and DCF_{total} in different environments

Table 8 Average dose conversion factors for the inhalation of unattached and aerosol-attached radon daughters

n…nucleation mode; a…accumulation mode; c…coarse mode; Z…aerosol particle concentrations

u…unattached ; ae…aerosol-attached radon daughters

	outdoor	**indoor**		**workplaces**			
	no sources	no sources	sources	no sources	sources	sources	
	30% n-mode	30% n-mode	100% a-mode	30% n-mode	30% n-mode	100% a-mode	
	67% a-mode	70% a-mode		70% a-mode	60% a-mode		
	3% c-mode				10% c-mode		
particle concentration	20 (10-40)	8 (3-20)	80 (20-500)	8 (3-20)	40 (20-60)	80 (50-500)	
Z (10^3.cm^{-3})							
nose breathing	1.2	0.75	0.75	1.2	1.2	1.3	1.7
v (m^3.h^{-1})							
DCF_u	1.5	1.9	0.2	3.1	0.6	0.3	0.6
(mSv/WLM)							
DCF_{ae}	9.1	6.1	4.0	8.4	10.6	5.4	6.5
(mSv/WLM)							
DCF_{total}	10.6	8	4.2	11.5	11.2	5.7	7.1
(mSv/WLM)							

The obtained DCF values for homes and workplaces with high aerosol particle concentrations are comparable with DCF = 3.8 mSv/WLM (homes) and DCF = 5 mSv/WLM from epidemiological studies and recommended by ICRP. But for places with lower particle concentrations the DCF are about 2xhigher (Porstendörfer, 2001).

5. Measuring methods and equipment

5.1 A general overview of devices and software

A list of environment characteristics and measuring devices/software used in this study

1. Laboratory gamma spectrometry measurement: coaxial HPGe detector 35% efficiency – 0.6 l Marinelli containers geometry, verification № 911-OL-Z 3122/200, Ortec
2. Air flow measurement: Testo 452, Testoterm, Germany
3. Kerma rate in air measurement: Tesla NB 3201 (№ B5-053) probe with energetic compensated plastic scintillation detector, Tesla Přemyšlení, CR
4. Gamma dose rate, X-ray and beta radiation measurements: RDS – 110, multi-purpose detector, Geiger tube, Germany
5. Activity concentration of radon in soil gas and in air: measuring set consisting of ERM 2 and IK 250 ionizing chambers, Froňka-Nuclear Technology, CR
6. Radon daughters measurement: PSDA with a pump, Tesla Přemýšlení, CR
7. Measurements of radon activity in water samples: RADIM4, SMM Ing. Jiří Plch, CR
8. Continuous radon activity concentration measurements in air: 8.4 l volume ionizing chamber in flow regime Radonic01; Froňka-Nuclear Technology, CR
9. Continuous radon concentration measurements in air: RADIM3(3A) monitor, Si detector, measurement step 0,5 h; SMM Ing. Jiří Plch, CR
10. Continuous radon activity concentration measurements in air: AlphaGuard, Saphymo GmbH, Germany
11. Continuous measurements of the unattached and attached fraction of radon daughter products in air: FRITRA4; SMM Ing. Jiří Plch, CR
12. Integral radon concentration measurements: Electret detectors – volume of chamber 0,5l; Froňka-Nuclear Technology, CR
13. Integral radon concentration measurements: RAMARN detectors, based on Bare Kodak LR 115, CR
14. Integral radon concentration measurements: SSNTDs, based on Bare Kodak LR 115, CR

15. Radon supply monitoring: FLIR ThermaCAM P25 IR camera, U.S., property of NRPI
16. Aerosol spectra measurements: SMPS, Nano SMPS (Scanning Mobility Particle Sizer), TSI Incorporated, U.S., property of the Institute of Chemical Process Fundamentals (ICPF) of the Academy of Sciences of the Czech Republic
17. Aerosol spectrum measurements: APS (Aerodynamic Particle Sizer); TSI Incorporated, U.S., property of the Institute of Chemical Process Fundamentals (ICPF) of the Academy of Sciences of the Czech Republic
18. Software: LUDEP 2.0 – program for dose calculation, based on the ICRP66 breathing model
19. Software: Genie2000 – program for gamma spectra analysis and mass activity of samples calculations, Canberra-Packard GmbH

5.1.1 Characteristics of selected radon monitors

PSDA

The measurement set consists of an analyzer based on an Si semiconductor detector and pump for air-grab sampling. The air is drawn for five minutes through a Millipore filter (3 l/min). Then the filter is inserted into an analyzer and is measured according to a time schedule, enabling the radon daughters concentration to be calculated. The apparatus enables equilibrium factor F to be determined while the radon concentration is simultaneously measured. One sample measurement takes 1 hour.

ERM2

The system is designated to measure soil air radon concentrations. The two main components of the ERM-2 Soil Radon Monitor are the ERM-2 Soil Radon Reader and the IK-250 Sampling Ionization Chambers. The ERM-2 Soil Radon Reader measures the ionization electric current produced by radon and its daughter products in the IK-250 Sampling Ionization Chamber. The soil-air with radon is sampled using a standard procedure.

IK-250 ionization chamber in measurement position

The ionization current is a measure of the activity of both radon and its daughter products. If the sampling requirements for the volume of soil-air and the time elapsed from the moment of sampling are satisfied, the ERM-2 Soil Radon Reader displays the soil-air radon concentration in kBq/m^3. The IK-250 Sampling Ionization Chamber is a rugged metallic, vacuum-tight container, with a built-in collecting electrode. The chamber can be opened to clean the grease and radon daughter products deposited on its inside surfaces. Due to the high concentration of radon-in-soil gas, the required minimum detection activity is 2 kBq/m^3.

RADONIC01

RADONIC01 is a type of continuous radon monitor, based on an ionization chamber detector, operating in current mode. The significant characteristic feature of the detection principle is its very fast response. Any real-time variations in radon concentrations are insignificantly influenced by the "memory effect", caused by radon decay products. The device enables standard monitoring of long-term variations (several weeks) of radon concentrations; monitoring and analysis of dynamic effects characterized by rapid variations in radon concentration (human activities in dwellings, ventilation and heating regime); rapid assessment of radon concentration values; radon transport and distribution monitoring (mapping of radon concentrations) – useful for building evaluations and for cave environment quality inspection. The RADONIC01 continuous radon monitor utilizes a cylindrical ionization chamber with an internal volume of 8.4 liters for the measurements. The chamber housing is a formed aluminum box with 1mm metal wall thickness. The unit's collecting electrode passes through a Teflon insulator inserted into a metal tube, functioning as a protective electrode. The direct operating voltage of the detector is 150V. The RADONIC01 radon monitor operates in active mode; external air is drawn in through an input ventilator, and passes through a set of filters into the detection chamber of the device. The filtration unit ensures dust suppression and effective radon progeny capture. The range of measured concentrations is between 30 – 12,000 Bq/m^3. Radonic01 is easily portable. The measurement results are saved in memory, and current values are displayed on the front panel.

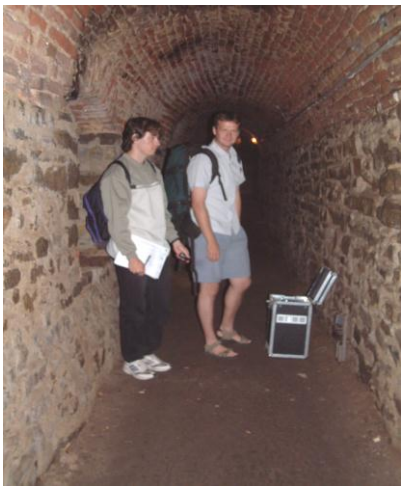

Measurements in Casemates under Vyšehrad, using RADONIC01

RADIM 3

RADIM (version 3 or 3A) continuously detects and records the following parameters, using selected measurement steps: radon activity concentration, temperature, air pressure and relative humidity. The radon measurement is based on the principle of electrostatic deposition of the radon decay product ^{218}Po on the surface of a Si-semiconductor alpha-detector. The subsequent ^{218}Po activity is determined by means of alpha spectrometry. Becasue it uses a specific determination of the short-lived decay product ^{218}Po, the RADIM3(3A) Radon Monitor has a very short response time to even large variations in radon concentrations. The air containing radon diffuses into a hemispherical chamber, which is adjacent to the detector. Inline filters prevent access of dirt and radon decay products. Because the emerging ^{218}Po resulting from the radon decay consists predominantly of positively charged ions, the surface of the chamber is connected to a positive output of a 2kV voltage source, while the surface of the detector is connected to the negative output. The resulting electrical field ensures a movement of polonium ions on the detector surface. The number of polonium ions is dependent on the air humidity. Particles with zero charge in terms of detection are lost. The measurement results are automatically corrected for prevalent moisture (up to 70%) and temperature. For use in a damp environment, e.g. in caves, a RADIM monitor must be placed in a plastic box containing a bowl with a desiccant. The device is not waterproof; the desiccant keeps the humidity around 50-60%, and thus protects the Radim internal electronics from corrosion, while it is inert toward radon. Care must be taken when servicing the unit, since long-term measurements in areas with high radon concentrations tend, over time, to contaminate the detector. Results are provided using intervals of 30 minutes or longer.

RADIM3 devices in a plastic box with a desiccant to decrease the humidity, and in a "free" cave atmosphere (in Bozkov Dolomite Caves)

RADIM 4

The RADIM4 continuous radon monitor is based on the same principle as the Radim3 monitor. In addition, Radim4 can measure the concentration of radon in water samples. The defined volume of 0.2 l water is bubbled for 5 minutes in a closed cycle through the measurement chamber, which contains a semiconductor detector. The total measurement period is 30 minutes for one sample. The results in Bq/l are guaranteed with relative error 20%.

Radon in water measurements outside the Kateřina's Cave

FRITRA4

The FRITRA4 unit measures the radon activity concentration in the following way:

The measured air is pumped into a chamber with volume V = 0.8 liters for 20 minutes. After it is created, most of the ^{218}Po is in the form of positively charged ions. A power supply positive output with potential 2kV is connected to the wall of the chamber, and the detector is connected to the negative output, which is also the unit's ground. Polonium is collected on an area detector. After the air collection phase is completed a 70-minute period is initiated, during which the alpha particles from polonium decay are detected. The equivalent activity of radon daughters in total (EEC), or as the attached and unattached fraction, is determined by measuring the alpha activity deposited on a Millipore filter and on a grid, which is followed by a second filter. The pulses are detected spectrometrically – the energy windows are set to peak ^{218}Po, ^{214}Po. The unattached fraction can either be determined by measuring the activity captured by the grid or calculated as the difference between activities captured on the filters.

FRITRA4, AlphaGuard, RADIM3 and RAMARN in the Bozkov Dolomite Caves

AlphaGuard

AlphaGuard is a continuous radon monitor. It works on the principle of an ionization chamber with a volume of 0.56 liters. Air is brought into the chamber through diffusion filters, which prevent access of dirt and radon decay products. The results are provided at intervals of 1 hour, and are stored in memory, from which they can be downloaded into a computer, after the measurements have been completed, and then used for further processing. The AlphaGuard monitor provides very reliable results with uncertainty of 5%, and is therefore often used as a standard in national laboratories. In our case, it was also used as a control gauge of continuous radon concentrations.

RAMARN

RAMARN is the certified detector for radon concentration measurements in the Czech Republic. It consists of a plastic chamber, which is conically cylindrical in shape and about 0.5 l in volume. Radon gas diffuses into the chamber throughout the exposure period, while the plastic box serves as a barrier for radon progeny attached to the aerosol particles. Bare LR 115Kodak film is placed on the bottom of the diffusion chamber (see the schematic view).

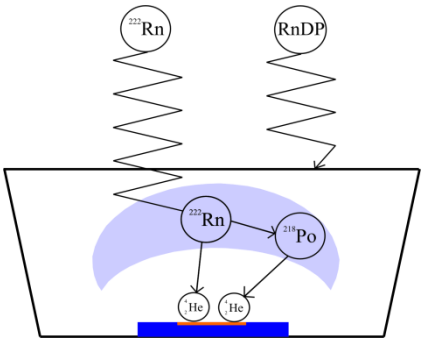

Schematic view: RAMARN measurement system

The size of the container was chosen to prevent the radon daughters deposited on the container walls from influencing the measurements. Kodak film has a spectrometric character - the tracks are visualized only for alpha particles with energies between 1 and 3 MeV that touch the foil; thus the effective volume is lens-shaped. The RAMARN detection system was accredited in 2004 (bare SSNTDs were used until 2003) (Figure 27). The range of sensitivity of the method is from 500 $kBq.h^{-1}.m^{-3}$ up to 160 $MBq.h^{-1}.m^{-3}$. Of course, no influence of differing unattached fractions in time and space is included in the calibration.

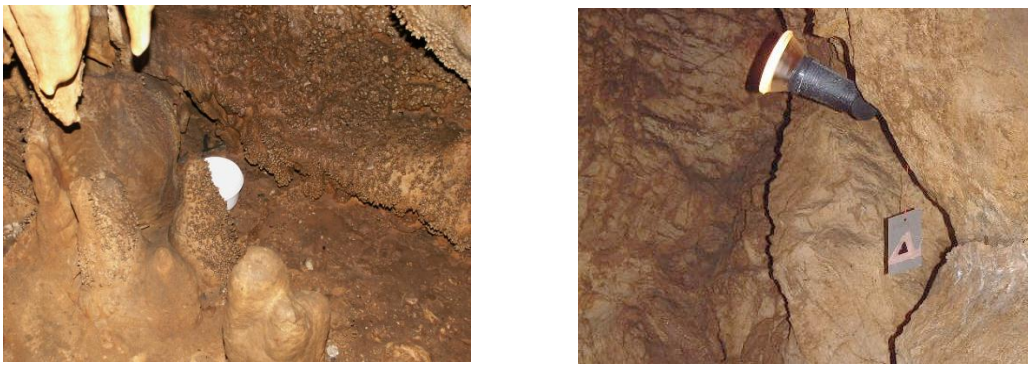

Figure 27 New RAMARN detectors, and the old SSNT detectors used in a cave

5.1.2 Calibration and verification of radon measuring equipment

Before field measurements were carried out in the caves, the FRITRA4 device was tested in the NRPI Radon Chamber (Ing. Karel Jílek). Further calibration of Fritra4 was performed, as a part of the service, during the measurement period. There was a grid fault, and the test instrument was repaired and calibrated by the manufacturer. The most important phase in verifying the correct function of the device was a 5-day comparative testing period in the *Bozkov Dolomite* Caves, where all FRITRA4 owners in the Czech Republic provided their units for testing, and also for another controlled comparison in the radon chamber. This multi-step method for checking the functions of the device was chosen deliberately, because in difficult field conditions in high humidity the devices must be monitored for any possible systematic shift in the measured values. The RADIM3 continuous monitors were also checked and calibrated.

AlphaGuard was also used as a control gauge for continuous radon concentration measurements. The results of these comparative measurements, confirming the actual measurement characteristics of RADIM3 and FRITRA4 monitors, are presented in (Thinová, 2007). An example of the results is shown in the Figure 28.

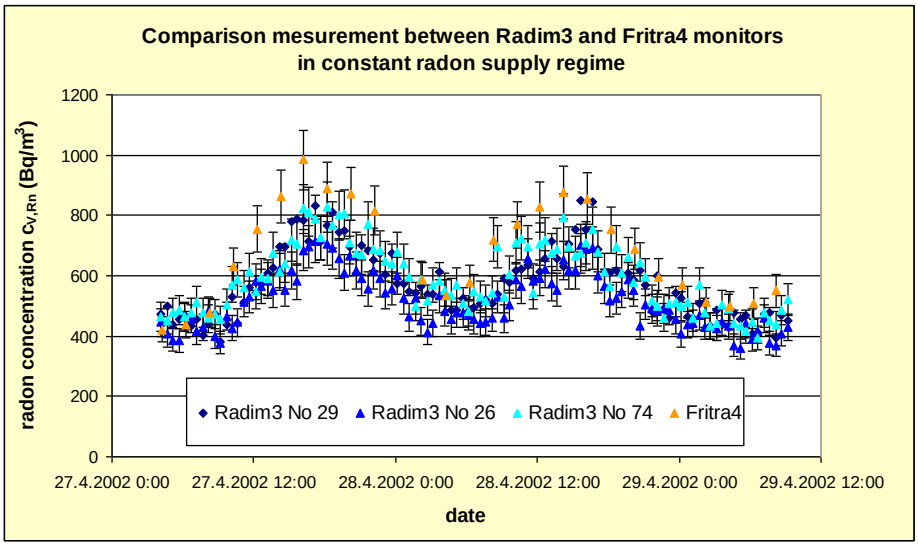

Figure 28 Comparison measurements between FRITRA4 and three RADIM3 units

Infrared Camera

A FLIR ThermaCAM P25 IR Camera was used for IR detection of the radon supply in the Zbrašov Aragonite Caves. The main characteristics of the camera are as follows:

- Temperature sensitivity 50/60Hz 0,08° C at 30°C
- Spectral range 7,5 - 13 um
- Precision (% of value) ± 2 ° C or ± 2%
- Measurements conducted in the range of -10°C to 55°C

FLIR ThermaCAM P25 IR Camera in the Zbrašov Aragonite Caves

5.1.3 Equipment for aerosol measurements

In order to evaluate the complex aerosol characteristics and behavior, a special assembly of dedicated test devices was integrated to form a test station. The following equipment was used:

The SMPS 3936NL Assembly (Scanning Mobility Particle Sizer), consisting of DMA 3085 and CPC 3025. In this kit, the air flow was set to 1.4 l/min and it detected aerosol particles 3 nm to 66nm in diameter. The second set SMPS 3934, comprising EC 3071 and CPC 3022, was used with airflow 0.3 l/min. SMPS 3934 detected aerosol particle diameters of approx. 14 nm to 530 nm. APS 3321 was used for measuring aerosols of larger size. At a

flow rate of 5 l/min, APS 3321 recorded particles in the range of approx. from 550 nm to 20 μm.

APS 3321 aerodynamic sorter

An aerodynamic particle separator (Aerodynamic Particle Sizer) measures aerosol particles according to their aerodynamic diameter. The unit's nozzle tapers, and the gas movement accelerates. The fewer particles adapt to the gas output velocity, the greater its aerodynamic diameter is. Two lasers are located behind the nozzle, with a mutual beam distance of approx. 10 μm. The particle size can be determined from the "relative flight time" of the particle between the two beams. This method is sensitive to aerodynamic diameters in the range from 300 nm to 20 μm. Smaller particles essentially accelerate with the speed of the gas, and cannot be accurately differentiated.

The device, on loan from ICPF ASCR, measured only the total number of particles in the range from 300 nm to 500 nm.

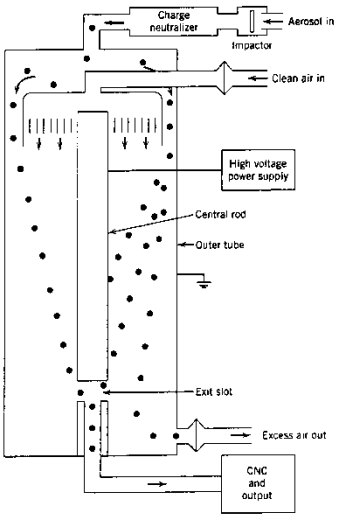

Schema: Scanning Mobility Particle Sizer (Hinds, 1998)

The equipment was used to evaluate the concentration of aerosols from 500 nm to 10 μm in the individual size fractions, resulting in a total of 50 categories. The device performs measurements using an air flow rate of 5l/min.

The manufacturer states the following range of operating conditions: temperature 10-40°C, pressure from 0.6 to 1.04 atm., relative humidity 10-90%, maximum particle concentration up to 1000 #/cm^3.

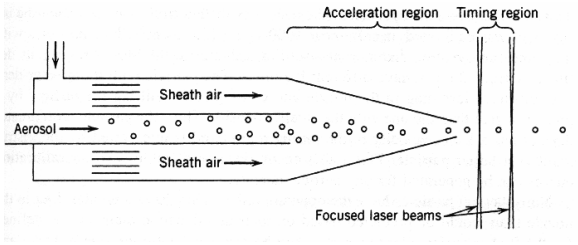

Schema: Aerodynamic Particle Sizer (Hinds, 1998)

CPC Condensation counter

The principle of the Condensation Particle Counter lies in increasing the "visible" size of a particle. The observed aerosol is mixed with saturated vapor (butane). The mixture is cooled in order to condense the vapor on the aerosol particles, and thus to increase their size. This causes the butane vapors to become saturated and to begin condensing on the particles. Condensation also partly forms on the walls of the chamber. As a result, the enlarged aerosol

particles are aerodynamically shifted into the focus of the laser beam in an optical cell. While passing through the optical cell, the particle reduces the intensity of the transmitted light, and it is registered. The unit can detect particles from 3 nm in size. The velocity used is from 0.3 to 1.5 l/min. Conditions recommended by the manufacturer: temperature 10-37° C, pressure from 0.7 to 1.1 atm., relative humidity up to 90%, maximum concentration of 10 million #/cm^3.

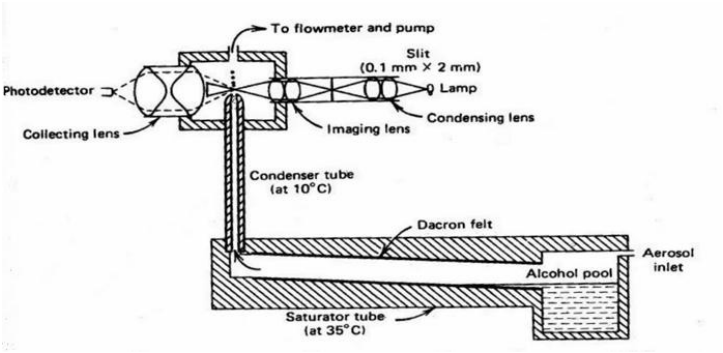

Schema: Condensation Particle Counter (Hinds, 1998)

DMA Differential mobility sorter (EC)

DMA (Differential Mobility Analyzer, O. 9) can distinguish particles in the range from 3 nm to 1 micron. EC is an older version of DMA. Aerosol particles pass through the neutralizer, and their charge distribution becomes Boltzmann (the parameters depend on the particle size). Then the particles are sent into an inner space between two vertical coaxial cylinders, where the outer cylinder has a negative or ground potential, while the outer cylinder has a positive voltage potential (usually less than 10 kV). The hole through which measured aerosol particles enter the space between the cylinders is located in the upper part on the surface of the outer cylinder.

Filtered air also enters between the cylinders. The air surrounds the inner cylinder and flows at the same speed as the aerosol. The distance travelled by the aerosol before it impacts the inner surface of the cylinder is proportional to its electrical mobility, and is hence proportional to the particle size.

At the end of the inner cylinder there is a narrow slit into which the given size fraction enters and is then fed to the CPC. The larger particles move on, while the small particles are caught on the cylinder much earlier. The sampled air flow is mostly in the range of 0.2 to 1.0 l /min. Recommended operating conditions: temperature 10-40° C, pressure 0.7 to 1.2 atm., relative humidity 90%.

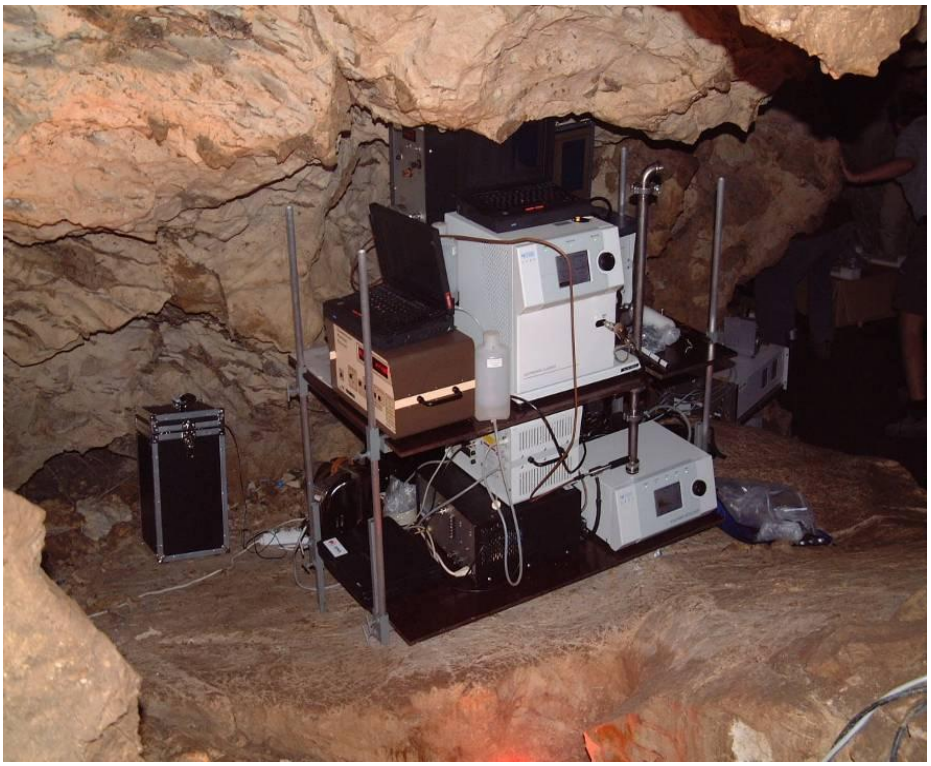

The set of devices used during the aerosol campaign in the Bozkov Dolomite Caves (Hell)

5.1.4 Dedicated software used in the measurements

Lung Dose Evaluation Program

LUDEP (NRPB, 1994) is a program running under MS DOS. This is an implementation of a model recommended by Respiratory Tract ICRP66. Basic information about the program and its operation can be found in the manual supplied with the program. The program is controlled using a keyboard.

For the purposes of this work, LUDEP was used to calculate the deposition of aerosol particles in the respiratory tract and batch conversion factors for radon transformation products. Prepared parameters describing the tidal volume, frequency, etc., can be used when calculating the deposition. The operator can also enter these values manually in "*advanced mode*". The user chooses what size AMAD she wants to use in the calculation. In "advanced mode," the operator can set the dispersion value, the size value, and the value for the shape factor and the density of the material from which the particles are composed. The program also allows the user to calculate the deposition for a given range of particle sizes. The output of this calculation is saved in a file.

To calculate the dose conversion factors, it is necessary to specify the amount of inhaled radionuclide. It is also necessary to select and calculate the AMAD size, to calculate the

deposition, and select the particle composition material behavior in terms of absorption. The absorption parameters can be entered manually, or can be selected from one of three programmed profiles - F, M and S. Finally, the user must choose the radionuclide for which the conversion factor is calculated. If the radionuclide has any conversion products, the program notifies the user and offers to include them in the calculation. The last step is to run the calculation. The output of this calculation is a table of batch conversion factors for the various compartments of the respiratory tract. In this table, conversion factors can be found first in the form of the unweighted equivalent dose, and then the weighted equivalent doses and the effective contribution to the total dose (weighing using a tissue weight factor). The program allows the user to change the regional, radiation and tissue weighting factors. The results are provided in *Sievert* units (Rovenská, 2007).

5.2 Description of the measurements

The establishment of a more precisely determined dose value would have a significant impact on radon remedies and/or on restricting the time workers stay underground. The approach to the calculation method might be improved on the basis of knowledge obtained by the following measuring procedures:

- continuous radon measurements (to capture the differences in $c_{V,Rn}$ between working hours and night-time, and also between daily and seasonal variations in radon concentration);
- regular measurements of radon and its daughters to estimate the equilibrium factor F and the presence of ^{218}Po;
- regular indoor air flow measurements to study the location of the radon supply and its transfer between areas of the cave;
- natural radioactive element content evaluations in subsoil and in water inside/outside the cave, a study of the radon sources in the cave;
- aerosol particle-size spectrum measurements to determine the free fraction;
- monitoring the behavior of guides and workers to record the actual time spent in the cave, in relation to the continuously monitored radon concentration levels.

These processes were integrated between the long-term measurements, which were focused on monitoring the variability of the measured values, and the short-term measurements, which

provided immediate values describing the cave environment at the time of sampling. The following measurement and experiments were carried out:

List of long-term measurements and experiments

- experiments with integral detectors (SSNTD and RAMARN)
- continuous radon concentration monitoring

List of short-term measurement and experiments

- air flow measurements
- measurements of the unattached and attached fraction of radon daughters
- aerosol particle-size spectrum measurements in the *Bozkov Dolomite* Caves
- gamma dose rate measurements
- in situ measurements of the radon concentration in water
- exhalation rate measurements and thoron occurrence measurements
- monitoring the concentration of radon along the visitors' path
- tests of the applicability of personal dosimeters

Laboratory gamma spectrometry measurements

- laboratory gamma spectrometry of rock and sediment samples, including bedrock

5.2.1 Long-term measurements and experiments

5.2.1.1 Integral radon detector testing

In the Czech Republic, the dose from radon is based on integral radon concentration measurements.

Between 1985 and 2003, bare solid state nuclear trace detectors (SSNTDs) were used for estimating the average equilibrium equivalent radon (EEC) activity in dwellings and workplaces. The exposure period was one year. This system never received a type approval, because the response was dependent on the equilibrium factor (F) and the occurrence of thoron. However, this approach was certainly sufficient to make a rough distinction in cases with higher concentrations (exceeding the investigation level). Since 2003, the new RAMARN measurement system has been certified. The RAMARN system shows lower levels of measured $c_{V,Rn}$ in the show caves than the earlier system, which used free LR 115.

The ratio of $c_{V,Rn}$ from bare SSNTD and from RAMARN varies in the range of 1.2–2.7 (Table 9, Figure 29), and, as was proven later, it is independent of F and f_p.

Note: A similar comparison was made for the measurement results in dwellings. Results were chosen from locations where the radon concentration exceeded 100 Bq/m^3. There was also a 20% decrease in the radon concentrations when SSNTDs were replaced by the RAMARN system.

Table 9 Ratios between the average seasonal radon concentrations measured by SSNTDs and by the RAMARN system, between 2001 – 2006

Location	**Summer season SSNTD/RAMARN**	**Winter season SSNTD/RAMARN**
Bozkov Dolomite Caves	1.7	2.1
Chýnov Caves	2	2.2
Javoříčko Caves	1.6	2.2
Na Špičáku Caves	2.3	2.7
Mladeč Caves	1.8	2
Balcarka Cave	2.6	2.2
Na Pomezí Caves	1.7	2.1
Koněprusy Caves	2.1	2.2
Zbrašov Aragonite Caves	1.2	2.3
Sloup-Šošůvka Caves	2.2	2.6
Kateřina Cave	2	2.1
Punkva Caves	1.8	2.5
Na Turoldu Cave	No measurements	No measurements

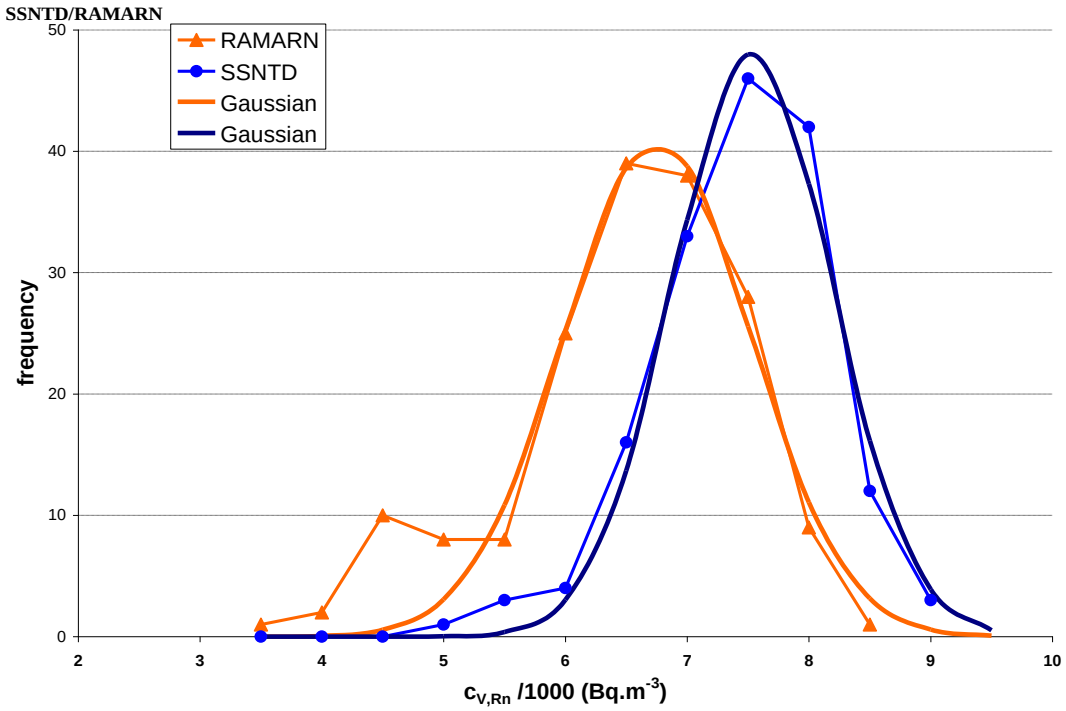

Figure 29 Comparison of results based on measurements of the integral average seasonal radon concentration in the Czech show caves using SSNTDs (in 2001-2003), and using the RAMARN system (in 2004-2006).

A single season lasts for an average of six months. According to Andersonov's statistical test, all processed data had a log normal distribution.

Separate experiments in two caves (the *Bozkov Dolomite* Caves and the *Zbrašov Aragonite* Caves), using around 200 detectors units, were started in 2006. The old system of integral radon detectors (bare SSNTD) and the new system (RAMARN) were tested together. The duration of the experiments was one year in the *Bozkov Dolomite* Caves, and 4 months (December 2006 – March 2007) in the *Zbrašov Aragonite* Caves.

The aim of the experiments was to determine the influence of the following effects:

1. *Measurement location* in the cave (cavity, clastogene sediments, limestone outcrops, elimination of the influence of different spot levels). The one-year experiment was carried out in the *Gallaš´s* Dome in the *Zbrašov Aragonite* Caves. Pairs of detectors (40 SSNT detectors and 40 RAMARN detectors) were placed or hung in various locations (free space, sediments, rock, etc.), and the influence of these locations on the radon concentration results was assessed (see Figure 30, Figure 31). A total of about one hundred detectors were tested. The radon concentration was checked by the RADIM3 continuous monitoring system.

Figure 30 Placement of RAMARN and SSNTD detectors in pairs for comparison in the *Zbrašov Aragonite* Caves; the main test in the *Gallaš´s* Dome

Figure 31 Placement of detectors in pairs along the visitor's path

2. *Period of exposure and high humidity including Ca, Mg ions*. (Solomon, 1996) described major differences between the overall measurement results for each quarter (of a year) and the results for the whole year. A relatively complicated system was used for the optimum time interval for integral radon measurements. Detectors were suspended in pairs in the cave environment, were inserted into cracks, or were placed on the sediments and exchanged according to a regular time schedule. A certain number of detectors were changed after one quarter, one half, and three-quarters of a year. The average annual $c_{V,Rn}$ was determined using the overall results. (In some cases, only the film inside the diffusion chamber was changed.) This one-year experiment (July 2006 – July 2007) was carried out in the *Robber's* Cave in the *Bozkov Dolomite* Caves, and a total 60 RAMARN-type detectors and 50 SSNTD-type detectors were tested. The experimental arrangement is shown in Figure 32. The radon concentrations were checked using the RADIM3 continuous monitoring system.

Figure 32 Integral detector test arrangement in the *Bozkov Dolomite* Caves

Figure 33 Dušan Milka, head of the *Bozkov Dolomite* caves, performing the continuous measurement test

3. *Presence of thoron*

The presence of thoron was measured in collaboration with NRBCPI, using a grab sampling method, in the *Bozkov Dolomite* Caves and in the *Zbrašov Aragonite* Caves. The air samples were taken from various parts of the caves, including fissures.

4. *Influence of a desiccant* (anhydrous calcium chloride) within the RAMARN diffusion chamber assessment. Short-term test.

5. The *number of outliers* among the results was monitored during both experiments, because some outliers may occur during measurements using track detectors. The outlying radon concentration values may lead to underestimation or overestimation of

the effective doses. The number of outliers was checked, and was compared with typical results from international comparative measurements.

An international comparison of integral radon detectors seemed to offer a useful supplement to detector testing. Two comparative measurements were carried out in the *Bozkov Dolomite* Caves. The RAMARN detectors were compared with detectors based on the CR39 material used in the NRPB (National Radiation Protection Board) laboratory (England), in 2007, and with new *Direct progeny sensor* (DTPS and DRPS) film detectors developed at the Radiological Physics & Advisory Division (RPAD) (Mumbai, India), in 2011.

Figure 34 Inter-comparative measurements in the *Bozkov Dolomite* Caves (RAMARN and DRPS/DTPS detectors; RAMARN and CR39 detectors in black plastic boxes)

5.2.1.2 Continuous radon concentration monitoring

Continuous radon concentration monitoring was mostly performed using RADIM3 monitors in a special configuration. The devices were enclosed (not hermetically) in a plastic box with desiccant powder to protect the electronic parts of the measuring system from excessive humidity. The test measurements demonstrated that sufficient interaction took place between the RADIMs in plastic boxes and the cave atmosphere. When compared with the integral monitoring continuous measurements (with a step of 0.5 hour), the configuration of the box enables the transfer of complete information about variations in concentration, humidity, cave temperature and atmospheric pressure. Despite initial problems with the power supply, the monitors worked well and are continuing to be used. Continuous monitoring was used in the following situations:

- Data obtained from the *Bozkov Dolomite* Caves from several years of measurements was utilized for establishing optimal seasons for integral monitoring.

- The data sets enabled a comparison of concentrations during working hours and at night, and verified the correctness of integral measurements for calculating the annual effective dose.
- After statistical processing, time data lines provided a better understanding of trends in the cave environment.
- A simple progression curve analysis can be made using a model of constant input and constant ventilation, to determine the ventilation coefficient (h^{-1}) and the radon inflow rate ($Bqm^{-3}.h^{-1}$).
- The continuous monitoring results were used for identifying outliers in the integral measurements.
- The continual monitoring results were used as control values in the comparison of international SSTN detectors.

5.2.2 Short-term measurements

5.2.2.1 Air flow measurements

Individual segments of underground areas are often interconnected by crevasses, sometime even leading to the surface of the earth, and thus also influenced by the external atmospheric conditions - pressure and temperature. The air flow in these areas is also affected by the movement of visitors in the cave. Air flow measurements provide very interesting information about the origin of "radon pockets" - air masses with a very high radon concentration - and enable a study of the location of the radon supply and its transfer among individual areas of the cave.

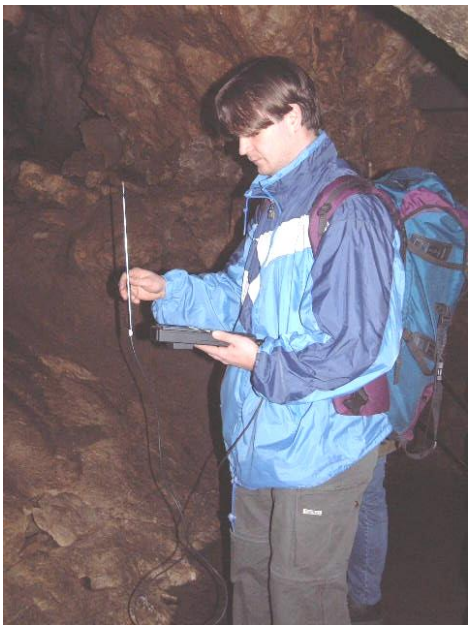

Air flow measurements in the Bozkov Dolomite Caves

Regular indoor air flow measurements at levels of 180 cm and 30 cm above ground were carried out in order to study the location of the radon supply and the air mass transfer process in individual areas of the cave, using a Testo 452 device.

5.2.2.2 Unattached fraction of radon daughter measurements

The quality of the environment in caves is different from the environment in flats or in houses. The measurements of the attached and unattached fraction of radon daughters in the underground environment were focused on quantifying these differences and their impact on dose assessment. The FRITRA4 continuous monitor was used for the unattached fraction measurements. FRITRA4 has two semiconductor detectors, filters, and a wire screen. Due to the measuring algorithm, it is able to determine the activity of radon, in general, and of radon daughters separately, for unattached and attached fractions. The ratio of the unattached and attached fraction and equilibrium factor F, which are important for dose assessment, were calculated from the measured results.

The FRITRA4 device was developed to make measurements in dwellings, and the required results should be obtained while spending the least possible time in a high humidity environment. However, the measurement time should affect the changes in the measured parameters that may occur in connection with the presence or absence of visitors or workers in the areas where the measurements are being made. A combination of the two requirements was taken into account, and the following measurements were carried out:

- Short-term (approx. three days in duration) unattached fraction measurements were carried out in each of the Czech show caves and speleotherapy areas, and in some underground workplaces (a mine tunnel, a wine cellar etc.).
- In addition to these routine measurements, a unique experiment in the *Bozkov Dolomite* Caves involved measurements at five different places in the cave at the same time. This experiment was focused on obtaining information about the variability of the unattached fraction in different areas of the cave. (All of the FRITRA4 devices available in the Czech Republic were used in this experiment.)
- Repeated measurements were performed each month in the *Bozkov Dolomite* caves and in the *Zbrašov Aragonite* Caves, using the FRITRA4 device. The measurements enabled the equilibrium factor to be determined and its variability to be observed.

In these measurements, the AlphaGuard continuous monitor was always used simultaneously as a control measuring instrument.

5.2.2.3 Aerosol measurements

In addition to the radon measurements, the aerosol particle size distribution was also measured, as one of the most important parameters for dose evaluation. The measurements were carried out in the *Bozkov Dolomite* Caves in August and September 2002. The measurements were supported by equipment and staff from the Institute of Chemical Process Fundamentals (ICPF) at the Academy of Sciences of the Czech Republic. Two researchers from NRPI also took part in the measurements. The list of devices that were used and their specifications is as follows:

- Nano SMPS (Scanning Mobility Particle Sizer), consisting of DMA 3085 and CPC 3025. The flow rate was adjusted to 1.4 l/min, and the range of detected particles was on an average approx. from 3 nm to 66 nm.
- SMPS 3934, consisting of EC 3071 and CPC 3022; the flow rate was adjusted to 0.3 l/min and the range of detected particles was on an average approx. from 14 nm to 530 nm.
- APS 3321 (Aerodynamic Particle Sizer), for detecting bigger aerosol particles; the flow rate was adjusted to 5 l/min, and the range of detected particles was on an average approx. from 550 nm to 20 μm.

The measurement campaign took four days. The time interval coincided with two days with visitors present in the cave (August 31st and September 1st), two nights (August 31st and September 1st), the "work in cave" regime, with the door open in the cave workers' entrance (September 1st, evening) and the "empty cave" regime (from September 2nd to September 3rd).

The measurements were carried out in the "*Hell*" location, which is the deepest cave area with reference to the cave entrance and exit levels; in addition, the highest radon concentrations are usually measured there. The checks for the sources of aerosols were conducted through NO_x measurements, which were performed by colleagues from ICPF. During the aerosol campaign, no aerosol sources were present (*see photo*).

Information about the number of particles of a given size in a volume of one cubic meter was obtained each six minutes during the measurement period. Any fluctuations in the number of particles were smoothed using

summation of 5 sampling intervals of six minutes duration. The result was assigned to the middle of each summer time interval (0.5 h). The smallest measurable aerosol particle had an average size of 2.89 nm. The concentration of the smallest particles (below 10nm) was very low, and for this reason the measurement error was very high. This made it impossible to determine the unattached mode.

Arrangement of the aerosol monitoring devices (the air was drawn in the left part of the Hell area, and after the aerosol particles had been processed it was exhausted into the Christmas caves, using a long tube)

Preparing the aerosol devices in the Hell area

The record of the continuous radon concentration measurements using a RADIM3 monitor (Figure 35, Figure 36) placed near the aerosol devices shows how the concentration and the temperature of the radon were influenced by air drawn out from the *Hell* area. Because the

radon concentration, the atmospheric pressure and the temperature were significantly influenced by the aerosol experiment, the radon concentration values for the dose calculation were taken from the time interval before the aerosol measurement started (from August27th to 30th).

The humidity was up to 100% throughout the experiment.

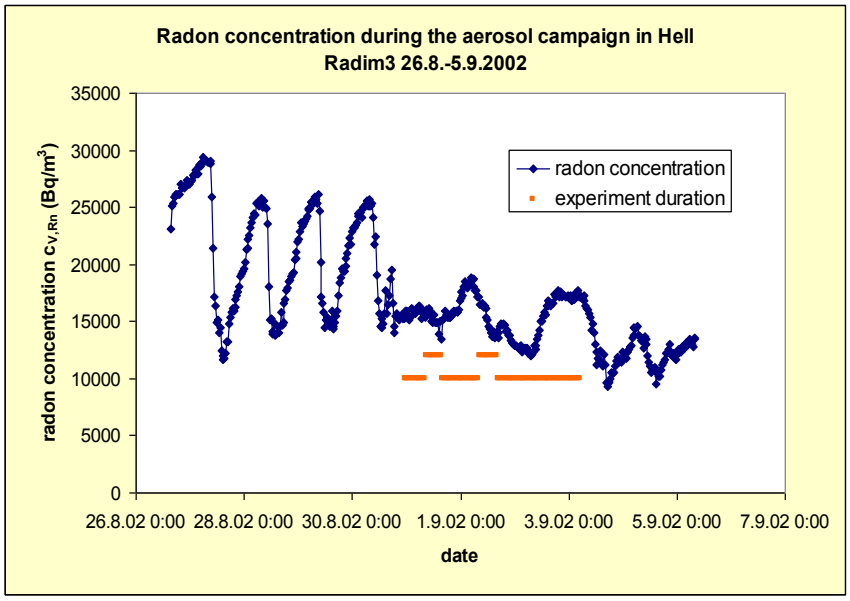

Figure 35 Continuous radon concentration record during the aerosol campaign in the *Hell* area

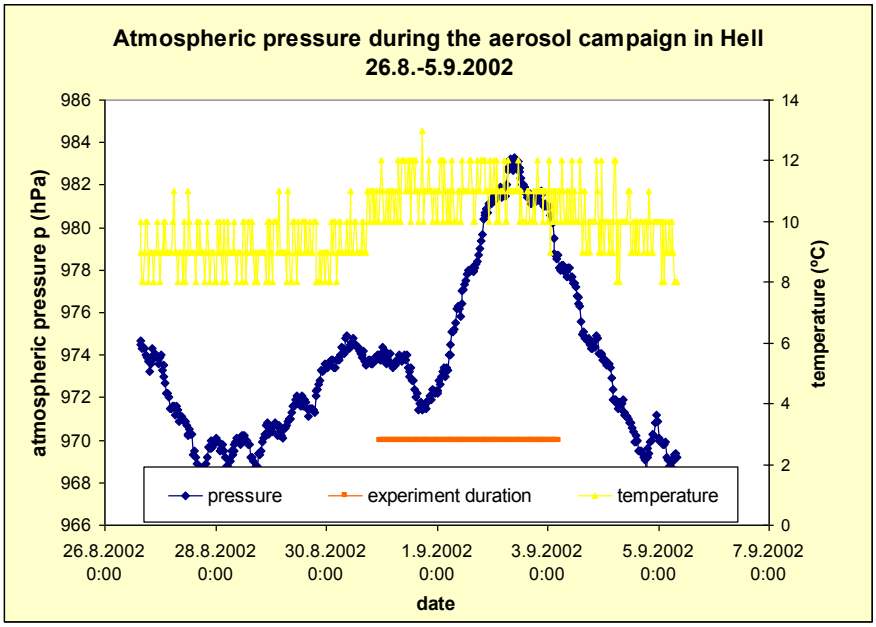

Figure 36 Continuous record of the inside atmospheric pressure and the temperature during the aerosol campaign in the *Hell* area

5.2.2.4 Kerma rate in air measurements

Kerma rate in air measurements were carried out using Tesla NB 3201 (№ B5-053), with the energy compensated plastic scintillation detector in current regime. The operating specifications were: directional dependence ±15% (from -3/4π to 3/4π, E_γ=60 keV), thermal dependence ±0,5% K^{-1}, and time instability ±5%. The total relative error should be less than ±10%. The stability and the setting of the device during the measurements were controlled before and at the end of the measurements, using a calibration source (^{137}Cs). The results for the kerma rate in air were expressed in (nGy/h). The device was not calibrated for the complicated geometry of the cave, and the measured dose rate values may be overvalued. (An overvaluation is acceptable within the principles of radiation protection.)

The dose rates were measured in all studied underground areas, along the visitors' path, and on contact with both outcrops and clastic sediments. Considering the complicated geometry of the cave, the results of the "on contact" measurements should not be significantly different from the measurements in the "open" air. The measured dose rate values were considered as background information only, and assisted in further decision making. On the basis of the results that we obtained, an assessment was made as to whether the values of the dose from external irradiation should be included in the calculation of the total dose.

5.2.2.5 Radon in water measurements

An essential aspect of identifying the radon sources in caves involved measuring radon concentrations in water. Samples of water 0.2 l in volume were measured in situ, using a portable RADIM4 monitor. The result in Bq/l of each sample measurement was available after a 30-minute measurement process. Samples of above/below surface water and dripping water present in small lakes were measured in each studied underground area. A total of 18 samples of water were measured. The use of a careful sampling method prevented any escape of radon from the water before measurement. The 5-minute bubbling process guaranteed approx. 95% transfer of radon from the water into the measurement chamber. The results were obtained with relative error 20%, which was sufficient for the purposes of identifying the radon sources.

5.2.2.6 Exhalation rate measurements

Measurements of the radon exhalation rate from clastic sediments and cave rock were performed in the *Bozkov Dolomite* Caves and the *Zbrašov Aragonit*e Caves. A difficulty noted with these measurements arises from the fact that the radon from the cave air can penetrate into the diffusion chamber through leaks, and can distort the measured results. The special structure of the diffusion chamber was used to reduce the inflow of high-concentration radon from the cave environment. Lucas cells were used for the radon concentration measurements. The exhalation rate measurement results could help to indicate the sources of high concentrations of radon in the caves.

These measurements were carried out by colleagues from NRCBPI Kamenná-Milín, and they are presented in this thesis to provide coherent information about the studied cave environment.

5.3 Laboratory gamma spectrometry measurements

The gamma spectrometry method is successfully used for a range of tasks in environmental monitoring and workplace monitoring. Over 150 samples of cave rock and sediments were collected in the studied caves and speleotherapy areas. The mass activity of the radionuclides that were present was determined for these samples, using laboratory semiconductor gamma spectrometric analysis. The equipment that was used comprised a coaxial HPGe detector (35% efficiency), with a built-in preamplifier (mfg. by EG&G Ortec), 2022 Canberra amplifiers, a Canberra Source VN31060, a built-in ADC analyzer, a Canberra analyzer model 4202 and a PC, with samples in the geometry of Marinelli containers (volume 0.5 l). The samples were dried and ground, and after being filled into containers they were hermetically closed for a minimum of 21 days, because equilibrium between ^{226}Ra and ^{222}Rn was required in the investigated samples. Knowledge of the mass related activities of the naturally radioactive elements (^{226}Ra (Bq/kg), ^{40}K (Bq/kg) and ^{228}Th (Bq/kg)) in the individual samples could be an important indicator for judging the samples or for categorizing them into the appropriate rock groups, from the point of view of their genesis. The ^{228}Th/^{226}Ra ratio was monitored. The ^{228}Th/^{226}Ra ratio enabled an evaluation of the origin of the clastogene sediments. The presence of man-made ^{137}Cs radionuclide can demonstrate that certain clastic sediments were transported into the cave from the surface during the time period since the Chernobyl accident.

The measurement time for the samples was selected to be between 30 and 80 thousands of seconds, depending on the sample activity in comparison with the background. SW Genie2000 was used for spectrum analysis in the energy range up to 3 MeV (the energy of naturally occurring radionuclides).

The ^{226}Ra mass activity was calculated from the energies of the Ra daughter ^{214}Bi, because equilibrium between U and Ra, especially in cave clastic sediments, was not expected. The energy of ^{226}Ra 0.186 MeV (4%) is much closer to the ^{235}U energy 0.185 MeV (54%). In the event of disequilibrium in the uranium decay chain, the mass concentration of ^{226}Ra as a mother radionuclide could be underestimated or overestimated.

The ^{228}Th radionuclide was used for the thorium mass activity calculation; because equilibrium in the thorium decay chain could be expected.

(IAEA, 2003a) states: *Thorium rarely occurs out of equilibrium in nature, and there are no disequilibrium problems with potassium. However, disequilibrium is common in the uranium decay series, and can occur at several positions in the ^{238}U decay series: ^{238}U can be selectively leached relative to ^{234}U; ^{234}U can be selectively leached relative to ^{238}U; ^{230}Th and ^{226}Ra can be selectively removed from the decay chain; and finally ^{222}Rn (radon gas) is mobile and can escape from soils and rocks into the atmosphere. Depending on the half-lives of the radioisotopes involved, it may take days, weeks or even millions of years for equilibrium to be restored. Disequilibrium in the uranium decay series is a serious source of error in gamma ray spectrometry.*

6. Overall measurement results

6.1 Selected results from experiments with integral radon detectors

6.1.1 The experiment in the *Bozkov Dolomite* Caves

The experiment started on 7th July 2006 and was finished on 5th July 2007. All detectors were evaluated in the *Integral Dosimetry Laboratory* of NRCBPI. RAMARN and SSNT detectors were mostly used in pairs. The scenario of the experiment was somewhat complicated (see photo below):

- The measurement period was divided into quarters (7/7/2006 - 6/10/2006; 7/10/2006 - 6/1/2007; 7/1/2007 - 2/4/2007; 3/4/2007 - 5/7/2007)
- The detectors were divided into three groups
    - group 4+4 "in a hollow" – 1 RAMARN and 1 SSNTD were removed each quarter for an assessment of the influences of thoron and of an enclosed space
    - group 4+4 detectors were suspended in the open air – all detectors were changed each quarter to define the length of exposure influence on the measurement results
    - group 12+12 detectors were suspended in the open air – 3 films inside RAMARN detectors were scheduled to be changed (plastic boxes remaining in place), 3 SSNTD detectors were scheduled to be changed. The exchange process is explained step by step:
        - first quarter, 3 to be changed,
        - second quarter, 6 to be exchanged,
        - third quarter, 9 to be exchanged,
        - after one year, 12 to be exchanged;

The aim of these changes was to assess the influence of humidity and dust sediment. This evaluation enabled us to make calculations combining the results from measurement intervals, and to make comparisons with the annual exposure quarterly test using a desiccant inside the RAMARN detectors, with the aim of assessing the influence of humidity on the results of the experiment.

The selected result from the experiment is expressed in Table 10 and Figure 37. Overvaluation of the radon concentration using SSNT detectors was confirmed; however the difference between the two types of detectors used here was smaller than in the previous measurements in caves (Table 9).

Table 10 Results of the experiment in the *Bozkov Dolomite* Caves, and a description of the measurement and calculation procedures (1-8)

	The measurement scenario
1	one year exposure in the hollow, as a summary of 4 quarters
2	one year exposure in the hollow
3	one year exposure in the open air, as a summary of 4 quarters, new detectors
4	one year exposure in the open air, as a summary of 4 quarters, new film
5	one year exposure in the open air, as a summary of 2 quarters and half a year
6	one year exposure in the open air, as a summary of quarter to year and quarter of a year
7	two quarters, summary
8	half a year exposure

Average integral radon concentration			
	RAMARN Bq/m^3	**SSNTD Bq/m^3**	**SSNTD/RAMARN**
1	3882	3936	1.01
2	3919	4140	1.06
3	4283	4835	1.13
4	4324	4796	1.11
5	4248	4930	1.16
6	3802	4265	1.12
7	2447	2762	1.13
8	2397	2756	1.15

The RAMARN detector results were controlled by continuous RADIM3 monitoring during each measurement time period. The average concentration from the RADIM3 monitor was within the radon concentration from the integral measurement +/- 10%.

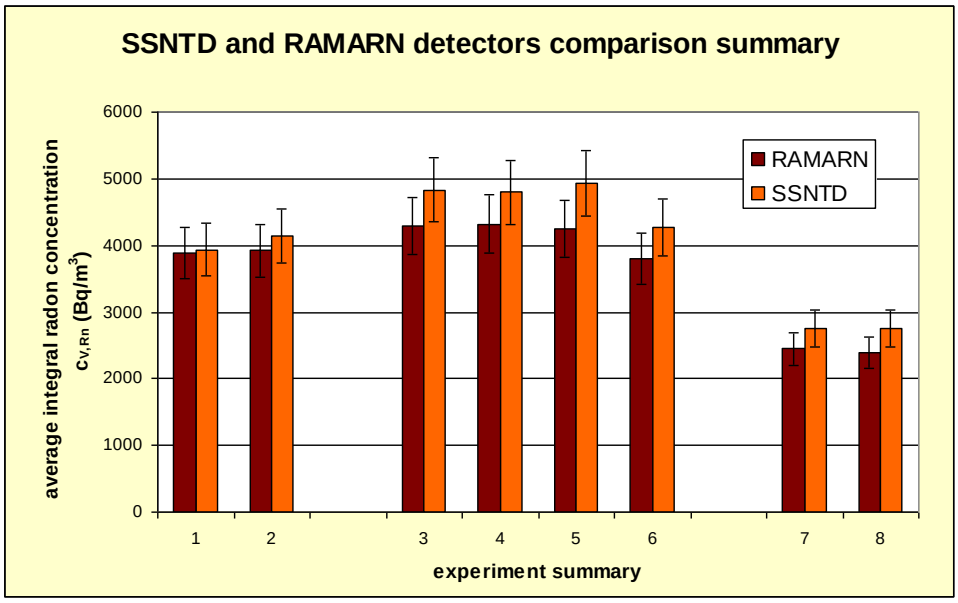

Figure 37 One of the results from the comparative measurements in the *Bozkov Dolomite* Caves

The best time interval for using RAMARN detectors was chosen on the basis of the results from the experiment. Figure 38 indicates that the half-year measurement interval was chosen as a result of an evaluation of the output of both SSNTD and RAMARN detectors, because the results from a quarter to a one year detectors´ exposure were under-valued (Figure 38 for SSNTD and Figure 39 for RAMARN).

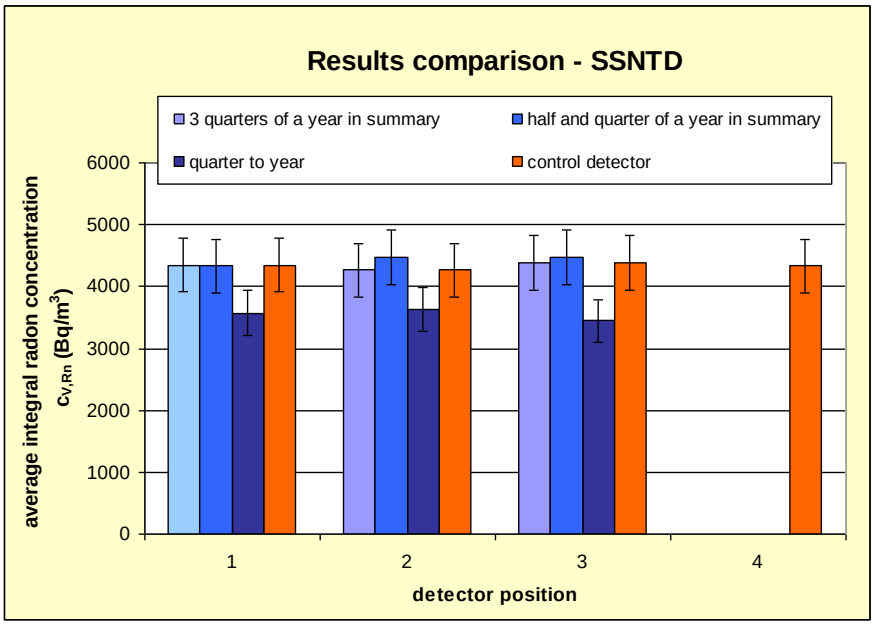

Figure 38 Part of the results of the experiment in the *Bozkov Dolomite* Caves for SSNT detectors

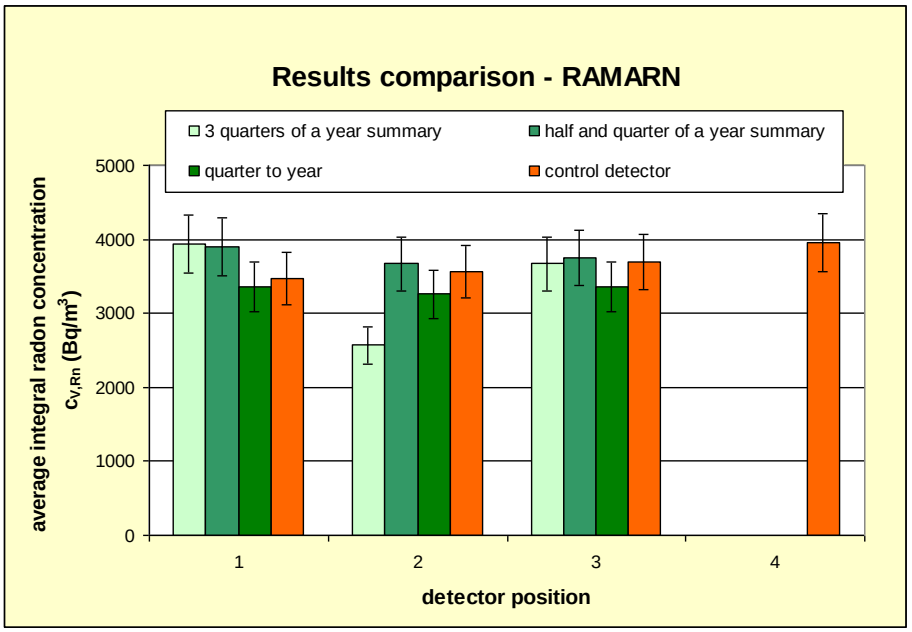

Figure 39 A part of the results of the experiment in the *Bozkov Dolomite* Caves for RAMARN detectors

6.1.2 The experiment in the *Zbrašov Aragonite* Caves

The experiment in the *Zbrašov Aragonite* Caves started in December 2006 and was completed in March 2007. All detectors were evaluated in the *Integral Dosimetry Laboratory* of NRCBPI. The illustrative photos in the previous chapter 5.2.1. show the experimental arrangement. The detectors were suspended in pairs in the open air, or were placed on the bottom of the *Gallaš´s* Dome. The group of detectors in pairs was distributed along the visitors' path or on the cave walls. The main results are shown in Figure 40.

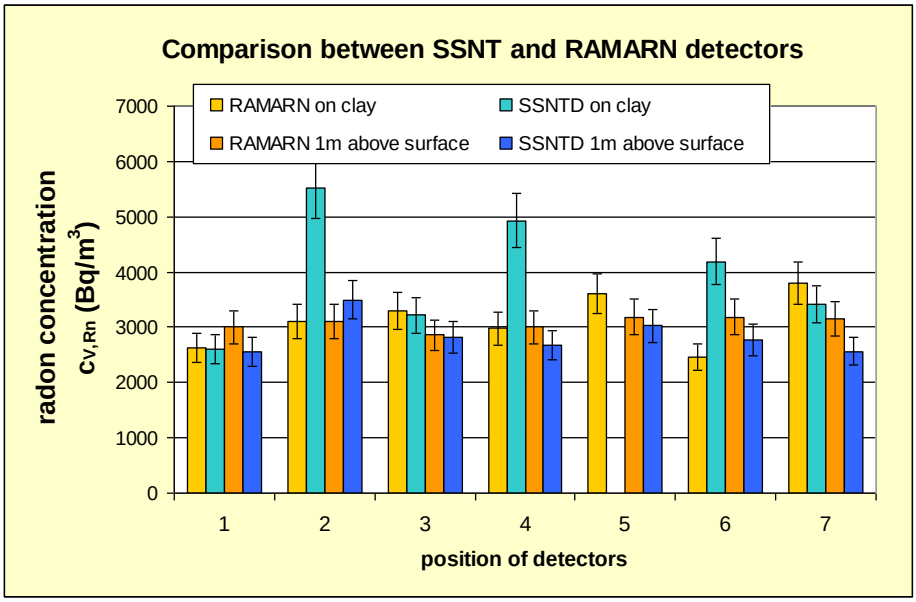

Figure 40 Results for a part of the comparative measurements in the *Zbrašov Aragonite* Caves (see the photo in section 5.2.1)

The influence of clastic sediments on the measured integral radon concentrations was proven. There were a total of 5 outliers in the two experiments (2.5%). An example of an outlier from the set of results is shown in Figure 41.

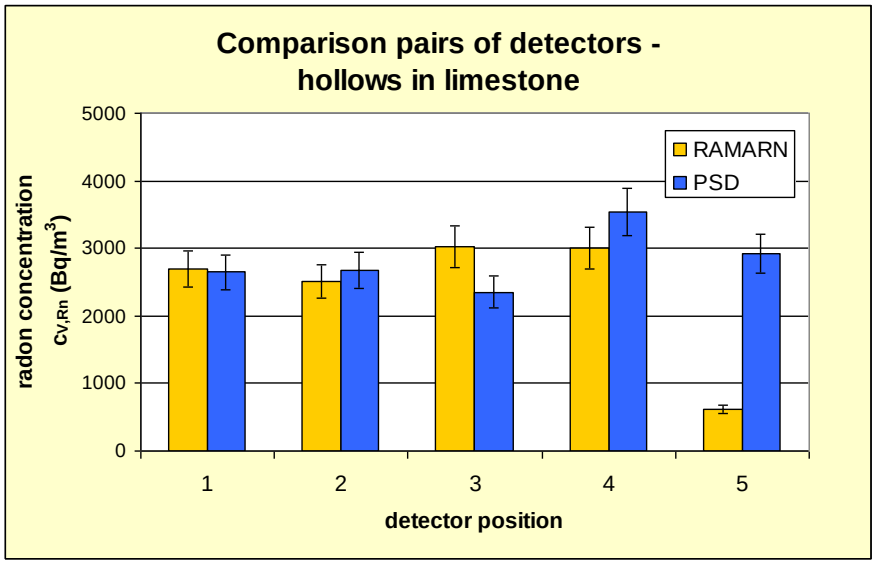

Figure 41 Example of an outlier in the comparative measurements in the *Zbrašov Aragonite* Caves

It follows from the results of the experimental measurements presented above that:

- The ideal length for seasonal measurements is half a year, because there was a decrease in the measured value when an interval of ¾ of a year was used.
- In a few cases, small specks of black mold were noted on the edge of the KODAK LR115 film. The radon concentration evaluation results were not affected by this.
- The RAMARN detectors could be placed in hollows, about 1.5 – 2 m above ground (at human breathing level).
- The locations containing clastic sediments, experienced local radon concentration inhomogeneity.
- Measurements in areas where there is dripping water is not recommended.

Definitely a wrong location for a RAMARN detector

6.1.3 Inter-comparative measurements of NRCBPI integral detectors (Czech Republic) and NRPB integral detectors (England)

The results of 4-week inter-comparative measurements comparing CR39 integral detectors in a plastic box with the RAMARN detection system (see photo) are summarized in Table 11. Continuous radon measurements were performed using the FRITRA4 monitor (see photo below) and were verified using the AlphaGuard monitor.

A total of 100 detectors were divided into 3 groups, and were exposed in three time intervals in 2007-2008: 14/12 - 29/12, 29/12 - 11/1 and 14/12 - 11/1.

Table 11 Results from integral concentration measurements (CR39, RAMARN) or averages from continual radon concentration measurements (Bq/m^3)

time interval (day/month)	AlphaGuard	FRITRA 4	NRPB (CR39)	difference FRITRA4-CR39	NRCBPI (RAMARN)	difference FRITRA4-RAMARN
2007-2008	(Bq/m^3)	(Bq/m^3)	(Bq/m^3)	(Bq/m^3)	(Bq/m^3)	(Bq/m^3)
14/12 - 29/12	1377	1284	1168	116	1201	83
29/12 - 11/1		1404	1396	8	1364	40
14/12 - 11/1		1390	1269	121	1283	107

No outliers were found in the results from NRPB or from NRCBPI. The concentration differs with a relative error not exceeding 10%.

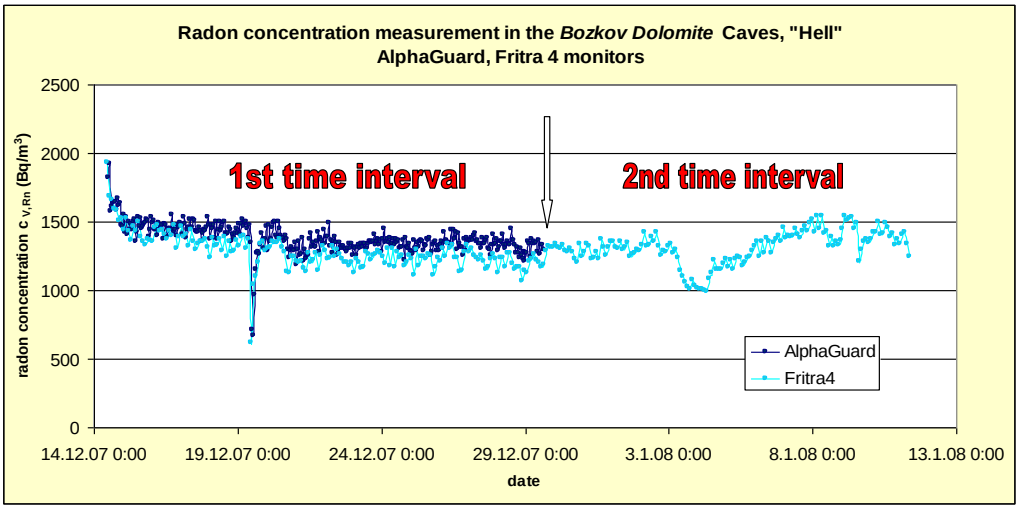

Figure 42 Record of continuous radon measurements during the comparison measurement

Inter-comparative measurements in Hell, the Bozkov Dolomite Caves

6.1.4 Inter-comparative measurements of NRCBPI RAMARN integral detectors (Czech Republic) and RPAD Direct progeny sensors (India)

Three locations were chosen for exposing the detectors: the *Bozkov Dolomite* Caves, the NRPI radon chamber, and the NRCBPI radon chamber. A total of 100 DRPS/DTPS detectors and 100 RAMARN detectors were exposed. DRPS are *Direct radon progeny sensors*, while DTPS are *Direct thoron progeny sensors*. The results are EERC (EETC) – equilibrium equivalent radon (thoron) concentration.

In the *Bozkov Dolomite* Caves, 5 plus 5 detectors were exposed in the *Lake* location for 100 days, and 5 plus 5 detectors were exposed in the *Pirate Ship* Cave location for 100 days. Four detectors were used as a personal dosimeters and one was placed in the guides' room as background. In addition, one detector was used for background during the detector transportation control. The experiment started on 26th April, 2011 and finished on 5th August, 2011.

The results from the comparative measurements in the cave are presented in Table 12 (integral measurements) and Table 13 (personal dosimeters). According to the measured values, the equilibrium factor F for the *Lake* location was 0.12, on an average (excluding the outlier), and for *Pirate Ship* Cave the equilibrium factor was also 0.12, on an average. In the previous measurements in the *Bozkov Dolomite* Caves, F varied around a value of 0.6. In this case, the DRPS detectors measured only 30% of the radon concentration, on an average. The

efficiency of the DRPS detectors was probably higher than is necessary for measurements of thousands of Bq/m^3, and this led to overlapping of the tracks.
Number of RAMARN outliers: 1.

Table 12 Results of the inter-comparative measurements in the *Bozkov Dolomite* Caves

Location	**RAMARN** $c_{V,Rn}$	**DRPS EERC**	**DTPS EETC**	**F**
	(Bq/m^3)	(Bq/m^3)	(Bq/m^3)	
Lake	2941	345	0.48	0.12
Lake	849	431	0.35	0.51
Lake	2712	385	0.55	0.14
Lake	2952	453	0.40	0.15
Lake	3149	243	0.49	0.08
Pirate Ship	4128	653	0.85	0.16
Pirate Ship	4749	332	0.76	0.07
Pirate Ship	4317	457	1.45	0.11
Pirate Ship	3752	582	1.1	0.16
Pirate Ship	4081	530	7.38	0.13

The second part of the experiment focused on the utilization of DRPS/DTPS detectors as dosimeters. Four cave guides wore the detectors on their jackets during the period of time in which the integral measurements were being made (100 days in total). The results for using DPS detectors as personal dosimeters are shown in Table 13. The equivalent radon concentrations (EERC) presented here are higher than the integral measurement results (see Table 12). The average radon activity concentration measured using RAMARN detectors in the *Lake* was 2938 Bq/m^3 and in the *Pirate Ship* the average radon activity concentration was 4205 Bq/m^3. The equilibrium factor is 0.72, when the total average radon activity concentration of 3571 Bq/m^3 is taken into account. This value corresponds better with the previous measurement in the *Bozkov Dolomite* Caves.

Table 13 shows that the experimental results with the use of DRPS/DTPS as personal detectors is more in agreement with the measurement results for the use of RAMARN detectors. When DRPS/DTPS detectors are to be used for long-term integral measurements, it is necessary to lower their sensitivity, because the present setting resulted in track overlapping.[2]

More information about the Direct *progeny sensors* was published in: Mishra, R., Mayya Y.S. (2008). Study of a deposition-based direct thoron progeny sensor (DTPS) technique for estimating equilibrium equivalent thoron concentration (EETC) in an indoor environment. *Radiation Measurements, Volume 43, Issue 8, September 2008, Pages 1408-1416.*

Table 13 Results of measurements using DRPS/DTPS as personal dosimeters worn by guides in caves (the names of the guides have been changed)

Name of guide (not the real name)	Time of exposure (hours)	DRPS minus DTPS EERC (Bq/m^3)
Jan	94	2271.21
Pavel	185	3098.80
Jana	117	2108.52
Pavla	118	2751.42
guides' room	100 days	33.70

6.1.5 Integral detector monitoring: a summary

After data processing, the following conclusions were reached:

- The influence of detector placement was noted only in the case of bare SSNTD detectors, which produced incorrect higher values when they were located near clay clastogene sediments. Similar results were observed for vertical inhomogeneous measurements, using electret detectors (chamber 0.5 l). In this case, the influence of thoron is probable.

[2] Inter-comparative measurements of integral detectors were also carried out in the framework of the *RADON 2007* international conference in September 2007. RAMARN and CR39 detectors were compared in the radon chambers of NRPI and NRCBPI. The integral radon concentration results were: NRPI radon chamber 3090 Bq/m^3, NRPB (CR39) 3059 Bq/m^3 (1% difference), NRCBPI (RAMARN) 3293 Bq/m^3 (6.6% difference).

- In some cases, a black mould appeared on the film inside the diffusion chamber, but this did not have any impact on the results.
- (Solomon, 1996) described major differences between the measurement result summation for the individual quarters (of a year) and the result of the whole year. The measurement results using the RAMARN system did not indicate significant differences. A total of 110 detectors were used, and the $c_{V,Rn}$ values were verified using the RADIM3 continual radon monitor.
- The number of outliers was less than 10%, while the causes of very low values were not clarified. The influence of a non-standard diffusion chamber cover was presumed. This issue was verified by an experiment in which the chamber covers were sealed and the $c_{V,Rn}$ results were compared with the results for non-sealed diffusion chambers. The sealed diffusion chambers received only half as much diffusion as the non-sealed chambers.

On the basis of the results discussed here and also on the basis of earlier experiments, cave monitoring for the purposes of worker dosimetry using the RAMARN integral system with six-month exposure is recommended. This period of time corresponds to the seasonal variations, and also conforms to the business operation of the caves. A shorter interval cannot be recommended. No significant impact of thoron or of possible mold was proven. The recommended detector position excludes places where there are clay clastogene sediments.

6.2 Continuous radon monitoring

Continuous monitoring of radon and environmental parameters in caves has certain advantages. It enables the entire variability of the parameters of interest to be observed. However, continuous monitoring has some disadvantages when used for long-term cave environment monitoring for the purposes of radon dose calculation. Firstly, the acquisition costs are very high (AlphaGuard costs around €14 000 and RADIM3A costs around €3 800). The probability that high humidity will reduce the working life of the equipment must also be taken into account. For dose calculation purposes, the devices must undergo metrological calibration at regular intervals; contamination of the detector in an environment with high radon concentration requires a frequent replacement of detectors; the working life of batteries or power supply requirements etc., also involve additional costs. It is therefore very important to verify the results for integral dosimeters as default information for dose calculation. Results

from continual monitoring enabled a comparison to be made between the radon concentrations during working hours and during non-working hours on each day.

6.2.1 A comparison of $c_{V,Rn}$ in working hours and in non-working hours

The first comparison was carried out in the *Koněprusy* Caves (Brandejsová, 2004). The differences between working hours and non-working hours in the *Mint*, the *Old Corridor* and *Prošek's Dome* were less than 5% of the measured concentration.

An example of a comparison of these two periods of time is shown in Figure 43 and in Table 14. The beginning of the recorded radon concentration values is typical for the winter season, when the differences between working hours and non-working hours are definitely negligible. The part of the recorded values where typical variations occurred was chosen for a comparison of the concentrations. The average radon concentration in the *Bozkov Dolomite* Caves (*Hell*) in the period from 12th March 2002 to 24th June 2002 was 3601 Bq/m^3 (1000 records with step 0.5 hour). The difference between the total average and the average for working hours was 5%, and for non-working hours the difference was 4%. The difference between working hours and non-working hours was 9%. No major differences were shown in the average $c_{V,Rn}$ during working time and during non-working time in the caves.

However the differences between two successive days may be higher than 100%, and this consideration alone supports the idea of long-term monitoring.

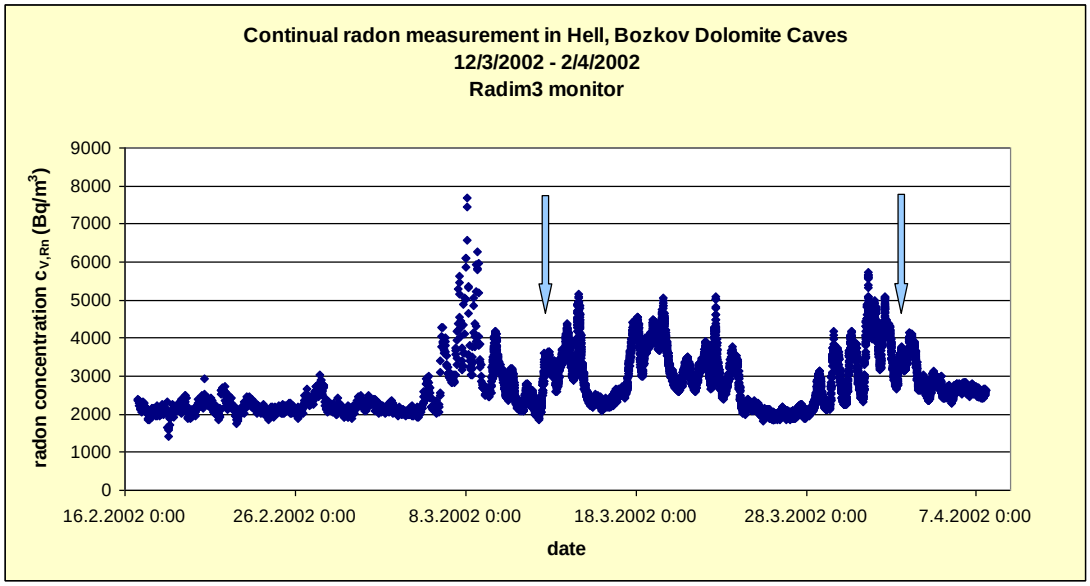

Figure 43 The continuously recorded radon concentration in *Hell, Bozkov Dolomite* Caves. The analyzed time period lies between the blue narrows.

During the time period from 12th June 2006 – 26th June 2006 in the *Gallaš´s* Dome (*Zbrašov Aragonite* Caves, 680 records with a step of 0,5 hour) the difference between the total concentration (2390 Bq/m^3) and the average concentration in working hours (2935 Bq/m^3) was 19% (Figure 44). During the same period, the difference between the total concentration (2835 Bq/m^3) and the average concentration in working hours (2875 Bq/m^3) in the *Jurik´s* Dome was 1.5%. The results obtained from continuous monitoring support the statement that the average radon concentration from integral monitoring can without any doubt be used for calculating the radon dose.

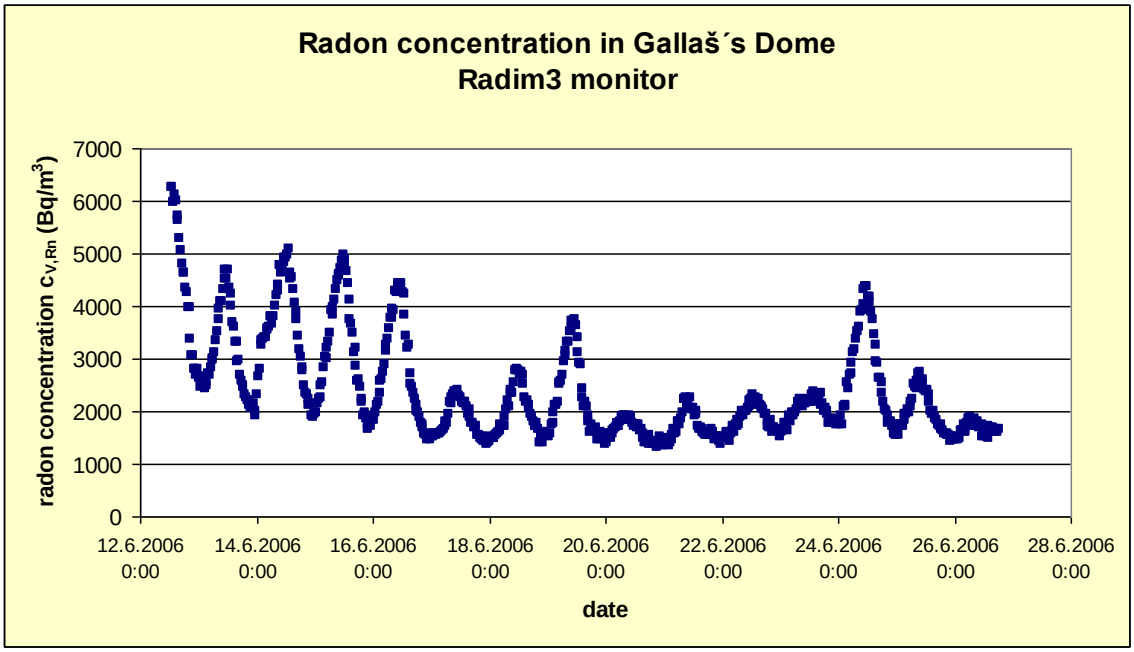

Figure 44 The radon concentration during the time period 12th June 2006 – 26th June 2006 in the *Gallaš´s* Dome, *Zbrašov Aragonite* Caves, using a comparison of working hours and non-working hours

If we compare results obtained by (Vaupotič, 2008), who described everyday minima for $c_{V,Rn}$ in *Postojna* Cave (Slovenia) at about 8 p.m., in the Czech caves minima (or maxima) for $c_{V,Rn}$ occurred during different time of day or in different season in different caves. For example in the *Zbrašov Aragonite* Caves the minima of $c_{V,Rn}$ in *Gallaš´s* Dome occurred near midnight, meanwhile in *Jurik´s* Dome (located deeper in the cave) about for 4 hours earlier (at about 8 p.m.). Totally reverse situation occurred in the *Bozkov Dolomite* Caves, where the minima for $c_{V,Rn}$ were measured in *Hell* area at about 6 a.m. (April), 9 a.m. (June, July), 8 a.m. (August). In the *Robber´s* Cave the minima for $c_{V,Rn}$ were measured at about 8 a.m. (June) and before noon (July). It could be said, that the deeper within the cave is a certain area located, the daily variations during the summer season are more noticeable; in winter months these variations are absent.

Table 14 A comparison of average radon concentrations (Bq/m^3), obtained from 14-day continuous monitoring, *Hell* (*Bozkov Dolomite* Caves)

	18:00 - 7:30	8:00 -17:30		18:00 - 7:30	8:00 -17:30
day	**non-working hours**	**working hours**	**day**	**non-working hours**	**working hours**
1	3584	3713	12	4511	5646
2	4280	3862	13	2454	2607
3	3294	6014	14	2241	2365
4	2522	2582	15	2128	2192
5	2712	2533	16	2153	2310
6	4401	3203	17	2547	2554
7	4755	3897	18	3060	3662
8	3568	4934	19	3451	4464
9	4073	3162	20	4711	5499
10	5055	3486	21	3567	4780
11	3979	6256	average	3478	3796
			%	1,04	0,95

6.2.2 A comparison of radon concentrations between winter season and summer season

After integral radon concentration monitoring was approved, the best measurement period had to be chosen. The radon concentration from 5 years of continuous radon concentration monitoring in the *Lake* (*Bozkov Dolomite* Caves) is shown in Figure 45.

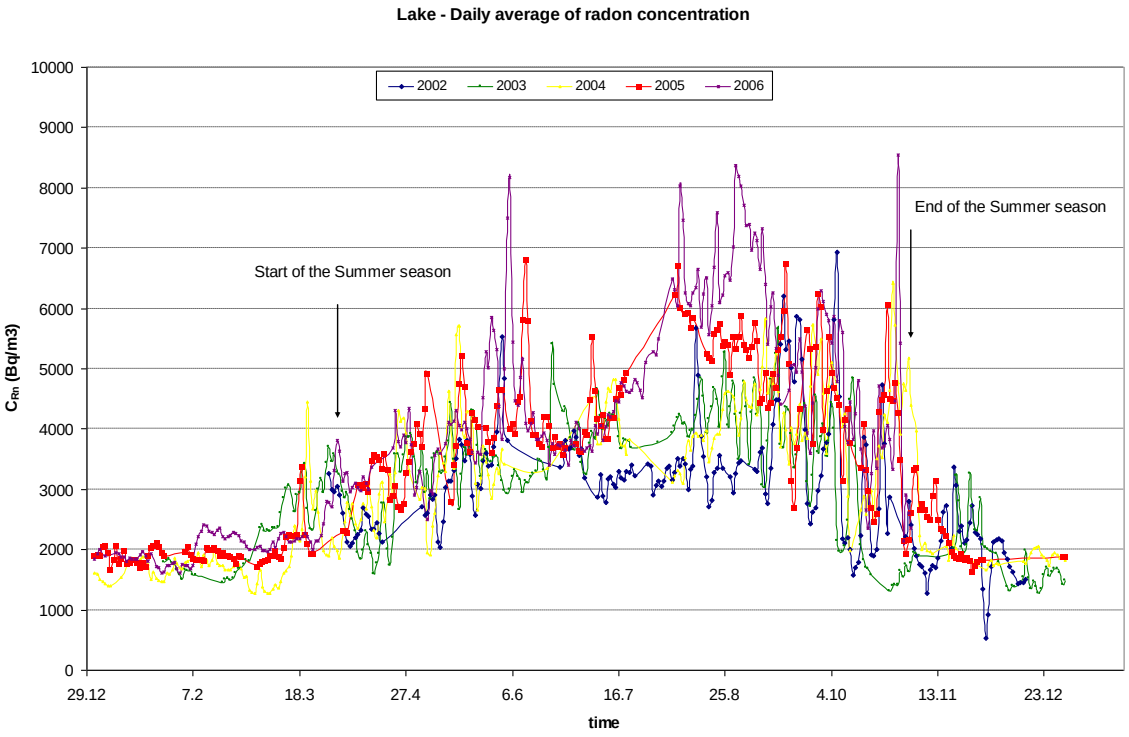

Figure 45 The seasonality of measured radon concentrations in the *Lake*, the *Bozkov Dolomite* Caves, between 2002 – 2006

On the basis of continuously monitored radon concentration records for the *Bozkov Dolomite* Caves, the best period for measurements during the "winter season" was from October 1st to March 31st; the remaining months are referred to as the "summer season". This period of time corresponds to the seasonal variations, and is also in conformity with the business operation of the caves.

6.2.3 A study of local radon concentration anomalies

The radon concentration along the visitors' path was measured in each underground area. All results were published in (Thinová, 2007). Figure 46 and Figure 47 show examples of the measured curves. This data can be used to locate the best position for integral radon detector placement.

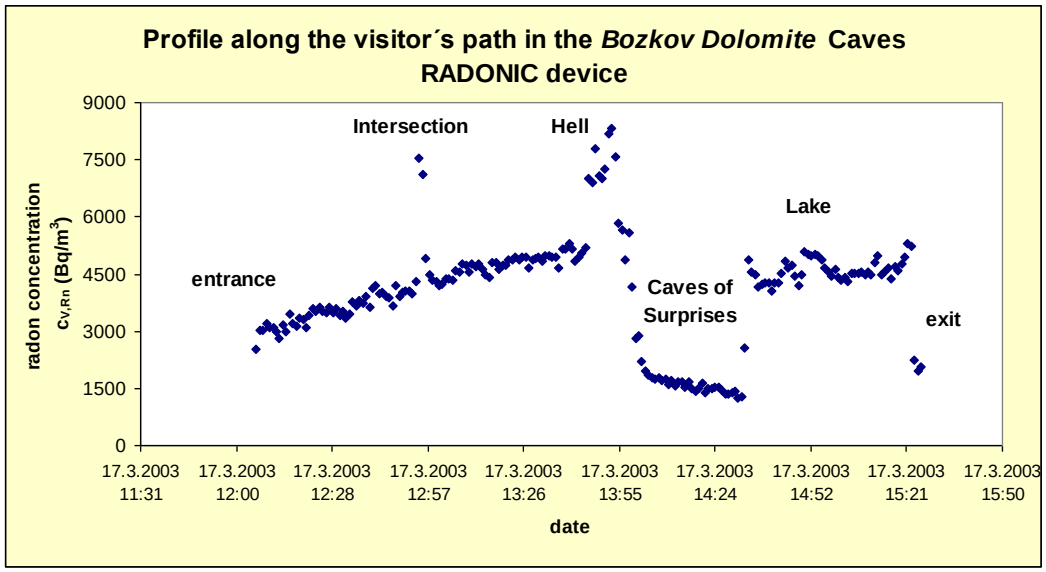

Figure 46 Radon profile along the visitors' path in the *Zbrašov Aragonite* Caves

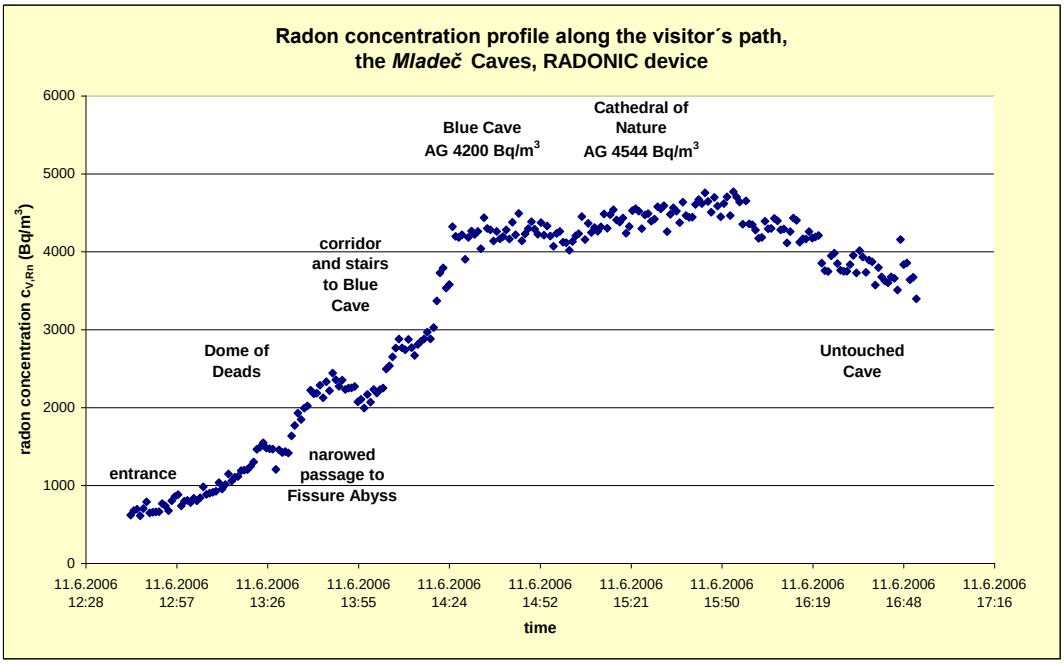

Figure 47 The profile along the visitors' path, *Mladeč* Caves, with a measurement step of 1 minute

6.2.4 A study of local radon concentration anomalies

In the *Zbrašov Aragonite* Caves, a local anomaly at the *Waterfall* was studied using electret detectors. The height profiles were measured in order to identify the radon sources. The results are shown in Figure 49, Figure 50, and Figure 51. The results confirm that the high concentration gradient of was associated with the intersection of three directions of air flow, see chapter 3. A very interesting result from the height profile is shown in Figure 49. The measurement confirmed the results from the RAMARN and SSNTD tests. The radon concentration was higher near the clastic sediments. During the summer season, the concentrations were higher as a result of the higher exhalation rate.

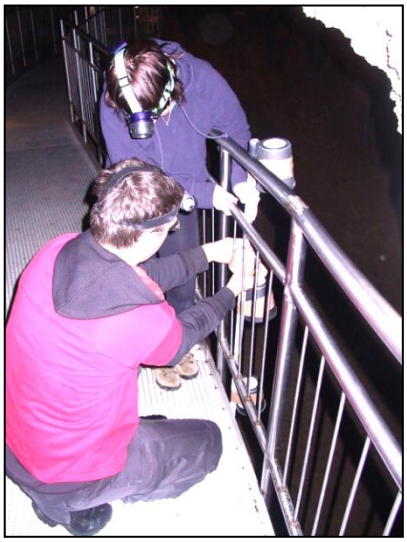

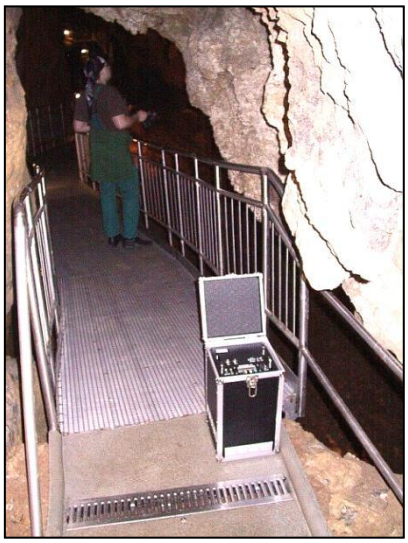

Preparations for the depth profile in the Gallaš´s Dome and for the profile along the visitors' path measurements, using a RADONIC continuous monitor

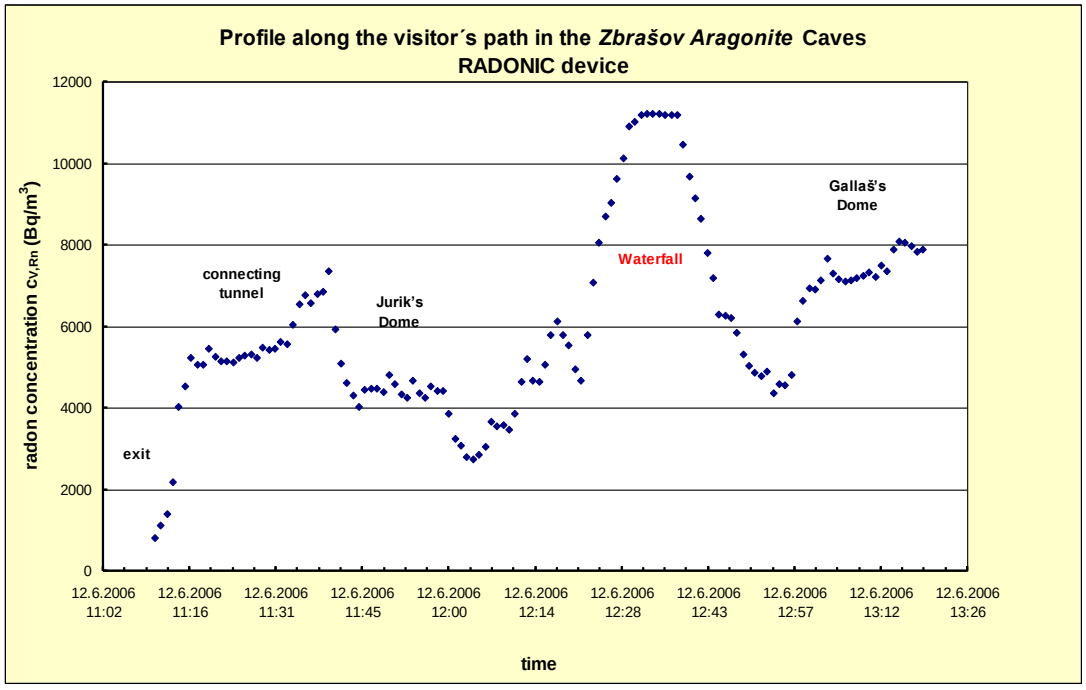

Figure 48 Radon profile along the visitors' path in the *Zbrašov Aragonite* Caves. Height profiles in the *Waterfall*

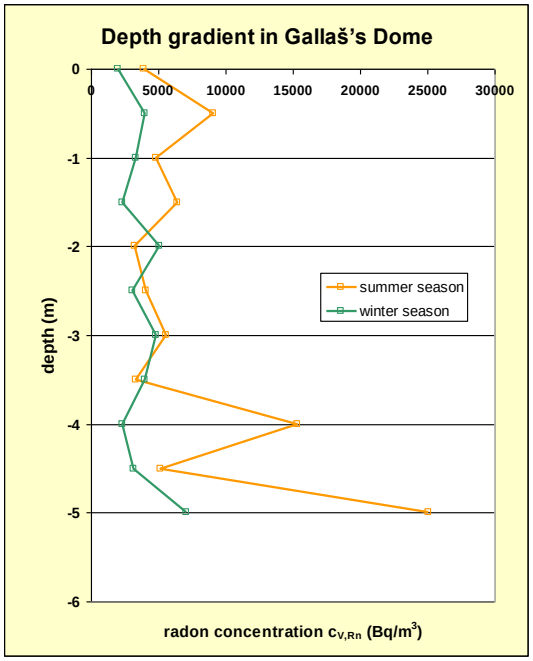

Figure 49 Height profile results for the *Gallaš´s* Dome, in winter season and in summer season

The radon concentrations measured by electret detectors are in good agreement with the previous values obtained using the RADONIC01 device. The radon concentration in the *Waterfall* area reached 15.10^3 Bq/m^3 in the location where three directions of air flow meet. Near the *Waterfall* (profile near the *Gas Lake* and in the *Gallaš´s* Dome) the concentrations were around 4,500 – 5,000 Bq/m^3.

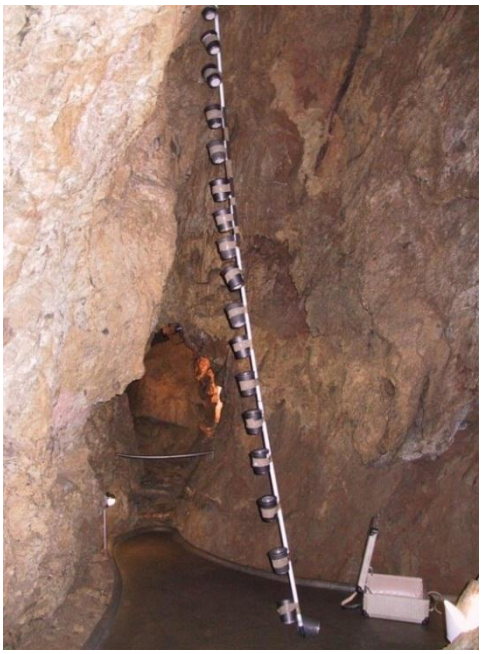

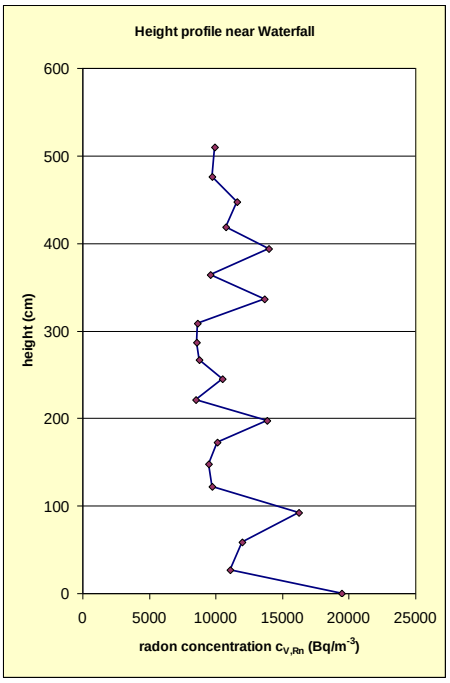

Figure 50 Results from the height profile near the *Waterfall*. The concentration is practically constant.

The next profile was measured in a place where there was a limonite core. The highest measured concentrations are in the most open part of the hollow (7,000 Bq/m^3).

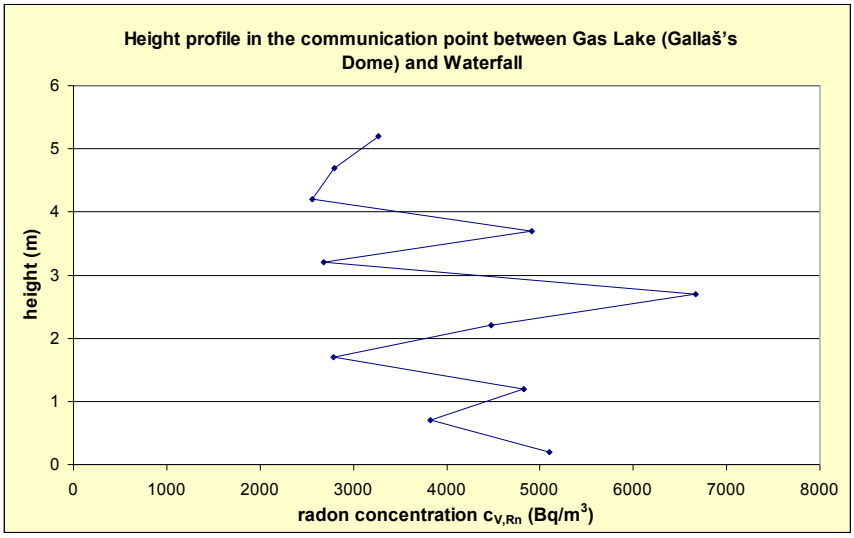

Figure 51 Results for the height profile in the area of the connecting hollow between the *Gas* Lake and the *Gallaš´s* Dome

Note: A final, important advantage of continuous radon monitoring is that statistical analyses can be made. Frequency analysis provides information about variations in radon concentration, and a simple analysis of the growth curve may be used to assess the ventilation parameters. An example of a simple analysis (assuming constant supplementation and ventilation, on different days) is presented in Figure 52. As the ventilation decreases, the radon supplementation rate grows according to present equation. (The stationary concentration was estimated for the purposes of calculation.)

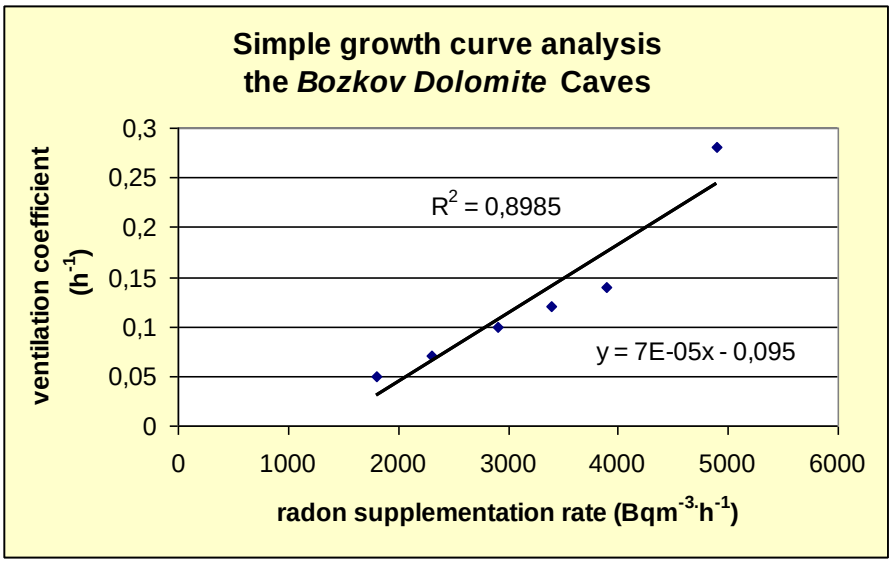

Figure 52 Example of a simple growth curve analysis. Measurements in the *Bozkov Dolomite* Caves (2006)

6.3 Air flow measurements

The results presented here were aimed at showing some long term (global) dependencies and some details concerning air flow changes. Some other results were included in section 4.3 (Description of the Environment) and in section 6.2 (Results of continuous monitoring).

From point of view of global dependencies, the most interesting result appears to be the shift between the decrease in radon concentration and outside temperatures during the summer season. This fact was documented in the one-year measurements in the *Mladeč* Caves (Figure 53 - continuous measurements in 2010) and in the *Bozkov Dolomite* Caves (continuous measurements in 2004, *Hell* - Figure 54 and the *Lake* – Figure 55). This result is especially interesting, because the locations for continuous monitoring were quite different from each other. In the *Bozkov Dolomite* Caves some portions of the annual records are unfortunately missing, due to problems with the power supply. In the *Mladeč* Caves, the RADIM3A monitor was placed in the deepest part of part of the cave, not open to the public, without strong air exchange with the surface, whereas the measurements in the *Bozkov Dolomite* Caves were carried out near the visitors' path. The results mentioned above could be caused by the fact that the air warms up successively, and the differences between daytime and night-time temperatures are greater during the summer. The situation described here may not apply to another year or to another cave, but it does seem to be the rule for the deeper part of most caves, where there is only weak air exchange with the surface.

Note: in the following graphs, which describe global tendencies, the trend connecting line is interposed using a 6^{th} degree polynomial.

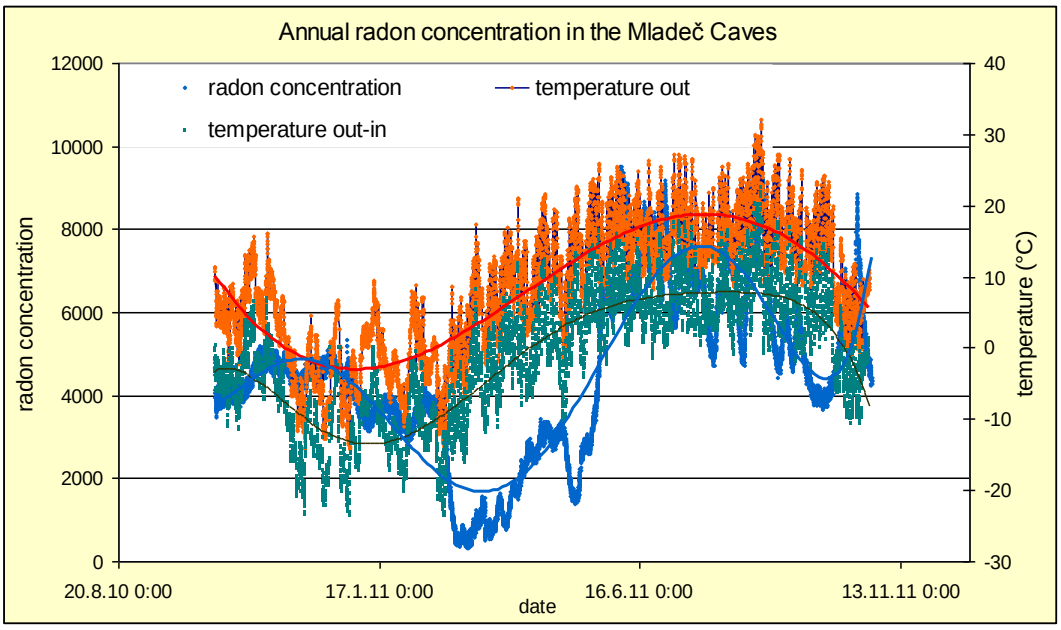

Figure 53 Record of the annual radon concentration and temperatures in the *Mladeč* Caves, between September 2010 and October 2011

The green curve demonstrates the difference between outside and inside temperatures. The radon concentration decreased when the difference grew to zero ºC. A decrease in the outside temperatures led to an increase in radon concentration, with a delay of about three months.

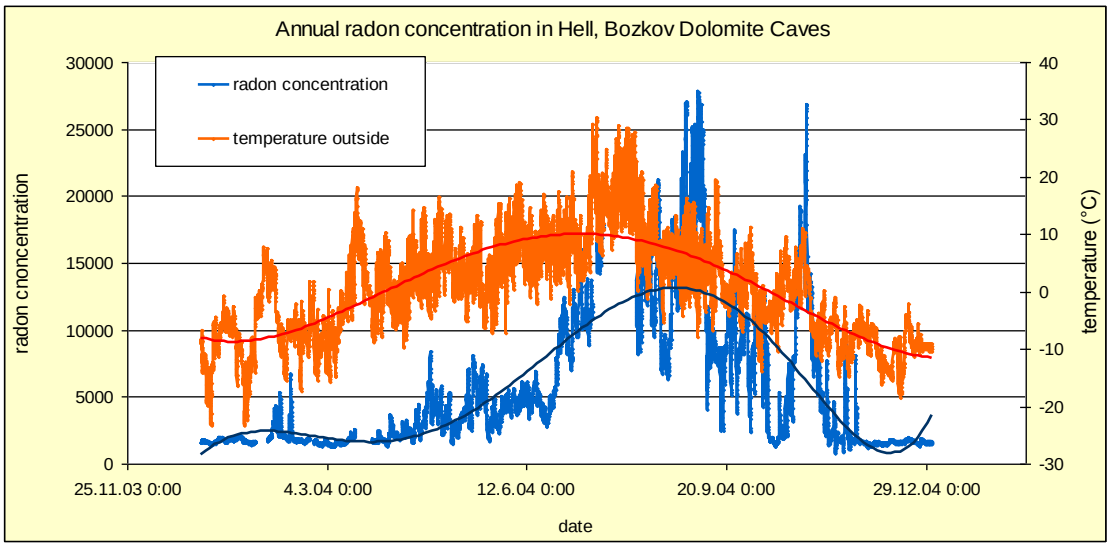

Figure 54 Record of the annual radon concentration and the outside temperatures in the *Bozkov Dolomite* Caves, *Hell*, from January 2004 to December 2004

The delay in the increase in radon concentrations in comparison with the increase in outside temperatures is approx. 3 months. The situation is slightly distorted, due to some gaps in the data.

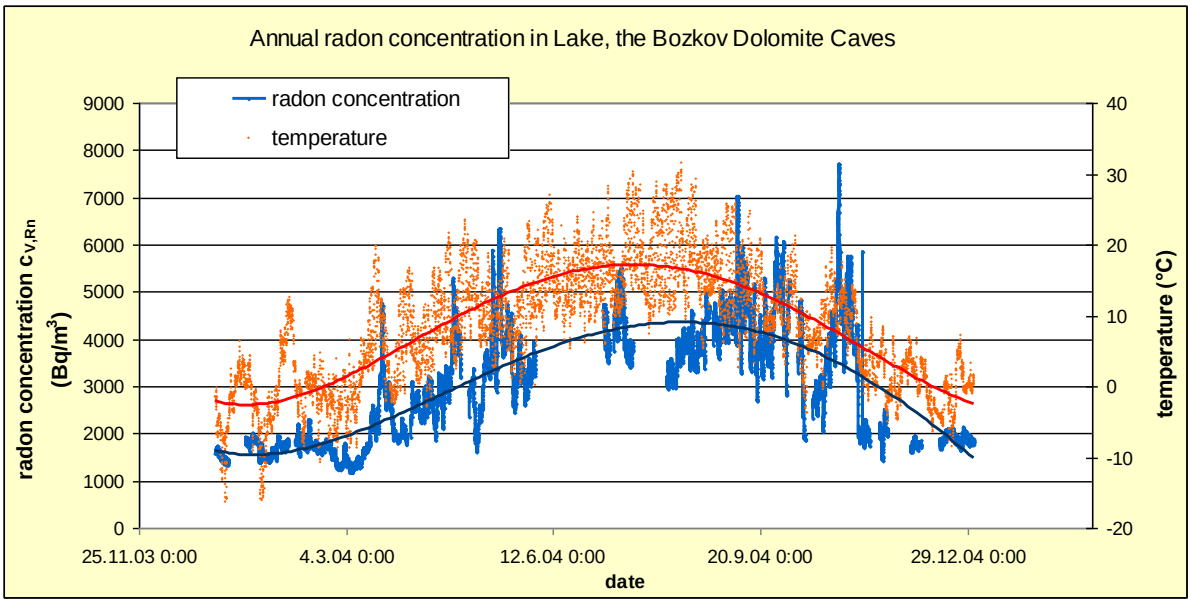

Figure 55 Record of the annual radon concentration and the outside temperatures in the *Bozkov Dolomite* Caves, the *Lake*, from January 2004 to December 2004

The delay in the increase in radon concentrations in comparison with the increase in outside temperatures is approx. 3 weeks. The *Lake* is located quite near the exit of the cave. The situation is slightly distorted, due to some gaps in the data.

The next example shows the results from five locations in the *Bozkov Dolomite* Caves for measurements taken over a period of three days (from June 30th to July 3rd 2005). The measurements were taken three times per day: in the morning (9 a.m.), in the middle of the day (1 p.m.) and in the night (11 p.m.). The results show how different behavior of the air masses influences the air transportation directions along the cave at two different heights (usually 30 cm and 180 cm above the ground, depending on the spatial possibilities of the measured area). Figures 56-62 present selected results of interest. Figure 56 shows that the air flow intensity may have changed significantly in the course of a few hours. In the *Robber's Cave* the direction of the air flow is changeable, decreasing or increasing in some way in the course of the measurements, at heights designated "down" and "up".

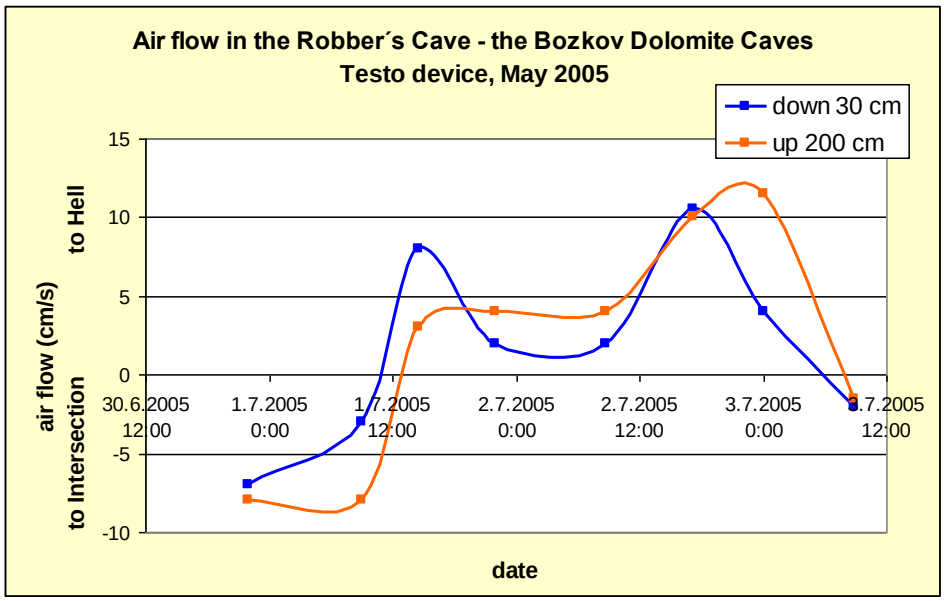

Figure 56 The air flow in the course of three days in the *Robber's* Cave

In the *Hell* area, the location with the highest radon concentration, the downward air flow is always positive (the air flow is aimed into the *Christmas Caves*), but at the height referred to as "up" the air circulates (Figure 57).

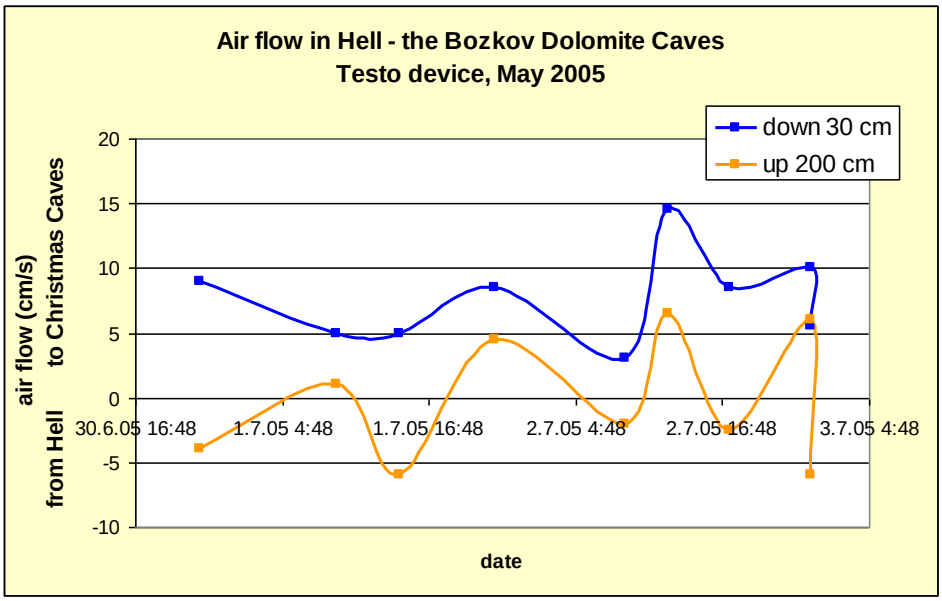

Figure 57 The air flow in the course of three days in the *Hell* section

There was an interesting situation in the *Intersection* area, where the direction of the air flow was permanently the same – parallel – near the ground, and also near the ceiling. Only the direction of the flow changed regularly (Figure 58).

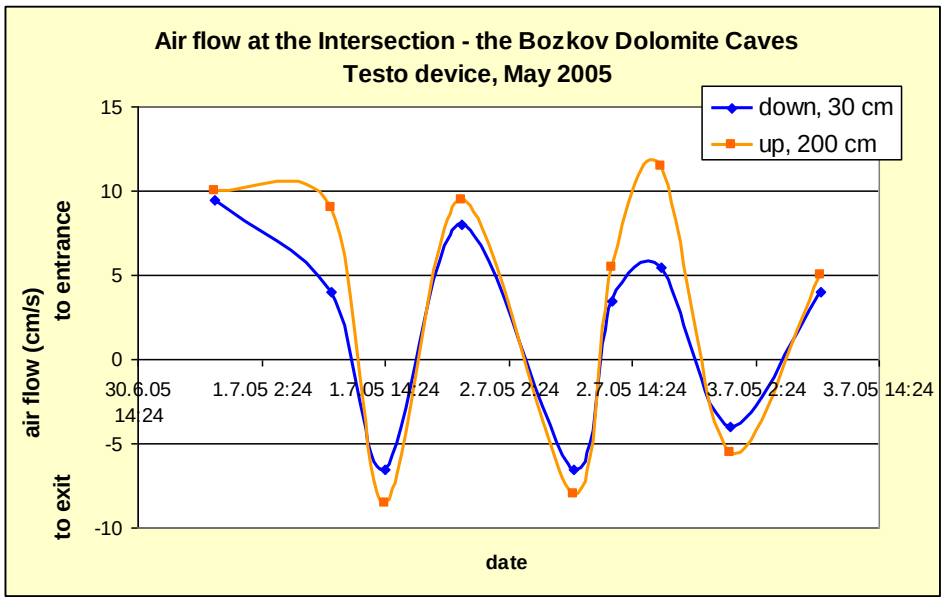

Figure 58 Air flow in the course of three days at the *Intersection*

The last demonstrated location is the *Lake*, which is close to the cave exit. There, the air flow is influenced by the opening of the door. Unlike at the *Intersection*, the directions of the air flow "down" and "up" are always opposite to each other (Figure 59).

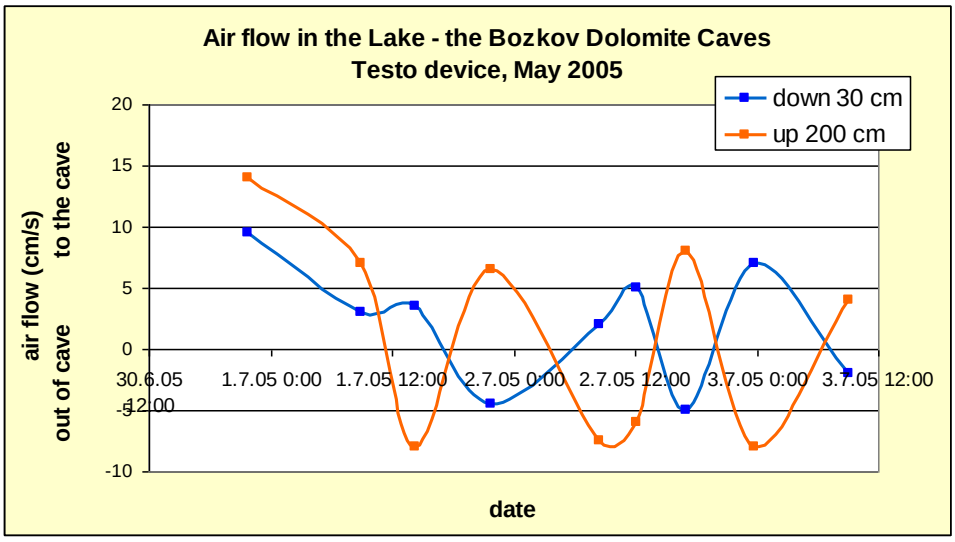

Figure 59 The air flow in the course of three days in the *Lake* area

Using the combination of data measured on July 7th 2006, it was possible to show the imaginary path of the air along one part of the main visitors' path in sequences of locations: Entrance – *Intersection* – *Hell* - *Pirate Shift* – *Lake* - Exit. The air is drawn in through the entrance and flows out through the exit. A change in direction was recorded in a location between *Intersection* and *Hell*, where the paths meet (at the *Robber's Cave* - *Hell* intersection,

and at the *Hell-Pirate Shift* intersection). An interesting situation in *Hell* - stable, low air flow in the direction into *Hell* - caused permanently higher radon concentrations, which are supplied by the non-accessed areas known as the *Christmas Caves* and the *New Year Caves (*Figure 60*).*

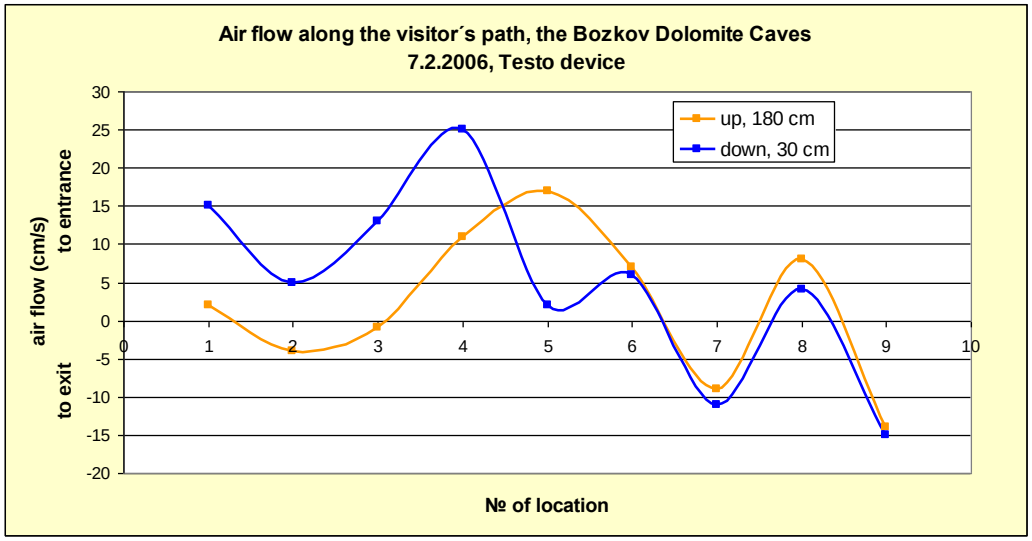

Location	Name		
1	The *Chapel*	6	The *Robber's Cave*
2	The *Midnight Cave*	7	The *Hell*
3	The *Intersection*	8	The *Pirate Shift*
4	The *Muddy Corridor*	9	The *Lake*
5	The *Parallel Corridor*		

Figure 60 Air flow along the visitors' path on July 7th 2006

The second type of measurement was focused on recording the air flow at the locations listed above throughout 2002. The measurements were carried out regularly, once per month, at midday. One part of the measurements was focused on the location *Lake*, and the air flow was measured with opened exit doors or with closed exit doors. The "up" and "down" direction of the air flow was always the same, irrespective of whether the door was open or closed. Opening the door influenced the flow only when both the day temperatures and the night temperatures were near or below zero ºC (Figure 61).

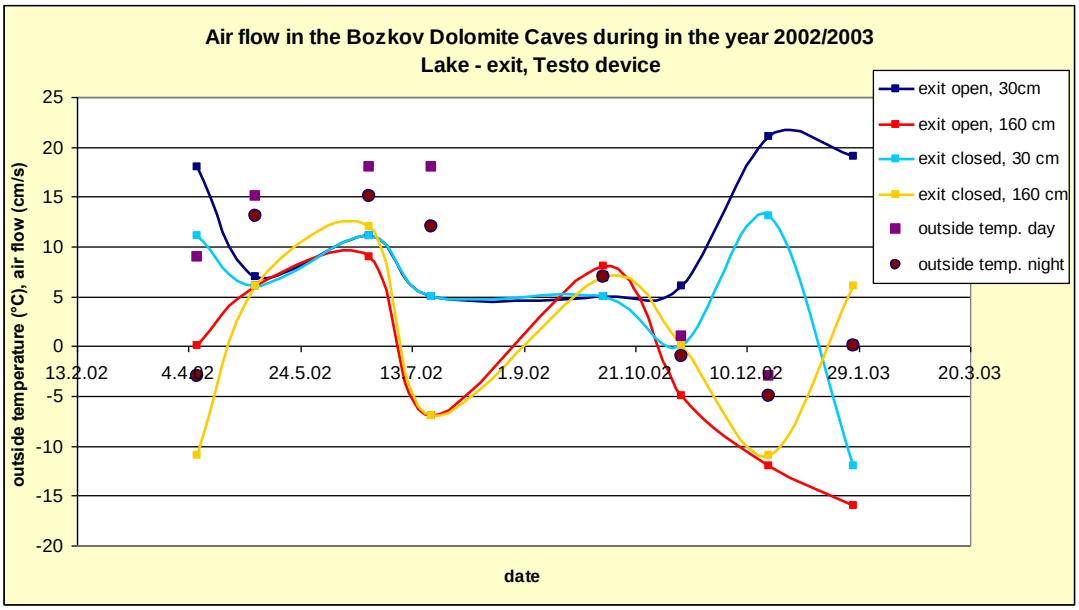

Figure 61 Air flow in the *Lake* in 2002. Measurements with open or closed exit door

Figure 62 shows the previous situation, and a study was made of the air flow in *Hell* and the *Swan Lakes*, which are located close to *Hell*. From the measured data, we concluded that whereas the air flow from the *Swan Lakes* into the *Hell* area varies in direction, the air flow at a height of 140 cm in the *Hell* area is positive (direction toward the *Christmas Caves*) and relatively stable during the summer season. This air flow maintained the high radon concentration that has accumulated there.

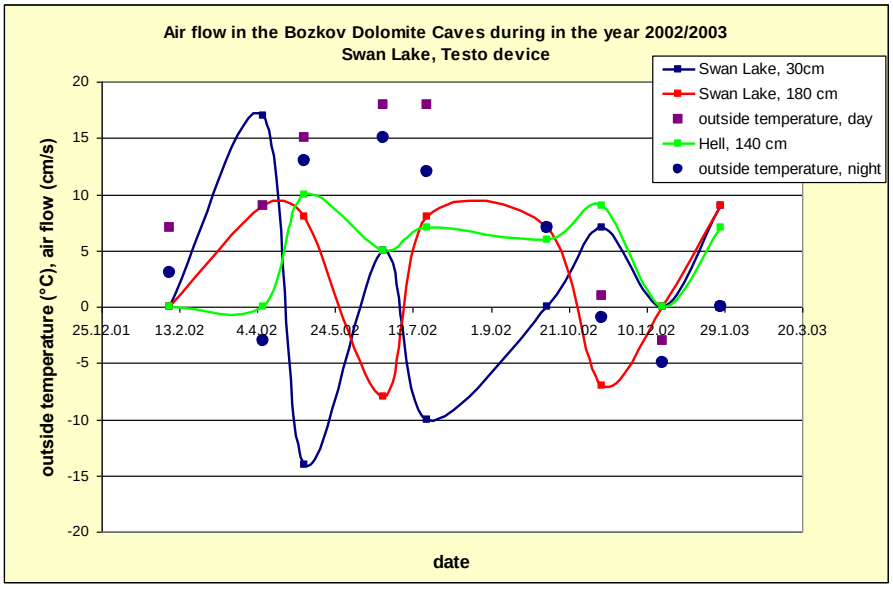

Figure 62 shows the direction of the air flow between summer season and winter season in the locations *Swan Lakes* and *Hell*

In summary, the results presented above indicate some relationships:

- The air flow in each underground area is quite individual, and only ambiguous air mass transportation rules can be proposed. These rules may change from day to day, and from year to year, depending on several parameters.
- The air flow significantly impacted the radon concentration levels at individual locations. However, for the purposes of calculating the dose from radon, it is not necessary to know the air flow in detail, only the radon concentrations, which must be measured continuously.
- In order to obtain detailed information about the air flow, long-term monitoring of each part of the caves is necessary, together with information about the outside meteorological parameters.
- It is indisputably very useful to make a study of the air flow as a part of the cave environment.

6.4 Unattached fraction measurements

The unattached and attached fractions of radon daughters were measured in all underground areas, using the FRITRA4 device. An example of the results is shown in Figure 63. The data obtained on radon concentration and radon daughters concentration enabled equilibrium factor F to be determined. To calculate the *individual cave factor*, we used mostly the data for the unattached fraction, measured on the wire screen (the calculation is presented in chapter 7). The measurements using the FRITRA4 device in the *Bozkov Dolomite* Caves (the center point of the study) and the *Kateřina´s* Cave (the highest individual cave factor) were repeated in order to verify the measurement results. In both cases, the results were within the declared relative error range of 10%, and the highest individual cave factor in the *Kateřina´s* Cave was confirmed in the year 2009.

Figure 64 shows the chosen measured data, using the FRITRA4 device. The measurements were carried out in *Hell* in the *Bozkov Dolomite* Caves in 2005. The average equilibrium factor was F=0.58, and the average unattached fraction was f_p=2.98%. The results from the simultaneous measurements in the *Chapel* (near the entrance) were: F=0.46 and f_p=1.77% (Figure 65), and in the *Lake* (near the exit) the results were: F= 0.49 and f_p=1.88%.

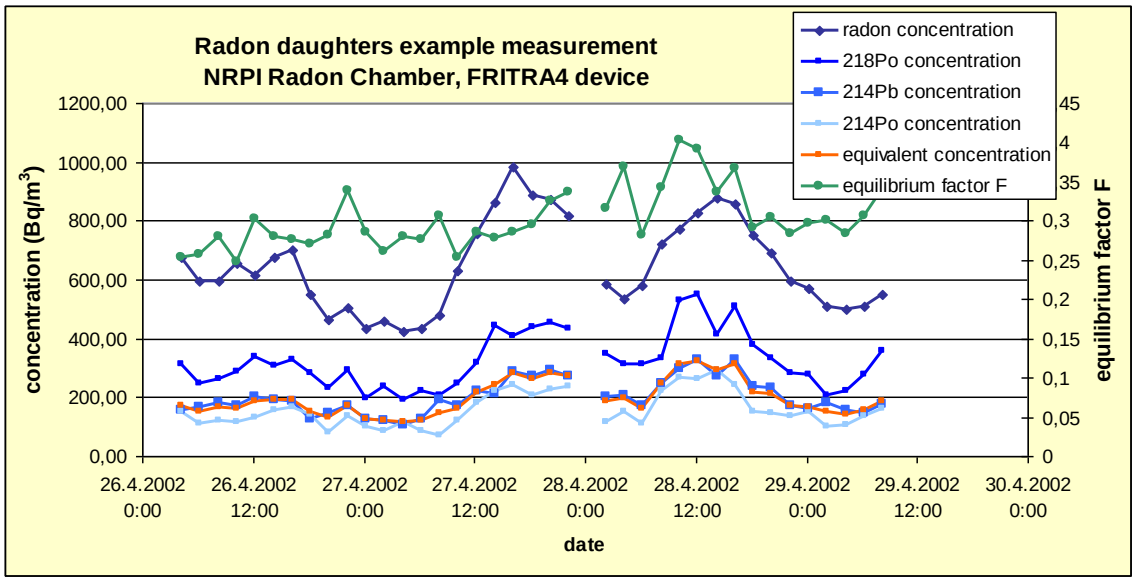

Figure 63 Verification measurements, using the FRITRA4 continuous monitor in the radon chamber

The results supported the conclusion that the unattached fraction value in different locations in the cave does not differ significantly. The measurements were repeated in July 2006 in the *Hell* area, and F was 0.47 and f_p was 2.83%.

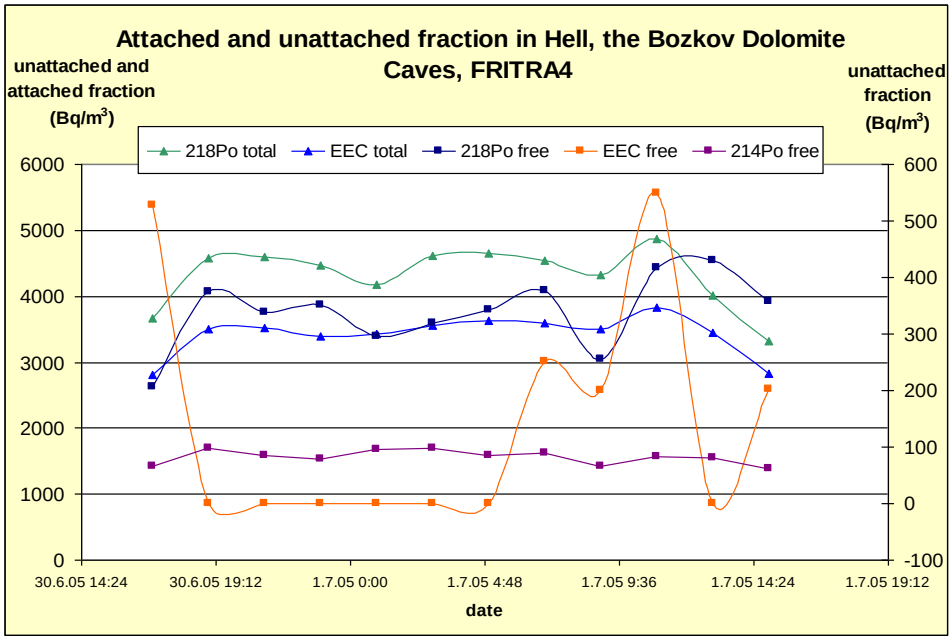

Figure 64 Continuous radon daughters monitoring in the *Bozkov Dolomite* Caves, using the FRITRA4 device

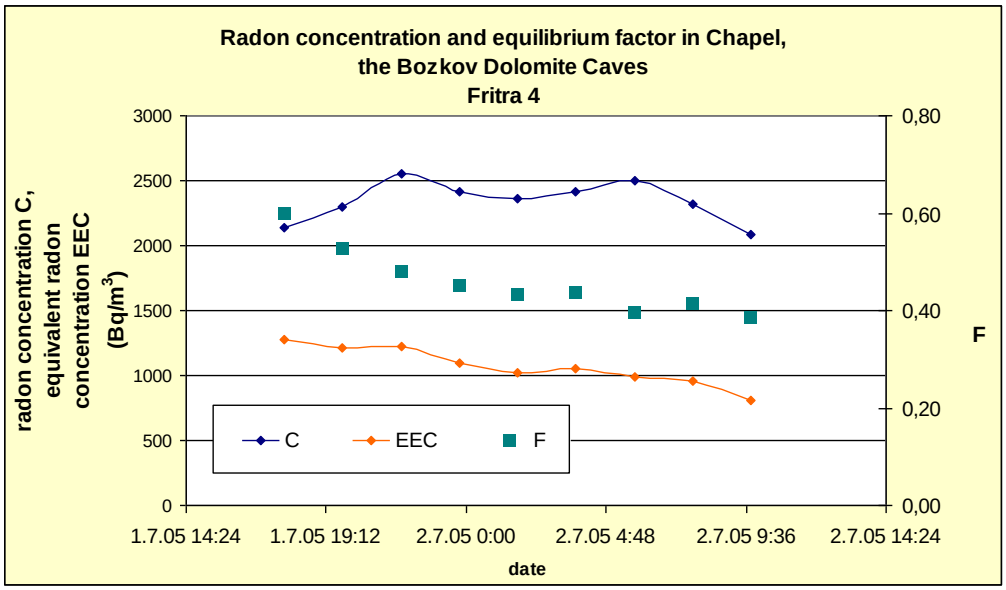

Figure 65 Continuous equilibrium factor monitoring in the *Bozkov Dolomite* Caves, using the FRITRA4 device

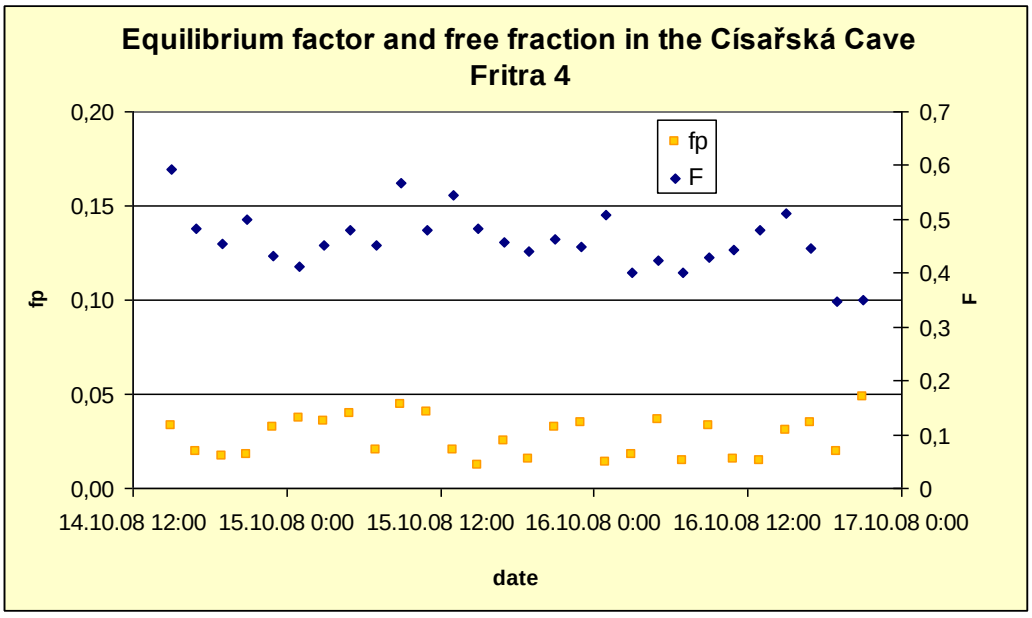

Figure 66 Measurements of F and f_p in the *Císařská* Cave speleotherapy area

In addition to the routine measurements discussed above, a unique experiment in the *Bozkov Dolomite* Caves enabled measurements to be made simultaneously in five different locations in the cave (*Chapel, Intersection, Robber's Cave, Hell, Lake*), using five Fritra4 devices. The devices were compared before and after the measurements in the radon chamber of the NRPI and during the measurements in the *Robber's* Cave. The results (Figure 67, Figure 68) show the variability of the unattached fraction and the equilibrium factor in different (most visited)

areas in the cave in the course of a guided tour. The percentage of unattached fraction was practically the same during the measurements, within 2.2% on an average. The equilibrium factor was on an average F = 0.58.

FRITRA4 and AlphaGuard devices during the measurements in the Kateřina´s Cave

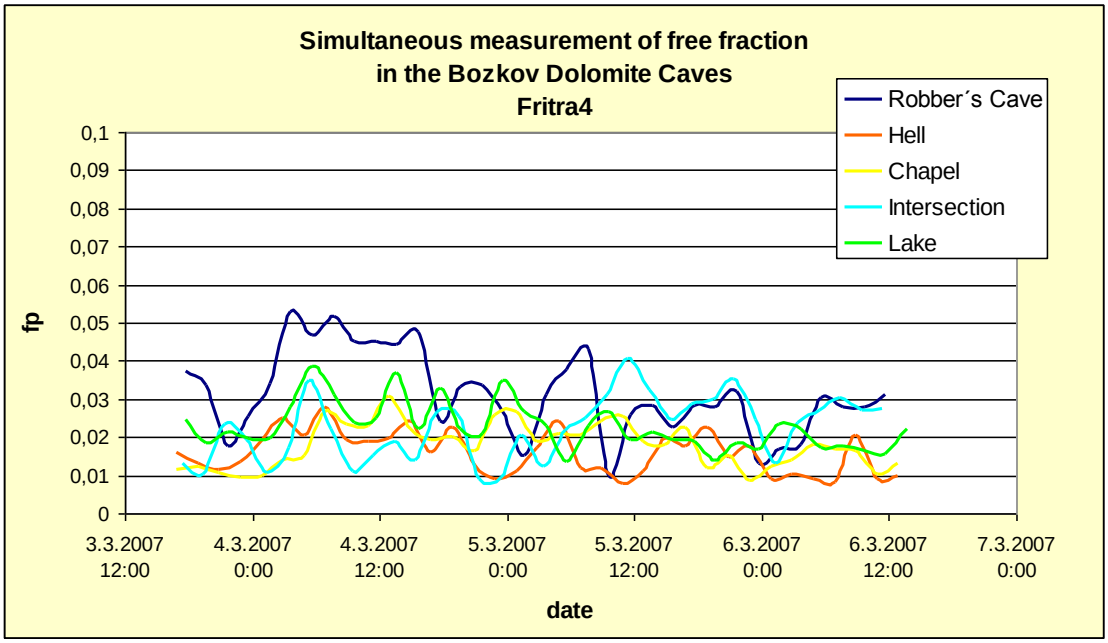

Figure 67 Results of simultaneous unattached fraction measurements at five locations in the *Bozkov Dolomite* Caves, using five FRITRA4 devices

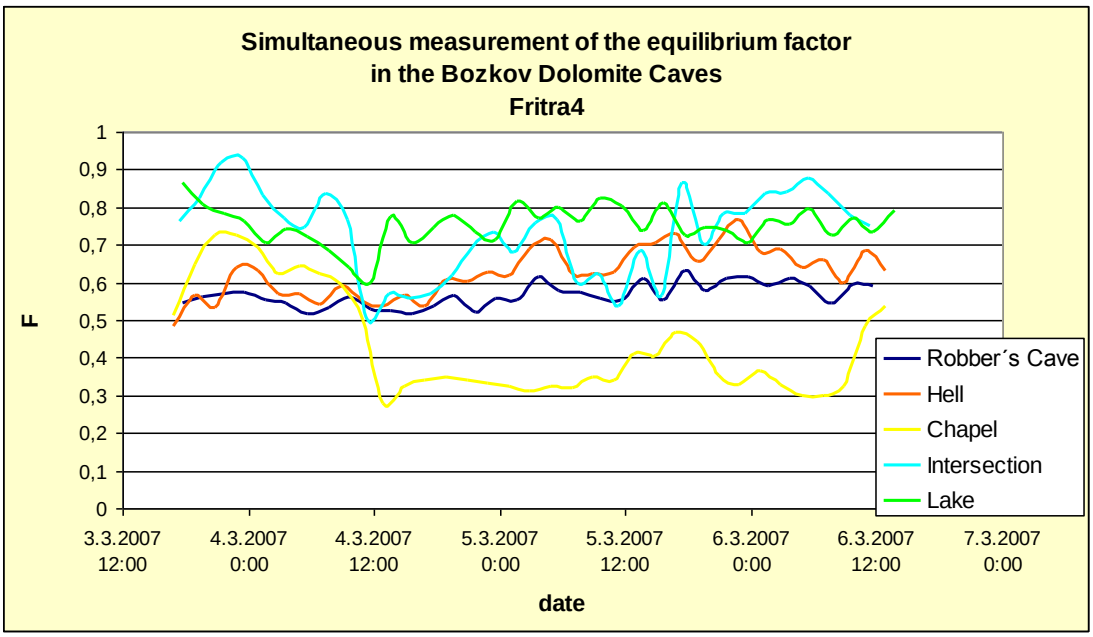

Figure 68 Results of equilibrium factor determination from simultaneous measurements at five locations in the *Bozkov Dolomite* Caves, using five FRITRA4 devices

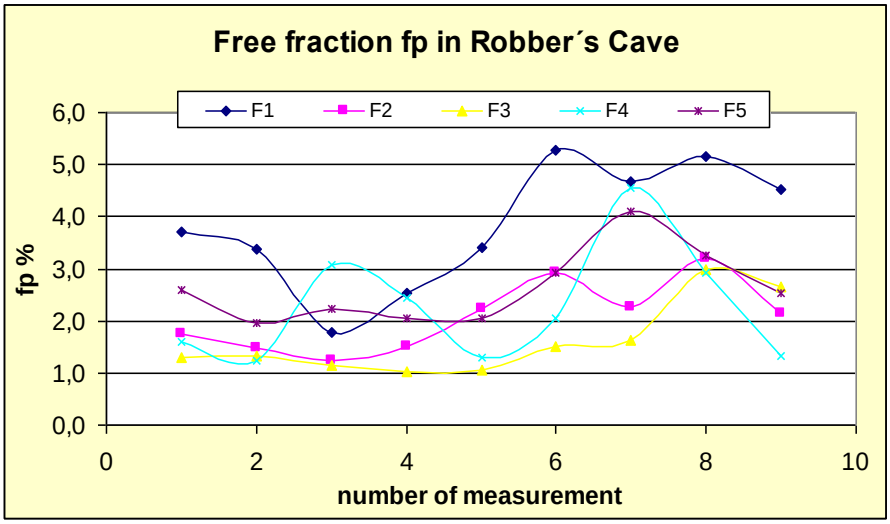

Figure 69 Results of comparative measurements in the *Robber's* Cave (F1-F5 is the number assigned to the FRITRA4 device) – unattached fraction measurements

The results of the measurements using the FRITRA4 continuous monitor show that the variability of the equilibrium factor is more significant in the cave environment than it is in apartments. The equilibrium factor differs from cave to cave and in different areas of the same cave, and changes over time (Figure 71, Figure 72). During the guided tour, F was 0.35 (σ = 0.1), and during the night F was 0.33 (σ = 0.06) on an average.

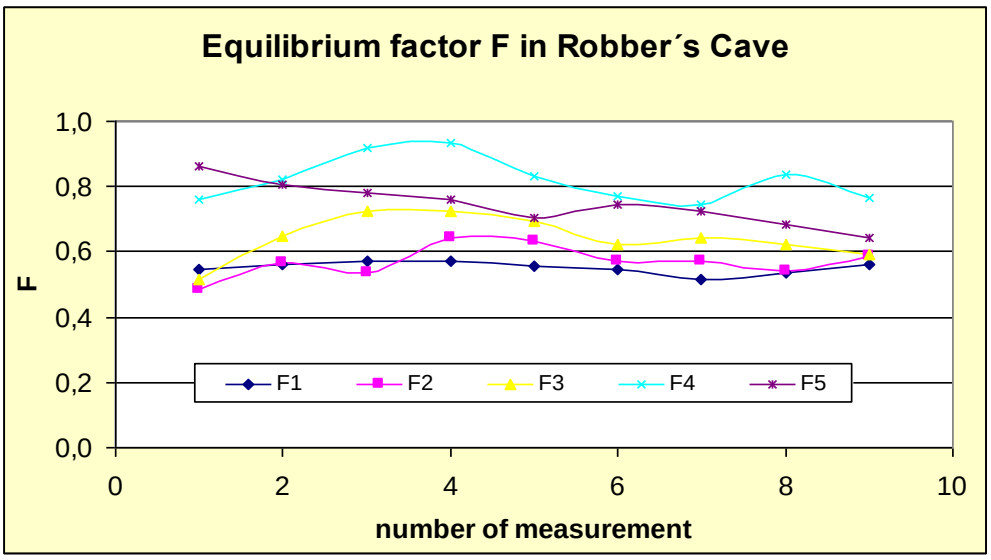

Figure 70 Results of comparative measurements in the *Robber's* Cave (F1-F5 is the number assigned to the FRITRA4 device) – equilibrium factor determination

The most accurate dose calculation should therefore be based on spectrometric determination of individual radon daughters and on categorizing them as unattached and attached fraction. However, radon monitoring in this way would be too expensive. For the purposes of radon dose calculation, it was considered adequate to determine the individual effective doses via routine integral seasonal radon concentration monitoring.

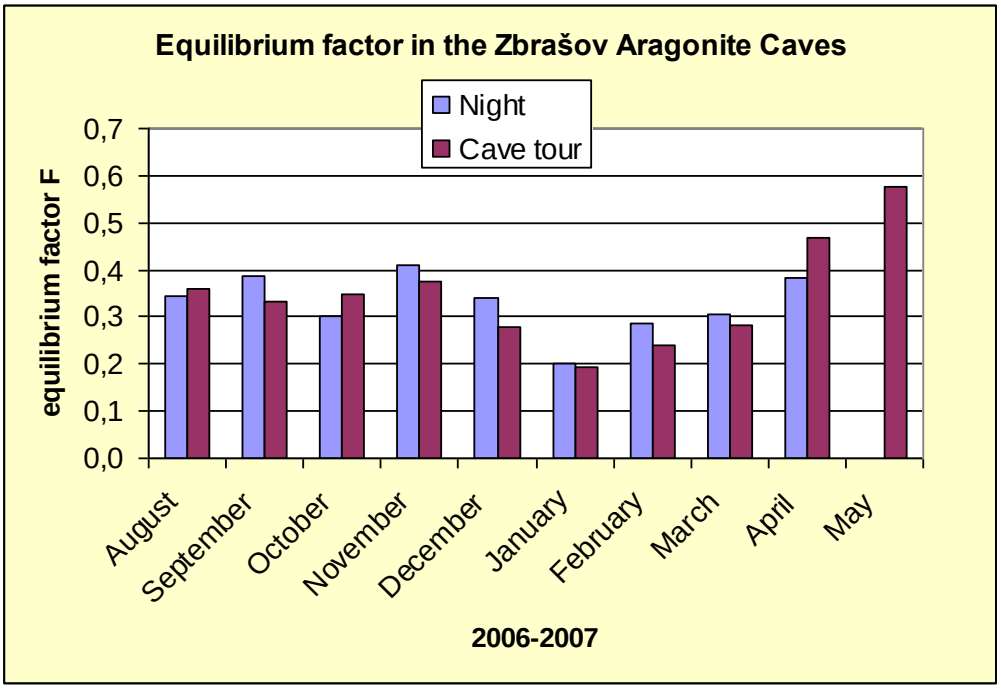

Figure 71 Annual course of the equilibrium factor in the *Zbrašov Aragonite* Caves, in 2006/2007

The equilibrium factor F in the *Bozkov Dolomite* Caves varied between 0.2 and 0.7 in the different locations in 2002 – 2003 (Figure 72). These results are based on the grab sampling method, using a PSDA radon daughters measurement device, and the radon concentration was determined with the use of IK250 ionizing chambers. It is probable that the results have a significant statistical error (systematic shift), because the radon concentration was often below the minimum detection activity of the ionizing chamber measurement system. However, the main trend in F variation is shown clearly.

As both radon measurements and radon daughter measurements were carried out each month, we were able to calculate the equilibrium factor time-dependence. The results presented in this graph imply that there is relatively intensive ventilation in practically all places, but that the ventilation decreased dramatically after the installation of a double door (July '02). The most intensive ventilation was found in the *Surprise* Caves, which are directly connected with the outside through a natural chimney; by contrast, the deepest point in the underground network is *Hell*, where the equilibrium factor was found to be among the highest. The high level of equilibrium at the *Lake*, which is close to the cave exit, was surprising, but the value can be explained by the spacious area there, which could retain a stable air composition with minimal influence of air flow.

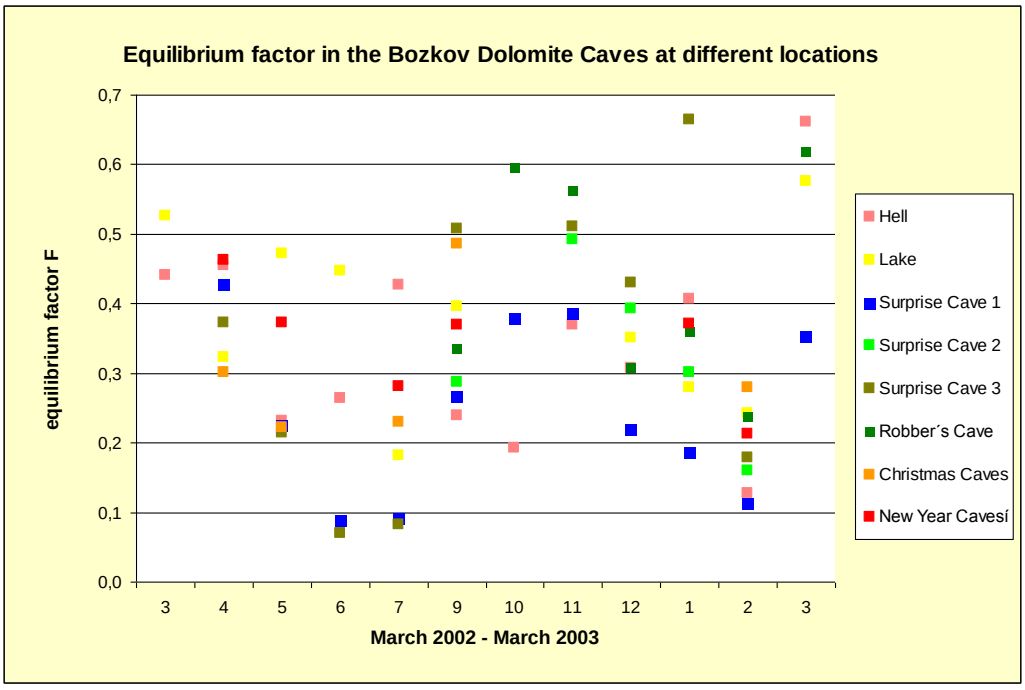

Figure 72 Annual course of the equilibrium factor in the *Bozkov Dolomite* Caves in 2002/2003, at various locations

Equilibrium factor F and unattached fraction f_p were determined using the FRITRA4 device in show caves and in some other underground workplaces. The results were used to calculate the individual cave factor (chapter 7), and are summarized in Table 15:

Table 15 Unattached fraction in the night period and in the daytime period at the measurement locations

Cave	f_p (night)	f_p (day)
Bozkov Dolomite Caves	0.02	0.03
Zbrašov Aragonite Caves	0.32	0.34
Kateřina Cave	0.58	0.48
Koněprusy Caves	0.34	0.36
Chýnov Caves	0.04	0.05
Javoříčko Caves	0.06	0.06
Mladeč Caves	0.11	0.12
Na Pomezí Caves	0.34	0.33
Na Špičáku Caves	0.08	0.08
Sloup-Šošůvka Caves	0.37	0.38
Balcarka Cave	0.32	0.32
Na Turoldu Caves	0.36	0.47
Zlaté Hory Edel Speleotherapy	0.03	0.02
Vojtěchov Speleotherapy	0.39	0.08
Císařská Cave Speleotherapy	0.03	0.03
Wine cellars, average	0.02	0.02
Mariánská Tunnel	0.10	0.10

Summary of the measurement results, using the FRITRA4 device:

The unattached fraction determined from the repeated measurements in 2005, 2006 and 2007 in the *Bozkov Dolomite* Caves varied between 0.2-0.3. The unattached fraction measured in the *Zbrašov Aragonite* Caves (a complicated environment with an artificial ventilation system

that is used to decrease the CO_2 concentration) in 2006/2007 varied from 0.3 to 0.5. This fact forms the basis for the estimation that the unattached fraction varies less in the range of typical values, but not significantly.

- The individual cave factor was calculated on the basis of the unattached fraction measurement results, which are given in Table 15.
- The experiments raised some questions, e.g. the relevance and the reproducibility of unattached fraction measurements (dependent on wire screen properties) in environments with different aerosol size distributions.
- Generally, the measurements in the caves open to the public in the Czech Republic demonstrated that each of them is a distinct site. The free fraction ranged from 0.03 to 0.6, and the arithmetical average unattached fraction was 0.13 for the "average Czech cave". The dose assessment methodology for caves in the Czech Republic was modified on the basis of these results.

6.5 Aerosol spectrum measurements and cave factor estimates

In addition to the radon measurements, the aerosol particle size distribution was also measured, as one of the most important parameters for dose evaluation. All results discussed in this chapter are based on a three-day aerosol campaign, which was carried out in the *Bozkov Dolomite* Caves. This chapter is compiled from a master's thesis (Rovenská, 2007) and from the final report of the VaV 12/2006 project (Thinová, 2007).

A brief description of the regime in the cave during the aerosol campaign:

August 30th – guided tours during the day – the devices were installed from 4 p.m. till 10 p.m. The measurements began. The measurement results were to be stored manually, once per hour, by a person entering the cave.

August 31st – measurements ongoing – guided tours during the day – the measurement results were to be stored manually, once per hour, by a person entering the cave.

September 1st – measurements ongoing – guided tours during the day – the measurement results were to be stored manually, once per hour, by a person entering the cave – a new automatic measurement system was installed from 6 p.m. till 12 p.m. (work in the cave with the door open).

September 2nd – measurements ongoing – no people in the cave, throughout the day and night.

September 3rd – measurements ended at 6 a.m.

The concentration of aerosol particles depended strongly on the presence of people, and on their behavior. The increase in the number of the smallest particles (between 3 to 200nm) was caused by work in the cave in the evening of September 1st, when a new detection system was being installed. The presence of people the cave led to the door being opened. The level of "stress" aerosols decreased slowly (Figure 73) after the work had been completed.

It was found that the presence of aerosol particles 1-10 μm in diameter is definitely caused by visitors or by the presence of personnel. When the cave was closed, the particles disappeared rapidly (after approx. 1 hour the concentration was about 10^{-4} #/cm^3). However, the concentration of particles about 200 nm in diameter is relatively stable (~10 #/cm^3). In the case of the largest particle size group (~10 nm), it seems that the aerosols are produced by intensive work or movement (the concentration is about 100-1000 #/cm^3).

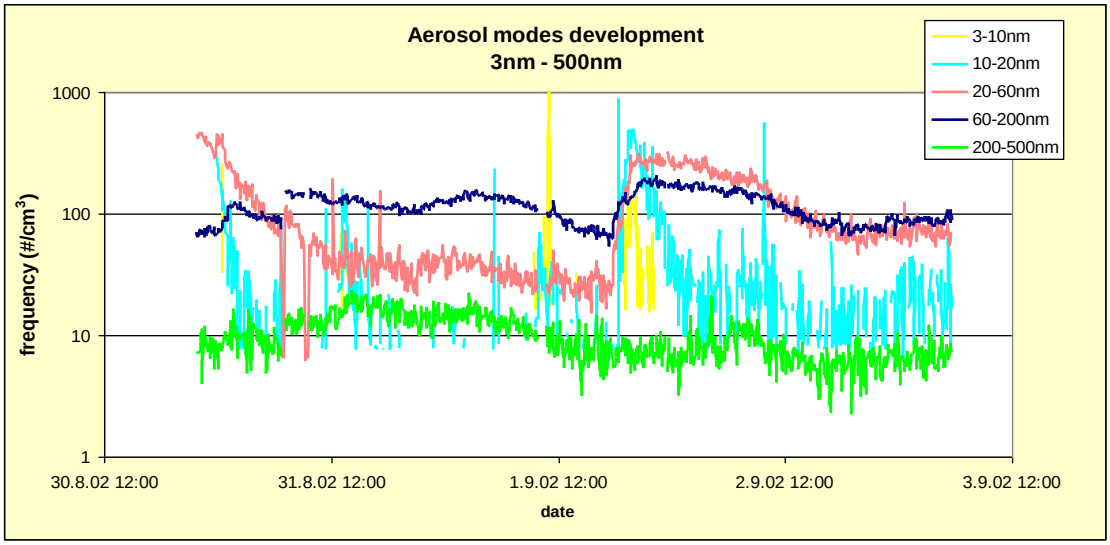

Figure 73 Development of aerosol modes with particle size between 3nm and 500nm during the aerosol campaign

The largest particle concentration (Figure 74, 2.5 – 10 μm) decreased rapidly when the cave was empty, i.e. when there were no people present. Guided tours and the presence of people for work led to a renewed increase in aerosols.

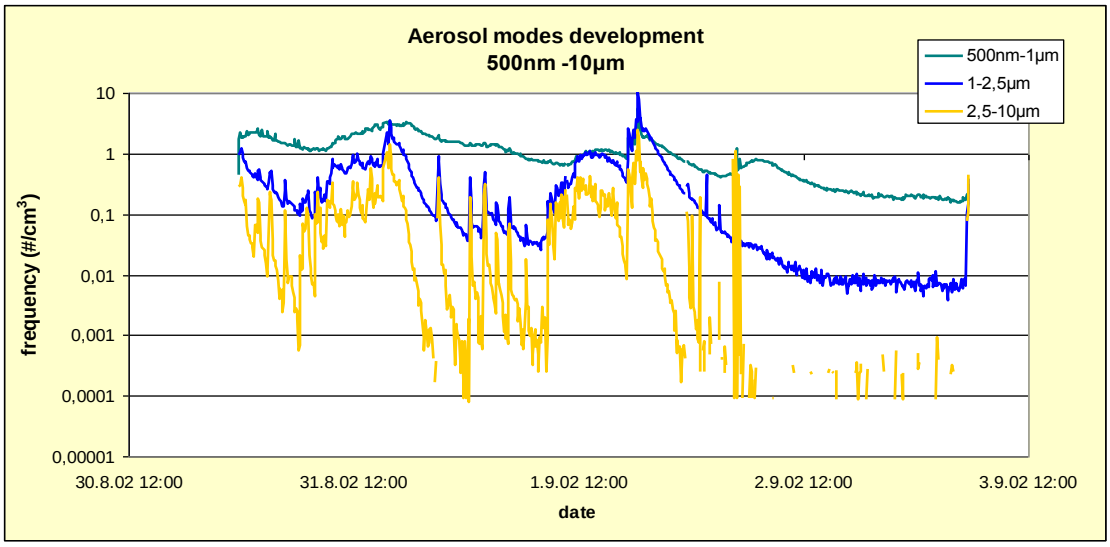

Figure 74 Development of aerosol modes between particle size 500 nm and 10 µm during the aerosol campaign

For the processing of the results, the measured data from the aerosol campaign was divided into time intervals (regimes), which followed the actions in the cave during the aerosol campaign: Night; Guided tour; Work in the cave; Night after the work; Cave tour without visitors; Empty cave. The aim of this process was to find the changes in particle concentration during the various work activities in the cave. From the point of view of calculating the radon dose, emphasis was put on the *Guided tour* regime in the cave. The average particle concentration during these time intervals is summarized in Table 16. This result shows that the particle concentration in the cave was about one order of magnitude lower than the usual concentration found in dwellings (Marsh, et al., 1998).

Table 16 Particle concentration from the aerosol campaign in the *Bozkov Dolomite* Cave in 2002

Profile	**Particle concentration (** #/cm^3)
Night	253
Guided tour	187
Work in the cave	536
Night after the work	494
Cave tour without visitors	292
Empty cave	197

The dose calculation is based on the aerosol spectra, an evaluation of the deposited activity on the aerosol particles and on the dosimetric model (Table 17 and Table 18).

Measurements performed with the FRITRA4 monitor provided this information (volume activity of radon decay products, radon concentration, equilibrium factor and unattached and attached fraction of radon daughter products). Repeated measurements (in 2005, 2006, 2007) showed a low proportion of free fraction in the *Bozkov Dolomite* Caves of about 2-3%. From the measurement results, the average F was taken equal to 0.6, and the average unattached fraction was 3%.

Table 17 Concentration of radon daughters – the *Bozkov Dolomite* Caves

(FRITRA4: 4.3. - 6.3.2007)

Profile: Guided tour

F	0.68	Attached (Bq/m^3)	^{218}Po	1069	^{214}Pb	870	^{214}Po	845
f_p	1.25%	Unattached (Bq/m^3)	^{218}Po	101	^{214}Pb	6	^{214}Po	0

Profile: Night

F	0.68	Attached (Bq/m^3)	^{218}Po	890	^{214}Pb	746	^{214}Po	737
f_p	1.25%	Unattached (Bq/m^3)	^{218}Po	95	^{214}Pb	4	^{214}Po	1

The dose was determined for the "Guided tour" profile and for the "Night" profile. Using the measured concentrations of aerosols, the activity deposited on individual aerosol modes was determined, using the equation published by Porstendörfer (Porstendörfer, 1994). The results of interpolation using the log-normal distribution for the "Night" and the "Guided tour" profiles are presented in Table 18.

Table 18 AMAD and dispersion for the "Night" profile and for the "Guided tour" profile

Night		**Guided tour**		
AMAD (nm)	**σ**	**AMAD (nm)**	**σ**	**EEC fraction**
140	1.80	143.8	1.65	72%
711	1.18	715.7	1.41	11%
		1900	1.90	17%

The measurements provided no information on the particle size of the free fraction. For the purposes of the calculations, sizes of 0.5 nm (lowest deposition in the bb and BB region) and 3 nm (the highest deposition in the bb and BB region) were chosen, see Table 22. In order to calculate the cave factor, information is required about the activity of the attached and free radon daughters and about the size of AMAD with dispersion σ. This data was taken from (Marsh, et al., 1998) and (Nazaroff, et al., 1988) (Table 19, Table 20).

Table 19 ***Activity concentration for radon daughters – apartments*** **(Marsh, et al., 1998)**

F	0.37	Attached (Bq/m^3)	^{218}Po	56.4	^{214}Pb	35.8	^{214}Po	27.1
f_p	6.4%	Unattached (Bq/m^3)	^{218}Po	15.9	^{214}Pb	1.4	^{214}Po	0

Table 20 ***AMAD and dispersion – apartments*** **(Marsh, et al., 1998)**

AMAD [nm]	σ
0.9	1.30
50	2
250	2
1500	1.5
Growth factor	1.5 (for unattached fraction)

The LUDEP program was used to calculate the dose conversion coefficients (Rovenská, 2007):

The breathing rate was considered to be the same for cave and for residential spaces - 0.778 m^3/h. Breathing was considered to be carried out only through the nose. The total dose coefficient for a given decay product was determined using equation 8:

$$DCF_x = \sum_{\text{mod}} C_x * DCF_{mod}(X) * fractionEEC_{mod} \qquad \textbf{Equation 8}$$

where X represents successively ^{218}Po, ^{214}Pb, ^{214}Bi; C_X is the volume activity of the appropriate decay product, and $fractionEEC_{mod}$ is the fraction of EEC on a given size mode. Total DCF can be obtained from equation 9:

$$DCF = \sum_x DCF_x / EEC \qquad \textbf{Equation 9}$$

where DCF_x are the results from equation 8 for individual decay products; EEC is the entire EEC; DCF is in nSv/Bqhm^{-3} units (Table 21).

Table 21 Dose conversion factors for individual radon daughters

	DCFs for apartments (Sv/Bqhm^{-3})		
AMAD (nm)	**^{218}Po**	**^{214}Pb**	**^{214}Bi**
0.9	9.45E-09	4.89E-08	3.73E-08
75	3.85E-09	1.82E-08	1.37E-08
375	1.29E-09	6.19E-09	4.66E-09
2250	2.45E-09	1.23E-08	9.39E-09

	DCFs for Bozkov D.C., Night profile (Sv/Bqhm^{-3})		
AMAD (nm)	**^{218}Po**	**^{214}Pb**	**^{214}Bi**
0.5	4.90E-09	2.59E-08	1.98E-08
3	1.69E-08	8.29E-08	6.28E-08
141	2.34E-09	1.11E-08	8.34E-09
711	7.93E-10	3.85E-09	2.91E-09

	DCFs for Bozkov D.C., Guided tour profile (Sv/Bqhm^{-3})		
AMAD (nm)	**^{218}Po**	**^{214}Pb**	**^{214}Bi**
0.5	4.90E-09	2.59E-08	1.98E-08
3	1.69E-08	8.29E-08	6.28E-08
143.8	2.25E-09	1.06E-08	8.01E-09
715.7	8.96E-10	4.36E-09	3.30E-09
1900	2.08E-09	1.04E-08	7.96E-09

The *individual cave factor* **j=1** for the *Bozkov Dolomite* Caves was determined on the basis of the aerosol campaign results. The *cave factor* can then be obtained as the ratio of DCF for a cave and DCF for a residential space. The cave factors for the "Guided tour" profile and for

the "Night" profile are plotted in Table 22. Figure 75 shows the activity distribution during “Guided tour” profile. The maxima for Aitken nuclei mode (0.144 μm), accumulation mode (0.716 μm) and coarse mode (1.9 μm) are in good agreement with the aerosol spectrum from the mine environment, where the maxima for particles of a given diameter were: from 0.001 to 0.08 μm, from 0.08 to 1.0 μm, and from 0.1 to 40 μm (Cantrell, et al., 1987). Only the maximum for the smallest particles in the *Bozkov Dolomite* Caves is shifted to larger particles (0.144 μm), mainly due to coagulation processes.

Table 22 The values of individual cave factor “j” for the *Bozkov Dolomite* Caves

Free fraction	0.5 nm	3 nm
Guided tour profile	0.83	1.06
Night profile	0.75	0.82

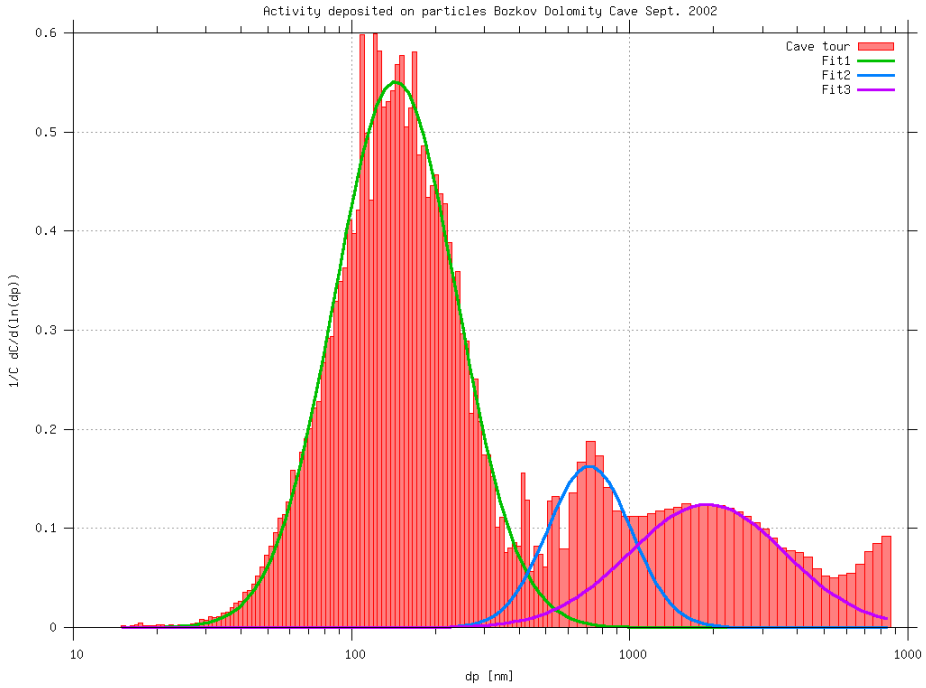

Figure 75 Aerosol modes during the measurements in the *Bozkov Dolomite* Caves – “Guided tour” profile (Rovenská, 2007)

6.6 Gamma dose rate for different underground location measurements

Table 23 summarizes the gamma dose rate measurement results in units of nGy/h (the kerma rate for gamma radiation in air is equal to the gamma dose rate). The column under the heading "air" presents the results of measurements in air, while the column under the heading "in contact" presents the results of measurements in contact with clastic sediments. The gamma dose rate in contact with the limestone was usually the same as, or slightly lower than, the dose rate measured in air. The gamma dose rate measurement in air was used for the dose from external irradiation calculation. The directional dependence of the TESLA NB3201 device was not taken into account. In most of the caves or underground spaces, the dose rate is lower than or comparable with measurements on the surface, whereby the average gamma dose rate from terrestrial radiation in the Czech Republic is 66 nGy/h (leading to an annual effective dose from external irradiation E = 0.40 mSv, when 8640 hours are taken into account).

The effective dose E (μSv, mSv) for a worker from external irradiation by gamma/year is calculated using:

$$E = B.(\dot{D} - \dot{D}_p).T \text{ ,} \qquad \textbf{Equation 10}$$

where:

$\dot{D}$ gamma dose rate in nGy/h,

$\dot{D}_p$ gamma dose rate from the natural background at the workplace in nGy/h; this is usually measured in the neighborhood of the workplace, or is known from previous measurements

T annual exposure of workers at a given location, in hours,

B photon dose equivalent, used for recalculation of gamma radiation from natural radionuclides into an effective dose in mSv/mGy. For a common mixture of radionuclides ^{40}K, ^{226}Ra, ^{228}Th, including their radon daughter products, the standard value is B = 0.7 mSv/mGy.

Table 23 shows that the effective doses calculated for time spent by workers annually under the ground are negligible (the information about working hours is from 2006), and due to the low number of working hours the values are not more than tens of μSv. Because the measured dose rates were so low, the background was not subtracted.

Considering all the facts mentioned above, the dose from external irradiation in caves is smaller than, or comparable with, the irradiation on the surface. It was therefore not taken into account when performing the total effective dose calculation.

Table 23 Results of gamma dose rate measurements in selected underground areas

Cave	gamma dose rate Ḋ (nGy/h)				
	air	in contact	inaccessible part	Working hours	E (μSv)
Mladeč Caves	65	180	to Gorge - 260	280	12.7
Sloup-Šošůvka Caves	36	68		300	7.6
Balcarka Cave	40	61		250	7.0
Kateřina Cave	36	65		200	5.0
Javoříčko Caves	90	126		500	31.5
Zbrašov Aragonite Caves	90	130		140	8.8
Koněprusy Caves	45	90		200	6.3
Na Pomezí Caves	36	72		180	4.5
Na Špičáku Caves	29	54		180	3.7
Chýnov Caves	54	72		200	7.6
Bozkov Dolomite Caves	130	137	Christmas Caves - 440	550	45.5
Na Turoldu Caves	30	36		*500**	10.5
Vojtěchov Tunnel	180	245		*500**	63
Dobrošov	97	126		*500**	34
Hanička	98	144		*500**	34

* Estimation

The measured gamma dose rates can be compared with the assessment of the dose rate based on the natural radionuclide content in rock and sediments (chapters 6.10). The average radon activity concentration values in individual caves (measured separately during the summer and winter season) corresponds well with average gamma dose rates values (Figure 76).

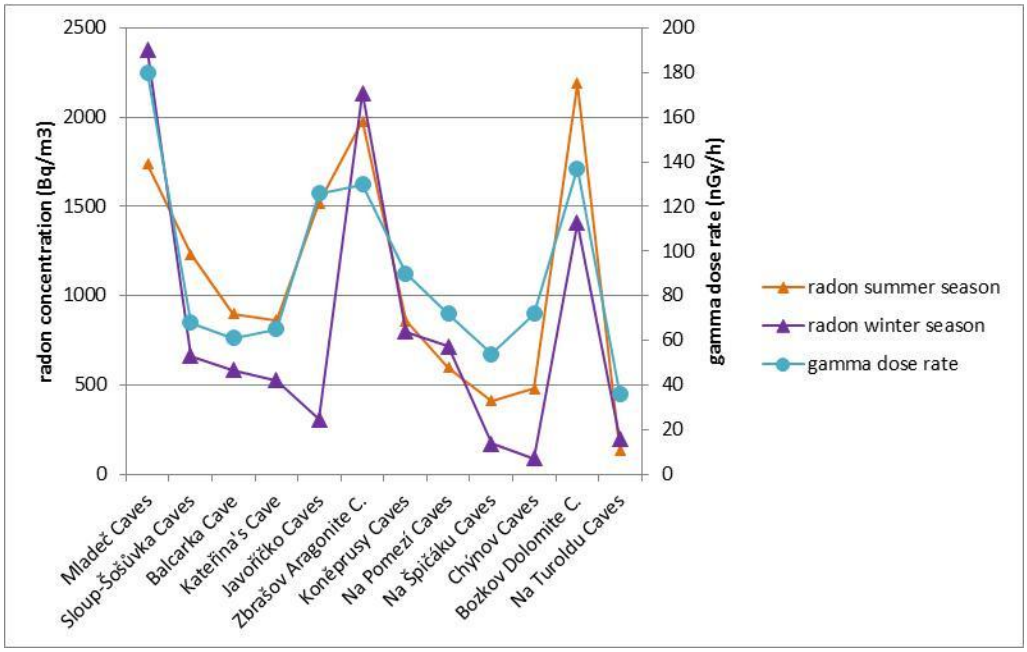

Figure 76 The comparison of average gamma dose rate values (measured on contact with clastic sediments) and average radon activity concentration (measured during summer and winter season)

Measurements in the Hanička underground Fortress. RADONIC01, NB3201 devices.

6.7 Radon in water measurements

Table 24 summarizes the results from the radon in water sample measurements. All measurements were carried out in situ, with relative error 20%. The MDA of the measurement system presented here is 2Bq/l. Two types of water samples were collected: water from lakes and water from small puddles of dripping water. The radon concentration in lakes was in the range of units Bq/l, and in dripping water the radon concentration was very low, practically below the detection limit.

Table 24 Results from radon in cave water measurements

Cave		Bq/l
Bozkov Dolomite Caves	Lake 1	7.1
	Lake 2	6.7
	Swan Lakes 1	8.3
	Swan Lakes 2	8.9
Sloup-Šosůvka Caves	Broušek Chamber	1.0
	before Silver Corridor	0
Chýnov Caves	water stream 1	3.9
	water stream 2	4.2
Na Pomezí Caves	Near Willow 1	0.1
	Near Willow 2	0.1
	Jewel Case	0.1
	Royal Dome - lake	0
Javoříčko Caves	Giant's Dome	2.4
	Happy Lake	1.3
Balcarka Cave	Gallery-small tank	12.3
	Big Dome	1.1
Kateřina Cave	Main Dome	0.9
	Near the Bear Stack	1.1

The low concentration of radon in the measured water, in combination with the low and stable temperature in the caves, leads to the conclusion that water cannot be the source of the high concentration of radon in the caves.

6.8 Determining the radon exhalation rate from the rock in selected show caves

All measurements mentioned below were carried out by NRCBPI staff (Petr Otáhal) in Kamenná-Milín (Thinová, 2007). The results were determined using two methods:

- In situ determination of the radon diffusive flux from the subsoil.
- Laboratory determination of the radon mass exhalation rate in selected types of sedimentary rocks.

6.8.1 In situ determination of the radon diffusive flux from the subsoil

In the *Bozkov* Dolomite Caves and in the *Zbrašov Aragonite* Caves, the radon diffusive flux was measured on the cave clastic sediments subsoil.

Basic methodology

When measuring the radon exhalation rate from the ground surface, the collecting container (a glass bottle) with a capacity of 12.8 liters is inserted into the ground soil, and is fastened in a stable position. Before the monitored area is entered, the container is flushed with outdoor air containing a minimal concentration of radon.

At time zero, the container input valve is opened, allowing the radon from the soil to diffuse into the container, which initially contained a minimal concentration of radon. The air in the container is sampled at regular intervals, using the exact volume that is transferred into the scintillation chamber. After radioactive equilibrium between ^{222}Rn and radon daughters is established, the radon activity concentration is determined. After data processing, the final result is the radon exhalation rate value per unit area, which is expressed in $mBq \cdot m^{-2} \cdot s^{-1}$.

Determining the radon diffuse flux results from the subsoil

In the *Bozkov Dolomite* Caves, the radon exhalation rate per unit area was determined in the area of the *Pirate Ship*. The detected radon exhalation rate per unit area from the clastic sediments was 45 ± 6 mBq $m^{-2} \cdot s^{-1}$.

In the *Zbrašov Aragonite* Caves, the flow of radon from the soil was determined on clastic sediments in the cave in the area of the *Gallaš´s* Dome bottom. The detected radon exhalation rate per unit area was 60 ± 8 $mBq \cdot m^{-2} \cdot s^{-1}$.

The results should be considered as local values.

6.8.2 Laboratory determination of the radon mass exhalation rate in selected types of sedimentary rocks

The radon mass exhalation rate was investigated in the clastic sediments in the cave and in dolomite in the material taken from the *Bozkov Dolomite* Caves and the *Zbrašov Aragonite* Caves.

Basic methodology

When determining the radon mass exhalation rate, a sample with defined mass is placed in an enclosed container. A series of air samples is collected in the following period of several hours and weeks (10 to 30 days). Each time, an air sample is transferred to a scintillation chamber to determine the radon activity concentration. The obtained values $c_{V,Rn}$ for individual time intervals become the input values for estimating the radon mass exhalation rate.

Results of laboratory determination of the radon mass exhalation rate from selected sedimentary rocks types

Table 25 summarizes the results of a radon mass exhalation rate test on samples of cave clastic sediment (CCS) and of dolomite sample measurements (Dolomite).

Table 25 Results for the radon exhalation rate of samples of clastic sediments and karst rock

Sample origin	a_m (μBq·s^{-1}·kg^{-1})
CCS Zbrašov 1	40.54±3.24
CCS Zbrašov 2	35.97±2.88
CCS Bozkov 1	40.28±3.17
CCS Bozkov 2	63.05±5.01
Dolomite Bozkov1	1.611±0.13
Dolomite Bozkov2	0.566±0.058

In relation to other measured samples, the values listed above were at the lower end of the radon mass exhalation rate scale. According to (UNSCEAR, 2000) and (Nazaroff, et al.,

1988), where an average emanation coefficient of 0.1 was used, the mass exhalation rate of radon in rock is nominally 10 $\mu Bq \cdot s^{-1} \cdot kg^{-1}$ (the lowest values were near 0.3 $\mu Bq \cdot s^{-1} \cdot kg^{-1}$).

6.9 Thoron measurements

The influence of thoron concentration on the radon concentration measurement results was verified in the *Zbrašov Aragonite* Caves, and the results presented in Table 26 were determined in studies by NRBCPI. The contribution of thoron to radon activity concentration was determined by a calculation process using results from 10 s measurement sets using Lucas cells (LUK4A device, Lucas cells 0.8l in volume). These results confirmed that no influence of thoron on the measured values for $c_{V,Rn}$ and EEC in the *Zbrašov Aragonite* Caves can be expected due to low thoron concentrations and diffusion rates. It is assumed that the contribution of thoron to the radon concentration was less than 10% in the open space where the RAMARN integral detectors are placed.

Table 26 Results of thoron measurements in the *Zbrašov Aragonite* Caves

Location	$c_{V,Rn}$ (Bq/m^3)	Error (Bq/m^3)	$c_{V,Tn}$ (Bq/m^3)	Error (Bq/m^3)	$c_{V,Rn}/c_{V,Tn}$
Gallaš Dome	2626	274	275	59	0.10
Waterfall	3258	136	566	67	0.17
Tunnel, fissure	8188	233	2252	660	0.28
Tunnel, wall surface	10915	293	1515	265	0.14

6.10 Laboratory gamma spectrometry measurements

The results from the laboratory gamma spectrometry measurements are summarized in Table 27 (clastic sediments) and Table 28 (rock, mainly limestone). A total of 142 samples were measured, using the laboratory gamma spectrometry method. The ^{226}Ra, ^{228}Th and ^{40}K mass activities were calculated using Genie 2000 Software. The ^{226}Ra mass activity (Bq/kg) was calculated from the energies of ^{214}Bi daughter, because it was assumed that there is a disturbance of the equilibrium between U and Ra in the sediments.

The lowest mass concentrations of all calculated radionuclides were in sinters, usually in the range of first units of Bq/kg. In limestone, the concentration of ^{226}Ra and ^{228}Th was usually

units of Bq/kg. The highest ^{226}Ra concentrations in rock were in *Vilémovický* limestone in the *Zbrašov Aragonite* Caves (40 Bq/kg), in the limestone in the *Javoříčko* Caves in the *Chamber of Hope* (41 Bq/kg), and in *Suchomastský* limestone in the *Koněprusy* Caves (30 Bq/kg). The concentration of ^{226}Ra in erlan (in the *Chýnov* Caves) was 22 Bq/kg.
The concentration of ^{226}Ra and ^{228}Th in clastic sediments was usually tens of Bq/kg. The highest ^{226}Ra concentrations in the sediment samples were in the *Mladeč* Caves, in the *Cathedral of Nature* (106 Bq/kg) and in the *Blue Cave* (183 Bq/kg). In the *Chýnov* Caves, 73 Bq/kg ^{226}Ra and 120 Bq/kg ^{228}Th were measured in the area of the *Sticky Corridor*.
Note: For clastic sediments collected in cave, there is no hundred percent certainty, regarding their original location (due to show caves modifications).

The ratio between Th (ppm) and U (ppm) in rocks usually varies between 3-4, which corresponds to a ratio higher than or equal to 1 (one) for calculations using Bq/kg units. In limestone the ratio is usually smaller than 1 (one), due to very low concentrations of Th.

The observed Th/Ra ratios in clastic cave sediments were mostly higher than 1; 1.5 on an average. But in some cases the ratio was surprisingly less than 1. This occurred for example in the *Mladeč* Caves, in the clastic sediments from the *Cathedral of Nature*, the *Deed's* Dome, the *Blue Cave*; in the *Javoříčko* Caves, in the *Brash* Dome, the *Sink* Dome, the *Garden*; in pelits (equivalent to *Rudické* layers) in the *Zbrašov Aragonite* Caves; in sand-clay sediments in the *Shooting of Žižka* (*Chýnov* Caves), and in all clastic sediments in the *Bozkov Dolomite* Caves. These clastic sediments probably contained a high proportion of autochthonous limestone material.

Sampling process with the help of a geologist (Milan Geršl) in the Sloup-Šošůvka Caves

Units of Bq/kg of ^{137}Cs were detected in the clastic sediment samples from the *Mint* area (*Koněprusy* Caves), in the *Near Willow* area (*Na Pomezí* Caves – 20 Bq/kg) and in phyllites (bedrock of the *Bozkov Dolomite* Caves).

Table 27 Results from laboratory gamma spectrometry measurements – clastic sediments

Cave	^{226}Ra (Bq/kg)			^{228}Th (Bq/kg)			^{40}K (Bq/kg)			Th/Ra	Th/Ra[2]
	min	max	a[3]	min	max	a[3]	min	max	a[3]		
Mladeč Caves	15	183	53	16	56	39	178	580	448	1.4	0.4
Sloup-Šošůvka Caves	14	33	28	33	57	44	447	674	598	1.6	
Balcarka Cave	16	33	25	23	48	38	443	667	565	1.6	
Kateřina´s Cave	26	30	28	14	43	27	239	495	390	1.0	
Javoříčko Caves	18	52	29	16	56	29	217	804	431	1.5	0.7
Zbrašov Aragonite C.	35	52	47	31	65	47	614	959	805	1.5	0.8
Koněprusy Caves	10	44	26	9	72	41	96	410	190	1.6	
Na Pomezí Caves	14	51	30	15	63	42	227	661	498	1.4	
Na Špičáku Caves	15	29	22	36	41	38	232	442	337	1.7	
Chýnov Caves	11	73	19	3	120	25	376	669	504	1.6	0.3
Bozkov Dolomite C.	18	51	32	10	20	15	114	468	318	-	0.5
Na Turoldu Caves			19			19			226	1.0	
Vojtěchov Tunnel	11	34	22	9	54	36	95	600	420	1.6	
Sloup-Šošůvka Cav.[1]			31			35			664	1.1	

[1]surface sediments (*Sloupský* stream)

[2]in some of the clastic sediment samples, the Th/Ra ratio was less than 1, probably because there is a significant contribution from the autochthonous material

[3]a = average

Table 28 The results from laboratory gamma spectrometry measurements – limestone and sinters

Cave		^{226}Ra (Bq/kg)	^{228}Th (Bq/kg)	^{40}K (Bq/kg)	Th/Ra
	rock	average	average	average	
Mladeč Caves	devonian limestone	4	2	47	0.5
Sloup-Šošůvka Caves	limestones and sinters	3	1	0	0.3
Balcarka Cave	limestone	11	4	83	0.2
Kateřina's Cave	limestone brash	8	6	83	0.8
Javoříčko Caves	limestone	27	2	15	0.1
Zbrašov Aragonite C.	*Vilémovický* limestone	40	3	101	0.1
	Hněvotínský limestone	14	11	303	0.8
Koněprusy Caves	*Suchomastský* limestone	25	14	150	0.6
	Koněpruský limestone	7	2	13	0.3
Na Pomezí Caves	limestone	6	2	30	0.3
Na Špičáku Caves	limestone	6	3	24	0.5
Bozkov Dolomite C.	dolomite				
	green phyllites (bedrock)	6	3	323	0.5
Na Turoldu Caves	sandy limestone	9	2	19	0.2
Vojtěchov Tunnel	limestone	7	1	13	0.1
Chýnov Caves	cryst. white limestone	1	1	0	1.0
	cryst. dark limestone	4	5	180	1.0
	erlan	22	14	493	0.6
	amphibolite	5	2	457	0.4
	amphibolite	5	2	346	0.4
	sinter	2	1	30	0.5

The laboratory gamma spectrometry measurement results can be shown in triangle graphs. Due to the order differences in concentrations, the concentrations of ^{40}K were reduced 10 times in order to show the results in better dimension. The samples labeled *S* or *L* represented clastic sediments or limestone (and sinters). Triangular Figure 77 – 90 show the distribution of the ^{226}Ra, ^{228}Th and ^{40}K mass concentrations in individual samples and locations. A significantly different content of radionuclides in a sample is indicated by the outlying position of the result.

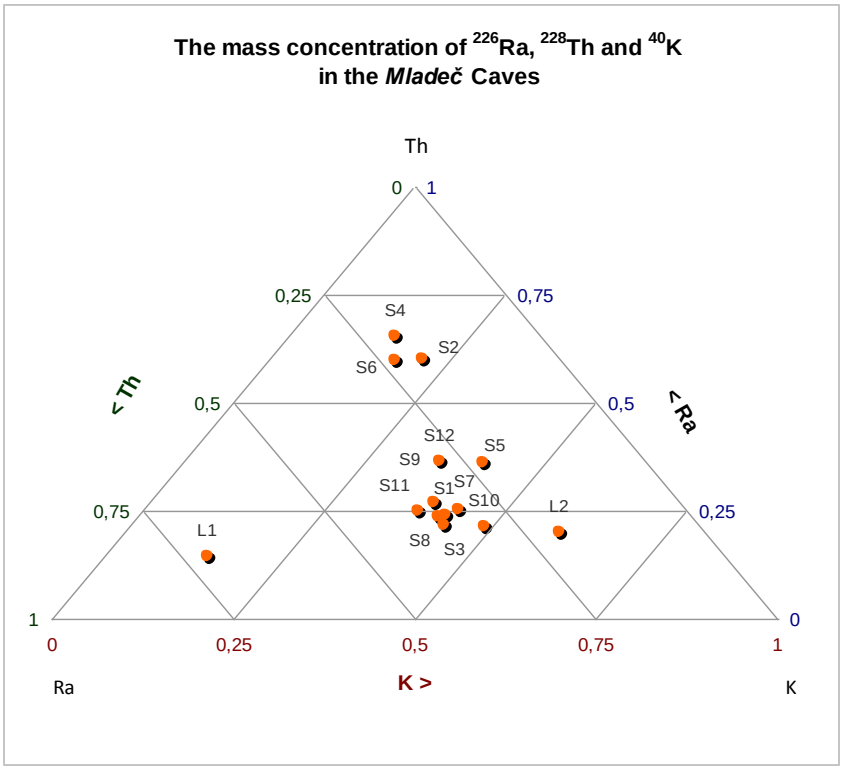

Figure 77 Concentration of ^{226}Ra, ^{228}Th and ^{40}K in the *Mladeč* Caves

S2, S4 and S6 are the sediments from the *Cathedral of Nature*, the *Deed's* Dome, and the *Blue Cave*. L1 and L2 are samples of *Devonian* limestone.

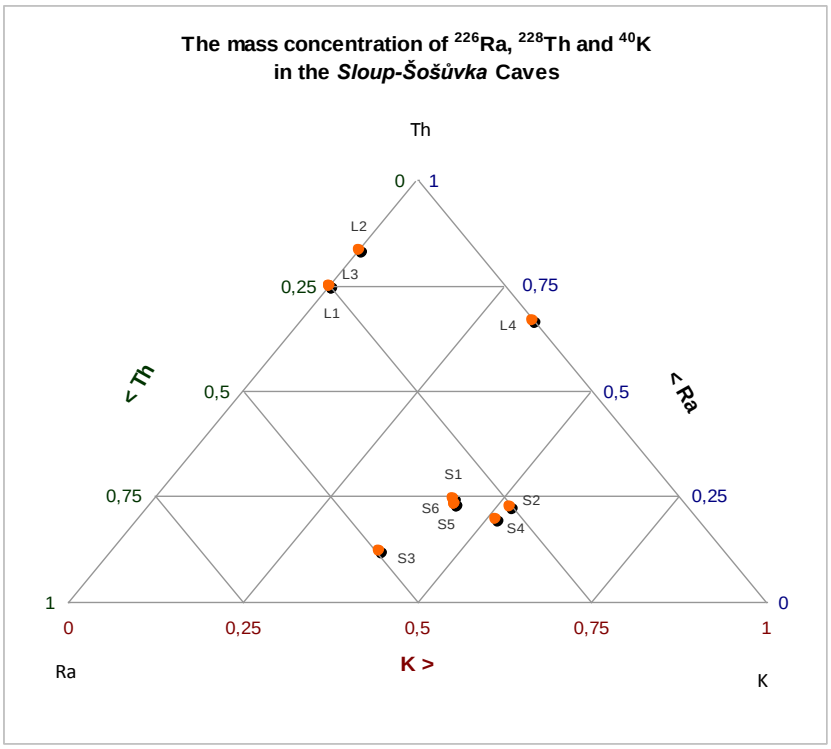

Figure 78 Concentration of ^{226}Ra, ^{228}Th and ^{40}K in the *Sloup-Šosůvka* Caves

Samples L1-L4 are sinters. The clastic sediment S3 comes from the connection corridor.

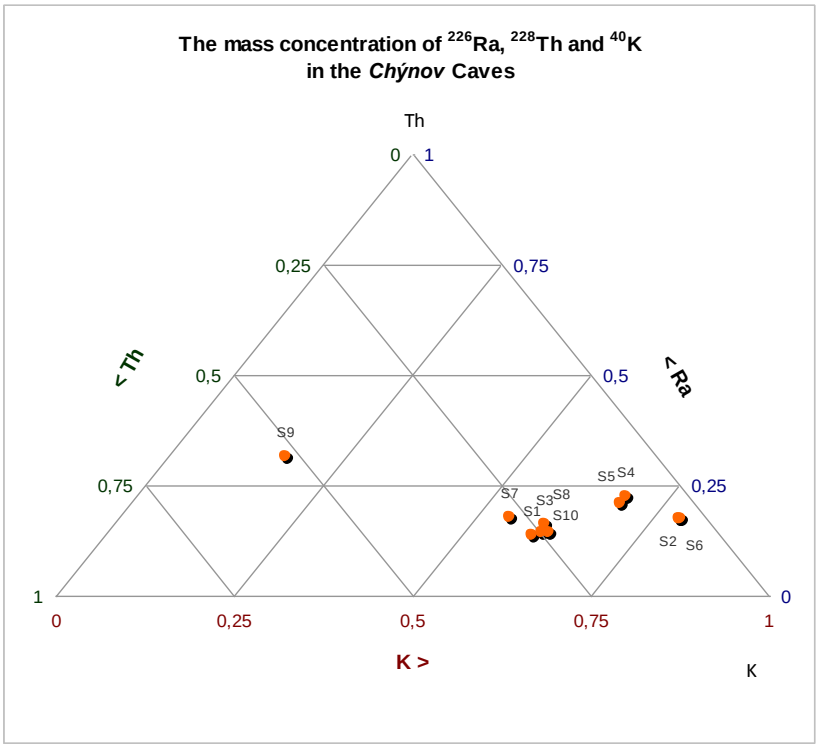

Figure 79 Concentration of ^{226}Ra, ^{228}Th and ^{40}K in the *Chýnov* Caves – clastic sediments

Sample S9 is a clay sediment and S2, S6 are sandy-clay sediment from the *Sticky* Corridor.

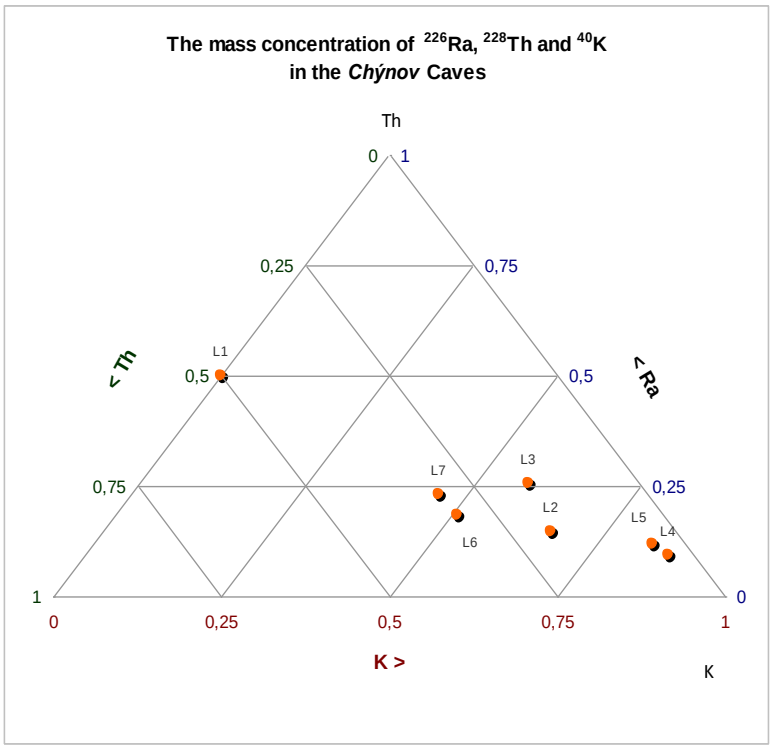

Figure 80 Concentration of ^{226}Ra, ^{228}Th and ^{40}K in the *Chýnov* Caves - sediments

Sample L1 is white crystalline limestone; L4 and L5 are samples of amphibolite.

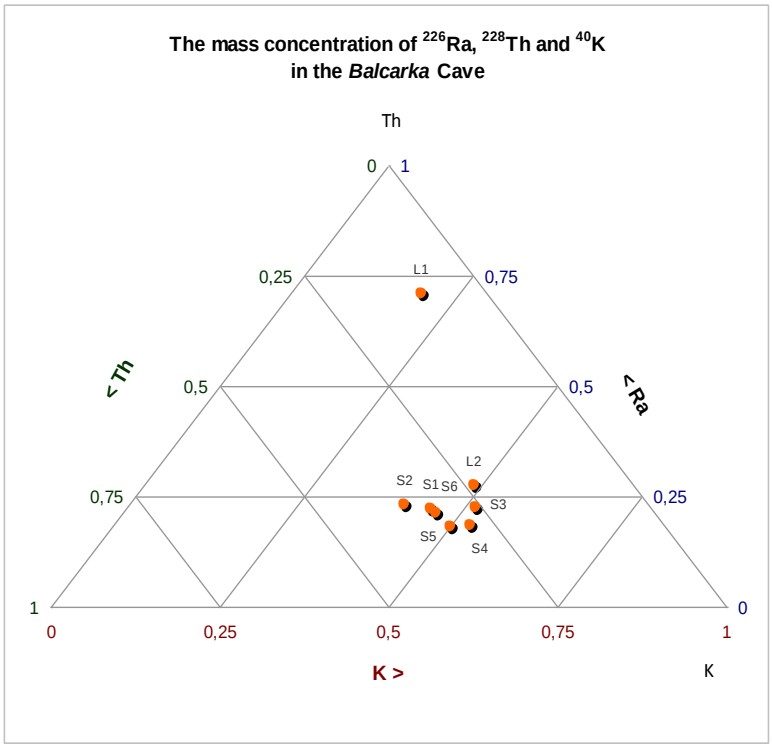

Figure 81 The concentration of ^{226}Ra, ^{228}Th and ^{40}K in the *Balcarka* Cave

All samples have similar radionuclide content. The L1 samples are from near the *Big Dome*, and L2 is from near the *Old Dome*.

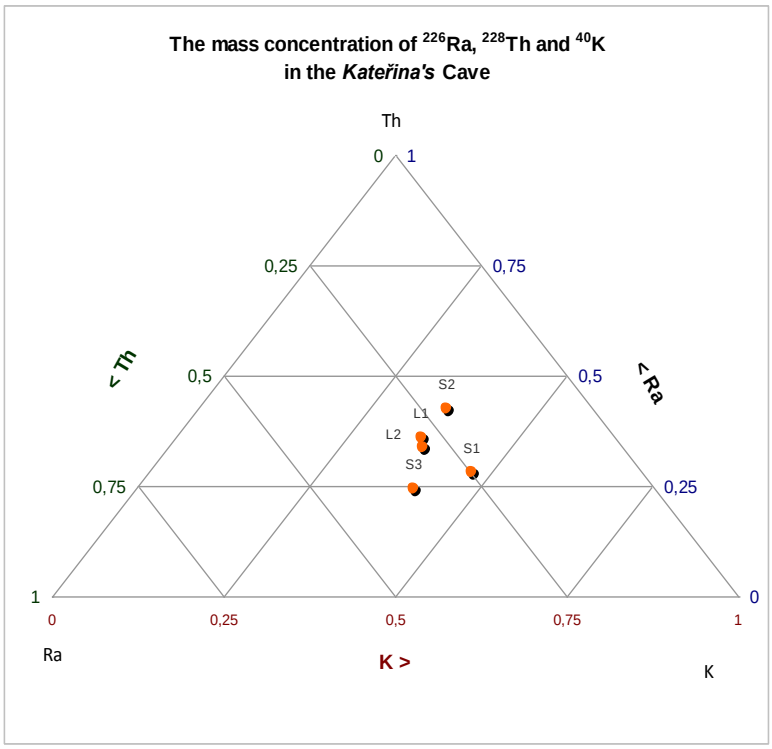

Figure 82 Concentration of ^{226}Ra, ^{228}Th and ^{40}K in the *Kateřina´s* Cave

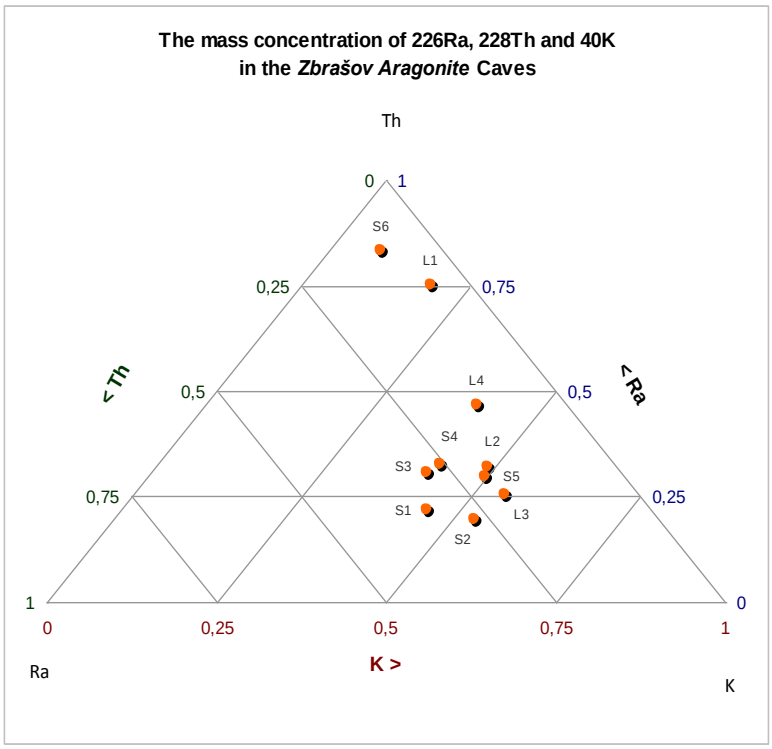

Figure 83 Concentration of ^{226}Ra, ^{228}Th and ^{40}K in the *Zbrašov Aragonite* Caves

Sediment S6 is yellow ochre, and sample L1 is *Vilémovický* limestone; L4 is *Hněvotínský* limestone.

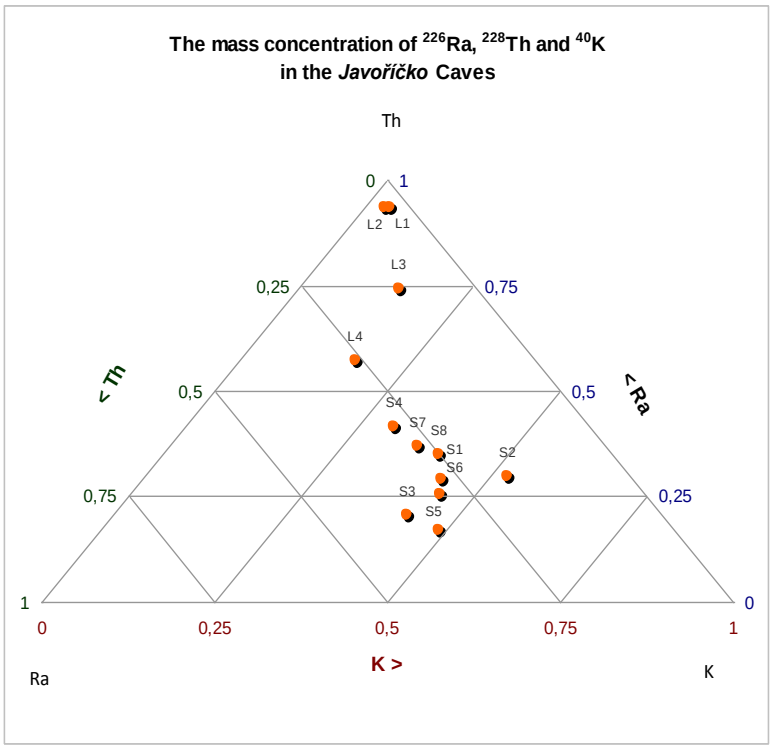

Figure 84 Concentration of ^{226}Ra, ^{228}Th and ^{40}K in the *Javoříčko* Caves

Limestone samples L1, L2, L3 are from the *Brash Dome*, the *Sink Dome*, and the *Garden*, and L4 is sinter from the *Fairytale* Cave.

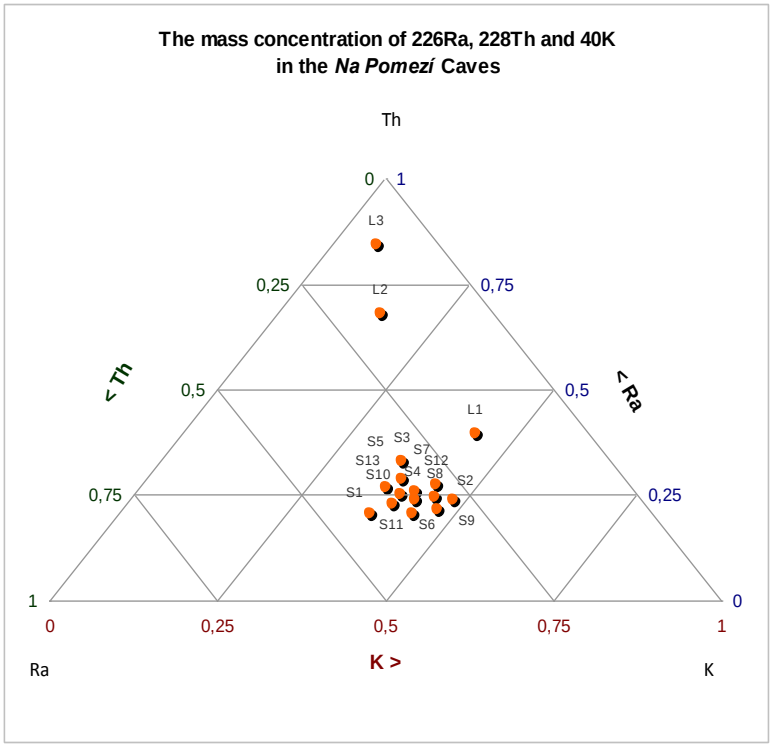

Figure 85 Concentration of ^{226}Ra, ^{228}Th and ^{40}K in the *Na Pomezí* Caves

L2, L3 are samples of marble. Sample L1 came from the *Royal* Dome.

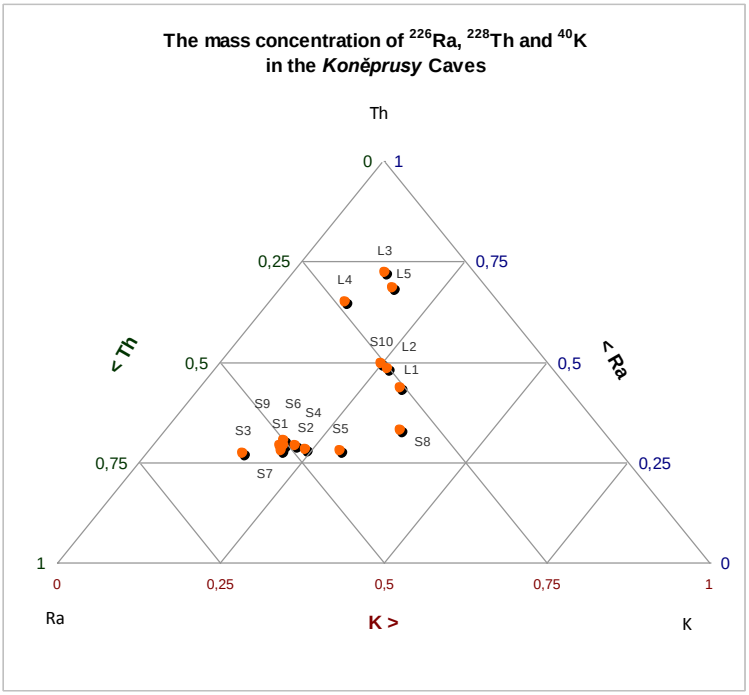

Figure 86 Concentration of ^{226}Ra, ^{228}Th and ^{40}K in the *Koněprusy* Caves

Samples L1, L2, and also sample S10 (sediment from *Peter's* Dome), are *Suchomasstký* limestone. Samples L3, L4, L5 were taken from the *Prošek's* Dome and the *Old Corridor*, and are *Koněpruský* limestone. Sample S8 is sediment from the *Jana's* Cave.

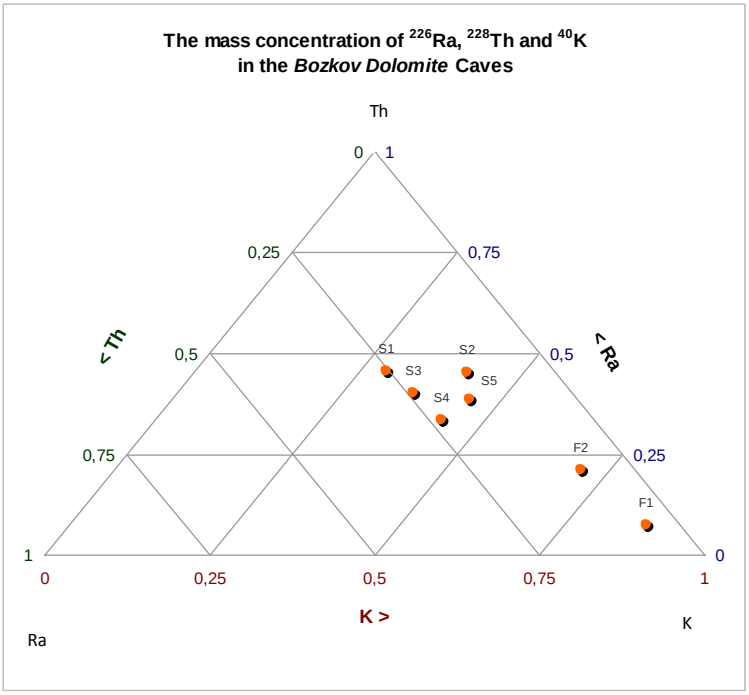

Figure 87 Concentration of ^{226}Ra, ^{228}Th and ^{40}K in the *Bozkov Dolomite* Caves

Samples F1, F2 are green *phyllites*, the cave bedrock material.

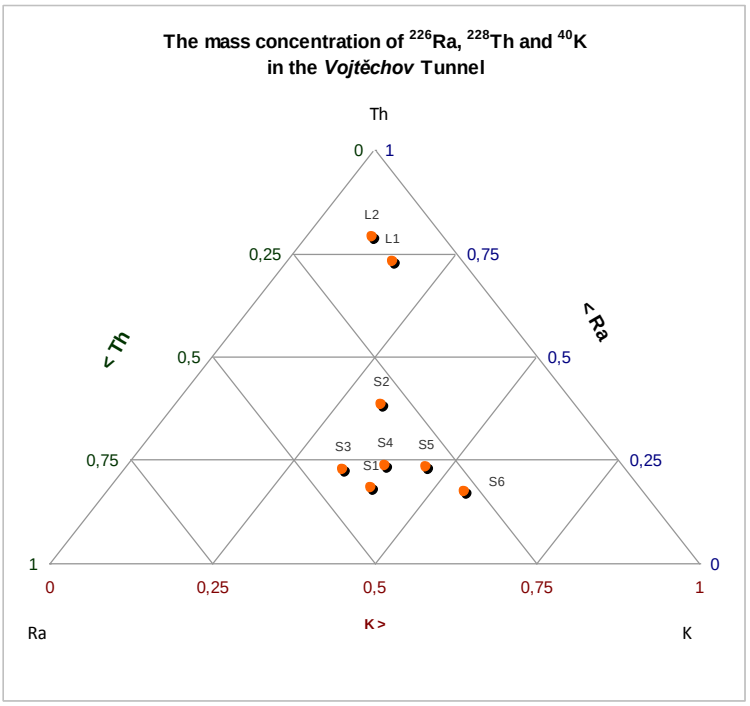

Figure 88 Concentration of ^{226}Ra, ^{228}Th and ^{40}K in the *Vojtěchov Tunnel*

Samples L1, L2 are limestone. Samples S2 and S6 are taken from the backfill material in corridor № 2.

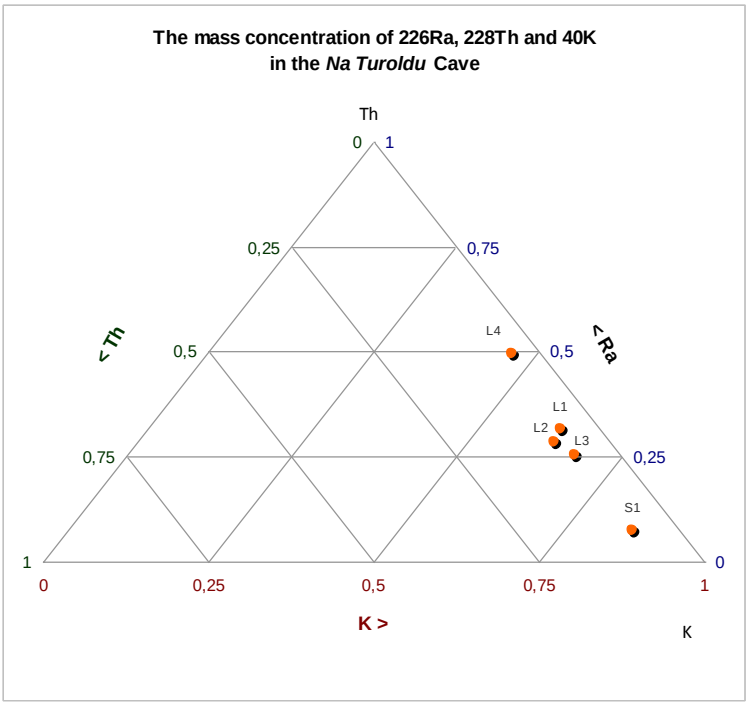

Figure 89 Concentration of ^{226}Ra, ^{228}Th and ^{40}K in the *Na Turoldu* Cave

Sample L4 is limestone from the *Chamber of the Ending*. All samples have a low concentration of Th and Ra in comparison with the higher concentration of K.

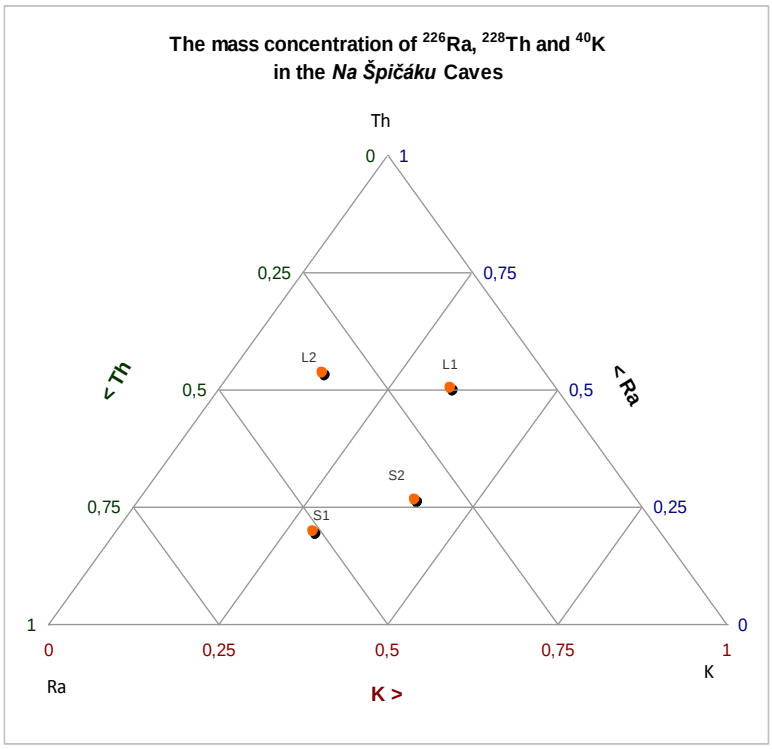

Figure 90 Concentration of ^{226}Ra, ^{228}Th and ^{40}K in the *Na Špičáku* Caves

The results of gamma spectrometry measurements in the *Na Špičáku* Caves display relatively high dispersion.

Table 29 summarizes the results from four-year integral monitoring of the radon concentration in the Czech show caves. The ratio between the average concentration in summer and in winter varies from the highest value 5.34 (4.91) in the *Chýnov* Caves (*Javoříčko* Caves) to an average ratio of 1.5. In the *Mladeč* Caves, the *Zbrašov Aragonite* Caves and the *Na Pomezí* Caves, the radon concentration is higher in winter than in summer.

The results summarized in Table 29 are expressed in Figure 91 - Figure 93. Because the content of ^{226}Ra in clastic sediments (in combination with a very low ventilation rate) is the main source of radon in the caves, the subsequent graphs show a comparison between them. The comparison of the average seasonal radon concentration in the summer season (in Bq/m^3) with the ^{226}Ra content in clastic cave sediments (in Bq/kg) seems to be similar in the *Zbrašov Aragonite* Caves and in caves from *Moravian Karst* (the correlation coefficient for all caves is 0.55, and when the *Zbrašov Aragonite* Caves and the *Moravian Karst* Caves are removed from the calculation to the special group, the correlation coefficients are 0.79 and 0.91). During the winter season there are no differences between the caves.

Table 29 A comparison between the average radon concentrations in summer (S) and in winter (W), measured over a period of four years (2004-2007) using the RAMARN integral measurement system and the ^{226}Ra content in sediments and rock

Cave name	Geol. Age	average concentration $c_{V,Rn}$ (Bq/m^3)		ratio	average mass concentration in sediments	average mass concentration in rock
		Summer season	Winter season	S/W	^{226}Ra (Bq/kg)	^{226}Ra (Bq/kg)
Mladeč Caves	Devonian	1738	2378	0.73	53	4
Sloup-Šošůvka Caves	Devonian	1234	662	1.86	28	3
Balcarka Cave	Devonian	900	583	1.54	25	11
Kateřina´s Cave	Devonian	863	526	1.64	18	8
Javoříčko Caves	Devonian	1518	309	4.91	29	27
Zbrašov Aragonite Caves	Devonian	1980	2137	0.93	47	7
Koněprusy Caves	Devonian	861	799	1.08	26	3
Na Pomezí Caves	Devonian	600	718	0.84	30	6
Na Špičáku Caves	Devonian	411	172	2.39	22	6
Chýnov Caves	Silurian	481	90	5.34	19	9
Bozkov Dolomite Caves	Silurian	2190	1410	1.55	32	7
Na Turoldu Caves	Jurassic	137			19	22

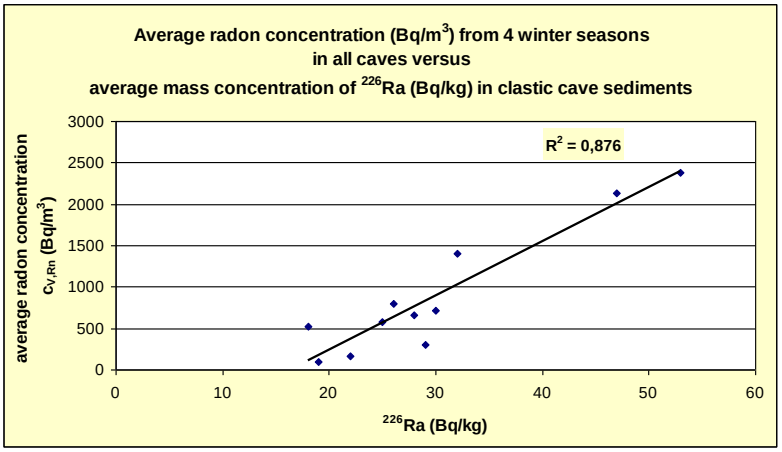

Figure 91 Comparison between the average radon concentration in four winter seasons and the ^{226}Ra content in clastic sediments

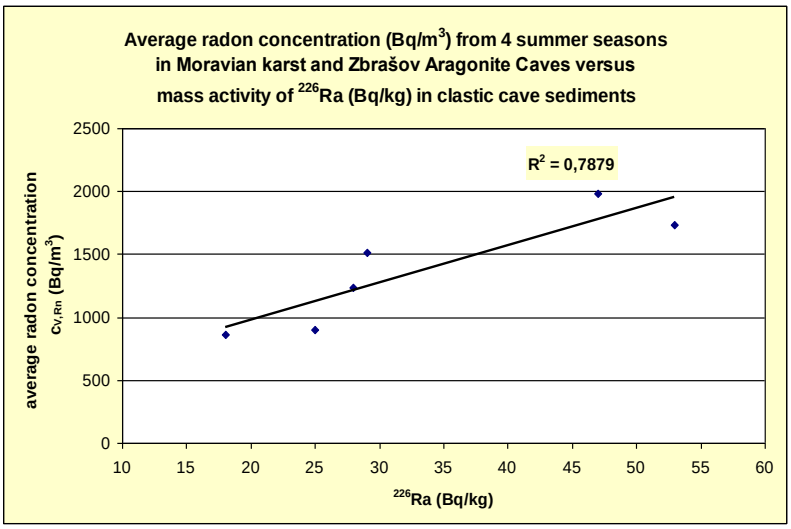

Figure 92 **Comparison between the average radon concentration in four summer seasons and the average Ra content in clastic sediments in the *Zbrašov Aragonite* Caves and the *Moravian Karst* caves**

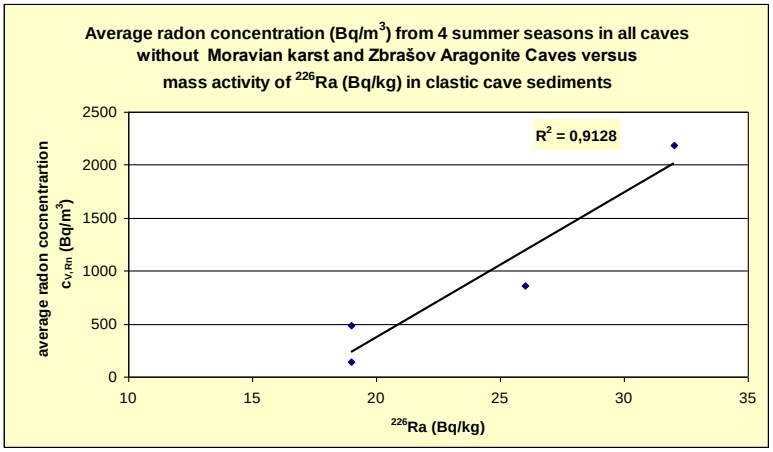

Figure 93 **Comparison between the average radon concentration in four summer seasons and the average Ra content in clastic sediments in the Czech show caves, excluding the *Zbrašov Aragonite* Caves and the *Moravian Karst* caves**

The following conclusions have been drawn on the basis of the results of laboratory gamma spectrometry measurements of cave sediments and rock:

- In limestone, the concentration of ^{226}Ra and ^{228}Th is usually units of Bq/kg.
- The concentration of ^{226}Ra and ^{228}Th in sediments is usually tens of Bq/kg.
- The highest ^{226}Ra concentrations in the sediment samples were in the *Mladeč* Caves in the *Cathedral of Nature* (106 Bq/kg) and in the *Blue Cave* (183 Bq/kg). In the *Chýnov* Caves, 73 Bq/kg ^{226}Ra and 120 Bq/kg ^{228}Th were measured in the *Sticky Corridor* area.
- The ^{228}Th/^{226}Ra ratios in sediments are mostly higher than 1; 1.5 on an average. In the *Mladeč* Caves, in the sediments from: the *Cathedral of Nature*, the *Deed's Dome*, the *Blue Cave*; in the *Javoříčko* Caves, in the *Brash Dome*, the *Sink Dome*, the *Garden*; in pelits (equivalent to *Rudické* layers) in the *Zbrašov Aragonite* Caves; in sand-clay sediments in the *Shooting of Žižka* (the *Chýnov* Caves) and in all sediments in the *Bozkov Dolomite* Caves the ratios are less than 1. The autochthonous material probably makes a significant contribution.
- Typical values for the ^{228}Th/^{226}Ra ratio for carbonate rocks (including amphibolite and erlan) varied between 0.2 -0.5.
- The ratio of ^{228}Th/^{226}Ra enabled us to assess the origin of the clastogene sediments. In the case of autochthonous speleogene sediments or allogenic and fluvial sediments, the ratio varies around 0.5 or 1.5.
- In three cases, the ^{137}Cs isotope was identified in the analyzed samples, suggesting a surface source of the sediments. These samples were located the near surface, and are clastogenic sediments flushed into the cave or they were transported artificially when the cave was modified.
- The laboratory gamma spectrometry method that was used did not enable us to determine the ratios of these radionuclides, which are in very low concentrations in the rock. For this purpose, we recommend the mass spectroscopy method, which has lower minimal detection activities.
- It is necessary to measure many more samples in order to make a detailed determination of the gamma spectrometry characteristics of the cave rock environment.

The measured mass concentrations of the radionuclides were compared with the results published in (Zimák, 2004b). A recalculation between ppm, % and Bq/kg was necessary for the purposes of the comparison. The following coefficients were used (IAEA, 2003a):

1ppm U = 12.35 Bq/kg U (or Ra when the equilibrium exists)

1 ppm Th = 4.06 Bq/kg Th

1 %K = 313 Bq/kg K

Considering that the comparison could be influenced by the following factors:

- The measured mass was different (approx. 1 kg of material in the laboratory and less than 1000 kg of material in situ, when the contribution from a hemisphere of about r = 100cm and 2.2 g/cm^3 soil density is taken into account). The locations of the in situ measurement most probably do not correspond with the location from which our samples were taken.
- The measured samples in the laboratory were dried, while the in situ material was wet.
- The correction on the measured material density was included in the laboratory measurement results.
- The number of samples measured in the laboratory was significantly lower than the number of in situ measurements. However, the average values were compared.
- The geometry of the in situ measurements could be different from the calibration geometry; the range of the gamma ray of natural radionuclide energies in the air may be hundreds of meters (see Appendix 3 Results of the MCNPX modeling simulation).
- Both the in situ measurements and in the laboratory measurements made use of a calculation of the ^{226}Ra concentration based on energies of ^{214}Bi (radon daughter), from the in situ measurement, only energy of 1.76 MeV was used; equilibrium was assumed between U and Ra, and between Ra and Rn, while equilibrium between ^{226}Ra and ^{222}Rn in the laboratory samples was established by hermetically closing the samples for the appropriate period of time; equilibrium between U and Ra, Ra and Rn in situ must be assumed.
- The eTh (ppm Th) concentrations from in situ measurement were calculated from the energy ^{208}Tl 2.6 MeV; the mass concentration of the ^{228}Th radionuclide was determined in the laboratory.

The following main comparison results are worth noting:

- The ^{40}K and ^{232}Th concentration results from measurements made in situ are higher than the laboratory measurement results (with the exception of the *Na Turoldu* Cave and the *Chýnov* Caves).
- The eU (Bq/kg) concentrations in all of the in situ measurements (rock and sediments) are significantly higher than the laboratory ^{226}Ra (Bq/kg) results (although the dry samples were measured in the laboratory), mainly in the *Zbrašov Aragonite* Caves and in the *Vojtěchov* speleotherapy area (with the exception of the *Na Turoldu* Cave and the *Chýnov* Caves).
- When compared with ratio values higher than 1 in the laboratory measurements, the Th/Ra(U) ratios lower than 1 (one) in clastic sediments, established during in situ measurements in most caves, indicate that the concentration of U determined in situ was overvalued.
- The gamma dose rates values, calculated according to (IAEA, 2003a) and based on in-situ gamma spectrometry measurement results, correspond well with in-situ gamma dose rate measurement. However the calculated gamma dose rate results based on laboratory gamma spectrometry measurements are undervalued. This confirms the influence of airborne radon concentration and of the measurement geometry on the measured K, U, Th radionuclides concentration.

The comparative results are summarized in Figure 94 (clastic sediments) and Table 30.

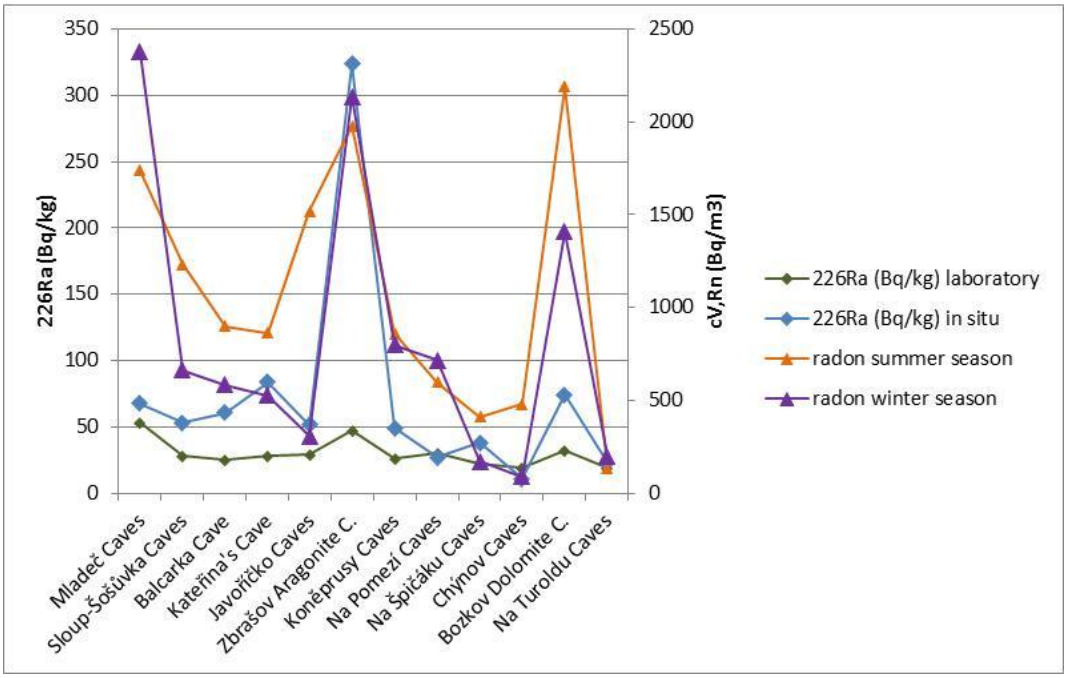

Figure 94 The comparative results from laboratory and in-situ gamma spectrometry measurement (^{226}Ra in clastic sediments)

Table 30 Comparison between laboratory gamma spectrometry measurements (black) and in situ gamma spectrometry measurements (blue) (Zimák, 2004b) in the show caves

Cave		^{226}Ra (Bq/kg)	^{228}Th (Bq/kg)	^{40}K (Bq/kg)	Th/Ra
	material	average	average	average	
Mladeč Caves	devonian limestone	4	2	47	0.5
		63	7	125	0.1
	sediments	53	39	448	1.4(0.4)
		68	35	470	0.5
Sloup-Šošůvka Caves	limestones and sinters	3	1	0	0.3
		31	7.3	188	0.2
	sediments	28	44	598	1.6
		53	37	595	0.7
Balcarka Cave	limestone	11	4	83	0.2
		45	8	156	0.17
	sediments	25	38	565	1.6
		61	34	501	0.6
Kateřina´s Cave	limestone brash	8	6	83	0.8
		48	3.6	94	0.08
	sediments	28	27	390	1.0
		84	18	250	0.2
Javoříčko Caves	limestone	27	2	15	0.1
		67	6	188	0.1
	sediments	29	29	431	1.5(0.4)
		52	17	313	0.3
Zbrašov Aragonite C.	*Hněvotínský* limestone	14	11	303	0.8
		275	22	376	0.08
	sediments	47	47	805	1.5(0.8)
		324	52	751	0.16
Koněprusy Caves	*Suchomastský* limestone	25	14	150	0.6
		32	17	188	0.5
	Koněpruský limestone	7	2	13	0.3
		29.6	10.5	125	0.35
	sediments	26	41	190	1.6
		49	65.4	376	1.3
Na Pomezí Caves	limestone	6	2	30	0.3
		27	4.5	157	0.2

Cave		^{226}Ra (Bq/kg)	^{228}Th (Bq/kg)	^{40}K (Bq/kg)	Th/Ra
	material	average	average	average	
Na Špičáku Caves	limestone	6 27	3 9	24 219	0.5 0.3
	sediments	22 38	38 31	337 501	1.7 0.8
Bozkov Dolomite C.	sediments	32 74	15 17.5	318 375	0.5 0.2
Na Turoldu Caves	sandy limestone	9 7	2 0.4	19 31	0.2 0.06
	sediments	19 11	19 11	221 219	1 1
Vojtěchov Tunnel	limestone	7 303	1 12	13 94	0.1 0.04
	sediments	22 348	36 50	420 501	1.6 0.1
Chýnov Caves	cryst. limestone dark	4 7.4	5 2.8	180 156.5	1.0 0.4
	erlan	22 12	14 13	493 501	0.6 1.1
	amphibolite	5 8.6	2 9.3	457 501	0.4 1.1
	sediments	19 11.1	25 16.6	504 470	1.3 1.5

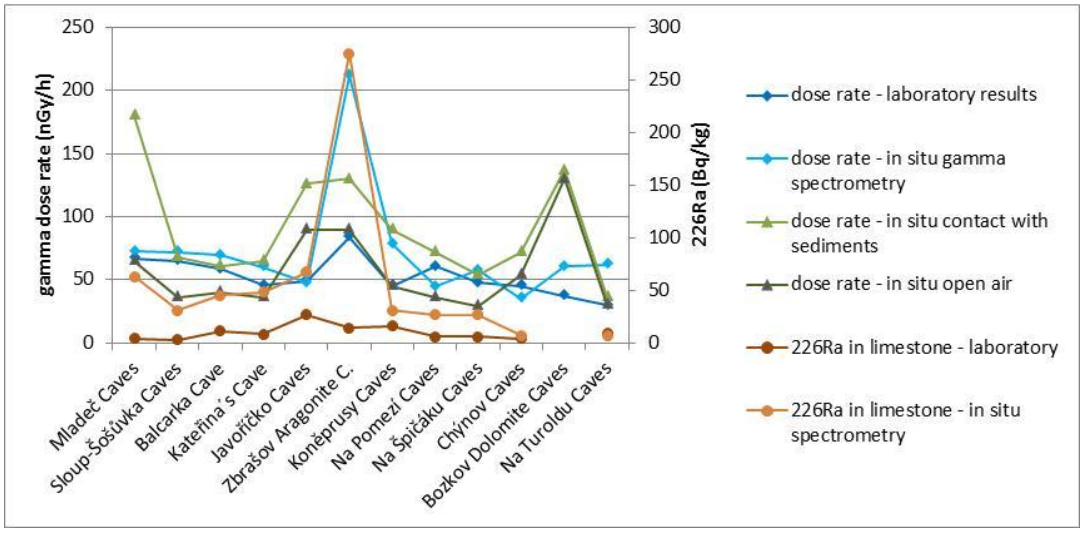

Figure 95 The comparative results from dose rate results based on laboratory and in-situ measurements or calculations (^{226}Ra in limestone)

7. Cave factor determination process

The data collected using the FRITRA4 monitor (chapter 6.4), the LUDEP program, and data from the aerosol campaign were used to determine the *individual cave factor* for each cave. The calculation procedure was identical to the procedure used for calculating the individual cave factor in the *Bozkov Dolomite* Caves (chapter 6.5), except that for the free fraction in caves we used the same value as for apartments, i.e. 0.9 nm.

Relationship $f_p = 0.022F^{-2.7}$ for the lowest point of Postojna Cave and $f_p = 0.075F^{-1.8}$ for the railway station and both together $f_p = 0.054F^{-2.0}$ was presented by (Vaupotič, 2008).

(Vargas, 2000) used the following approach for dose calculation: there is a direct dependence between equilibrium factor F and the size of free fraction f_p, which can be described using a Log-Power expression (equation 11). This expression overestimated f_p only for very low and very high equilibrium factor values.

$$\ln(1/f_p) = a*\ln(1/F)^b \qquad \textbf{Equation 11}$$

The calculated values for coefficients *a* and *b* for the measured free fraction values from a wire screen (FRITRA4 device) from all measurement in caves and in underground areas were $a = 1.85$ and $b = -1.096$.

Vargas made indoor measurements in four groups of houses in different parts of Catalonia, and the coefficients obtained from the Log-Power expression for his measurement were:

$a = 1.90$ and $b = -0.68$.

Interpolation and all measured values are plotted in Figure 96. Outliers with $\ln(1/f_p)$ value around 3 and ln(1/F) value around 2 - 2.5 originate from the first measurements in the *Zbrašov Aragonite* Caves in April 2006 (in April 2007, the $\ln(1/f_p)$ value was 1.3 on an average and the ln(1/F) value was 0.9 on an average). At the time when the measurements were performed, the floodwater in the cave was diminishing. The cave had abnormal water-drip. It is likely that these special conditions also influenced the processes around radon. In the measurement results, the outliers with $\ln(1/f_p)$ value around 0.05 and ln(1/F) value around 2 originate from measurements in the *Tunnel* area of the tour route. This area is man-made, and is closed by two doors. The measurements were carried out at a time when the cave was being visited only for maintenance purposes. The free fraction f_p was as high as 98%. The wine cellars provided a special group of measurement results. These areas were man-made, and the building materials were usually bricks.

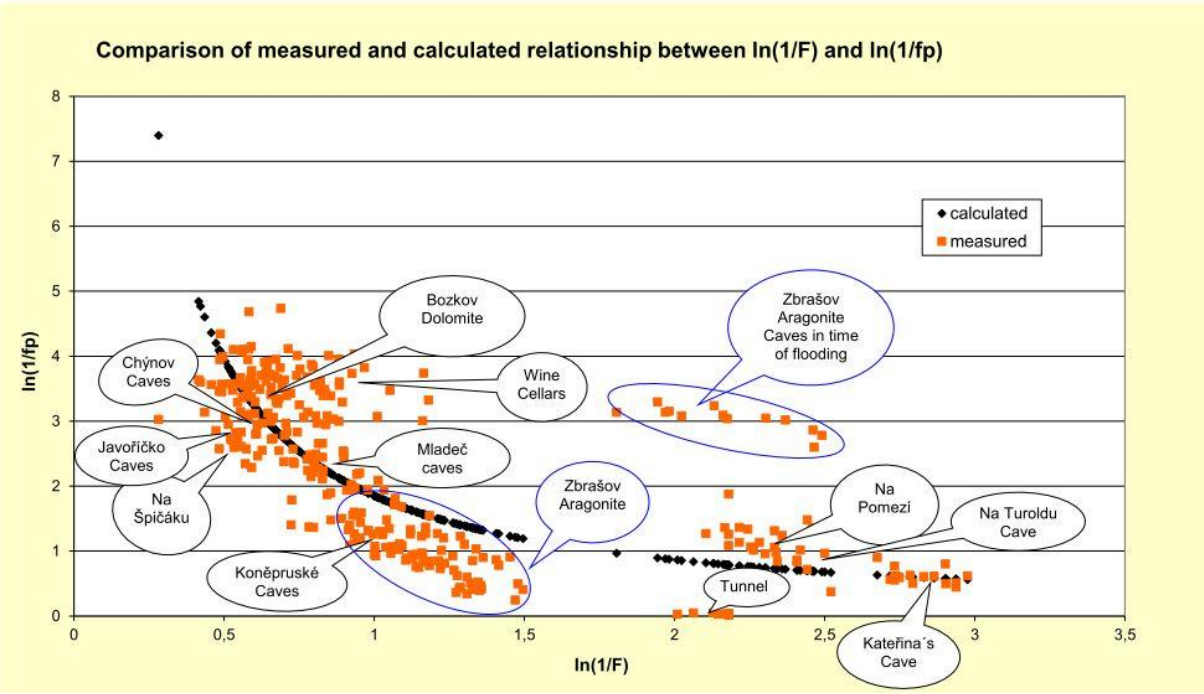

Figure 96 Fitting the relationship of F and f_p, and making a comparison with the measured values. The dependence of f_p on F is represented by the function $\ln(1/f_p) = a*\ln(1/F)^b$

The dose calculation using the Log-Power relationship could be performed in the following manner:

$$E = (DCF_F * f_p + DCF_A * (1-f_p)) * F * c_{V,Rn} * T \qquad \text{Equation 12}$$

where DCF_F is the dose conversion factor for the free (unattached) fraction, f_p is the size of the free fraction, which can be obtained from equation 10; DCF_A is the dose conversion factor for the attached fraction; $c_{V,Rn}$ is the radon activity concentration; F is the equilibrium factor, and T is the time spent in the workplace.

Dose determination using the above procedure thus depends only on the equilibrium factor F, and on predetermined coefficients *a*, *b*, DCF_F and DCF_A. This approach is relatively promising, because it includes the relationship between the free fraction and the equilibrium factor, not in its very approximate linear form but in a more complex relationship which is closer to reality.

For practical applications, it is necessary to perform many more measurements of F and f_p in different environments to obtain a good correlation. It is also important to determine the DCF for the free faction and for the attached fraction. It is therefore first necessary to determine the aerosol modes and then the appropriate DCF.

In Table 31, the cave factors were determined by following the process described in chapter 6.5 (based on the dose conversion factors calculated using LUDEP program) (Thinová, 2007).

Table 31 Summary of the results for individual cave factor development

Cave	night f_p	day f_p	Individual cave factor
Mladeč Caves	0.11	0.12	1.1
Sloup-Šošůvka Caves	0.37	0.37	1.7
Balcarka Cave	0.32	0.32	1.6
Kateřina Cave	0.58	0.48	2.4
Javoříčko Caves	0.06	0.06	1
Zbrašov Aragonite Caves	0.32	0.34	1.5
Koněprusy Caves	0.34	0.36	1.6
Na Pomezí Caves	0.33	0.34	1.7
Na Špičáku Caves	0.08	0.08	1
Chýnov Caves	0.04	0.05	1
Bozkov Dolomite Caves	0.02	0.03	1
Na Turoldu Caves	0.36	0.47	2
Edel Zlaté hory – speleotherapy area	0.03	0.02	1
Wine cellars	0.02	0.02	1
Hanička and *Dobrošov* military fortresses	0.09	0.09	1
Mariánská Mines Tunnel	0.10	0.10	1

Calculation results:

The *individual cave factor* for the investigated underground areas was calculated on the basis of the results from the aerosol campaign in the Bozkov Dolomite Caves in 2002; and from the unattached and attached fraction and equilibrium factor measurements, using the FRITRA4 continuous monitor.

Unfortunately, no information about the size of the aerosols of the unattached fraction was available, so AMTD 0.9 nm was used (Porstendörfer, 1994).

The recommended aerosol modes for dwellings were taken into account (Marsh, et al., 1998).

The dose conversion coefficients were calculated using LUDEP software (Rovenská, 2007).

The dependence of f_p on F was represented by the function ln(1/fp) = a*ln(1/F)^b (Vargas, et al., 2000). The results from all measurements carried out under the ground were:

- a = 1.816
- b = - 1.167

It was recommended for future to calculate the effective dose using equation 12:

$E = (DCF_F * f_p + DCF_A * (1-f_p)) * F * c_{V,Rn} * T$

The dose from radon under the ground cannot be calculated using the individual cave factor. If a new underground area is utilized as a workplace, a cave factor of 2 should be put into the effective dose calculation (to keep to the principles of radiation protection), or the unattached fraction should be measured and the individual cave factor should be calculated.

The recommendations described above are nowadays used as the methodology for calculating the dose for underground workplaces: caves, wine cellars, mines (*with the exception of* active mines), tail-race tunnels, bank vaults, etc., issued by the State Office of Nuclear Safety.

8. Research conclusions

On the basis of the research, measurements and calculations carried out between 2002 and 2010 in the Czech show caves and in other underground areas, the following conclusions can be drawn:

8.1 Results of long term measurements and experiments

8.1.1 Integral radon measurement verification

- The influence of detector placement was noted only in the case of bare SSNTD detectors providing incorrect higher values when located near clay clastic sediments. Similar results were observed for vertical inhomogeneous measurements, using electret detectors (chamber 0.5 l). Locations containing clastic sediments experience local radon concentration inhomogeneity. In this case, the influence of thoron is probable.
- In an open space where the RAMARN integral detectors are placed, the contribution of thoron to the radon concentration is expected to be less than 10%.
- In some cases, a black mold appeared on the film inside the diffusion chamber, but this did not have any impact on the results.
- (Solomon, 1996) described major differences between the measurement result summation for individual quarters of a year and the results for the whole year. The measurement results using the RAMAN system did not indicate significant differences of this kind. A total of 110 detectors were used, and the $c_{V,Rn}$ values were verified using the RADIM3 continuous radon monitor.
- The number of outliers was less than 10%, while the causes of very low values were not clarified. The influence of a non-standard diffusion chamber cover was assumed. This issue was verified by an experiment in which the chamber covers were sealed and the $c_{V,Rn}$ results were compared with the results for non-sealed diffusion chambers. The sealed diffusion chambers received only half as much diffusion as the non-sealed chambers.
- On the basis of knowledge of the underground working environment, including the behavior of guides, and on the basis of the results from comparative measurements, we conclude that integral radon monitoring can provide more consistent results for calculating the effective doses that are received.

- RAMARN detectors can be placed in hollows, about 1.5 – 2 m above ground (human breathing level).

8.1.2 Continuous radon monitoring results

- Using the continuously monitored radon concentration records for the *Bozkov Dolomite* Caves, it was determined that the best period for "winter season" measurements was from October 1st to March 31st; the remaining months are referred to as the "summer season". These periods of time correspond with the seasonal variations, and also conform to the business operation of the caves.
- No major differences were shown in the average $c_{V,Rn}$ during working time and non-working time in the caves.
- The results obtained from continuous monitoring indicate that the average radon concentration from integral monitoring can be confidently used for calculating the radon dose.
- Height profiles were measured in order to identify sources of radiation. The high concentration gradient was solved as an intersection of the air flow. The radon concentration was higher near clastic sediments and in the summer season.

8.2 Short-term measurement results

8.2.1 Air flow measurement results

- The air flow in each underground area is quite individual, and only ambiguous rules for air mass transportation can be proposed. These rules may change from day to day and from year to year, depending on several parameters.
- The air flow significantly impacted the radon concentration levels in individual locations. However, in order to calculate the dose from radon it is not necessary to know the air flow in detail, only the radon concentrations, which must be measured continuously.
- For detailed information about the air flow, long-term monitoring of each part of the caves is needed, including information about the outside meteorological parameters. A study of the air flow as a part of the cave environment is indisputably very useful.
- The ratio between the outside temperature and the inside temperature influences the air flow in underground spaces. The radon concentration decreases when the difference between these temperatures approaches zero ºC. Existing continuous

measurements show that a decrease in the outside temperature manifests itself as an increase in radon concentration, with a delay ranging from a few days to three months, depending on the depth of the study area inside the cave.

8.2.2 Unattached fraction measurement results

- The results from unattached fraction measurements using the FRITRA4 device were the source for individual cave factor calculations.
- The experiments highlighted some questions, e.g. the relevance and reproducibility of unattached fraction measurements (dependent on wire screen properties) in environments with different aerosol size distributions.
- Generally, the measurements in caves in the Czech Republic that are open to the public demonstrated that each cave is a distinct site – the free fraction ranged from 0.03 to 0.6; with arithmetical average for the unattached fraction was 0.13 for the hypothetical "average Czech cave". These results led to a modification of the methodology for assessing the dose in caves in the Czech Republic.

8.2.3 Aerosol spectrum measurement results

- In addition to radon measurements, were made measurements of the aerosol particle size distribution, one of the most important parameters for dose evaluation.
- The presence of aerosol particles 1-10 μm in diameter is definitely caused by the presence visitors or personnel; when the cave was closed, the particles rapidly disappeared (after approx. 1 h the concentration was about 10^{-4} #/cm^3. By contrast, the concentration of particles about 200 nm in diameter is relatively stable (~10 #/cm^3). For the ~10 nm particle size group, it seems that the aerosols are produced by intensive work or movement (the concentration is about 100-1000 #/cm^3).
- The activity deposited on each mode was determined using the measured aerosol concentrations. For "Night" profile, the AMADs were 140nm and 710nm; for "Guided Tour" profile, the AMADs were 144, 715 and 1900 nm. Using LUDEP (Rovenská, 2007), dose conversion factors were obtained for individual radon daughters DCF_{mod} (X).
- The *individual cave factor* **j=1** for the *Bozkov Dolomite* Caves was determined on the basis of the results of the aerosol campaign.

8.2.4 Dose rate measurements, and the dose from external irradiation calculation results

- The effective doses calculated for the time spent annually by workers under the ground (information from 2006) are negligible. The values are not higher than units of μSv. The dose from external irradiation in caves is smaller than, or comparable with, the irradiation on the surface, and it was not taken into account when performing the total effective dose calculations.

8.2.5 Radon in water sample measurement results

- Two types of water samples were collected: water from lakes and water from small puddles of dripping water. The radon concentration in lakes was in the range of units Bq/l. In dripping water, the concentration was very low, practically below the detection limit.
- The low concentration of radon in the measured water samples, together with the low and stable temperature in caves, leads to the conclusion that water cannot be the source of a high concentration of radon in caves.

8.2.6 Exhalation rate measurement results

- The detected radon exhalation rate per unit area from the clastic sediments in the *Bozkov Dolomite* caves was 45 ± 6 $mBq.m^{-2}\cdot s^{-1}$. The detected radon exhalation rate per unit area in the *Zbrašov Aragonite* Caves was 60 ± 8 $Bq.m^{-2}\cdot s^{-1}$.
- The radon mass exhalation rate test results obtained from individual samples of cave clastic sediments and from dolomite sample measurements were at the lower end of the radon mass exhalation rate scale. According to (UNSCEAR, 2000) and (Nazaroff, et al., 1988), using average emanation coefficient 0.1, the mass exhalation rate of radon in rock is nominally 10 $\mu Bq\cdot s^{-1}\cdot kg^{-1}$ (the lowest values were near 0.3 $\mu Bq\cdot s^{-1}\cdot kg^{-1}$).

8.3 Results of laboratory gamma spectrometry measurements

- In limestone, the concentration of ^{226}Ra and ^{228}Th is usually units of Bq/kg.
- The concentration of ^{226}Ra and ^{228}Th in sediments is usually tens of Bq/kg.
- The highest ^{226}Ra concentrations in samples of sediments were in the *Mladeč* Caves, in the *Cathedral of Nature* (106 Bq/kg) and in the *Blue Cave* (183 Bq/kg). In the *Chýnov* Caves 73 Bq/kg ^{226}Ra and 120 Bq/kg ^{228}Th were measured in the *Sticky Corridor* area.

- The $^{228}Th/^{226}Ra$ ratios in sediments are mostly higher than 1; they are 1.5 on an average. In the *Mladeč* Caves, in the sediments from the *Cathedral of Nature*, the *Deed's Dome*, the *Blue Cave*; in the *Javoříčko* Caves, in the *Brash Dome*, the *Sink Dome*, the *Garden*; in pelits (equivalent to *Rudické* layers) in the *Zbrašov Aragonite* Caves, in the sand-clay sediments in the *Shooting of Žižka* Cave (*Chýnov* Caves) and in all sediments in the *Bozkov Dolomite* Caves, the ratios are less than 1. The contribution of the autochthonous material is probably significant.
- Typical values for the $^{228}Th/^{226}Ra$ ratio for carbonate rocks (including amphibolite and erlan) varied between 0.2 - 0.5.
- The ratio of $^{228}Th/^{226}Ra$ enabled the origin of the clastogene sediments to be assessed. For autochthonous speleogene sediments the ratio varies around 0.5, and for allogenic and fluvial sediments the ratio varies around 1.5.
- In three cases, the ^{137}Cs isotope was identified in the analyzed samples, suggesting a surface source of the sediments. These samples were located near the surface. They are clastogene sediments flushed into the cave, or they were transported artificially when the cave was modified.
- The gamma spectrometry method that we used did not enable us to determine other radionuclides ratios, which are in very low concentrations in the rock. The mass spectroscopy method, which has lower minimum detection activities, is recommended for this purpose.
- In order to make a detailed determination of the gamma spectrometry characteristics of a cave rock environment, many more samples need to be measured.

8.4 Cave factor determination results

- The direct dependence between equilibrium factor F and the size of the free fraction f_p was described using the Log-Power expression $\ln(1/f_p) = a*\ln(1/F)^b$. .
- The calculated values for coefficients *a* and *b* for measured free fraction values from a wire screen (FRITRA4 device) from the all measurements made in caves and in underground areas were $a = 1.85$ and $b = -1.096$.
- Unfortunately, no information was available about the size of the aerosols in the unattached fraction. AMTD 0.9 nm was therefore used (Porstendörfer, 1994).
- Recommended aerosol modes for dwellings were taken into account (Table 19, Table 20) (Marsh, et al., 1998).

- The dose conversion coefficients were calculated, using LUDEP software.
- The *individual cave factor* (Table 31) was calculated for investigated underground areas on the basis of results from the aerosol campaign in the *Bozkov Dolomite* Caves in 2002 (unattached and attached fraction and equilibrium factor measurements, using the FRITRA4 continuous monitor).
- The dose from radon in the underground can be calculated using the individual cave factor. When a new underground area is to be used as a workplace, an individual cave factor of 2 should be used in the effective dose calculation, or the unattached fraction should be measured and the individual cave factor should be calculated.
- A new methodology was recommended for use in all underground workplaces – caves, wine cellars, mines (*with the exception of* active mines), tail-race tunnels, bank vaults, etc.

The main source of radon is the ^{226}Ra radionuclide content in the rock and sediments present in the underground space – in the material of these areas, or coming from the bedrock. Very high concentrations are caused by transport of radon from the deeper parts of these areas, where they are retained due to very low ventilation. It is impossible to remove these sources, but for the purposes of radiation protection the doses can be kept within the limits by regulating the time spent under the ground.

Appendix 1 Relative error assessment in determining the annual effective dose from radon in caves and its practical impact

An assessment of the relative error of the determined dose (annual effective dose from radon) could not be ignored in an evaluation of the health impact on cave workers and visitors, and had to be implemented in The Quality Assurance program (Instructions for work in the Czech Republic show caves environment), following the basic principles of radiation protection.

As mentioned in chapter 4.1.1, the dose calculation was defined SONS Recommendation 2006: "A methodological process for measurements in workplaces where a significant increase in irradiation from natural sources could occur: determining the effective dose" (SÚJB, 2006). The relative error in dose assessment must be determined in accordance with the main ideas of the quoted recommendation, especially:

- Decisions on whether the workers' dose **can exceed** the reference level according to § 88 article 2 of the Ordinance, i.e. an effective dose of 6 mSv per year. The most important aim of repeated measurements is to determine the effective doses, and thus the health risks, as precisely as possible. This process does not determine **when the the reference level is exceeded**, as such, but rather **the possibility of the reference level being exceeded** (see §88 article 2, second sentence).
- Given that the possibility of exceeding the reference level of 6 mSv is not established in repeated measurements, §89 article 3 section d) of the Ordinance applies - the measurements and the determination of the effective dose shall not be conducted in following years, unless there is a change in the working conditions, manufacturing processes or materials used...
- One of the consequences of determining that the reference level could be exceeded is the requirement to calculate the effective doses for all workers at the site repeatedly, every calendar year. (i.e. **measurements are conducted regularly every year**)...
- In cases where it is proven that after accepting steps toward lowering the irradiation, the reference level of 6 mSv per year cannot be exceeded for any of the workers, §88 article 1 section d) applies, and measurements need not be performed in the following years, unless there is a change in the working conditions, manufacturing processes or materials used...

It is evident from this Recommendation that with the strict aim of preventing negative health impacts, the estimate of the relative error in determining the dose must lead to an assessment of every possibility that the reference level of 6 mSv might be exceeded. On the basis of this assessment, the radon concentration measurement regime in individual caves can later be adjusted.

- The personal annual effective dose comprises doses received due to radon and its daughter products inhalation, including external irradiation received. It is calculated according to the (SÚJB, 2006) using equations 3.
- Based on the results from chapter 6.6, only the dose received through radon daughter products inhalation, was taken into consideration in the dose error assessment.

It can generally be stated that the level of uncertainty in dose calculation differs for various parameters and conditions in specific exposure situations. Thus it is not possible to set a universal level of uncertainty. It is only possible to make an estimate, and use the estimate judiciously. It can be assumed that the uncertainty in estimating radiation doses from internal irradiation, including radionuclide biokinetics is higher than for external exposure, which does not have to be monitored in caves. The impact of the internal exposure cannot be observed in vivo, and the data applied to humans often comes from research on animals. Of course, the level of uncertainty also differs among radionuclides (ICRP, 2007). The entire inaccuracy of the relative error in determining the annual effective radon dose, which is a measure of the health impact on workers in underground locations, consists of a chain of uncertainties and variables that will be addressed below.

The **uncertainties** associated with the radiation dose estimates and the health impact estimates are related to the credibility of the measured data entered into the annual dose calculations, and also to the credibility of parameters resulting from estimates based on the models that are used (Dosimetric model for human respiratory track (ICRP, 1994)), or epidemiological studies. These are uncertainties that will impact the annual effective dose from radon calculation results, which are later compared with the constraints.
In our case, the uncertainties are associated mainly with:

- errors in integral measurements of radon concentration $c_{V,Rn}$,while the detecting system must be approved within the methodology;

- errors in determining the unattached fraction f_P for a specific environment;
- establishing the equilibrium factor F for a specific environment;
- conversion factor h_p (including influence value for the radiation weight factor for alpha particles w_T).

We should also include here the error of the dose determination system given in currently valid Methodological Procedures. These uncertainties will be analyzed below.

Variability (more exactly *biological variability*) is related to quantitative differences between various evaluated members of a population, with respect to their physiological and metabolic parameters, gender or ethnicity. Variability is an important source of uncertainty in determining the annual dose value.

The distribution of the absorbed dose in the human body for radionuclides emitting alpha particles (particles with high LET, or with a short path), e.g. among radon daughter products, can be highly heterogeneous (ICRP, 2007). This heterogeneity is due to the various deposition rates of radon daughter products in various areas of the lung (tissues) and in bronchial mucus (ICRP, 1994). Thus there are various opportunities for transferring energy to target cells in relation to their location, their response in the region of low doses, the method of extrapolation and in relation to acceptance of LTN model. Variability can also be due to the impact of smoking (Böhm, 2003), or due to the effect of other damage to the lung tissue caused by the presence of harmful substances in the working or living environment.

In these cases, the dose is determined for a specific tissue area that is considered to be a target for the development of radiation-induced cancer, labeled an average dose, due to the fact that the impact of these influences cannot be encompassed for an individual.

For obvious reasons, the variability listed above cannot be included in the determination of total error in determining the annual effective dose.

In the case of a cave environment, however, we can include the inter-annual and seasonal variability of radon concentration under *variability*.

The measured radon concentration is a random quantity, so the radon concentration in individual caves cannot be predicted into the future. Continuous historical observations have shown that the radon concentration value in some years and seasons can differ by as much as 400 percent! It is impossible to encompass this in a mathematical model, and to forecast future values on this basis. The only solution would be to determine the probability that the measured values would fall within a certain interval (chapter 4.3.3.1), (Štolba, 2012). The variability in some of caves is more pronounced (the *Zbrašov Aragonite* Caves, the *Bozkov*

Dolomite Caves, the *Balcarka* Cave, etc.). In other caves, the variability is less noticeable (the *Chýnov* Caves, the *Javoříčko* Caves). The following graphs show with certainty that the average $c_{V,Rn}$ value in individual caves is dependent on more or less the same inter-annual trend. The variability is manifestly dependent on meteorological parameters (variations in external temperature, intensity and duration of precipitation, variations in atmospheric pressure, etc.) in a given year. On the basis of the multi-year measurement campaign, among all the variabilities mentioned above, only the inter-annual variability can be captured and taken into account in forming a comprehensive estimate of the annual effective radon dose in caves.

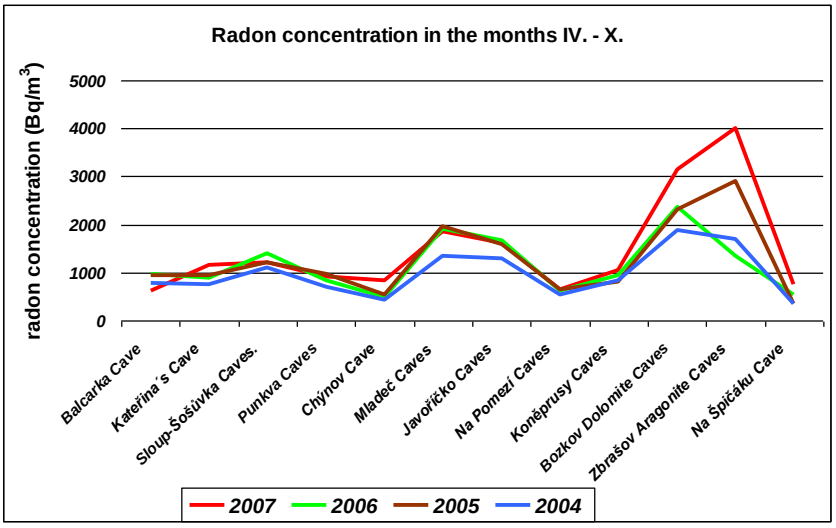

Figure 97 Radon concentration in the show caves in 2004-2007, summer season

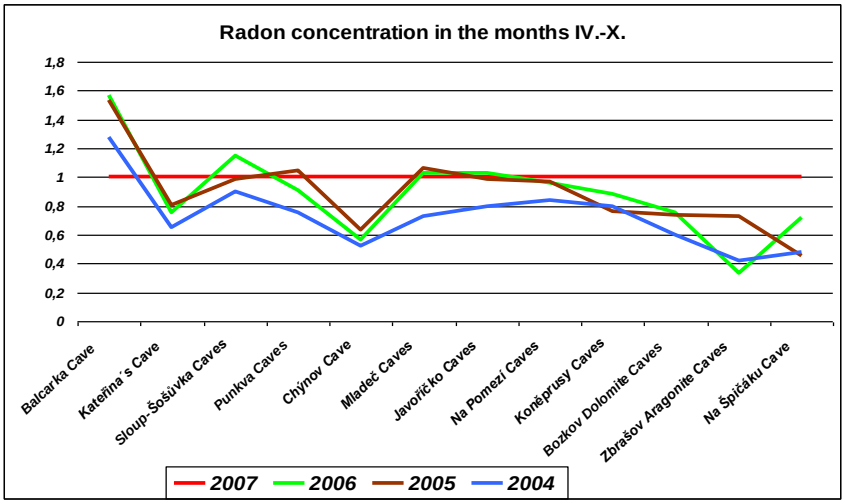

Figure 98 Radon concentration in the show caves in 2004-2007, summer season (standardized by year 2007)

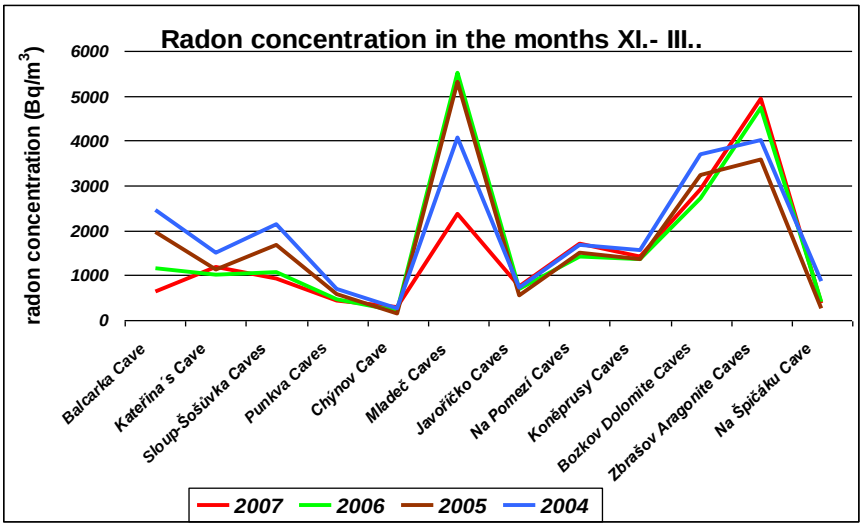

Figure 99 Radon concentration in the show caves in 2004-2007, winter season

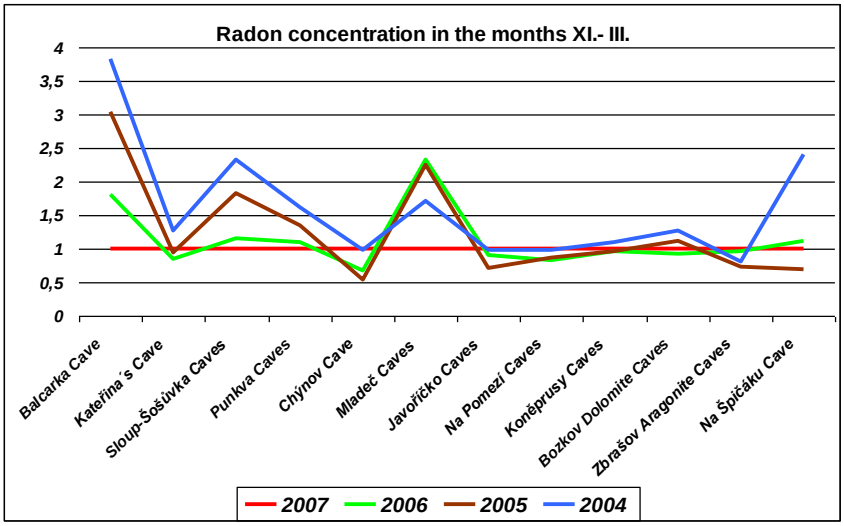

Figure 100 Radon concentration in the show caves in 2004-2007, summer season (standardized by year 2007)

Specifically in the calculations of the personal effective dose from radon inhalation in a cave environment suggested here, the following **uncertainties** of the measured values and their relative errors enter into consideration:

Radon concentration (Bq/m^3) – integral of radon activity concentration measured by RAMARN detectors.

In accordance with the measurement methodology issued by NRCBPI, annual measurements with average radon activity concentration lower than 15000 Bq.m^{-3}are guaranteed. Higher activities are loaded with greater uncertainty related to the increased number of undistinguishable tracks (in the film). At radon volume activity above 400 Bq.m^{-3} and after

one year exposure, the extended measurement uncertainty (at the 95% probability level) is lower than 16%. This uncertainty is given through calibration and evaluation of track density. The extended measurement uncertainty (at the 95% probability level) is caused by exclusion of thoron and its daughter products, estimated at <1%. The test results in the *Bozkov Dolomite* Caves and in the *Zbrašov Aragonite* Caves established experimentally that the measurement error was less than 16% (Thinova, et al., 2008). Outlying values occurred in fewer than 1% of the detectors that were used, which confirms the NRCBPI measurement quality was very good (see chapter 6.1.1, 6.1.2).

T (hours) – registered duration of stay underground.

h_p (nSv*m^3*h^{-1}*Bq^{-1}) – conversion factor – based on the ICRP 65 Recommendation – the error entering the calculation cannot be quantified, but may be as high as several 100% - for the purposes of error evaluation, this error, and also the radiation weight factor value will not be considered.[3]

j_p – individual cave factor – the error in determination this factor is the sum of the estimates of the following errors:

- measurement and aerosol spectrum recalculation errors (according to information from V. Ždímal) of approx. 20%, depending on the size of the specific fraction;
- errors in determining the free fraction (approx. 20%, according to the method that is used);
- errors of the calculation process that was selected on the basis of the level of knowledge at the time, and which cannot currently be estimated; these errors will not be included.

The entire relative error in determining the cave factor is estimated to be on an average 30%.

The error in determining the radon concentration and the error in determining the cave factor were taken for an estimate of the entire error in determining the personal effective dose. The

[3] w_R = 20 – radiation weight factor – is based on the ICRP recommendation, and has not been changed during our research. The average quality factor for 6 MeV alpha particles slowed down in tissues was estimated from calculations that utilize data for alpha particles slowing in tissues, the function Q(L) and is set to a value of 20. The limited human data (epidemiological and experimental studies) that enables the alpha particles RBE value to be estimated shows values around 10-20 for lung cancer (ICRP, 2007).

errors in determining the duration of stay and in determining the conversion factor were not included in the estimate. Using the process for error determination of indirectly measured values, the total error is established as a total differential, in which the individual differentials are replaced by concrete increases in the measured values, calculated from knowledge of the relative errors. The process leads to a calculation with a result that represents **the entire error in determining the effective dose from radon inhalation in caves**. This value is 46% (equal to the sum of the relative errors).

The error estimated using this process is further used for estimating the possibility of workers in individual caves exceeding the reference level of 6 mSv. The input data for radon concentrations obtained in 2004 – 2007, measured using RAMARN integral detectors, was provided by Petr Zajíček (Czech Cave Administration). Year 2007 was selected for the evaluation, because the radon concentrations reached the highest values in that year, and in addition none of the monitored caves were under reconstruction. If the worker effective doses are recalculated for year 2007 (the dose database was provided with permission from the Czech Cave Administration), taking into consideration the 46% relative error of dose determination, the reference level of 6 mSv was exceeded only in the *Zbrašov Aragonite* Caves, and only by two workers. The reference level had already been exceeded there in 2004, when the cave was under reconstruction. In the other caves, the reference level was not exceeded. Due to the large amount of data, the results table is not included here.

Exceeding the 6 mSv reference level can be eliminated by establishing a maximum length of stay for the workers in each cave. This length of time was calculated for the maximum individual cave factor value (the calculated value of an individual cave factor was raised by the 30% relative error) and also the maximum measured $c_{V,Rn}$ values (the measured value in each year was raised by the 16% relative error) for specific cases, see Table 32 .
Year 2007 was selected for the calculation of the maximum stay period, as in the previous procedure. From radon concentration values, the maximum permissible length of time for workers to stay in a cave was determined in such a way that the 6 mSv reference level would not be exceeded for the season with the highest $c_{V,Rn}$, i.e. for the summer months, with the exception of the *Na Pomezí* Caves, where the highest $c_{V,Rn}$ levels occurred in the fall of 2007.
The calculated maximum length of stay was compared with real maximum underground stay by workers, and those caves were selected where there was a possibility, or a probability, that

the reference level would be exceeded. For those caves, the values were recalculated more precisely.

For the *Bozkov Dolomite* Caves and the *Zbrašov Aragonite* Caves, where the calculated maximum length of stay came close to the hours actually spent underground, the precision of the calculation was improved by statistically weighting $c_{V,Rn}$ for individual time periods in accordance with the records of workers' maximum underground stays. The statistical weights used for the *Bozkov Dolomite* Caves were 0.3; 0.5; 0.2, and for the *Zbrašov Aragonite* Caves the weights were 0.2; 0.7; 0.1.

According to these results, the Zbrašov Aragonite Caves is the only cave complex where the reference level of 6 mSv might be exceeded, due to the fact that the time spent underground by workers approaches the calculated maximum time.

The conclusions based on the information given above summarize the practical impact of including the total relative error in the effective dose calculation:

1. The gamma dose rates (due to radionuclides in the rocks and due to radon daughter products) in underground workplaces do not ordinarily reach the common natural background values, because the cosmic radiation component is missing (due to the shielding effect of the caves) and the contribution of external background radiation is very low in such an environment, and can thus be excluded.
2. At the *Na Turoldu* Cave, the reference level cannot be exceeded, so it is not necessary to monitor $c_{V,Rn}$ or calculate the dose.
3. When the effective dose in caves was calculated and the total relative error of 46% was included, it was calculated that the reference level 6 mSv was exceeded only in the *Zbrašov Aragonite* caves, in 2004 by several workers in the course of reconstruction works, and by two workers in 2007).
4. A comparison between the maximum permissible number of hours that can be spent underground without exceeding the reference level of 6 mSv (calculated from the radon concentrations in 2007, raised by the measurement error) and the real, documented hours spent underground, the permissible time spent underground was exceeded only in the *Zbrašov Aragonite* Caves.

Table 32 Radon concentration (Bq/m^3) in the caves and years used for optimizing the annual working time

		$c_{V,Rn}$ (Bq.m^{-3})								T	
	year	**2007**		**2006**		**2005**		**2004**		**2007**	
Cave	j_{ipmax}	I-III + XI-XII	IV-X	I-III + XI-XII	IV-X	I-III + XI-XII	IV-X	I-III + XI-XII	IV-X	real T (h)	allow T (h)
Balcarka Cave	2.1	643	616	1168	968	1958	944	2464	787	365	1346
Kateřina Cave	3.1	1184	1169	1012	884	1124	938	1492	766	229	473
Sloup-Šošůvka C.	2.2	920	1223	1070	1405	1676	1204	2135	1100	475	638
Punkva Caves	2	433	922	472	841	586	963	698	694	566	959
Chýnov Cave	1.3	281	838	189	472	154	534	274	437	522	1583
Mladeč Caves	1.4	2365	1848	5511	1907	5320	1957	4064	1352	195	652
Javoříčko Caves	1.3	754	1621	682	1667	543	1597	735	1292	333	818
Na Pomezí Caves	2.2	1712	650	1419	625	1490	632	1667	544	267	745*
Koněprusy Caves	1.3	1409	1058	1357	930	1368	808	1557	844	621	737
Bozkov Dolomite C.	2	2923	3148	2698	2374	3235	2315	3696	1880	447	583
Zbrašov Aragonite C.	1.3	4945	3992	4730	1350	3567	2908	4008	1682	352	247
Na Špičáku Cave	2	362	744	404	535	248	340	870	358	101	1783
Výpustek C.		0	865							231	1022

j_{ipmax} maximum individual factor

T time spent under the ground

4008 cave under reconstruction

352 cave exceeded the reference level

Conclusion:

According to Methodology, the obligation to carry out $c_{V,Rn}$ monitoring and dose calculations applies only to the *Zbrašov Aragonite* Caves. For all the other show caves, it was proven that the 6 mSv reference level cannot be exceeded, provided that existing schedule and the present number of hours spent underground are maintained. If planned reconstruction or other work would increase number of hours spent working underground, monitoring will therefore be necessary. (In case of the *Zbrašov Aragonite* Caves, some workers spent more than 8 hours per day underground in the summer season, or worked at the weekend.)

For the *Bozkov Dolomite* Caves, the *Na Pomezí* Caves and the *Sloup-Šošůvka* Caves continued monitoring can be recommended (due to the occasional occurrence of an effective dose of around 5 mSv– see), if the Cave Administration agrees. Since a unique batch of data is being obtained and workers can be informed accurately about the dose that they have actually received, without guessing, we recommend that monitoring be continued in all caves (with the exception of the *Na Turoldu* Cave), using at least one RAMARN detector placed in the location with historically highest $c_{V,Rn}$.

Table 33 Number of workers in each year that have exceeded a maximum effective dose of 5 mSv (including the calculated relative error)

year	cave	number of staff	cave	number of staff
2004	*Zbrašov Aragonite* Caves	12 (reconstruction)	*Bozkov Dolomite* Caves	1
2005	*Na Pomezí* Caves	6 (reconstruction)		
2006	*Sloup-Šošůvka* Caves	1	*Bozkov Dolomite* Caves	1
2007	*Zbrašov Aragonite* Caves	2	*Bozkov Dolomite* Caves	1

Appendix 2 Practical impact of the new methodology for assessing the dose from radon for underground workers

The *individual cave factor* (ICF) was determined for Czech show caves (and for some historical tunnels, wine cellars and old mines that are in operation as museums), and the "Methodology for measurements at workplaces where there could be a significant increase in irradiation from natural radioactive sources", was updated (in accordance with the results of the research described in this thesis) in 2009. The solution presented here is based on the latest scientific knowledge and on the capabilities of state-of-the-art devices for radon measurement and dose from radon assessment in caves. It should be noted that these values differ significantly from the values measured in dwellings. Cave environments are characterized by relative humidity near to 100%, the absence of sources of aerosols, a very low ventilation coefficient, and the need to conserve these natural conditions. The proposed method can be applied to other underground workplaces, and the **individual cave factor** is determined on the basis of unattached fraction measurements. These measurements are carried out by the Radon Department of NRCBPI Kamenná-Milín. The updated Methodology is available on www.sujb.cz.

The impact of the new methodology on obligatory radon measurements in the Czech show caves can be summarized as follows:

- The only caves in which the reference level of 6mSv is likely to be exceeded are the *Zbrašov Aragonite* Caves. It is recommended that the existing radon monitoring be continued.
- A level of 5mSv can be exceeded in the *Bozkov Dolomite* Caves and in the *Sloup-Šošůvka* Caves. It is recommended that the existing radon monitoring also be continued in these caves.
- When any cave reconstruction work is being carried out, there is a high probability that the reference level will be exceeded. During reconstruction work, it is recommended that each cave be monitored.
- Monitoring in the *Na Turoldu* Cave is considered unnecessary.
- Personal dosimeters were found not to be effective in caves.

- It is recommended to continue with radon monitoring in all of the other show caves, using a single RAMARN detector that which will be placed in the area where the radon concentration is expected to be highest. This procedure will enables the Cave Administration to be sure that the workers are safe. It will also be very useful to maintain a unique data set of long-term radon measurements from the Czech show caves.
- The maximum "safe or permissible" working hours for each show cave has been calculated. It seems very useful to prepare a "nomogram" based on the equation (Cigna, 2005)

  $T = 10^6 * D / 7.784 * F * C$

  Where T time spent in under the ground

  D dose limit (e.g. 20 mSv)

  F equilibrium factor

  C average radon concentration ($Bq.m^{-3}$)

  This "nomogram" makes it very simple to read the allowed time for a given dose limit.

A brief statistical estimate of the practical impact of the new methodology reveals the following information: in the caves that were monitored before the new methodology was introduced, about 60 RAMARN detectors were used each year. After 2009, the number of detectors fell to approx. 24, leading to a reduction in costs of at least CZK 20 000 per year. The costs for staff medical tests can also be reduced.

Appendix 3 Results of the MCNPX modeling simulation

There were some differences between the data from laboratory gamma spectrometry measurements of rock samples and the in situ gamma spectrometry measurements (Zimák, 2004b) concerning the mass concentrations of ^{40}K, ^{226}Ra (eU) and ^{232}Th (eTh) in rock and in clastic sediments. Differences in the measurement conditions, which may have influenced the results, were discussed in chapter 6.10. A matter for discussion was the extent to which the high radon concentration in the cave atmosphere contributed to the in-situ gamma spectrometry (ppm eU) mass concentration measurement results. In cases when gamma spectrometry measurements are performed in the open air 1m above the Earth's surface, the contribution of radon daughters (mainly of the ^{214}Bi isotope) is negligible, approximately 5-7% for average dose rate 115 nGy/h (Klusoň, et al., 2011). It depends on the level of the gamma dose rate in the measurement location and on the measurement geometry. In caves, the situation is different. The radon concentration in the cave atmosphere is significantly higher (hundreds and thousands Bq/m^3) than the units of Bq/m^3 in the open atmosphere. In comparison with the 2π geometry which is typical for above ground measurements and calibration, radionuclides present in the rock contribute more to the dose rates because the walls are relatively close to the detector (several meters away), surrounding the detector.

A simple model using the MCNPX method (Figure 101) was developed to estimate the contributions of different geometries of the measurement configuration and of different radon concentrations in the underground atmosphere. The cave was approximated using a sealed tunnel model with variable average radius (2, 4, 6 and 10 meters) and length (4, 10, 20 and 30 meters). The parameters considered in the calculation are listed in Table 34. The thickness of the walls was taken as 1 meter, based on previous calculations, which indicated that the contribution of a layer of greater thickness was less than 3%. The response of the detector in the 1.66-1.86 MeV energetic window (IAEA, 2003a) (near to energy of ^{214}Bi 1.76 MeV) was compared using the Tally8 MCNPX card. Examples of results from the MCNPX model of the Gamma Surveyor gamma spectrometry probe (FG Instruments) with a 3"x3" NaI(Tl) detector attached (similar to a GS256 device) are presented in Table 35, Table 36 and in Figure 102.

Photons with energy 1.76 MeV in the air have a range of hundreds of meters, and it is apparent that the influence of a complicated cave surface and a high indicated concentration of radon, for a given equivalent radon concentration, will depend on the concentration of the Ra in the walls, on the concentration of ^{214}Bi in the air, and on the volume of air in the cave.

The higher the concentration of Ra, the larger the cave volume that is necessary for a significant contribution of airborne Bi.

The deposition of the radon daughters on the walls was also taken into account. The surface concentration of ^{214}Bi (Bq/m^2) was consulted with Ivo Burian (NRCBPI), and was calculated by him using the WIEN_III.BAS program for very low air flow velocity, ventilation coefficient 0.1 (h^{-1}), average F=0.45 and free fraction f_p = 0.5 (and 0.13 as the average value from measurements in the Czech show caves in 2006-2007).

Table 34 List of changeable parameters which were taken into consideration for response calculation

Changeable parameters					
Cave radius (m)	2	4	6	8	10
Cave length (m)	4	10	20	30	
Mass concentration of ^{226}Ra in the walls (Bq/kg)	5	10	20		
EEC (Bq/m^3) (c_A depends on F)	500	1000	4000		
Free fraction 0.5 and deposition of ^{214}Bi/1Bq (Bq/m^2)	0.70				
Free fraction 0.13 and deposition of ^{214}Bi/1Bq (Bq/m^2)	0.11				
Ratio between the real cave surface and model surface	10	100			

Table 35 Example of the contribution of the air to the total count in specific conditions

20 Bq/kg ^{226}Ra in the walls; EEC=1000 Bq/m^3; appropriate surface deposition of ^{214}Bi=700Bq/m^2 for f_p=0.5; ratio of real surface to ideal surface = 10

	Contribution from the air to the total counts					**Total counts**			
	Internal length of the cave (m)					Internal length of the cave (m)			
Internal cave radius (m)	4	10	20	30		4	10	20	30
2	0.217	0.254	0.275	0.284		0.877	0.927	0.922	0.953
4	0.284	0.366	0.401	0.404		1.003	1.072	1.162	1.164
6	0.318	0.421	0.482	0.506		1.049	1.237	1.284	1.328
8	0.360	0.458	0.539	0.546		1.103	1.299	1.429	1.522
10	0.364	0.499	0.559	0.600		1.113	1.350	1.569	1.612

Table 36 Comparison of results for 2π geometry (open atmosphere) and 4π geometry (cave 4x4 m) for in situ gamma spectrometry measurements

^{226}Ra (Bq/kg)	$c_{Rn,V}$=5 Bq/m^3 2π geometry; open atmosphere		EEC=500 Bq/m^3 4π geometry; f_p=0.5		EEC=1000 Bq/m^3 4π geometry; f_p=0.5	
10	0.153	total	0.502	total		
			0.354	walls		
			0.142	air		
			0.005	deposition		
20	0.306	total			1.003	total
					0.708	walls
					0.285	air
					0.010	deposition

The results from the model support the following conclusions:

- The contribution of a high radon concentration in the air, which is typical for the cave environment, to the total count of the gamma spectrometry measurement (or to the energy window of ^{214}Bi 1.66-1.86 MeV) always occurs (when EEC is higher than 100 Bq/m^3, the contribution is in range of tens of %; below this value, the contribution is units %, depending of the cave air volume).
- The total count (imp/s) in this energy window consists of three main components: the contribution of the walls (which is constant), the contribution of the air (which grows with the size of the cave) and the contribution of the deposition of radon daughters (which is negligible).
    - The contribution of the ^{214}Bi contained in the cave walls or in clastic sediments (mass concentration in Bq/kg) is constant for caves of usual size.
    - The contribution of the ^{214}Bi concentration present in the air grows with the size of the cave chamber or tunnel chamber.
    - The contribution of the radon daughter ^{214}Bi that is deposited on the walls is negligible. For free fraction 0.5 and 0.13 it is about 2 orders less and 3 orders less, respectively, than the contribution from the walls or air, when the ratio of the real surface to the model surface is 10. The cave surface is very

complicated, and the ratio could be 100 or more. As the ratio rises the contribution of the deposition decreases.

- Due to influence of stripping ratio values on calculated concentrations, the high concentration of airborne radon will have impact on the concentration of K and Th as well.

The model has proven to be quite effective, and the simulations will be continued in the future. The model will be verified, using gamma spectrometry measurements, in the *Mladeč* Caves at a specific location where long-term continual radon monitoring is being carried out.

Figure 101 Model illustration using MCNPX Visual Plotter Version X-24E

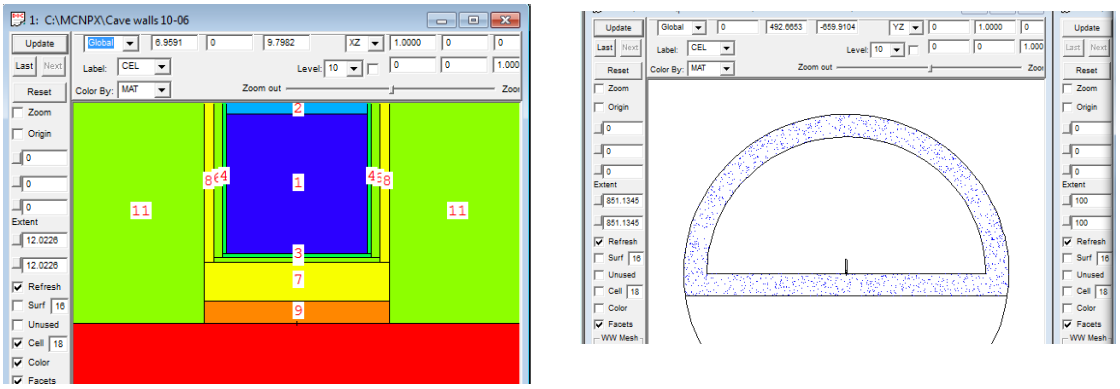

Source: walls, 6m radius and 10m length,1m thickness

Figure 102 Comparison of contributions to the total count in the 1.66-1.86 MeV energy window under different conditions

A: cave length 4m, EEC=500Bq/m^3, f_p=50%, a_m (^{226}Ra) =10Bq/kg

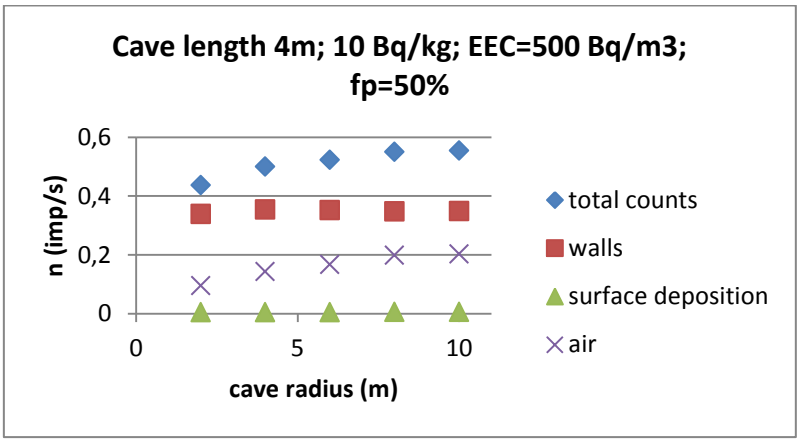

B: cave length 20m, EEC=500Bq/m^3, f_p=50%, a_m (^{226}Ra) =10Bq/kg

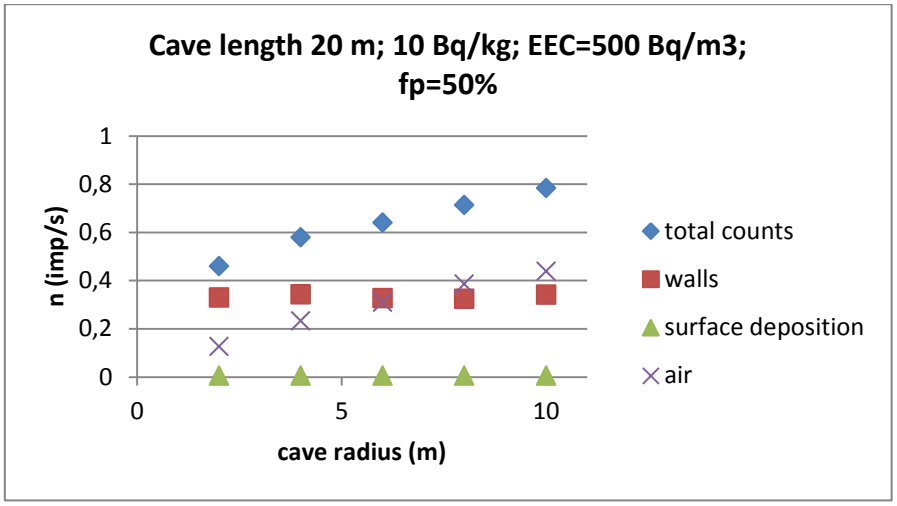

C: cave length 4m, EEC=1000Bq/m^3, f_p=13%, a_m (^{226}Ra) =10Bq/kg

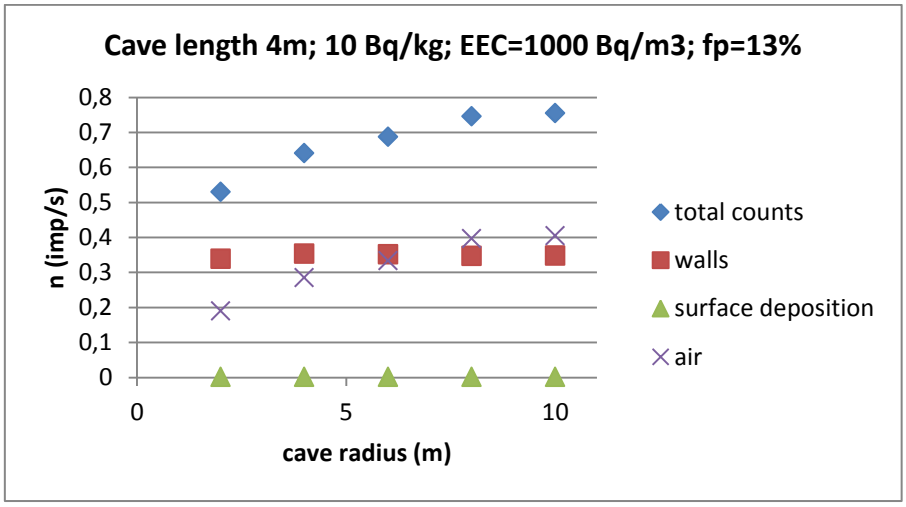

D: cave length 20m, EEC=1000Bq/m^3, f_p=13%, a_m (^{226}Ra) =10Bq/kg

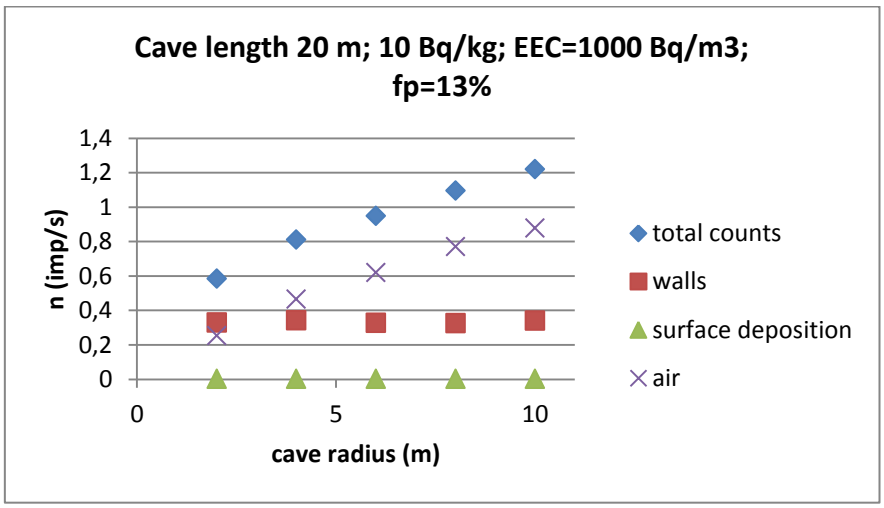

E: cave length 4m, EEC=1000Bq/m^3, f_p=50%, a_m (^{226}Ra) =20Bq/kg

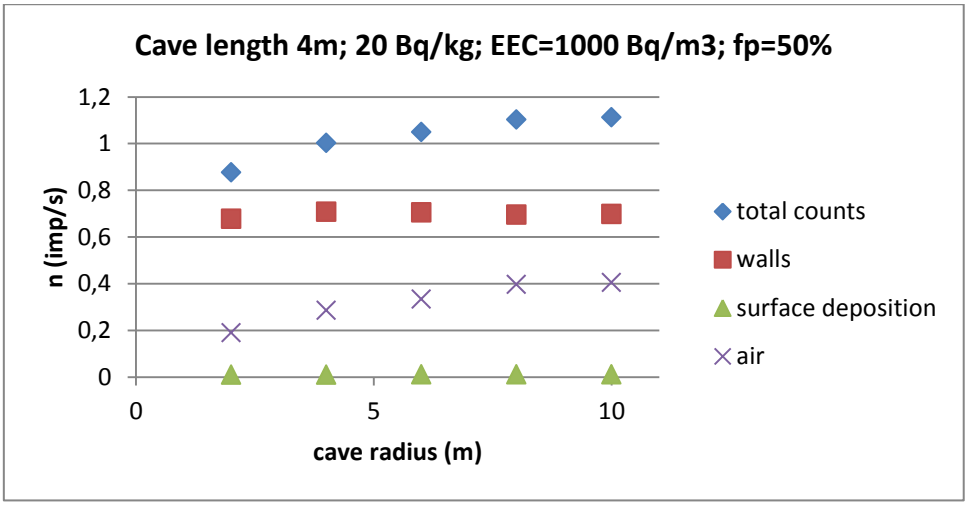

F: cave length 20m, EEC=1000Bq/m^3, f_p=50%, a_m (^{226}Ra) =20Bq/kg

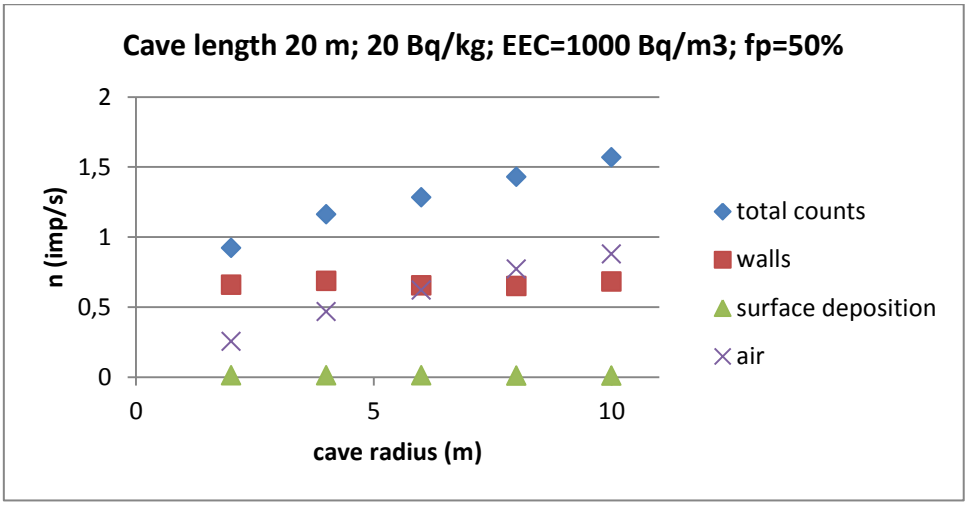

Acknowledgement

I would like to thank Jaroslav Šolc for his help with the MCNPX model and for making the calculations, and Ivo Burian for the surface deposition calculations.

List of symbols

Symbol	Unit	Description
AMAD		Activity median aerodynamic diameter. The value of aerodynamic diameter where 50% of the airborne activity in a given aerosol is associated with particles smaller than the AMAD, and 50% of the activity is associated with particles larger than the AMAD. The AMAD is used in internal dosimetry as a means of simplifying the true distribution of aerodynamic diameters of a given aerosol as a single value. It is used to describe those particle sizes for which deposition depends chiefly on inertial impaction and sedimentation.
AMTD		Activity median thermodynamic diameter. For smaller particles, deposition typically depends primarily on diffusion, and the activity median thermodynamic diameter (AMTD) - defined in an analogous way to the AMAD, but with reference to the thermodynamic diameter of the particles - is used.
$a_{V, Rn}$ VAR, C_{Rn}	Bq/m^3	Radon activity concentration.
$c_{V, Rn}$	Bq/m^3	Radon activity concentration in this thesis.
$\dot{D}$	nGy/h	Dose rate, absorbed dose rate. Dose rate is defined as the ratio of an incremental dose, dD, in a time interval, dt, to the time interval, $\dot{D} = dD/dt$. Gamma dose rate in air is used for the description of terrestrial radiation, and is usually expressed in nGy/h. 1 pGy/s = 3.6 nGy/h.
DCF	mSv/WLM	Dose conversion factor.
E	Sv	Effective dose is a sum of multiples of equivalent doses in separate human organs and particular organ weighting factors w_T. $E = \Sigma\, w_T H_T$. Effective dose is expressed in mSv and usually reported per annum. For environmental gamma radiation the estimate is $E = \dot{D}_a \times t \times 0.7 \times 10^{-6}$, where E is the effective dose (mSv), $\dot{D}_a$, is the dose rate in air (nGy/h), t is the exposure time (h) and 0.7 is the conversion coefficient (Sv/Gy) for human organs (UNSCEAR, 1988). For $\dot{D}_a$ = 100 nGy/h, t = 8760 h (1 year), E = 0.613 mSv.
EEC C_{RnDp}	Bq/m^3	The activity concentration of radon gas in equilibrium with its short-lived progeny that would have the same potential alpha energy concentration as the existing non-equilibrium mixture. $EEC = 0.1065c_{218Po} + 0.515c_{214Pb} + 0.379C_{214Bi}$
F		Equilibrium factor, which is ratio of the equilibrium equivalent radon activity concentration to the radon activity concentration. The ratio of potential alpha energy concentration for the actual mixture of radon decay product to that which would apply at radioactive equilibrium. Assuming 7000 h/year indoors or 2000 h/year at work, and F = 0.4 (ICRP,2003).
f_p f_{un}		Free fraction, unattached fraction. The fraction of the potential alpha energy concentration of short-lived radon progeny that is not attached to the ambient aerosol. $f_{un} = PAEC_{un}/(PAEC_{un} + PAEC_{att})$
f_a		Attached fraction. The fraction of the potential alpha energy concentration of short-lived radon progeny that is attached to the ambient aerosol.
h_p DCF_E	$nSv/Bqhm^{-3}$	Dose conversion factor based on epidemiological studies, dose conversion convention = 4mSv/WLM at home and =5 mSv/WLM at workplace.

HRTM		Human Respiratory Tract Model. Model used in Publication 66 (ICRP, 1994) to evaluate the deposition and clearance of inhaled particles in the respiratory airways, as well as the resulting dose to the lung tissues.
PAEC		The concentration of short-lived radon or thoron progeny in air in terms of the alpha energy emitted during complete decay from radon-222 progeny to lead-210, or from radon-220 progeny to lead-208, of any mixture of short-lived radon-222 or radon-220 in a unit volume of air. For radon progeny: 1 Bq/m^3 of radon at equilibrium = 3.47 • 10^4 MeV/m^3 = 5.56 • 10^9 J/m^3 . For thoron progeny: 1 Bq/m3 of thoron at equilibrium = 4.72 • 105 MeV/m^3 = 7.56 • 10^8 J/ m^3.
RAMARN		Integral radon detector with Kodak LR115 film as an alpha track detector.
RBE		Relative biological effectiveness.
Reference level		Existing controllable exposure situations, this represents the level of dose or risk above which it is judged to be inappropriate to plan to allow exposures to occur, and below which optimization of protection should be implemented. The chosen value for a reference level will depend upon prevailing circumstances of the exposure under consideration.
SSNTD		Solid state nuclear track detector.
WL		Is defined as ^{218}Po, ^{214}Bi, $^{214}Pb/^{214}Po$ being in a radioactive equilibrium (equilibrium factor, F=1) with 100 pCi L^{-1} (1 pCi L^{-1}=37 Bq m^{-3}) of ^{222}Rn, resulting in potential alpha energy concentration of 1.3×10^5 MeV 1 WL = 100 pCi/l = 3.76 Bq/m^3 = 1.3 • 10^8 MeV/ m^3 = 2.08 • 10^5 J/ m^3
WLM		Working-levelmonth is the exposure gained by 170 h breathing in the air with the activity concentration of short-lived radon decay products of 1 WL 1 WLM = 3.54 • 10^3 Jh/ m^3 = 6.37 • 10^5 Bqh/ m^3 equilibrium equivalent concentration of radon = 6.37 • 10^5/FBqh/ m^3 of radon, where F = equilibrium factor • 1 Bq/m^3 of radon over 1 year = 4.4 · 10^3 WLM at home * • 1 Bq/m^3 of radon over 1 year = 1.26 · 10^3 WLM at work * *Assuming 7000 h/year indoors or 2000 h/year at work, and F = 0.4 (ICRP, 1993). WLM = 4.68 · 10^4 Bqh/ m^3 equilibrium equivalent concentration of thoron
#		Number of particles.

List of tables

List of figures

Works Cited

Abt, L. 2010. Komplexní geologické zhodnocení jesenického krasu. *Diplomová práce. Masarykova Universita Brno.* 2010.

BEIRIV. 1999. Health Effects of Exposure to Radon. 1999.

Bezek, M. and Gregorič, A. et all. 2012. Diurnal and seasonal variations of concentration and size distribution of nano aerosols (10-1100 nm) enclosing radon decay products in the Postojna Cave, Slovenia. *Radiation Protection Dosimetry.* Vol. 152, No. 1-3, pp. 174-178, 2012.

Bílková, D., et al. 2002. *Podzemí v Čechách, na Moravě a ve Slezku.* Praha : Olympia, 2002. 80-733-519-X.

Birchall, A. et al. 1996. Respiratory track model. NRPB-SR287. Chilton. Didcot. Oxon OX11 0RQ. 1996.

Böhm, R. 2003. Modelovanie radiačného rizika indukovaného radónom a zdrojmi. *Dizertační práce.* Fakulta matematiky, fyziky a informatiky, UK, Bratislava, 2003.

Böhm, R., Nikodémová, D. and Holý, K. 2002. Dosimetric and micro-dosimetric approach for the estimation of radon–induced damages in human lungs. *Book of abstract XXIV.DRO. Slovakia.* 2002.

Bochicchio, F., McLaughling, J.P. and Piermattel, S. 1995. Radon in indoor air. Report EUR 16123 Environmental quality of life. Luxemburg , 1995, ISBN 92 827 0119 0.

Bosák, P. 1988. Jeskyňářství v teorii a praxi. *Česká speleologická společnost ve Státním zemědělském nakladatelství. Praha.* 1988.

Brandejsová, E. 2004. *Dose assessment in connection with the inhalation of radon by caves guides.* Praha : CTU in Prague, 2004. Diploma thesis.

Briestensky, M., et al. 2011. The use of caves as observatories for recent geodynamic activity and radon gas concentrations in the Western Carpathians and Bohemian Massif. *Radiation Protection Dosimetry.* 2011, Vols. 145, No. 2-3, p. 166-172, ISSN 0144-8420.

Bruthans, J. and Zeman, O. 2001. Nové poznatky o charakteru a genezi podzemních krasových forem v Českém krasu a dalších oblastech bez soustředěných ponorů v České republice. *Český kras 27, pp. 21-29, Beroun 2001,ISSN 1211-1643.* 2001.

Burian, I. and Štelcl, O. 1990. Radon and its daughters in the tourisitic caves of the Moravian Carst. *Studia Carsologica 3.* GGÚ ČSAV, 1990.

Cantrell, B.K., et al. 1987. Monitoring and measurement of in-mine aerosol: Diesel emissions. *BuMines IC 9141.* Washington DC, pp. 18-40, 1987.

Cappa, B.G., et al. 1996. Radiation protection and radon concentration measurements in Italian caves. *BOSSEAMCMXCV. Proc. Int. Symp. Show caves and Environmental monitoring.* Cuneo, Italy, 1996.

Cigna, A. 2005. *Radon in Caves.* Bologna : International Journal of Speleology. Societá Speleologica Italiana, 2005. ISSN 0392-6672.

Cohen, A. B.L. 1993. Relationship between exposure to radon and various types of cancer. *Health Physics.* Vol. 65(5), pp. 529-531, 1993.

Darby, S., et al. 2005. Radon in homes and risk of lung cancer; collaborative analysis of individual data from 13 European case-control studies. *Br. Med. J.* 2005, Vols. 330, pp. 223-227.

Denman, A.R. and Parkinson, S. 1996. Estimations of radiation dose to National Health Srvice workers in Northamtonshire from rised radon levels. *Br. J. Radiol. 69. pp. 72-75.* 1996.

Dickin, P.A. 2005. *Radiogenic Isotope Geology.* New York : Cambridge University Press, 2005. ISBN 978-0-521-53017-0.

Dvořák, J. and Friáková, O. 1978. Stratigrafie paleozoika v okolí Hranic na Moravě. *Výzk. Práce Ústř. úst. geol., 18, 50 str. Praha.* 1978.

Dvořák, J. 1994. Styk geologických struktur jesenického a drahanského regionu mezi Mohelnicí, Uničovem a Litovlí.- Geol. vyzk. Mor. Slez. v r. 1993, s 30-31. Brno. *Geol. vyzk. Mor. Slez. v r. 1993, s 30-31. Brno.* 1994.

Dvořák, V. 2004. Orientační strukturní analýza vápenců hranického krasu. *Geol. výzk. Mor. Slez. v r. 2003, Brno.* pp. 42-45, 2004.

Fabík, M. 1975. Výsledky ložiskového průzkumu vápenců konického devonu. *Sbor. GPO, 9.* 1975.

Genrich, V. AlphaGuard PQ2000/MC50 Multiparameter Radon Monitor-Characterissation of its physical properties under normal clinic and servereenvironmental conditions, Genitron Instruments GmbH, Frankfurt am Main.

Gillmore, G.K., et al. 2000. Radon Hazards, Geology, and Exposure of cave Users: A Case Study and Some Theoretical Perspectives. *Ecotoxicology and Environmental Safety.* Vol. 46. pp. 279-288, 2000.

Grundel, M. and Porstendörfer, J. 2004. Differences between the activity size distribution of the different natural radionuclide aerosols in outdoot air. *Atmos. Environ.* 2004, Vols. 38, pp.3723-3728.

Haninger, T. 1997. Size distribution of radon progeny and their influence on lung. *Abstract for 7th Tohwa University International Symposium.* 1997.

Harley, N.H., Fisenne, I.M. and Robbins, E.S. 2012. Attempted validation of ICRP 30 and ICRP 66 respiratory models. *Radiation Protection Dosimetry.* Vol. 152, No. 1, pp. 14-17, 2012.

Havíř, J., Bábek, O. and Otava, J. 2004. Vztah struktur, stratigrafie a krasovění ve Zbrašovských aragonitových jeskyních. *46–50, Geol. výzk. Mor. Slez. v r. 2003, Brno.* 2004.

Hinds, C. Williams. 1998. *Aerosol Technology: properties, behavior, and measurement of airborne particles.* New York : John Wiley & Sons, Inc., 1998. ISBN 0-471-19410-7.

Hladil, J. 1994. Geologický atlas České republiky – stratigrafie. *Česká geologická společnost. Praha.* 1994.

—. 1983. Cyklická sedimentace v devontských karbonátech macošského souvrtství. *Zemní plyn a nafta.* 1983, Vols. Hodonín, Sv. 28, str. 1-15.

Hladil, J. et al. 2003. A pragmatic test of the early origin and fixation of gamma-ray spectrometric (U, Th) and magneto-susceptibility (Fe) patterns realted to sedimentary cycle boundaries in pure paltform limestones. *Carbonates and Evaporites.* Springer Niederlands, 2003, Vol. 18, ISSUE 2, pp 89-107.

Hladil, J. 1997. Obsah izotopů 13C a 18O v devontských karbonátech Moravského krasu: specifický sekvenční vzor. *Geologický výzkum na Moravě a ve Slezku.* Brno, Sv. 3, str. 56-63, 1997.

Hladil, J., et al. 2003. Metamorphosed carbonates of Krkonoše Mountains and Paleozoic evolution of Sudetic Terranes (NE Bohemia, Czech Republic). *Geol. Carpathica, 54, s. 281-297.* 2003.

Hromas, J. 1997. Tektonická stavba krasových ostrovů v oblasti Bozkov-Jesenný . *In Kučera B., Turnovec I. (eds.): Příroda 9. Kras Krkonoš a Podkrkonoší, s. 22-49. AOPK ČR, Praha.* 1997.

Hromas, J. a kol. 2009. *Jeskyně. Chráněná území sv. XIV.* Praha : Agentura ochrany krajiny a přírody ČR a EkoCentrum Brno, 2009. ISBN 978-80-87051-17-7.

Cháb, J. and Žáček, V. 1994. Geology of the Žulová pluton mantle (Bohemian Massif, Central Europe). *Věst. Ústř. Úst. geol., 69, s. 1-12.* 1994.

Chábera, S. 1982. Geologické zajímavosti jižních Čech. *Jihočeské nakladatelství České Budějovice.* 1982.

—. 1982. Geologické zajímavosti jižních Čech. *Jihočeské nakladatelství České Budějovice.* 1982.

Chaloupský, J. et al. 1989. Geologie Krkonoš a Jizerských hor. *ÚÚG Praha.* 1989.

Chlupáč, I. 2002. Geologická minulost České republiky. *Academia Praha.* 2002.

IAEA. 2003a. Guidelines for radioelement mapping using gamma ray spectrometry data. IAEA-TECDOC-1363. 2003a.

—. 2003. Radiation Protection Against Radon in Workplaces other than Mines. *Vienna.* 2003.

—. 2003. *Safety reports Series No. 33. Radiation Protection against radon in Workplaces other than Mines.* Vienna : International Atomic Energy Agency, 2003. ISBN 92-0-113903-9.

ICRP. 2005. Assessing dose of the representative individual for the purpose of radiation protection for the public. *DRAFT.* 2005.

—. 1994. ICRP Publication 66: Human respiratory tract model for radiological protection. 1994.

—. 1981. ICRP Publications. Pergamon Press, Oxford, 1981, Vol. 26.

—. 2010. Lung Cancer Risk from Radon and Progeny and Statement on Radon. *ICRP Publication 115, Ann. ICRP 40(1).* 2010.

—. 1994. Protection against Radon-222 at Home and at Work. *ICRP Publication 65.* 1994.

—. 1993. *Publication 65. Protection Against Radon-222 at Home and at Work.* Oxford : Pergamon, 1993. ISSN 0146-6453.

—. 2007. The 2007 Recommendations of the International Commission on Radiological Protection. ICRP Publication 103. Annn. ICRP 37 (2-4). 2007.

James, A.C., Birchall, A. and Akabani, G. 2004. Comparative dosimetry of BEIRVI revisited. *Rad. Prot. Dosim.* 2004, Vols. 108, pp.3-26.

Jirka, Z. et al. 2001. *Speleoterapie. Principy a zkušenosti.* Olomouc : Universita palackého, 2001. ISBN 80-244-0346-3.

Klusoň, J. and Thinová, L. 2011. Contribution of atmospherical radon to in-situ scintillation gamma spectrometry data. *Applied Radiation and Isotopes.* Vol. 69, pp. 1143–1145, 2011.

Knutson, G.E.O., et al. 1983. Radon daughter plateout-II. Prediction model. *Health Physics.* Vol. 45, No.2.pp. 445-452, 1983.

Kučera, B., Hromas, J. and Skřivánek, F. 1981. Jeskyně a propasti v Československu. *Academia Praha.* 1981.

Květoň, P. 1951. Stratigrafie krystalinickým sérií v okolí severomoravských grafitových ložisek. *Sbor. ÚÚG, LXVIII/1951, Odd. geol., 18.* 1951.

Lang, M. 2010. Cirkulace vzduchu v jeskynním prostředí (Císařská jeskyně, Moravský kras). *Bakalářská práce. Přírodovědecká fakulta Masarykovy univerzity. Brno.* 2010.

Lippmann, M. 1977. Regional Deposition of Particles in the Human Respiratory Track. *in Lee, D.H.K., Falk, H.L., Murphy, S.O., and Geiger, S.R. (Eds.), Handbook of Physiology, Reaction to Environmental Agents, American Physiological Society.* Bethesda, MD, 1977.

Manová, M. Matolín, M. 1995. *Radiometrická mapa České republiky 1:500 000.* Praha : ČGÚ, 1995.

Mareš, S. et al. 1979. Úvod do užité geofyziky. SNTL Praha, 1979.

March, J.W. and Birchall, A. 2000. Sensitivity analysis of the weighted equivalent lung dose per unit exposure from radon progeny. *Rad. Prot. Dosim.* 2000, Vols. 87, pp.167-178.

March, J.W., et al. 2002. Uncertainty analysis of the weighted equivalent lung dose per unit exposure from radon progeny in the home. *Radiation Protection Dosimtry.* Vo. 102, pp. 229-248, 2002.

Marsh, J.W. and Birchall, A. 1998. Sensitivity Analysis of the Weighted Equivalent Lung Dose Per Unit Exposure from Radon Progeny. *NRPB-M929.* 1998.

Mc Laughlin, J. 2012. An historical overview of radon and its progeny applicationa nad health effects. *Radiation Protection Dosimetry.* Vol. 152, No. 1-3, pp. 2-8, 2012.

Michovská, J. 1957. Typizace Československého krasu. *Čs.kras, 10, s.60-68.* 1957.

Mísař, Z. et al. 1993. Geologie ČSSR I. Český masiv. *SPN Praha.* 1993.

Musil, R. et.al. 1993. Moravský kras-labyrinty poznání. *Geo program, Adamov.* 1993.

Nazaroff, W. W. and Nero, A.V. 1988. Radon and its decay products in indoor air. *New York, John Wiley.* 1988.

Nováková, K. 2011. Dynamika teplotních změn v Chýnovské jeskyni. *Diplomová práce. Masarykova Universita Brno.* 2011.

NRPB. 1994. LUng Dose Evaluation Program. 1994.

Otáhal, P. 2006. Radioaktivita horninového prostředí jeskyní Moravského krasu. *Diplomová práce. Masarykova universita v Brně.* 2006.

Panoš, V. 1964. Der Urkarst in Ostflugel der Böhmischen Masse. *Z. Geomorphol.* N.F. 8(2), pp. 105-164, 1964.

—. 2001. Karsologická a speleologická terminologie. Knižné Centrum Žilina, 2001, ISBN 80-8064-115-3.

Papastefanou, C. 2008. *Radioactive Aerosols.* Amsterdam : Elsevier, 2008. ISBN 978-0-08-044075-0, ISSN 1569-4860.

Pashenko, S. and Dublyansky, V.Y. 1997. Generation of cave aerosols by alpha particles: critical evaluation of the hypothesis. *Journal of Cave and Karst Studies.* 59/3), pp. 103-109, 1997.

Porstendörfer, et al. 2005. Fraction of the positive 218Po and 214Pb clusters in indoor air. *Radiat Prot Dosimetry.113(3):342-51. Epub 2005 Apr 13.* 2005.

Porstendörfer, J. 2007. Electrical charge and the concentration fo the non aerosol-attached radon progeny in indoor air. *5th International Conference on Protection against at Home and at Work.* Prague, 2007, Vol. oral presentation.

—. 2001. Physical parameters and dose factors of the radon and thoron decay products. *Radiation Protection Dosimetry.* Vol. 94 (4), pp. 365-371, 2001.

—. 1994. Properties and behaviour of radon and thoron and their decay products in the air. *Journal of Aerosol Science.* 1994, Vols. Vol. 25, No. 2, pp.

—. 1996. Radon: measurement related to dose. *Environ. Int.* Vol.22, pp. 563-583, 1996.

Porstendörfer, J., Butterweck, G. and Reineking, A. 1994. Daily variation of the radon concentration indoors and outdoors and the influence of meteorological parameters. *Health Physics* . Vol. 67(3). Pp. 283-287, 1994.

Porstendörfer, J., Wicke, A. and Schraub, A. 1978. The influence of exhalation, ventilation and deposition processe upon the concentration of radon (222Rn), thoron (220Tn) and their decay products in room air. *Health Physics.* Vol. 34, pp. 465-473., 1978.

Přibyl, P. et al. 1992. Základy karsologie a speleologie. *1. vyd. Praha: Academia.* 1992, Vols. ISBN 80-000-0084-4.

Přichystal, A. 1996. Moravskoslezské bradlové pásmo. *Geol. výzk. Mor. Slez. v r. 1995, s. 113-118. Brno.* 1996.

Puskin, J.S. and James, A.C. 2006. Radon exposure assessment and dosimetry applied to epidemiology and risk estimation. *Radiat Res. 2006 Jul;166(1 Pt 2):193-208.* 2006.

Quinn, C.J.A. 1990. Factors that may affect radon daughter concentrations in Whipple Cave and Gushute Cave, Nevada. *The NSS Bulletin. Pp 104-109.* 1990.

RADONIC01. Continual radon monitor with very fast response. Návod k použití. Nuclear Technology. Prague.

Raes, F. 1985. Description of the properties of unattached 218Po and 212Pb particles by means of the classical theory of cluster formation. *Health Physics.* Vol.49, No. 6, pp.1177-1187, 1985.

Reineking, A., et al. 1992. Thoron gas concentration and aerosol characteristics of thoron decay products. *Rad. Prot. Dosim.* 1992, Vols. Vol. 45, pp. 353-356.

Rovenska, K. and Thinova, L. 2010. Seasonal variation of radon in the Bozkov cave. *Nukleonika Journal.* 2010, Vols. Vol 55, no.4, p. 483-490, ISSN 0029-5922.

Rovenská, K. 2007. *Dose from radon calculation.* Prague : CTU in Prague, 2007. Diploma thesis.

Rovenska, K., Thinova, L. and Zdimal, V. 2008. Assessment of the Dose from Radon and its Decay Products in the Bozkov Dolomite Cave. *Radiation Protection Dosimetry.* 2008, Vols. vol. 130, no. 1, p. 34-37, ISSN 0144-8420.

Sainz, C., et al. 2007. Analysis of the main factors affecting the evaluation of the radon dose in workplaces: the case of tourist caves. *Hazard Mater. 2007 Jul 16;145(3):368-71. Epub 2006 Nov 21.* 2007.

Scott, A.G. 1983. Scott, A.G. Radon daughter deposition velocities estimated from field measurements. *Health Physics.* Vol. 45. No.2.pp. 481-485, 1983.

Shimo, M. and Ikebe, Y. 1984. Measurements of radon and its short-lived decay products and unattached fraction in air. *Radiation Protection Dosimetry.* Vo. 8, No. 4, pp.209-214, 1984.

Schery, D.S. 2001. *Understanding Radioactive Aerosols and Their Measurement.* Dordrecht, Niederlands : Kluwer Academic Publishing, 2001. ISBN 0-7923-7068-6.

Skoček, V. 1980. Nové poznatky o litologii devonských bazálních klastik na Moravě. *VÚÚG, 31, 120–127. Praha.* 1980.

Skřivánek, F. and Valášek, K. 1997. Jeskyně ve vápnitých dolomitech fylitové zóny u Bozkova na Železnobrodsku. *In Kučera B., Turnovec I.(eds.) Příroda 9. Kras Krkonoš a Podkrkonoší, s. 50-69. AOPK ČR, Praha. .* 1997.

Sládek, P. 2009. Jeskynní mikroklima a radioaktivita. **—** In: Mackovčin P. – Sedláček M.(eds.): Chráněná území ČR XIV.: Jeskyně. Agentura ochrany přírody a krajiny ČR a EkoCentrum Brno, 107-109. Praha. 2009.

Sládek, P., Navrátil, O. and Sas, D. 2001. Mikroklima a fyzikální parametry ve speleoterapii. In Jitka, Z. a kol. Speleoterapie – principy a zkušenosti. 1. vyd. Olomouc: Univerzita Palackého, 2001, s. 98 – 152. . 2001, Vols. ISBN 80-244-0346-3.

Smetanová, I. 2009. VARIÁCIE OBJEMOVEJ AKTIVITY RADÓNU VO VRTOCH A V PODZEMNÝCH PRIESTOROCH. *DIZERTACNÁ PRÁCA.* Bratislava, 2009.

Smith, A.C., Wynn, P.M. and Barker, P.A. 2013. Natural and anthropogene factors which influence aerosol distribution in Ingleborough Show Cave, UK. *International Journal of Speleology.* Vol.42(1). 49-56., 2013.

Solomon, B.S. et al. 1996. OCCUPATIONAL EXPOSURE TO RADON IN AUSTRALIAN TOURIST CAVES. *FINAL REPORT OF WORKSAFE AUSTRALIA RESEARCH GRANT (93/0436).* 1996.

Solomon, S.B., et al. 1992. Radon exposure in a limestone cave. *Radiation Protection Dosimetry* . Vol. 45. No. ¼. Pp. 171-174, 1992.

Solomon, S.B., et al. 1992. Radon exposure in limestone cave. *Radiation Protection Dosimetry.* Vol. 45, pp. 171-174, 1992.

STATGRAPHIC® Centurion XVI, statistical programe. 2012. 2012.

Stranden, E. 1980. Thoron and radon daughters in different atmospheres. *Health Physics.* Vol. 38, pp. 777-785, 1980.

SÚJB. 2006. Methodological procedures for measurements at workplaces where a significant increase in irradiation from natural sources can occur, and for determining the effective dose. 2006.

Suk, M., et al. 1991. Hluboké vrty v Čechách a na Moravě a jejich geologické výsledky. *Gabriel, 62. Praha.* 1991.

—. 1991. Hluboké vrty v Čechách a na Moravě a jejich geologické výsledky. *Gabriel, 62. Praha.* 1991.

Svoboda, J. and al., et. 1956. Závěrečná zpráva o základním geologickém výzkumu hranického devonu. *Geofond, P 8629. Praha.* 1956.

Svoboda, J. et al. 1966. Regionální geologie Československa I. Český Masiv I. Krystalinikum. II. Algonkuim až kvartér. *Praha.* 1966.

Štelcl, J. and Zimák, J. 2006. Přirozená radioaktivita horninového prostředí Moravského krasu. UP Olomouc. 2006.

—. 2011. Přirozená radioaktivita horninového prostředí speleoterapeutických léčeben v Císařské jeskyni a Sloupskošošůvských jeskyních (Moravský kras, Česká republika). *Geol. výzk. Mor. Slez., Brno 2011/2.* 2011.

—. 1998. Výsledky gamaspektrometrických měření v Javoříčských jeskyních. - *Geologický výzkum Moravy a Slezka, 1997, s. 112-115, Brno.* 1998.

Štolba, M. 2012. Statistické modelování koncentrace radonu ve vybraných jeskyních ČR. *Diplompvá Práce. VŠB Ostarva.* 2012.

Thinova, L. and Burian, I. 2008. Effective Dose Assessment for Workers in Caves in the Czech Republic: Experiments with Passive Radon Detectors. *Radiation Protection Dosimetry.* 2008, Vols. vol. 130, no. 1, p. 48-51, ISSN 0144-8420.

Thinova, L. and Rovenska, K. 2011. Radon dose calculation methodology for underground workers in the Czech Republic. *Radiation Protection Dosimetry.* 2011, Vols. vol. 145, no. 2-3, p. 1233-237, ISSN 0144-8420.

—. 2008a. Radon Dose Determination for Cave Guides in Czech Republic. *The Natural Radiation Environment.* Melville, New York: American Institute of Physics, 2008a, Vols. vol. 1, p. 141-144, ISBN 978-0-7354-0559-2.

Thinova, L. et al. 2005. Effective dose calculation using radon daughters and aerosol particles measurement in Bozkov Dolomite Cave. *HIGH LEVELS OF NATURAL RADIATION AND RADON AREAS: RADIATION DOSE AND HEALTH EFFECTS.* Book Series: INTERNATIONAL CONGRESS SERIES, 2005, Vols. Vol. 1276, pp. 381-382 .

Thinová, L. et al. 2007. *Závěrečná zpráva VaV12/2006. Radon v jeskyních.* Praha : ČVUT, 2007.

Thinová, L. 2005. Personal Dosimetry Enhancement for Underground Workplaces. Acta Polytechnica. Praha. *Acta Polytechnica. Praha.* 2005.

Thinová, L., Otáhal, P. and Rovenská, K. 2006. Dílčí zpráva o průběhu řešení úkolu VaV 12/2006 SÚJB. ČVUT, Praha, 2006.

Thinova, L., Otahal, P. and Rovenska, K. 2010. Environmental and radon measurements in the underground workplaces in Czech Republic. *Nukleonika Journal.* 2010, Vols. Vol 55, no.4, p. 491-494, ISSN 0029-5922.

Thomas, J. 1999. Odhad osobních dávek průvodců v jeskyních přístupných. *Vnitřní metodika SUJB.* 1999.

—. 1999a. Profesionální radiační riziko z přírodních radionuklidů v jeskyních. *SÚJB.* 1999a.

Toohey, R.E., et al. 1984. Measuremetns of the deposition rates of radon daughters in indoor surfaces. *Radiation Protection Dosimetry.* Vol. 7, No. 1-4. pp. 142-146., 1984.

UNSCEAR. 2000. *Sources and Effects of Ionizing Radiation. Report of the United Nations Scientific Committee on the Effects of Atomic Radiation to the General Assembly.* 2000.

Vaillant, L. and Bataille, C. 2012. Management of radon: a review of ICRP recommendations. *Journal of Radiological Protection.* 32, R1-R12, 2012.

Vanmarcke, H. and Berkvens, P. 1989. Radon versus radon daughters. *Health Physics.* Vol. 56.pp.229-231, 1989.

Vargas, A., Ortega, X. and Porta, M. 2000. Dose conversion factor for radon concentration in indoor environment using a new equation for the F-fp correlation. *Health Physics.* Vol 28, Issue 1, 2000.

Vaupotič, J. 2008. Nanosize radon short-lived decay products in the air of the Postojna Cave. *Science of the total environment* . Vol. 393, pp. 27-38, 2008.

Wysocka, M. 2011. Radon in Jurassic Caves of the Kraków-Czestochowa Upland. *Geochemical Journal.* Vol. 45. (No. 6), pp. 447-453, 2011.

Zimák, J. - Štelcl, J. 2004b. *Přirozená radioaktivita horninového prostředí v jeskyních České republiky.* Olomouc : Universita Palackého, 2004b. ISBN 80-244-0938-0.

Zimák, J. and Štelc, J. 2004a. Přirozená radioaktivita horninového prostředí v jeskyních Na Pomezí u Jeseníku. *Geol. výzk. Mor. a Slez. v r. 2003, s. 107-108, Brno.* 2004a.

Zimák, J. and Štelcl, J. 2004c. Výsledky gamaspektrometrických měření v Chýnovské jeskyni (závěrečná zpráva). *MS. PřF UP Olomouc a PřF MU Brno.* 2004c.

—. 2004d. Výsledky gamaspektrometrických měření v Koněpruských jeskyních (závěrečná zpráva). *MS. PřF UP Olomouc a PřF MU Brno.* 2004d.

Zimák, J., Štelcl, J. and Hofírková, P. 2004e. Výsledky gamaspektrometrických měření v Bozkovských dolomitových jeskyních (závěrečná zpráva). *MS. PřF UP Olomouc a PřF MU Brno.* 2004e.

Ženatá, I., Thinová, L. and Rovenská, K. 2009. *Novelizace-Metodický návod pro měření na pracovištích, kde může dojít k významnému zvýšení ozáření z přírodních zdrojů, a určení efektivní dávky.* Praha : SÚJB, 2009.

www.caves.cz

www.ssj.sk